Baoxue Yang
Jeff M. Sands   *Editors*

Urea Transporters

Principle and Function of Urea Transport

Second Edition

Springer

Subcellular Biochemistry

Volume 118

The book series SUBCELLULAR BIOCHEMISTRY is a renowned and well recognized forum for disseminating advances of emerging topics in Cell Biology and related subjects. All volumes are edited by established scientists and the individual chapters are written by experts on the relevant topic. The individual chapters of each volume are fully citable and indexed in Medline/Pubmed to ensure maximum visibility of the work.

Baoxue Yang • Jeff M. Sands
Editors

Urea Transporters

Principle and Function of Urea Transport

Second Edition

Springer

Editors
Baoxue Yang
Department of Pharmacology,
School of Basic Medical Sciences
Peking University
Beijing, China

Jeff M. Sands
Department of Medicine
Emory University School of Medicine
Atlanta, GA, USA

If disposing of this product, please recycle the paper.

Preface

As described in its contents, the first edition of *Urea Transporters*, published in 2014, focused on the mathematical modeling, genes, proteins, structure, expression regulation, biochemical properties, transport characteristics, physiological functions, small molecule inhibitors, and clinical aspects of urea transporters. Since the publication of the first edition, this book has been welcomed by readers and downloaded more than 32,000 times. The second edition of *Urea Transporters* represents an extensive revision and a considerable update of the first edition. For this second edition, as in the first edition, our approach has been not just to describe what urea transporters are and where they are expressed but to emphasize their protein structure, physiological functions, pathophysiological roles in diseases, and drug discovery as a novel diuretic target. The contents were redesigned with 10 updated chapters. We hope readers like it as much or more than the first edition.

Here we are grateful to the readers who have taken the trouble to write to us with constructive comments and suggestions. We thank all authors and colleagues for their contribution to this book.

Beijing, China   Baoxue Yang
Atlanta, GA, USA   Jeff M. Sands

Contents

Chapter 1
Genes and Evolution of Urea Transporters

Yi Ying, Bo Kan, Baoxue Yang, and Jeff M. Sands

Abstract Urea transporters (UTs) are a group of membrane channel proteins that specifically facilitate the permeation of urea, from bacteria to mammals, playing an essential role in urea reabsorption and water conservation. In mammals, there are two subfamilies of UT: the UT-A group originally isolated from the kidney inner medulla, and UT-B originally isolated from erythrocytes. The human UT-B gene (*Slc14a1*) arises from a single locus located on chromosome 18q12.1-q21.1, which is close to the UT-A gene (*Slc14a2*). The human *Slc14a1* gene includes 11 exons, with the coding region extending from exon 4 to exon 11, and is approximately 30 kb in length. The rat *Slc14a2* gene is very large, containing 24 exons, approximately 300 kb in length, and encodes 6 different isoforms. The *Slc14a2* gene has two promoter elements: promoter I, located upstream of exon 1, drives the transcription of UT-A1, UT-A1b, UT-A3, UT-A3b, and UT-A4; promoter II, located within intron 12, drives the transcription of UT-A2 and UT-A2b. This chapter will summarize the evolution and genetic characteristics of UTs.

The urea transporters (UTs), including UT-A isoforms and UT-B, are a group of membrane channel proteins that specifically facilitate the permeation of urea, which play an essential role in urea reabsorption and water conservation. UT-A isoforms,

Y. Ying · B. Yang (✉)
State Key Laboratory of Vascular Homeostasis and Remodeling, Department of
Pharmacology, School of Basic Medical Sciences, Peking University, Beijing, China
e-mail: baoxue@bjmu.edu.cn

B. Kan
Department of Clinical Laboratory, The Second Hospital of Jilin University,
Changchun, Jilin, China

J. M. Sands (✉)
Renal Division, Department of Medicine, Emory University School of Medicine,
Atlanta, GA, USA
e-mail: jsands@emory.edu

UT-A1-UT-A4 in mammals, are critical for renal urea recycling that contributes to the maintenance of osmotic pressure in kidney. UT-A5 and UT-A6 are expressed in testis and colon, respectively, but not in kidney. UT-B is expressed in various tissues, especially in red blood cells and endothelial cells, where it facilitates urea transport across membranes, regulating urea concentrations in tissues.

Cloning and characteristics of Urea Transporters

UT-A1

UT-A1, the largest isoform in the UT-A subgroup, was cloned by Shayakul et al. in 1996. The UT-A1 cDNA encodes a peptide of 532 amino acids, exhibiting 67% sequence similarity with UT-A2 [1]. UT-A1 is expressed in the apical plasma membrane and in the cytoplasm of the IMCD in rat [2–7], mouse [8], and human medulla [9]. When expressed in Xenopus oocytes, rat, mouse, and human UT-A1 are stimulated by cyclic AMP [1, 8–11]. Polyclonal antibodies have been raised against three portions of UT-A1: the N-terminus [12], the intracellular loop region [13], and the C-terminus [7, 14]. These antibodies often detect more than one UT-A protein since the various UT-A isoforms result from alternative splicing of the UT-A gene. However, they can be distinguished by the different sizes that are detected on Western blot. In the inner medullary tip region, all anti-UT-A1 antibodies detect protein bands at 97 and 117 kDa by Western blot [7, 13, 14]. The 97- and 117-kDa proteins are glycosylated versions of a non-glycosylated 88-kDa UT-A1 protein [15].

UT-A2

UT-A2 was the first cloned urea transporter and was discovered by You et al. in 1993 [16]; in 1995 and 1996, its homologs in rats and humans were cloned, respectively [17, 18]. UT-A2 and UT-A1 possess identical C-terminal amino acid sequences (and 3′ cDNA) but exhibit differences at the N-terminal (5′ cDNA) region [1, 8, 9]. Hence, UT-A2 is simply the C-terminal half of UT-A1. UT-A2 is recognized as a 55 kDa protein band in the renal medulla. Immunohistochemical examination demonstrated that UT-A2 is expressed in the thin descending limb of the loop of Henle [4, 7, 12, 19–23]. Specifically, UT-A2 is exclusively found in the final 28~44% of the thin descending limb of short-looped nephrons [24]. Cyclic AMP analogs fail to activate UT-A2 when produced in either Xenopus oocytes or human embryonic kidney (HEK) 293 cells [1, 10, 11, 16, 17, 25, 26]. However, vasopressin does enhance urea flow in MDCK cells that are stably transfected with mouse UT-A2, mUT-A2-MDCK cells. Urea flow is also enhanced by forskolin and elevated intracellular calcium in mUT-A2-MDCK cells. Inhibiting PKA with H-89 does not

influence forskolin-stimulated urea flow in mUT-A2-MDCK cells [27]. In humans, single-amino acid mutations in UT-A2, such as Val/Ile 227 or Ala/Thr 357, have been associated with a decrease in blood pressure [28]. These UT-A2 mutations have also been linked to increased efficacy of the antihypertensive drug nifedipine [29] and have more recently been shown to be associated with metabolic syndrome [30].

UT-A3

UT-A3 was cloned by Karakashian et al. in 1999 [26]. UT-A3 and UT-A1 share the same N-terminal amino acid sequence (and 5′ cDNA sequence) but differ at the C-terminal (3′-cDNA) end, making UT-A3 essentially the N-terminal half of UT-A1 [26, 46, 108]. Mouse UT-A3 shares 93% amino acid identity with rat UT-A3, 68% with rat UT-A2, and 63% with rat UT-B [26, 31]. Histological analysis suggests that UT-A3 is in the basolateral membrane of principle cells in inner medullary collecting ducts (IMCDs) and facilitates transepithelial urea transport across the IMCD. Cyclic AMP analogs can stimulate urea transport by UT-A3 when expressed in Xenopus oocytes or HEK 293 cells [26, 32], although one study did not observe this effect in oocytes [33]. Additionally, vasopressin enhances urea transport through a PKA-dependent pathway in cells stably transfected with mouse UT-A3 (mUT-A3-MDCK cells) [34]. UT-A3 has a single glycosylation site at N279, and altering this site diminishes its membrane expression and urea transport efficacy. The mature version of UT-A3 is extensively changed by sialic acid, with ST6GalI, not ST3GalIV, being responsible for its sialylation, which improves both membrane trafficking and activity. Furthermore, PKC activation facilitates the sialylation of UT-A3, while PKC inhibition blocks this process and decreases membrane expression. Sialylation also increases the protein's stability, and greater levels of sialylation correspond with increased urea transport activity [35].

UT-A4

UT-A4 was cloned by Karakashian et al. in 1999 [26]. UT-A4 and UT-A1 have similar N- and C-terminal amino acid sequences (as well as 5′ and 3′ cDNA sequences). However, UT-A4 is smaller, including mostly the N-terminal quarter of UT-A1 spliced with the C-terminal quarter of UT-A [26]. The UT-A4 cDNA encodes a peptide of 466 amino acids, which is 84% similar to UT-A2. UT-A4 and UT-A3 exhibit 87% homology. UT-A4 mRNA is found in rat kidney outer or inner medulla (although its specific tubular location is uncertain) and is activated by cyclic AMP analogs when produced in HEK-293 cells [26]. Unlike in rats, UT-A4 has not been discovered in mouse kidneys [36]. Induction by cisplatin may modify the UT-A4 protein, and further research should ascertain if glycosylation influences the function of UT-A4 [37].

UT-A5

UT-A5 was cloned by Fenton et al. in 2000 [32]. UT-A5 cDNA is 1.4 kb. UT-A5 was isolated and characterized from the testes, signifying a new isoform of the UT-A transporter family. It has been identified just in the outermost layer of the seminiferous tubules inside the testes, and not in the kidneys. The mRNA level of UT-A5 corresponds with the stage of testicular development and rises about 15 days after birth, corresponding with the commencement of fluid flow in the seminiferous tubules. The UT-A5 cDNA has a predicted open reading frame that encodes a protein consisting of 323 amino acids [32]. The inferred amino acid sequence of UT-A5 commences with methionine 139 in mouse UT-A3, subsequently exhibiting 100% homology and a shared C-terminus with mouse UT-A3 [32].

UT-A6

UT-A6 was cloned by Smith et al. in 2004. UT-A6 is a unique urea transporter within the UT-A family that has been discovered in the human gastrointestinal system, especially in the colon [38]. Interestingly, UT-A6 is poorly expressed only in the adult colon and is not detectable in the human fetal colon, showing that the expression of UT-A6 is controlled by the contents of the intestinal mucosa. Expression of colon UT-A6 may be modulated by hyperosmolarity, similar to the previously characterization of renal UT-A transporters [39]. The UT-A6 transcript encodes a protein with 235 amino acids, making it the smallest member of the UT-A family.

UT-B

UT-B was cloned by Olives et al. in 1994 [40] and was subsequently cloned from rat and mouse [31, 41, 42]. There are two transcripts for UT-B. UT-B1 mRNA is widely expressed and has been detected in many tissues, including kidney, brain, liver, colon, small intestine, pancreas, testis, prostate, bone marrow, spleen, thymus, heart, skeletal muscle, lung, bladder, and cochlea [3, 10, 18, 40–54]. Several polyclonal antibodies have been made to either the N- or C-terminus of human UT-B1 [46, 53, 55]. These antibodies also detect UT-B1 in rodents [46, 53, 55]. On Western blot, UT-B1 protein is detected as a broad band between 45 and 65 kDa in human red blood cells and 37–51 kDa in rat or mouse red blood cells [42, 53]. UT-B1 protein is detected in kidney medulla as a broad band between 41 and 54 kDa [53]. In both red blood cells and kidney medulla, deglycosylation converts the broad band detected on Western blot to a sharp band of 32 kDa. Human, mouse, and rat kidney show UT-B1 immunostaining in the non-fenestrated endothelial cells that are

characteristic of descending vasa recta [20, 42, 46, 53, 55–57]. UT-B1 protein is also present in rat liver, colon, testis, brain, heart, lung, aorta, cochlea, spinotrapezius muscle, urothelial, and mesenteric artery [3, 44, 46, 47, 49, 50, 53, 54, 58, 59].

UT-B2 mRNA transcripts can be found in sheep and cow rumens, and their expression is influenced by gastric acidity and alkalinity, rumen ammonia concentration, and the type of food consumed in the digestive system of sheep and cows [60–65]. The variation in UT-B2 abundance in ruminants to the level of nitrogen in their food parallels the response of UT-B1 abundance in rats to fluctuations in urea load or urine urea concentration [48, 66, 67].

Comparison of Amino Acid Sequences of Human Urea Transporters

Figure 1.1 presents the amino acid sequences of 4 human isoforms of UTs: UT-A2; UT-A3; UT-A6; and UT-B. The amino acid sequences of UT family members exhibit a number of similarities. Typically, UT proteins have 10 predicted transmembrane helices; however, in the UT-A isoform, the combination of 2 tandem UT domains leads in a total of 20 predicted transmembrane helices. Significant similarity exists between the first five and final five transmembrane helices within each UT domain, indicating that this protein may have developed from the duplication of a primordial five-transmembrane helix protein. Additionally, comparative examination of the UT sequences has shown a significant feature: each five-transmembrane repeat contains a conserved motif, which is thought to be essential for urea permeability [68–71].

The three major protein variants produced by the human UT-A gene include UT-A1, UT-A2, and UT-A3. UT-A2 shares a common C-terminal amino acid sequence with UT-A1, consisting of 397 amino acids. Meanwhile, UT-A3 shares a common N-terminal amino acid sequence with UT-A1. UT-A6 features only three membrane-spanning domains and an extracellular carboxy terminus. The characteristics of human UT-A6 indicate that the encoded protein is 235 amino acids in length, making it the smallest member of the UT-A family yet characterized. In hUT-A6, there exists a unique atypical region after amino acid 216 that is specific to the UT-A family, consisting of 19 hydrophilic amino acids. This region is derived from a newly identified 127-base pair alternative splicing exon, which encodes these 19 amino acids along with a stop codon. Furthermore, this exon contains a potential N-glycosylation site (N-I/N-T-W/G) located at the amino terminus at position 223 [38]. Human UT-B protein encodes a peptide of 389 amino acids and exhibits over 60% identity with UT-A2. Notably, the UT-B peptide contains a unique "ALE" motif that is not found in other urea transport proteins [40, 72].

Previous studies have identified amino acids involved in urea binding: Q24/V25/F27 (Pa), F80/L84 (T3a), L129/T130 (T5a), E187/V188/F190 (Pb), F243/L247 (T3b), and L293/T294 (T5b) (Fig. 1.1c). Notably, these amino acids are highly conserved among the human UT-A and UT-B subtypes, as illustrated in Fig. 1.1 [71].
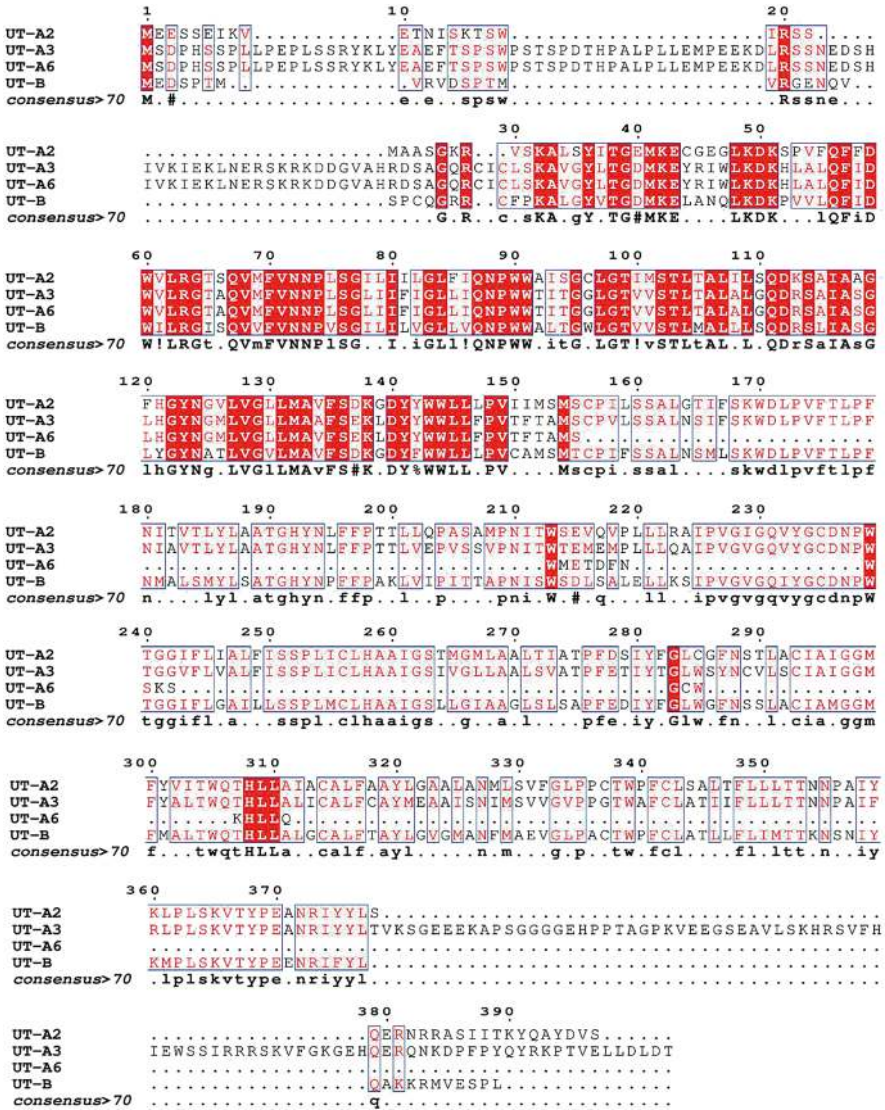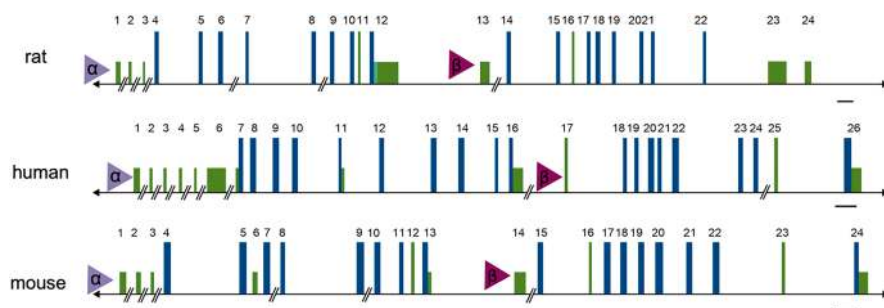
```
              1              10                            20
UT-A2      MEESSEIKV............ETNISKTSW....................IRSS....
UT-A3      MSDPHSSPLLPEPLSSRYKLYEAEFTSPSWPSTSPDTHPALPLLEMPEEKDLRSSNEDSH
UT-A6      MSDPHSSPLLPEPLSSRYKLYEAEFTSPSWPSTSPDTHPALPLLEMPEEKDLRSSNEDSH
UT-B       MEDSPTM.J...........VRVDSPTM...................VRGENQV..
consensus>70 M.#.....................e.e..spsw....................Rssne...

                        30            40              50
UT-A2      ..................MAASGKR...VSKALSYITGEMKECGEGLKDKSPVFQFFD
UT-A3      IVKIEKLNERSKRKDDGVAHRDSAGQRCICLSKAVGYLTGDMKEYRIWLKDKHLALQFID
UT-A6      IVKIEKLNERSKRKDDGVAHRDSAGQRCICLSKAVGYLTGDMKEYRIWLKDKHLALQFID
UT-B       ...............SPCQGRR...CFPKALGYVTGDMKELANQLKDKPVVLQFID
consensus>70 ....................G.R..c.sKA.gY.TG#MKE....LKDK...lQFiD

           60        70        80        90       100       110
UT-A2      WVLRGTSQVMFVNNPLSGILIILGLFIQNPWWAISGCLGTIMSTLALILSQDKSAIAAG
UT-A3      WVLRGTAQVMFVNNPLSGLIIFIGLLIQNPWWTITGGLGTVVSTLALALGQDRSAIASG
UT-A6      WVLRGTAQVMFVNNPLSGLIIFIGLLIQNPWWTITGGLGTVVSTLALALGQDRSAIASG
UT-B       WILRGISQVVFVNNPVSGLILIVGLLVQNPWWALTGWLGTVVSTLMALLLSQDRSLIASG
consensus>70 W!LRGt.QVmFVNNPlSG..I..I.iGLl!QNPWWW.itG.LGT!vSTLtAL.L.QDrSaIAsG

          120      130       140        150       160       170
UT-A2      FHGYNGVLVGLLMAVFSDKGDYYWWLLLPVIIMSMSCPILSSALGTIFSKWDLPVFTLPF
UT-A3      LHGYNGMLVGLLMAAFSEKLDYYWWLLFPVTFTAMSCPVLSSALNSIFSKWDLPVFTLPF
UT-A6      LHGYNGMLVGLLMAVFSEKLDYYWWLLFPVTFTAMS.....................
UT-B       LYGYNATLVGVLMAVFSDKGDYWWWLLLPVCAMSMTCPIFSSALNSMLSKWDLPVFTLPF
consensus>70 lhGYNg.LVGlLMAvFS#K.DY%WWLL.PV....Mscpi.ssal....skwdlpvftlpf

          180      190       200       210       220       230
UT-A2      NITVTLYLAATGHYNLFFPTTLLQPASAMPNITWSEVQVPLLLRAIPVGIGQVYGCDNPW
UT-A3      NIAVTLYLAATGHYNLFFPTTLVEPVSSVPNITWTEMEMPLLLQAIPVGVGQVYGCDNPW
UT-A6      ...................WMETDFN........................W
UT-B       NMALSMYLSATGHYNPFFPAKLVIPITTAPNISWSDLSALELLKSIPVGVGQIYGCDNPW
consensus>70 n....lyl.atghyn.ffp..l..p....pni.W.#.q...ll..ipvgvgqvygcdnpW

          240      250       260       270       280       290
UT-A2      TGGIFLIALFISSPLICLHAAIGSTMGMLAALTIATPFDSIYFGLCGFNSTLACIAIGGM
UT-A3      TGGVFLVALFISSPLICLHAAIGSIVGLLAALSVATPFETIYTGLWSYNCVLSCIAIGGM
UT-A6      SKS.......................GCW............
UT-B       TGGIFLGAILLSSPLMCLHAAIGSLLGIAAGLSLSAPFEDIYFGLWGFNSSLACIAMGGM
consensus>70 tggifl.a...sspl.clhaaigs..g..a.l....pfe.iy.Glw.fn..l.cia.ggm

          300      310       320       330       340       350
UT-A2      FYVITWQTHLLAIACALFAAYLGAAALANMLSVFGLPPCTWPFCLSALTFLLLTTNNPAIY
UT-A3      FYALTWQTHLLALICALFCAYMEAAISNIMSVGVPPGTWAFCLATIIFLLLTTNNPAIF
UT-A6      .......KHLLQ.....................
UT-B       FMALTWQTHLLALGCALFTAYLGVGMANFMAEVGLPACTWPFCLATLLFLIMTTKNSNIY
consensus>70 f....twqtHLLa..calf.ayl.....n.m...g.p..tw.fcl....fl.ltt.n..iy

          360      370
UT-A2      KLPLSKVTYPEANRIYYLS.
UT-A3      RLPLSKVTYPEANRIYYLTVKSGEEEKAPSGGGGEHPPTAGPKVEEGSEAVLSKHRSVFH
UT-A6      ............................
UT-B       KMPLSKVTYPEENRIFYL.........................
consensus>70 .lplskvtype.nriyyl.......................

                        380       390
UT-A2      .......................QERNRRASIITKYQAYDVS......
UT-A3      IEWSSIRRRSKVFGKGEHQERQNKDPFPYQYRKPTVELLDLDT
UT-A6      .......................................
UT-B       .......................QAKKRMVESPL............
consensus>70 .......................q...........
```

Fig. 1.1 Amino acid sequence alignment of human UTs

Genes of Urea Transporters

The Slc14a2 (UT-A) Gene

The *Slc14a2* (UT-A) gene was initially cloned from rat [73] and subsequently cloned from human and mouse [9, 74]. The rat UT-A gene is a very large gene (Fig. 1.2) with 24 exons and is approximately 300 kb in length (Fig. 1.2) [73, 75].

Fig. 1.2 Comparison of the genomic organization of the urea transporter UT-A gene (*Slc14a2*) for human, rat, and mouse. Above are schematic representations of the gene structure for each species. Exon width is representative of actual size, and intronic distance is scaled. Introns >5 kb are represented by //and are not scaled. Triangles denote the α and β promoters. Coding exons and untranslated exons (green) are drawn to scale. (Figure is reproduced with permission of the American Physiological Society from Klein et al. [79])

UT-A1 is encoded by exons 1–12 spliced to exons 14–23 (exon 13 is not used for UT-A1). UT-A3 is encoded by exons 1–12. UT-A4 is encoded by exons 1–7 spliced to exons 18–23. There is a common transcription start site in exon 1 and translation start site in exon 4 for UT-A1, UT-A3, and UT-A4. In contrast, UT-A2 is encoded by exons 13–23 with an unique translation start site in exon 16. UT-A1b and UT-A2b utilize exon 24, which is located in the 3′ untranslated region of the UT-A gene. UT-A1b and UT-A2b have the same coding regions as UT-A1 and UT-A2, respectively, but their cDNA transcripts differ due to use of exon 24 in the 3′ untranslated region [76]. UT-A3b also results from expression of an alternative 3′-untranslated region and results in a transcript that is ~1.5 kb longer than UT-A3 cDNA [76].

The rat *Slc14a2* (UT-A) gene contains two promoter elements: promoter I is located in the typical position, upstream of exon 1, and drives the transcription of UT-A1, UT-A1b, UT-A3, UT-A3b, and UT-A4; while promoter II is located within intron 12 and drives the transcription of UT-A2 and UT-A2b. When the 1.3 kb of UT-A promoter I that is located immediately 5′ to exon 1 is cloned into a luciferase reporter gene construct and transfected into mIMCD3, MDCK, or LLCPK1 cells, it shows evidence of promoter activity [36, 77]. This 1.3-kb promoter sequence does not contain a TATA motif but does contain three CCAAT elements [36, 77]. UT-A promoter I activity is significantly increased by hyperosmolality, and it contains a tonicity enhancer (TonE) element [36, 77]. Dexamethasone, at a dose equivalent to a level found during stress, reduces the activity of UT-A promoter I by 70% and decreases the mRNA abundances of UT-A1, UT-A3, and UT-A3b in the rat inner medulla [36, 77].The repressive effect of dexamethasone on UT-A promoter I activity does not occur via the consensus glucocorticoid response element (GRE) that is present in UT-A promoter I [36, 77].

UT-A2 is under the control of a unique internal promoter, UT-A promoter II, which is located within intron 12 [73, 76]. The transcription start site for UT-A2 is located in exon 13, which is almost 200 kb downstream from exon 1 [73, 76]. Within

intron 12, there is a TATA box 40 bp upstream of the UT-A2 transcription start site and a cAMP response element (CRE) 300 bp upstream of the UT-A2 transcription start site [73, 76]. This internal promoter region of intron 12 shows evidence of promoter activity when it is transfected into mIMCD3 cells, along with a luciferase reporter gene, and the cells are stimulated with cAMP; no promoter activity is detected under basal conditions [73, 76].

The human *Slc14a2* (UT-A) gene is approximately 67.5 kb in length (Fig. 1.2). The human gene is significantly shorter than the rat gene because: (1) it does not contain an exon in the 3′-untranslated region that is analogous to rat exon 24; and (2) the 5′-untranslated region is almost entirely located in exon 1 in humans, while in rat, it spans the first 3 widely spaced exons [9, 73]. However, human UT-A does contain an extra exon, exon 5a, which has not been reported in rat [38]. Exon 5a was subsequently renumbered as exon 6, with a renumbering of all the downstream exons [75]. The human UT-A gene gives rise to UT-A1, UT-A2, and UT-A3, similar to rat, and to a shorter isoform, UT-A6 [75]. UT-A6 is encoded by human exons 1–11 (original nomenclature is exons 1–10 but including exon 5a) and is expressed in colon [38].

The structure of the mouse *Slc14a2* (UT-A) gene is very similar to the rat *Slc14a2* gene (Fig. 1.2), with the exception that a mouse UT-A4 isoform has not been detected [74]. The mouse UT-A gene contains 24 exons, is >300 kb in length, and has two promoter elements, which are named α and β [74, 75]. UT-A promoter α, which corresponds to promoter I in rat, contains a TonE element, and its promoter activity is increased by hypertonicity [74]. In contrast to rat, the activity of mouse UT-A promoter I (α) is increased by cAMP, even though no consensus CRE element is present in promoter I (α) from either species [73, 74]. The mouse gene also gives rise to a testis-specific isoform, UT-A5, which is encoded by exons 6–13 [32, 74, 75]. While all mouse UT-A isoforms originate from a single mouse gene, the transcription start site of UT-A5 has not been determined and may be located downstream from mouse UT-A1 and UT-A3 [74]. Thus, whether UT-A5 is driven by promoter α or by a novel promoter element is not known, nor is it known whether UT-A5 is expressed in humans or rat (Table 1.1). UT-A promoter α has been further characterized using a transgenic mouse in which 4.2 kb of the 5′-flanking region of the UT-A gene is linked to a β-galactosidase reporter gene [78]. UT-A5 differs slightly with its amino terminus in the hydrophobic region, and UT-A6 contains only three membrane spanning domains with an extracellular carboxy terminus [32, 38]. The largest isoform, UT-A1, represents a duplication of this structure linked by a large hydrophilic intracellular loop [71]. The regulation of β-galactosidase transgene by water restriction and glucocorticoids is similar to the regulation of the endogenous UT-A promoter I (α) [36, 74, 77, 78].

Table 1.1 Mammalian facilitated urea transporter gene families

Gene	Isoform	RNA (kb)	Protein (kDa)	AVP	Location	References
Slc14a1	UT-B1	3.8	43		DVR, RBC[a]	Olives et al. [40], Couriaud et al. [41], Promeneur et al. [10], Tsukaguchi et al. [31], Berger et al. [43], Timmer et al. [53].
	UT-B2	3.7	43–54	No	Bovine rumen	Stewart et al. [62], Tickle et al. [63]
Slc14a2	UT-A1	4.0	97, 117	Yes	IMCD	Shayakul et al. [1]., Bradford et al. [15], Bagnasco et al. [9].
	UT-A1b	3.5			Medulla[b]	Bagnasco et al. [76]., Nakayama et al. [73]
	UT-A2	2.9	55	No[c]	tDL, liver	You et al. [16], Smith et al. [17], Olivès et al. [18], Promeneur et al. [10], Nielsen et al. [7], Doran et al. [3], Potter et al. [27]
	UT-A2b	2.5			medulla[b], heart	Karakashian et al. [26], Bagnasco et al. [76]., Duchesne et al. [85].
	UT-A3	2.1	44, 67	Yes	IMCD	Karakashian et al. [26], Fenton et al. [32], Shayakul et al. [33]., Terris et al. [86].
	UT-A3b	3.7			medulla[b]	Bagnasco et al. [76].
	UT-A4d	2.5	43	Yes	medulla[b]	Karakashian et al. [26]
	UT-A5[e]	1.4			Testis	Fenton et al. [32]
	UT-A6[f]	1.8			Colon	Smith et al. [38]

Isoform names are based upon the urea transporter nomenclature proposed in [87]; AVP, urea flux is stimulated by vasopressin; *DVR* descending vasa recta; *RBC* red blood cells
[a]also expressed in several other tissues and endothelial cells; *IMCD* inner medullary collecting duct; *tDL* thin descending limb
[b](exact tubular location unknown)
[c]no in rat but yes in mouse
[d]cloned from rat only
[e]cloned from mouse only
[f]cloned from human only

The Slc14a1 (UT-B) Gene

UT-B is encoded by a different gene, *Slc14a1,* than the UT-As [80]. However, UT-A and UT-B contain tandem repeat sequences that may represent a urea transporter signature sequence [81]. The *Slc14a1* (UT-B) gene was initially cloned from a human erythropoietic cell line and subsequently cloned from rats and mice [31, 41, 42]. The human *Slc14a1* (UT-B) gene includes 11 exons, with the coding region extending from exon 4 to exon 11, and is approximately 3917 bp in length (Fig. 1.3) [82]. There are two mRNA transcripts, 4.4 and 2.0 kb, which result from alternative polyadenylation signals; both are expressed in reticulocytes and encode a single 45-kDa protein [82].
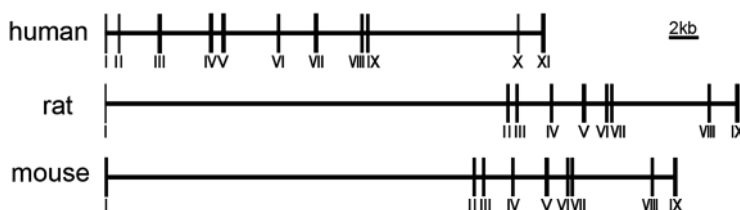
Fig. 1.3 Comparison of the genomic organization of the UT-B gene (Slc14a1) for human, rat, and mouse. Above are schematic representations of the gene structure for each species

Two rat cDNA sequences were originally reported for UT-B1 that differed by only a few nucleotides at their 3′ end [31, 41]. It is unknown whether these small differences may represent polymorphisms or sequencing artifacts.

The cDNA for mouse UT-B was cloned, encoding a protein of 384 amino acids, which is expressed in the kidney, spleen, brain, ureter, and urinary bladder. In 2002, Yang et al. first generated UT-B knockout mice through targeted deletion of exons 3–6 to analyze the mouse UT-B gene. They found that UT-B-dependent urea countercurrent exchange accounted for approximately one-third of the total capacity for urine concentration in the kidneys, while contributing even more significantly to the intrinsic ability of the kidneys to concentrate urea [42].

The Slc14a2 (UT-A) and Slc14a1 (UT-B) Genes Localization

Slc14a1, the human UT-B gene, arises from a single locus located on chromosome 18q12.1- q21.1 (Fig. 1.4), which is linked with *Slc14a2*, the human UT-A gene. The analogous mouse genes, UT-B (*Slc14a1*) and UT-A (*Slc14a2*), also occur in tandem on mouse chromosome 18 [83].

Evolution of Urea Transporters

The discovery and evolution of urea transporters (UTs) illustrates the capacity of many species to adapt to their unique environmental challenges and physiological requirements. Homologues are predominantly found in vertebrate animals and bacteria, excluding other eukaryotes and archaea. Analyses of sequence, structure, and phylogeny reveal conserved regions and residues, indicating that a primordial genetic element encoding five transmembrane helical segments (TMS) underwent duplication to create a ten TMS-encoding element early in evolutionary history, coinciding with the divergence of eukaryotes from prokaryotes. Two conserved, highly amphipathic, putative alpha-helices preceding both 5 TMS repeat motifs are expected to possess structural, functional, or biogenic significance. An additional duplication event, or gene fusion event, occurred throughout the evolution of the
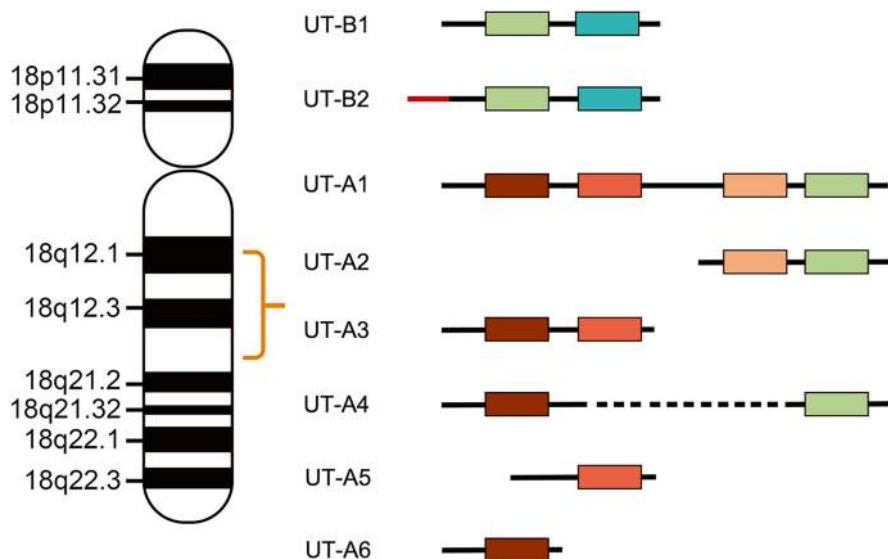
Fig. 1.4 Schematic representation of the human UT-B (*Slc14a1*) and UT-A (*Slc14a2*) genes on chromosome 18 and encoded isoforms of UT-A and UT-B urea transporters, respectively. The different boxes represent regions of hydrophobic amino acids. The black lines show coding sequences that are common, while the red lines show coding sequences that are unique to that particular isoform (i.e., derived from novel exons) [84]

vertebrate lineage, resulting in 20 TMS mammalian homologues. The statistics indicate that vertebrates acquired UT genetic information from bacteria a single time, and all existing orthologues and paralogues in animals originated from this singular system [69].

In lower organisms, such as bacteria, urea transporters are typically simpler and often consist of single-domain proteins. Bacteriologists typically consider that urea flows across bacterial membranes predominantly via passive diffusion. Yut [88] and UreI [89, 90], two energy-independent urea transporters, appear to be channel-like structures that allow urea to enter the cytoplasm via a urea pore driven by a favorable concentration gradient from gastric juice urea, which is maintained by rapid urea hydrolysis by intrabacterial urease [88, 91].

As organisms evolved into more complex forms, including invertebrates and early vertebrates, the genetic structure of UTs became progressively complex. In these organisms, UTs started to diversify, with some species exhibiting numerous isoforms of the protein. This diversity reflects the increased necessity for more detailed control over nitrogen waste excretion and osmotic equilibrium as organisms acquired more complex excretory systems during evolution.

In vertebrates, the principal metabolic process involved in urea synthesis is the ornithine–urea cycle (OUC). A significant evolutionary feature of this system is its obvious derivation from ancestral metabolic pathways prevalent in almost all animals [92]. One of the primary evolutionary novelties leading to the development of

the OUC is the duplication of the cytosolic enzyme carbamoyl phosphate synthetase II (CPSII), and its transfer to the mitochondria, becoming CPSI (in tetrapods) or III (in fishes). This mechanism was once considered a metazoan innovation; however, current developments in comparative genomics indicate that the evolution of mito-chondrial CPS predates metazoans, since it is seen in choanoflagellates and other diatom species [93, 94]. This characteristic was likely subsequently lost in many metazoan lineages, and the exploration of its physiological importance in early eukaryotes requires additional inquiry [95, 96].

Current models of UT evolution in mammals suggest two key duplication events originating from an ancestral UT gene (Fig. 1.5). In fish and amphibians, this gene encodes proteins ranging from 380 to 475 amino acids, with 8 to 10 transmembrane segments. The first duplication is believed to have led to the UT-B gene, which
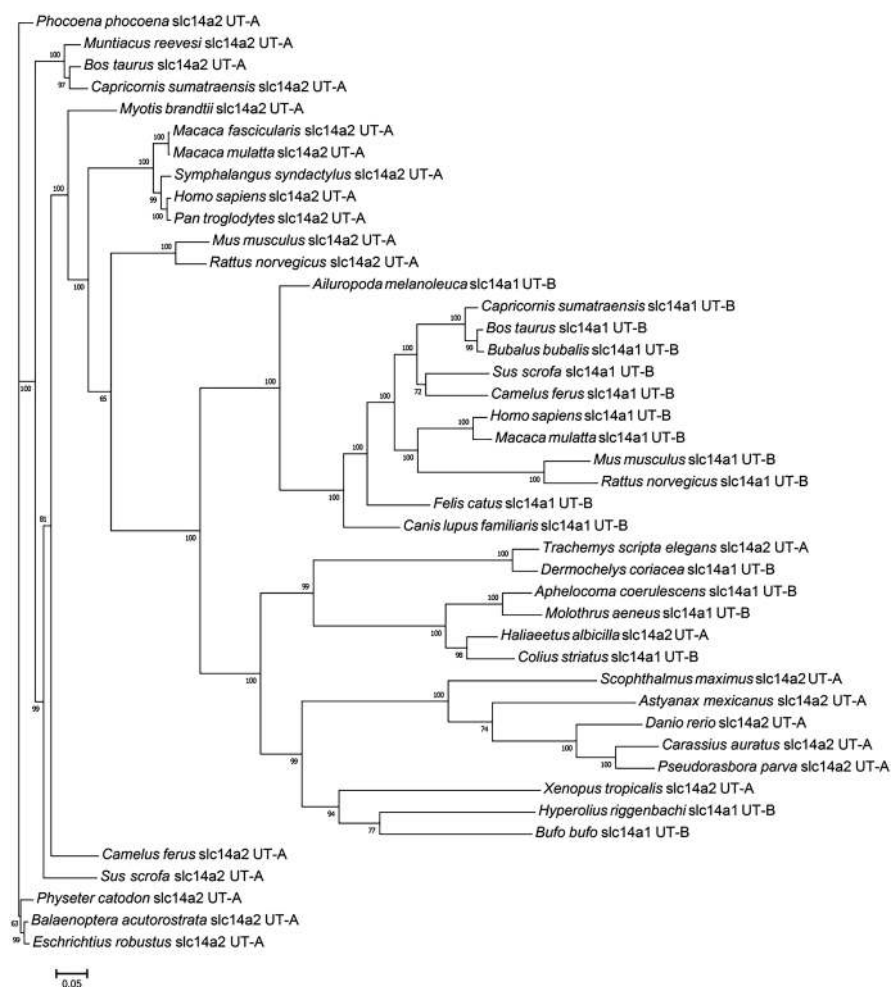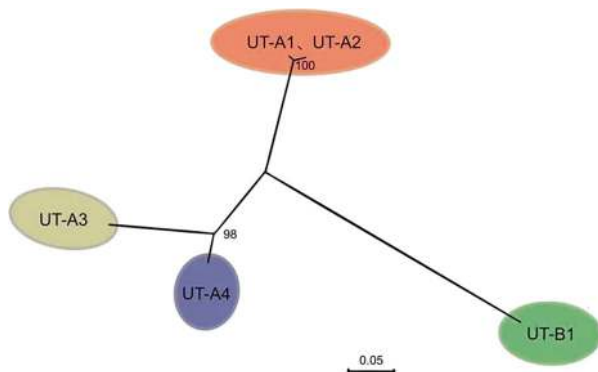

Fig. 1.5 The phylogenetic tree of UTs

Fig. 1.6 The phylogenetic tree of 5 rat UTs. The tree shows UT-A1, UT-A2 (orange oval); UT-A3 (light yellow oval); UT-A4 (puple oval) and UT-B1 (green oval)

evolved a distinct amino acid sequence aligned with its role in red blood cells and related tissues. The second duplication event led to the enlargement of the UT-A gene, producing two highly homologous halves. When fully transcribed and translated, this gene produces the UT-A1 isoform, while alternative splicing generates five additional isoforms (UT-A2 through UT-A6) with diverse, tissue-specific expression patterns. Phylogenetic analyses indicate that the duplication and differentiation of UT-B occurred before the internal duplication within UT-A (Fig. 1.6).

All UT-A and UT-B isoforms exhibit significant structural homology at both the nucleotide and amino acid levels. Their predicted primary structure includes 10 transmembrane domains organized into two hydrophobic repeats, an extracellular loop, intracellular N- and C-termini, a single N-glycosylation site, and multiple phosphorylation sites for protein kinase A (PKA) and protein kinase C (PKC). This structural organization highlights the functional versatility of UT isoforms in nitrogen waste excretion and osmoregulation across species.

Conflicts of interest The authors have no conflicts of interest.

References

1. C. Shayakul, A. Steel, M.A. Hediger, Molecular cloning and characterization of the vasopressin-regulated urea transporter of rat kidney collecting ducts. J. Clin. Invest. **98**(11), 2580–2587 (1996)
2. M.A. Blount et al., Expression of transporters involved in urine concentration recovers differently after cessation of lithium treatment. Am. J. Physiol. Renal Physiol. **298**(3), F601–F608 (2010)

3. J.J. Doran et al., Tissue distribution of UT-A and UT-B mRNA and protein in rat. Am. J. Physiol. Regul. Integr. Comp. Physiol. **290**(5), R1446–R1459 (2006)
4. Y.H. Kim et al., Expression of urea transporters in the developing rat kidney. Am. J. Physiol. Renal Physiol. **282**(3), F530–F540 (2002)
5. J.D. Klein et al., Phosphorylation of UT-A1 on serine 486 correlates with membrane accumulation and urea transport activity in both rat IMCDs and cultured cells. Am. J. Physiol. Renal Physiol. **298**(4), F935–F940 (2010)
6. S.W. Lim et al., Ultrastructural localization of UT-A and UT-B in rat kidneys with different hydration status. Am. J. Physiol. Regul. Integr. Comp. Physiol. **290**(2), R479–R492 (2006)
7. S. Nielsen et al., Cellular and subcellular localization of the vasopressin- regulated urea transporter in rat kidney. Proc. Natl. Acad. Sci. USA **93**(11), 5495–5500 (1996)
8. R.A. Fenton et al., Characterization of mouse urea transporters UT-A1 and UT-A2. Am. J. Physiol. Renal Physiol. **283**(4), F817–F825 (2002)
9. S.M. Bagnasco et al., Cloning and characterization of the human urea transporter UT-A1 and mapping of the human Slc14a2 gene. Am. J. Physiol. Renal Physiol. **281**(3), F400–F406 (2001)
10. D. Promeneur et al., Evidence for distinct vascular and tubular urea transporters in the rat kidney. J. Am. Soc. Nephrol. **7**(6), 852–860 (1996)
11. C. Shayakul et al., Segmental localization of urea transporter mRNAs in rat kidney. Am. J. Phys. **272**(5 Pt 2), F654–F660 (1997)
12. J.B. Wade et al., UT-A2: a 55-kDa urea transporter in thin descending limb whose abundance is regulated by vasopressin. Am. J. Physiol. Renal Physiol. **278**(1), F52–F62 (2000)
13. A. Kato et al., Long-term regulation of inner medullary collecting duct urea transport in rat. J. Am. Soc. Nephrol. **9**(5), 737–745 (1998)
14. M. Naruse et al., Glucocorticoids downregulate the vasopressin-regulated urea transporter in rat terminal inner medullary collecting ducts. J. Am. Soc. Nephrol. **8**(4), 517–523 (1997)
15. A.D. Bradford et al., 97- and 117-kDa forms of collecting duct urea transporter UT-A1 are due to different states of glycosylation. Am. J. Physiol. Renal Physiol. **281**(1), F133–F143 (2001)
16. G. You et al., Cloning and characterization of the vasopressin-regulated urea transporter. Nature **365**(6449), 844–847 (1993)
17. C.P. Smith et al., Cloning and regulation of expression of the rat kidney urea transporter (rUT2). J. Clin. Invest. **96**(3), 1556–1563 (1995)
18. B. Olivès et al., Molecular characterization of a new urea transporter in the human kidney. FEBS Lett. **386**(2–3), 156–160 (1996)
19. B. Maciver et al., Functional characterization of mouse urea transporters UT-A2 and UT-A3 expressed in purified Xenopus laevis oocyte plasma membranes. Am. J. Physiol. Renal Physiol. **294**(4), F956–F964 (2008)
20. T.L. Pallone, Z. Zhang, K. Rhinehart, Physiology of the renal medullary microcirculation. Am. J. Physiol. Renal Physiol. **284**(2), F253–F266 (2003)
21. T.L. Pannabecker et al., Mixed descending- and ascending-type thin limbs of Henle's loop in mammalian renal inner medulla. Am. J. Physiol. Renal Physiol. **278**(2), F202–F208 (2000)
22. T.L. Pannabecker, C.S. Henderson, W.H. Dantzler, Quantitative analysis of functional reconstructions reveals lateral and axial zonation in the renal inner medulla. Am. J. Physiol. Renal Physiol. **294**(6), F1306–F1314 (2008)
23. J. Yuan, T.L. Pannabecker, Architecture of inner medullary descending and ascending vasa recta: pathways for countercurrent exchange. Am. J. Physiol. Renal Physiol. **299**(1), F265–F272 (2010)
24. X.Y. Zhai et al., Aquaporin-1 is not expressed in descending thin limbs of short-loop nephrons. J. Am. Soc. Nephrol. **18**(11), 2937–2944 (2007)
25. Z.M. Ashkar et al., Urea transport in initial IMCD of rats fed a low-protein diet: functional properties and mRNA abundance. Am. J. Phys. **268**(6 Pt 2), F1218–F1223 (1995)
26. A. Karakashian et al., Cloning and characterization of two new isoforms of the rat kidney urea transporter: UT-A3 and UT-A4. J. Am. Soc. Nephrol. **10**(2), 230–237 (1999)

27. E.A. Potter, G. Stewart, C.P. Smith, Urea flux across MDCK-mUT-A2 monolayers is acutely sensitive to AVP, cAMP, and [Ca2+]i. Am. J. Physiol. Renal Physiol. **291**(1), F122–F128 (2006)
28. K. Ranade et al., Genetic variation in the human urea transporter-2 is associated with variation in blood pressure. Hum. Mol. Genet. **10**(19), 2157–2164 (2001)
29. X. Hong et al., Genetic polymorphisms of the urea transporter gene are associated with antihypertensive response to nifedipine GITS. Methods Find. Exp. Clin. Pharmacol. **29**(1), 3–10 (2007)
30. H.J. Tsai et al., Genetic variants of human urea transporter-2 are associated with metabolic syndrome in Asian population. Clin. Chim. Acta **411**(23–24), 2009–2013 (2010)
31. H. Tsukaguchi et al., Cloning and characterization of the urea transporter UT3: localization in rat kidney and testis. J. Clin. Invest. **99**(7), 1506–1515 (1997)
32. R.A. Fenton et al., Molecular characterization of a novel UT-A urea transporter isoform (UT-A5) in testis. Am. J. Physiol. Cell Physiol. **279**(5), C1425–C1431 (2000)
33. C. Shayakul et al., Molecular characterization of a novel urea transporter from kidney inner medullary collecting ducts. Am. J. Physiol. Renal Physiol. **280**(3), F487–F494 (2001)
34. G.S. Stewart et al., Acute regulation of mUT-A3 urea transporter expressed in a MDCK cell line. Am. J. Physiol. Renal Physiol. **292**(4), F1157–F1163 (2007)
35. X. Qian et al., Modulation of kidney urea transporter UT-A3 activity by alpha2,6-sialylation. Pflugers Arch. **468**(7), 1161–1170 (2016)
36. Y. Nakayama et al., The TonE/TonEBP pathway mediates tonicity-responsive regulation of UT-A urea transporter expression. J. Biol. Chem. **275**(49), 38275–38280 (2000)
37. C.A. Ecelbarger et al., Expression of salt and urea transporters in rat kidney during cisplatin-induced polyuria. Kidney Int. **60**(6), 2274–2282 (2001)
38. C.P. Smith et al., Characterization of a human colonic cDNA encoding a structurally novel urea transporter, hUT-A6. Am. J. Physiol. Cell Physiol. **287**(4), C1087–C1093 (2004)
39. A. McGrane, G. Stewart, Hyperosmolality regulates UT-A6 urea transporter expression in the Caco-2 cell line. Physiol. Rep. **4**(18), e12984 (2016)
40. B. Olives et al., Cloning and functional expression of a urea transporter from human bone marrow cells. J. Biol. Chem. **269**(50), 31649–31652 (1994)
41. C. Couriaud, P. Ripoche, G. Rousselet, Cloning and functional characterization of a rat urea transporter: expression in the brain. Biochim. Biophys. Acta **1309**(3), 197–199 (1996)
42. B. Yang et al., Urea-selective concentrating defect in transgenic mice lacking urea transporter UT-B. J. Biol. Chem. **277**(12), 10633–10637 (2002)
43. U.V. Berger, H. Tsukaguchi, M.A. Hediger, Distribution of mRNA for the facilitated urea transporter UT3 in the rat nervous system. Anat Embryol (Berl) **197**(5), 405–414 (1998)
44. D. Collins et al., Differential protein abundance and function of UT-B urea transporters in human colon. Am. J. Physiol. Gastrointest. Liver Physiol. **298**(3), G345–G351 (2010)
45. G.D. Hall et al., Novel urothelium specific gene expression identified by differential display reverse transcriptase-polymerase chain reaction. J. Urol. **175**(1), 337–342 (2006)
46. M.C. Hu et al., Massive reduction of urea transporters in remnant kidney and brain of uremic rats. Kidney Int. **58**(3), 1202–1210 (2000)
47. H. Inoue et al., Identification and characterization of a Kidd antigen/UT-B urea transporter expressed in human colon. Am. J. Physiol. Cell Physiol. **287**(1), C30–C35 (2004)
48. H. Inoue et al., Regulated expression of renal and intestinal UT-B urea transporter in response to varying urea load. Am. J. Physiol. Renal Physiol. **289**(2), F451–F458 (2005)
49. Y.S. Kwun et al., Immunohistochemical localization of urea transporters A and B in the rat cochlea. Hear. Res. **183**(1–2), 84–96 (2003)
50. N. Lucien et al., UT-B1 urea transporter is expressed along the urinary and gastrointestinal tracts of the mouse. Am. J. Physiol. Regul. Integr. Comp. Physiol. **288**(4), R1046–R1056 (2005)
51. N. Lucien et al., Antigenic and functional properties of the human red blood cell urea transporter hUT-B1. J. Biol. Chem. **277**(37), 34101–34108 (2002)

52. W.P. Prichett et al., Identification and cloning of a human urea transporter HUT11, which is downregulated during adipogenesis of explant cultures of human bone. J. Cell. Biochem. **76**(4), 639–650 (2000)
53. R.T. Timmer et al., Localization of the urea transporter UT-B protein in human and rat erythrocytes and tissues. Am. J. Physiol. Cell Physiol. **281**(4), C1318–C1325 (2001)
54. M.M. Trinh-Trang-Tan, J.P. Cartron, L. Bankir, Molecular basis for the dialysis disequilibrium syndrome: altered aquaporin and urea transporter expression in the brain. Nephrol. Dial. Transplant. **20**(9), 1984–1988 (2005)
55. Y. Xu et al., Endothelial cells of the kidney vasa recta express the urea transporter HUT11. Kidney Int. **51**(1), 138–146 (1997)
56. T.L. Pannabecker et al., Role of three-dimensional architecture in the urine concentrating mechanism of the rat renal inner medulla. Am. J. Physiol. Renal Physiol. **295**(5), F1271–F1285 (2008)
57. M.M. Trinh-Trang-Tan et al., UT-B1 proteins in rat: tissue distribution and regulation by antidiuretic hormone in kidney. Am. J. Physiol. Renal Physiol. **283**(5), F912–F922 (2002)
58. L. Wagner et al., Urea transporters are distributed in endothelial cells and mediate inhibition of L-arginine transport. Am. J. Physiol. Renal Physiol. **283**(3), F578–F582 (2002)
59. R.A. Fenton et al., Coordinated expression of UT-A and UT-B urea transporters in rat testis. Am. J. Physiol. Cell Physiol. **282**(6), C1492–C1501 (2002)
60. A. Ritzhaupt et al., Isolation of a RT-PCR fragment from human colon and sheep rumen RNA with nucleotide sequence similarity to human and rat urea transporter isoforms. Biochem. Soc. Trans. **26**(2), S122 (1998)
61. N.L. Simmons et al., Dietary regulation of ruminal bovine UT-B urea transporter expression and localization. J. Anim. Sci. **87**(10), 3288–3299 (2009)
62. G.S. Stewart et al., UT-B is expressed in bovine rumen: potential role in ruminal urea transport. Am. J. Physiol. Regul. Integr. Comp. Physiol. **289**(2), R605–r612 (2005)
63. P. Tickle et al., Novel bUT-B2 urea transporter isoform is constitutively activated. Am. J. Physiol. Regul. Integr. Comp. Physiol. **297**(2), R323–R329 (2009)
64. P.A. Ludden et al., Effect of protein supplementation on expression and distribution of urea transporter-B in lambs fed low-quality forage. J. Anim. Sci. **87**(4), 1354–1365 (2009)
65. K. Abdoun et al., Modulation of urea transport across sheep rumen epithelium in vitro by SCFA and CO2. Am. J. Physiol. Gastrointest. Liver Physiol. **298**(2), G190–G202 (2010)
66. D. Kim et al., Urea may regulate urea transporter protein abundance during osmotic diuresis. Am. J. Physiol. Renal Physiol. **288**(1), F188–F197 (2005)
67. L. Yu et al., Physiological functions of urea transporter B. Pflugers Arch. **471**(11–12), 1359–1368 (2019)
68. Levin, E.J. and M. Zhou, Structure of urea transporters. Subcell. Biochem., 2014. 73: p. 65–78, Springer Netherlands
69. R. Minocha, K. Studley, M.H. Saier Jr., The urea transporter (UT) family: bioinformatic analyses leading to structural, functional, and evolutionary predictions. Recept. Channels **9**(6), 345–352 (2003)
70. G. Stewart, The emerging physiological roles of the SLC14A family of urea transporters. Br. J. Pharmacol. **164**(7), 1780–1792 (2011)
71. C. Shayakul, B. Clémençon, M.A. Hediger, The urea transporter family (SLC14): physiological, pathological and structural aspects. Mol. Asp. Med. **34**(2–3), 313–322 (2013)
72. F. Sidoux-Walter et al., At physiological expression levels the Kidd blood group/urea transporter protein is not a water channel. J. Biol. Chem. **274**(42), 30228–30235 (1999)
73. Y. Nakayama et al., Cloning of the rat Slc14a2 gene and genomic organization of the UT-A urea transporter. Biochim. Biophys. Acta **1518**(1–2), 19–26 (2001)
74. R.A. Fenton et al., Structure and characterization of the mouse UT-A gene (Slc14a2). Am. J. Physiol. Renal Physiol. **282**(4), F630–F638 (2002)
75. C.P. Smith, R.A. Fenton, Genomic organization of the mammalian SLC14a2 urea transporter genes. J. Membr. Biol. **212**(2), 109–117 (2006)

76. S.M. Bagnasco et al., Differential expression of individual UT-A urea transporter isoforms in rat kidney. J. Am. Soc. Nephrol. **11**(11), 1980–1986 (2000)
77. T. Peng, J.M. Sands, S.M. Bagnasco, Glucocorticoids inhibit transcription and expression of the UT-A urea transporter gene. Am. J. Physiol. Renal Physiol. **282**(5), F853–F858 (2002)
78. R.A. Fenton, A. Shodeinde, M.A. Knepper, UT-A urea transporter promoter, UT-Aalpha, targets principal cells of the renal inner medullary collecting duct. Am. J. Physiol. Renal Physiol. **290**(1), F188–F195 (2006)
79. J.D. Klein, M.A. Blount, J.M. Sands, Urea transport in the kidney. Compr. Physiol. **1**(2), 699–729 (2011)
80. S.M. Bagnasco, The erythrocyte urea transporter UT-B. J. Membr. Biol. **212**(2), 133–138 (2006)
81. G. Rousselet, P. Ripoche, P. Bailly, Tandem sequence repeats in urea transporters: identification of an urea transporter signature sequence. Am. J. Phys. **270**(3 Pt 2), F554–F555 (1996)
82. N. Lucien et al., Characterization of the gene encoding the human Kidd blood group/urea transporter protein. Evidence for splice site mutations in Jknull individuals. J. Biol. Chem. **273**(21), 12973–12980 (1998)
83. R.A. Fenton et al., The murine urea transporter genes Slc14a1 and Slc14a2 occur in tandem on chromosome 18. Cytogenet. Cell Genet. **87**(1–2), 95–96 (1999)
84. Sands, J.M. and M.A. Blount, Genes and proteins of urea transporters. Subcell. Biochem., 2014. 73: p. 45–63, Springer Netherlands
85. R. Duchesne et al., UT-A urea transporter protein in heart: increased abundance during uremia, hypertension, and heart failure. Circ. Res. **89**(2), 139–145 (2001)
86. J.M. Terris, M.A. Knepper, J.B. Wade, UT-A3: localization and characterization of an additional urea transporter isoform in the IMCD. Am. J. Physiol. Renal Physiol. **280**(2), F325–F332 (2001)
87. J.M. Sands, R.T. Timmer, R.B. Gunn, Urea transporters in kidney and erythrocytes. Am. J. Phys. **273**(3 Pt 2), F321–F339 (1997)
88. F. Sebbane et al., The Yersinia pseudotuberculosis Yut protein, a new type of urea transporter homologous to eukaryotic channels and functionally interchangeable in vitro with the Helicobacter pylori UreI protein. Mol. Microbiol. **45**(4), 1165–1174 (2002)
89. M.A. Hediger et al., Structure, regulation and physiological roles of urea transporters. Kidney Int. **49**(6), 1615–1623 (1996)
90. D.L. Weeks et al., A H+-gated urea channel: the link between Helicobacter pylori urease and gastric colonization. Science **287**(5452), 482–485 (2000)
91. G. Sachs et al., Urea transport in bacteria: acid acclimation by gastric Helicobacter spp. J. Membr. Biol. **212**(2), 71–82 (2006)
92. P.M. Anderson, Glutamine- and N-acetylglutamate-dependent carbamoyl phosphate synthetase in elasmobranchs. Science **208**(4441), 291–293 (1980)
93. J. Hong et al., Carbamyl phosphate synthetase III, an evolutionary intermediate in the transition between glutamine-dependent and ammonia-dependent carbamyl phosphate synthetases. J. Mol. Biol. **243**(1), 131–140 (1994)
94. T.P. Mommsen, P.J. Walsh, Evolution of urea synthesis in vertebrates: the piscine connection. Science **243**(4887), 72–75 (1989)
95. C.M. LeMoine, P.J. Walsh, Evolution of urea transporters in vertebrates: adaptation to urea's multiple roles and metabolic sources. J. Exp. Biol. **218**(Pt 12), 1936–1945 (2015)
96. A.E. Allen et al., Evolution and metabolic significance of the urea cycle in photosynthetic diatoms. Nature **473**(7346), 203–207 (2011)

Chapter 2
Protein Structures of Urea Transporters

Mengyao Xiong, Shenming Huang, Jinpeng Sun, and Baoxue Yang

Abstract Urea transporters (UTs) facilitate the rapid transport of urea from the extracellular space to the intracellular space through a selective transport mechanism driven by urea concentration gradients. Advances in Cryo-electron microscopy and X-ray crystallography have enabled us to solve the homotrimer structures of UT-A and UT-B, which share a common feature comprising two homologous domains surrounding a continuous transmembrane pore, indicating that UTs transport urea via a channel-like mechanism. By analyzing the structures of ligand-protein complexes, results from molecular dynamics simulations, and functional data on urea analogues and small molecule permeation inhibitors, we can gain a deeper understanding of the conservation and specificity of the urea channel architecture, and clearly recognize how urea is transported by UTs and the mechanisms of small molecule inhibition. This will provide an important structural basis for drug design and development.

M. Xiong · B. Yang (✉)
State Key Laboratory of Vascular Homeostasis and Remodeling, Department of Pharmacology, School of Basic Medical Sciences, Peking University, Beijing, China
e-mail: baoxue@bjmu.edu.cn

S. Huang
Advanced Medical Research Institute, Cheeloo College of Medicine, Shandong University, Jinan, Shandong, China

State Key Laboratory of Bioactive Molecules and Druggability Assessment, Jinan University, GuangZhou, China

J. Sun (✉)
Advanced Medical Research Institute, Cheeloo College of Medicine, Shandong University, Jinan, Shandong, China

Department of Physiology and Pathophysiology, School of Basic Medical Sciences, State Key Laboratory of Vascular Homeostasis and Remodeling, Beijing Key Laboratory of Cardiovascular Receptors Research, Peking University, Beijing, China
e-mail: sunjinpeng@sdu.edu.cn

Structural Studies of Urea Transporters

Structural and Functional Insights into Urea Transporters

Within the lipid bilayer of cells, two kinds of key transmembrane proteins, namely "channels and transporters", play crucial roles in mediating the transport of substances across the cell membrane. Channels facilitate transport by forming continuous, semirigid pores spanning the bilayer, whereas transporters possess a central substrate-binding site that alternately exposes itself to either side of the bilayer through a series of conformational changes.

Proteins of the Urea Transporter (UT) family, which transport urea passively at high speeds of $10^4 \sim 10^6$ molecules per second, exhibit selectivity for urea and a few analogues, and reach saturation at high urea concentrations [1–4]. The amino acid sequences of UT family members share numerous characteristics, typically including 10 predicted transmembrane helices. UT-A1 may be composed of two tandem UT domains, possibly containing a total of 20 transmembrane helices. Notably, the regions corresponding to the first and last five transmembrane helices of each UT domain exhibit significant homology with each other, suggesting that the protein may have arisen from the duplication of an ancestral five-transmembrane helix protein [5]. Analysis of UT sequences has revealed a conserved motif LPXXTXPF every five transmembrane repeats, which is crucial for urea permeation [6]. This consistency with channel behavior implies that urea transporters are essentially urea channels.

To gain a deeper understanding of the functional properties of urea channels, atomic-level structural resolution is indispensable. This chapter discusses the structures of several members of the UT family, elucidating their permeation and selectivity mechanisms. Furthermore, the structures of UTs with inhibitors reveal the specific mechanism of small molecule inhibitors in their action process, providing valuable insights for us to understand and optimize the function of such inhibitors.

Determination of UT Structures Across Multiple Species

High-resolution structures are usually the basis for understanding the mechanisms of protein function. In this exploration process, X-ray crystallography, Cryo-electron microscopy (Cryo-EM), and Nuclear magnetic resonance (NMR) techniques play a crucial role. A high-resolution structure typically serves as an essential prerequisite for elucidating the mechanistic basis of a protein's function. Given the general stability and relative ease of crystallization exhibited by bacterial proteins, initial efforts to obtain the structure of UTs through X-ray crystallography predominantly centered on bacterial homologs. Bacteria can utilize urea for two purposes: firstly, as a nitrogen source essential for the synthesis of amino acids and

nucleotides, and secondly, in the specific case of enteric bacteria, to generate ammonia, serving as a protective buffer against the highly acidic environment of the gastrointestinal system [7, 8].

In 2002, Sebbane and colleagues cloned and sequenced a UT, yUT, from the enteric pathogen *Yersinia pseudotuberculosis*, demonstrating its ability to functionally complement UreI, a proton-gated urea channel derived from the ulcer-causing pathogen *Helicobacter pylori* [9]. Surprisingly, yUT possessed no detectable homology to UreI, but instead shared 21% ~ 25% sequence identity to the mammalian UTs. Subsequently, the crystal structure and cryo-EM structure of UreI in closed and open conformations were analyzed successively, revealing the fine gating mechanism of UreI [10, 11]. As more bacterial genomes became available, other bacterial UTs were identified and characterized, including ApUT from *Actinobacillus pleuropneumoniae* [12]. ApUT was the first UT to be purified in detergent and subsequently reconstituted into proteoliposomes, which were used in stopped-flow fluorimetry assays of urea permeation [13]. Research demonstrated that ApUT facilitated rapid, downhill flux of urea and exhibited sensitivity to inhibition by phloretin, a defining feature shared by mammalian UTs [14]. The findings indicated that bacterial UTs could serve as suitable model systems for conducting structural investigations of the UT family.

The initial crystal structure of a UT family member to be determined was that of dvUT, the homolog derived from the bacterium *Desulfovibrio vulgaris* [15]. Subsequently, the structure of bovine UT-B was determined by overexpressing the mammalian protein in insect cells, adding to the growing body of structural knowledge within the UT family [16]. As cryo-EM technology became increasingly mature and widely used, researchers have cleverly utilized detergents to successfully extract and purify overexpressed target proteins, such as human UT-A, from the cell membranes of insect cells or the human embryonic kidney cell line, HEK293F. Through this cutting-edge technique, researchers not only revealed the high-resolution cryo-EM structure of UT-A3 but also delved into the mechanism of how a selective inhibitor, UT-B$_{inh-14}$, effectively inhibits UT-B at the structural perspective [17].

Additionally, the discovery of phospholipid molecules closely related to the function of the urea channel significantly enriched our understanding of the biophysical characteristics of these channels [17]. Simultaneously, researchers focused on the UT-A family, successfully resolving the structures of multiple members of the UT-A family and their complexes with various small molecule inhibitors. These structures encompass UT in its resting state, urea binding state, and inhibitors binding state. Combining with the molecular dynamics simulation techniques, researchers further revealed the complex and subtle dynamic binding mechanisms between drugs and proteins, providing a solid structural basis and dynamic perspective for in-depth understanding of the urea channel transport mechanism and the mechanism by which small molecule drugs inhibit the urea channel, which might promote the development and optimization of treatment strategies for related diseases [18].

Structural Characteristics of the Urea Transporters

Topological Structures of UT-A and UT-B

Among the reported members of the UT-A family, the cryo-EM structures of UT-A2 and UT-A3 have been thoroughly studied. The cryo-EM structure of UT derived from *zebrafish*, zfUT, encoded by the *Slc14a2* gene, has also been unveiled [17, 18]. The structure of human UT-B was analyzed in detail after the structure of dvUT and bovine UT-B were elucidated. Consistent with UT-A2, UT-A3, and zfUT, these UT proteins exhibit a similarity protein backbone structure and share the same overall folding pattern [15–17]. These proteins form trimers with parallel orientations within the membrane, and there is a large cavity located at the trimer interface (Fig. 2.1a–d). Each UT unit is composed of 10 complete transmembrane helices and 2 half-helices along the axis of the urea transport channel, designated as 1a-5a, 1b-5b, Pa and Pb, and their urea transport channels are tightly enclosed by helices from both symmetric halves, including 3a, 3b, 5a, 5b, Pa and Pb. Pa and Pb are designated as "re-entrant" helices, meaning they constitute segments of structures that initiate their entry into the membrane from one side, penetrate only partially through the bilayer, and subsequently re-exit on the same side. These two re-entrant helices in the UT structures extend roughly halfway into the membrane and are tilted at approximately 45° relative to the bilayer plane. Assuming that the UT proteins obey the "positive-inside" rule [19], it can be inferred that the N-terminal and C-terminal of each UT subunit are oriented towards the intracellular side (Fig. 2.2). This topology is consistent with the location of known sites of posttranslational modifications, notably including N-glycosylation sites located on the extracellular
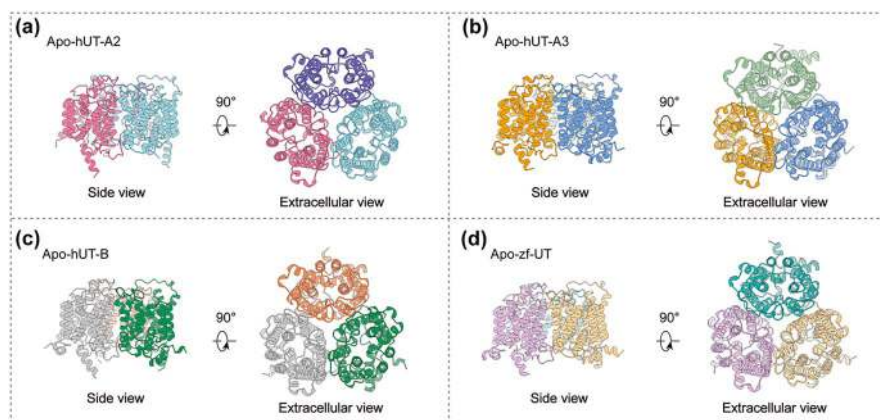
Fig. 2.1 Structural representation of hUT-A2, hUT-A3, hUT-B and zf-UT. (**a**–**d**) Structural representations of apo-hUT-A2 homotrimer (**a**), apo-hUT-A3 homotrimer (**b**), apo-hUT-B homotrimer (**c**) and apo-zf-UT homotrimer (**d**), from the side view (left) and the extracellular view (right), respectively. (Data cited from ref. [18])
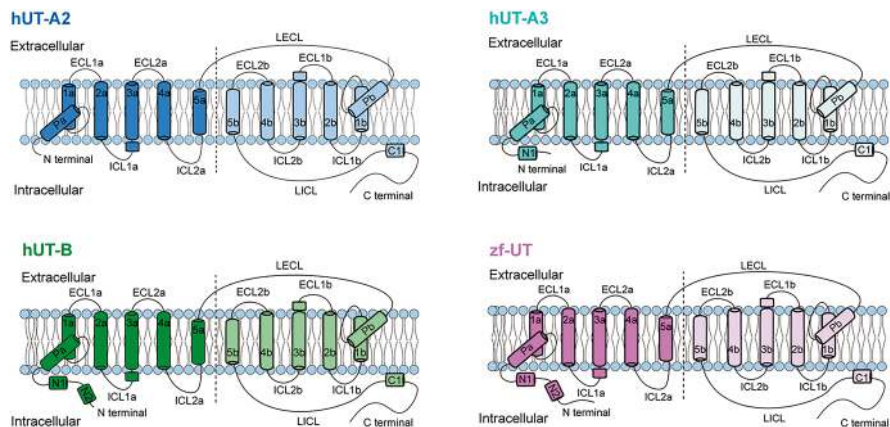
Fig. 2.2 Diagram of the topology of transmembrane helices of hUT-A2, hUT-A3, hUT-B and zf-UT. Oriented with the intracellular side on bottom, equivalent helices between the two homologous repeats are marked with a and b. ECL indicates the extracellular loop and the ICL indicates the intracellular loop. LECL (long extracellular loop). LICL (long intracellular loop). (Data cited from ref. [18])

loop between the fifth and sixth transmembrane helices of both UT-A and UT-B [20, 21], as well as phosphorylation sites on the N-terminus of UT-A1 and UT-A3 [22].

The first five and last five transmembrane helices in the UT protomer each form a separate domain with an approximate semicircular shape, known as the a-half and b-half, are cleverly linked by a long extracellular loop (LECL) (Fig. 2.2), and the two domains also each contain one re-entrant helix. Consistent with their sequence homology [5], the two domains are similar and can be aligned with a root mean square deviation (RMSD, a measure of the average distance between equivalent atoms in two structures) of less than 1 Å. Because their topology is inverted with respect to each other, the two repeats give the UT fold twofold pseudosymmetry along an axis parallel to the plane of the membrane. Inverted internal structural repeats are found frequently in membrane proteins and have been observed previously in a number of channel and transporter folds [23–29]. The three-dimensional structures of UT-A and UT-B are similar, as their urea transport channels are tightly enclosed by helices from both symmetric halves, including 3a, 3b, 5a, 5b, Pa, and Pb.

Structural Conservation and Differences Between UT-A and UT-B

Mammals have two UT genes that, via alternative splicing, are used to construct different proteins with at least five unique transmembrane domains. The bovine UT-B and dvUT have only approximately 33% sequence identity, and yet the RMSD between their transmembrane helices is less than 1 Å. UT-A and UT-B family members exhibit a high degree of structural similarity, both being homotrimers. Each UT

channel is composed of 10 complete transmembrane helices and 2 half-transmembrane helices that are symmetrically arranged along the axis of the urea transport pathway, responsible for the transport of urea.

Comparative studies show that the basic features of the core hydrophobic regions of UT protomers, including the ten transmembrane helix topology and the location of the permeation pathway, are conserved across the UT family [18]. Channel proteins typically have close interactions with lipid molecules, which assist in facilitating the functional roles of the channel proteins. These lipid molecules help to enhance the stability of the proteins within the cell membrane, increase enzymatic activity, and maintain osmotic pressure gradients, among other functions [30–35].

The cryo-EM maps of both HsUT-A and HsUT-B structures reveal distinct characteristics that are in harmony with phospholipids. These discernible features are located on the extracellular side of the transmembrane surface, with one notable feature residing between the subunits. MS analysis identified specific phospholipid molecules associated with UT-B, including phosphatidylethanolamines (PEs) and phosphatidylinositols (PIs), which may contribute to the stability of the trimeric structure or confer selectivity in the permeation of urea and other similar solutes. Further investigation is warranted to elucidate whether lipid molecules are present within the central pore of the trimer, potentially influencing its functional properties.

The soluble regions of various mammalian UT proteins exhibit considerable variability. For example, the UT-A isoforms UT-A1 and UT-A3 have an N-terminal domain of approximately 90 residues, which is predicted to be unstructured. In contrast, the N-terminus of UT-B is relatively short, and UT-A1 has an intracellular linker over 100 residues long connecting the two UT domains. The N-terminus of hUT-B is similar to that of zf-UT, and compared to hUT-A2, it contains two additional helical structures, named N1 and N2 respectively (Fig. 2.2). Compared to the corresponding position of UT-A2, the C1 helix of UT-B rotates outward by approximately 11°, the intracellular terminal of 4a, LECL, and long intracellular loop (LICL) shift inward. Notably, despite the commonalities between the different UT-A subtypes, significant structural differences exist among UT-A family members, primarily focused on the N-terminal, C-terminal, LECLs, and LICLs. Specifically, compared to hUT-A2, hUT-A3 possesses an additional α-helix at its N-terminus, and its C1 helix is one helical turn shorter, rotated outward by approximately 8°. Additionally, when compared to hUT-A2, the C1 helix of zf-UT is rotated outward by about 6°, accompanied by inward shifts of both the LECL and LICL [18]. Post-translational modifications in these regions likely account for differences in how the mammalian UT isoforms are regulated and trafficked [36].

The surface negative charge of UT-A3 is much greater than that of UT-B family members. HsUT-A3 shows significantly more negative surface charge on its extracellular side compared to members of the UT-B family, especially for dvUT [17]. While the individual subunits of different UT proteins likely have highly similar folds, the oligomeric state among all homologs remains less definitive.

Native gel electrophoresis and a low-resolution projection map from 2D crystals suggested that the bacterial homolog ApUT forms a dimer [13]. Because the UT-A1 isoform contains two tandem UT domains, it is unable to form a three-domain

homotrimer similar to UT-B. Furthermore, the formation of a heterotrimer between UT-A1 and UT-B, or any of the single-domain UT-A isoforms, appears improbable due to their spatial segregation within renal tissues. UT-A3 and UT-A1 are both expressed in the epithelia of the inner medullary collecting ducts, but UT-A1 is localized to the apical membrane [37], while UT-A3 is localized to the basolateral membrane [38]. One possibility is that UT-A forms a higher-order complex than UT-B, such as a hexamer. Because the permeation pathway is enclosed within a single protomer, differences in the number of subunits may not have a significant effect on the function of the protein. Alternatively, urea binding to dvUT exhibits a Hill coefficient of ~3 [15], which could be indicative of strong positive cooperativity between the different subunits. Additional structural studies on the UT-A homologs will likely be necessary to resolve this issue.
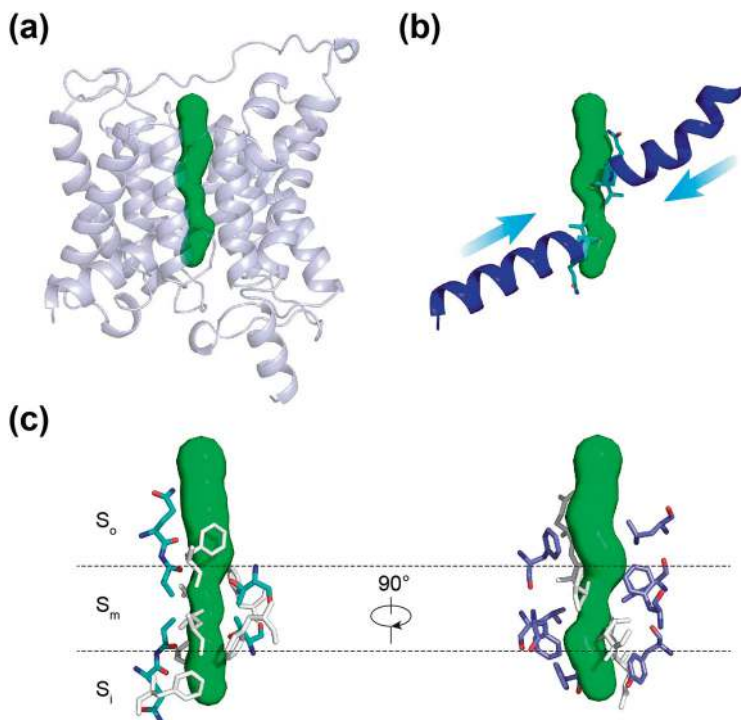
Features of the Permeation Pathway

The clear perspectives of Fig. 2.1 reveal the unique architecture of the UT trimer at the convergence center of its three subunits. A significant large cavity is highlighted in the core region, which is a distinctive feature of the UT trimer. Although this cavity is located at the center, it is surrounded by hydrophobic residues on both sides of the membrane. It is likely that some lipid molecules are also filled inside the cavity, forming a stable structure. Further observation of the UT trimer reveals that each subunit contains a channel, a solvent-accessible pore that spans from one side of the bilayer to the other (Fig. 2.3a).

Through sequence alignment analysis, the amino acids in these channels have been confirmed to be composed of a series of highly conserved residues that are closely arranged. These conserved residues have remained unchanged throughout the long evolutionary process, strongly suggesting their core role in the function of the UT trimer. It is likely that they serve as important gateways for the transport of urea and other small molecules across cellular membranes. By delving into these intricate structural features, we not only gain a more comprehensive understanding of the specific mechanism of the UT trimer in cellular membrane transport but also provide valuable structural foundations for the development of novel drugs targeting the UT trimer.

The UT pore can be divided into three regions: two hydrophilic vestibules that form the entrances to the pore on either side, which are wide enough for an entering urea molecule to retain its hydration waters, and a narrower region approximately 15 Å long at the center of the pore, lined with highly conserved residues. This constricted region, referred to as the selectivity filter, ranges in diameter from ~1 to 3 Å across and is roughly rectangular in cross section. The pseudosymmetry axis of the protein runs directly through the center of the pore. The structural elements forming the four walls of the pore include the two pore helices (Fig. 2.3b), the third transmembrane helices from each pseudosymmetry repeat (T3a and T3b), and the fifth transmembrane helices from each repeat (T5a and T5b). These last two helices are

Fig. 2.3 The urea transporter permeation pathway. (**a**) The central pore in a bUT-B protomer is shown as a green surface. Residues lining the pore are shown as sticks. (**b**) The locations of the pore helices are shown relative to the UT pore. (**c**) The UT selectivity filter shown from two orientations, divided into the So, Sm, and Si regions. Conserved residues capable of forming hydrophilic (left) or hydrophobic (right) interactions with ligands within the filter are highlighted with color. (Data cited from ref. [16])

actually shorter than the full length of the membrane, so that the regions forming the selectivity filter are unwound and expose backbone elements to the lumen of the pore. In the UT-A structure, the urea transport channel connecting the extracellular section to the intracellular region is composed of helices 3a, 3b, 5a, 5b, Pa and Pb. This region also corresponds to the location of the conserved signature motifs [6].

The selectivity filter can be further subdivided into outer, middle, and inner regions, referred to as So, Sm, and Si (Fig. 2.3c). So and Si are related by the pseudosymmetry axis and have a similar architecture. One wall of the pore at these sites is formed by a row of oxygen atoms contributed by backbone carbonyls and side chains located on the C-terminal ends of the pore helices, which point directly into the selectivity filter. The ability of these atoms to act as hydrogen bond acceptors would therefore likely be strengthened by the helix dipole moments. These oxygen atoms are flanked by hydrophobic residues from T3a and T3b, which form the two perpendicular walls of the selectivity filter. The Sm site is the narrowest region of the pore and is hydrophobic except for a pair of threonine residues from the conserved LPXXTXPF motifs on the N-terminal ends of T5a and T5b. These residues form a hydrogen bond that crosses the center of the selectivity filter.

## Structural Basis of Permeable Urea and Selective Inhibitors

The structures of UT-A and UT-B series proteins have laid a solid foundation for the in-depth analysis of the binding and permeation mechanisms of urea and its analogs. Notably, in the structures of hUT-A2 and zf-UT, urea molecules and their paired water molecules exhibit clear density maps. By further integrating molecular dynamics simulation studies, we can more thoroughly elucidate the specific mechanisms of UTs in the process of urea transport, thereby deepening our understanding of their physiological functions and pathological implications. Notably, selective inhibitors of UTs have demonstrated significant potential as high-efficiency diuretic drugs. Through in-depth investigations into the structures of small molecule compounds in complex with UT-A and UT-B, we can precisely reveal the mechanisms of these inhibitors. This not only provides valuable structural insights for designing novel inhibitors with higher selectivity and lower side effects but also opens up new avenues for drug discovery and optimization.

Potential Urea Permeation Mechanism of UT-A and zf-UT

There are two urea-binding pockets in the hUT-A2 channel, one in the extracellular urea binding pocket (EUBP) and the other in the cytoplasmic urea binding pocket (CUBP), and the two urea molecules are separated by about 10 Å. EUBP is composed of 7 residues, and CUBP is composed of 5 hydrophobic residues and 2 polar residues (Fig. 2.4a). Urea molecules in EUBP and CUBP form a symmetrical polar interaction and hydrophobic accumulation. This process involves the interaction of urea molecules with specific amino acid sites in the hUT-A2 protein channel.

First of all, free urea molecules in solution are captured by the flexible side chain of Q231[Pb] in the extracellular region (So region). The urea molecules are then brought into the So region of the transport channel by the rotation of the side chain of Q231[Pb] and coordinated by water molecules. At this stage, the two basic nitrogen atoms of the urea molecule form a salt bridge with the main chain oxygen atoms of Q231[Pb] and V232[Pb] and a hydrogen bond with the hydroxyl group of T338[5b].

Then, the flexibility of the side chains of L131[3a] and F287[3b] and hydrogen bond transfer mediated by the side chain of T338[5b] pull the urea molecules into the Sm region. The Sm region of the UT transport channel constitutes a comparatively confined cavity consisting of three residue pairs, namely, T176[5a]-T338[5b], L127[3a]-L291[3b], and F179[3a]-F341[3b] (Fig. 2.4b). The analysis indicated that the side chains of T176[5a] and T338[5b] underwent an another rotation of approximately 40°. Subsequently, the side chains of T176[5a]-T338[5b] and F179[3a]-F341[3b] underwent rearrangement, facilitating the passage of urea molecules through the Sm region. Urea molecules formed hydrogen bonds with the hydroxyl group on the side of T338[5b], as well as the carbonyl group on the side chain of T176[5a] and the main chain of V232[Pb] (Fig. 2.4c). Moreover, the rearrangement of the configurations of the residue pairs L127[3a]-L291[3b] and F179[3a]-F341[3b] may allow the entry of urea molecules.
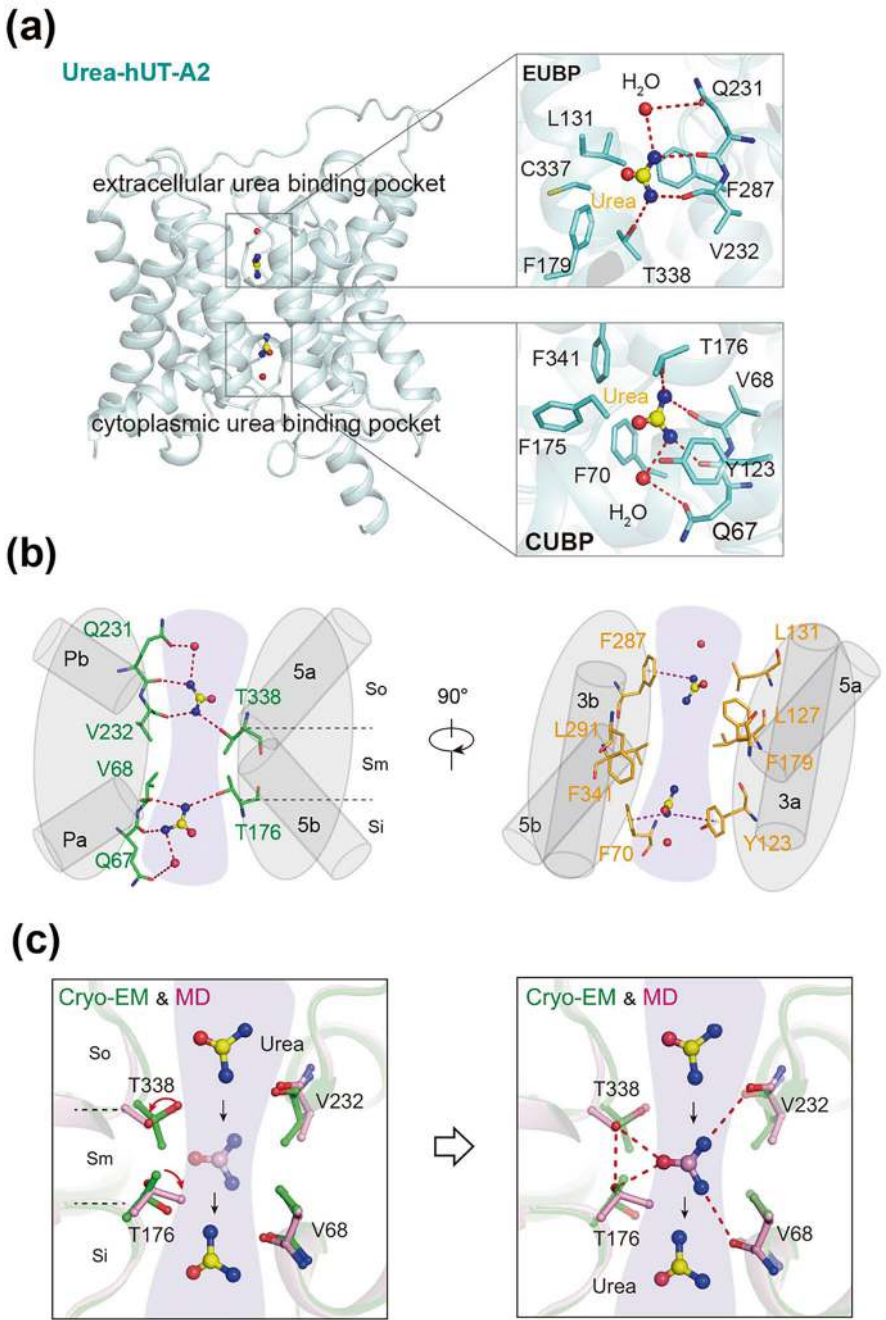
Fig. 2.4 Urea permeation mechanism of the human urea transporter UT-A2. (**a**) The extracellular urea binding pocket (EUBP) and the cytoplasmic urea binding pocket (CUBP) of hUT-A2.

Finally, the movement of the T176[5a] side chain may transfer the urea molecules from the Sm region to the Si region, where they may adopt an interaction pattern that mirrors the symmetry observed in the So region, because the distribution of amino acids in the So and Si regions of the channels is relatively symmetrical [15, 16]. Consequently, the urea bound to the Si region is released into the cytoplasm, marking the completion of its transport from the extracellular side to the intracellular side.

In comparison to the cryo-EM structure of urea-hUT-A2, the structure of urea-zf-UT exhibits an additional EM density connected to the "So" region on the extracellular side, which is named the "So'" region, a cavity surrounded by the side chains of F135[3a], L284[3b] and P335[ECL3b] (Fig. 2.5a, b). The molecular dynamics simulations indicated that F135[3a] and L284[3b] form transient interactions with urea during urea transport. On the intracellular side, the EM density of zf-UT-urea enabled the identification of two additional urea binding sites, Si' and Si", which are linked to the Si region through an "L"-shaped configuration. Specifically, urea in the Si' region contacts F300[3b] and L363[LICL], and urea in the Si" region interacts with Y121[3a] and S160[4a] (Fig. 2.5a, c). Urea showed similar interaction modes in the So and Si regions to those in the urea-hUT-A2- structure, including the polar network constituted by the Q231[Pb]-T338[5b]-T176[5a]-Q67[Pa] motif and hydrophobic interactions involving L131[3a], F287[3b], F70[Pa] and Y123[3a]. These findings indicate that a common mechanism and conserved motifs govern urea transport across UTs from different species.

Interactions with Urea and Urea Analogs of UT-B and dvUT

Structures have been solved for dvUT bound to the urea analog 1,3-dimethylurea (DMU) [15, 39] and bovine UT-B bound to selenourea [16] (Fig. 2.6a). Both structures contain two molecules of the substrate bound to the selectivity filter, one in So and the other in Si (Fig. 2.6b, c). Both DMU and selenourea are oriented with their amide nitrogens positioned to form hydrogen bonds with the oxygen atoms at the ends of the pore helices. In the DMU-bound structure, ordered water molecules are also visible forming hydrogen bonds with the oxygen atoms on both DMU molecules, suggesting that the substrate is not fully desolvated in these regions. Comparison of the binding sites of the two substrates shows that their locations are


Fig. 2.4 (continued) The key residues interacting with urea in EUBP and CUBP are shown as sticks while the urea and water molecules are displayed as stick-balls and red balls, respectively. The H-bond is shown as red dash line. (**b**) The hydrogen bonding and hydrophobic interactions of urea in the urea transport channel of hUT-A2. The black dashed lines were used to separate So, Sm and Si regions of the channel. The H-bond is shown as red dashed line and the cation-π interaction are shown as purple dashed lines. (**c**) Metadynamics simulations elucidate the passage of urea through the Sm region. This process involves a rotation of the side chains of T176[5a] and T338[5b], facilitating the rearrangement of T176[5a]-T338[5b] side chains. Notably, hydrogen bond formations between urea and specific residues, including T338[5b] and T176[5a], are depicted. The H-bond is shown as red dashed line. (Data cited from ref. [18])
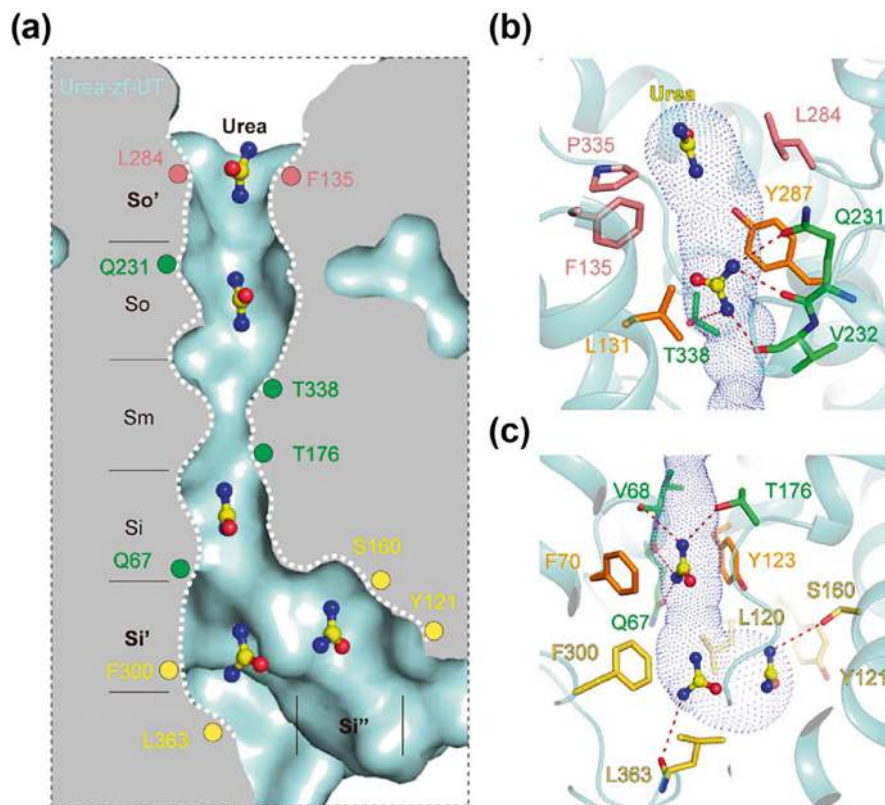
Fig. 2.5 Structural analysis of urea transport in zf-UT. (**a**) The location of the urea molecules is modeled into six regions shown as So′, So, Sm, Si, Si′ and Si″ in the zf-UT channel surrounding with presentation of key interacting residues. The urea transport channel of zf-UT is depicted by a white dotted line with the inner urea molecules displayed as stick-balls. The conserved Q^{Pb}-T^{5b}-T^{5a}-Q^{Pa} motif is shown as green dots. (**b** and **c**) The interactions between urea and the key residues in the zf-UT urea transport channel is shown as blue dots. In the extracellular side of the channel (**b**), the urea molecules form H-bond with side chains of $Q231^{Pb}$ and $T338^{5b}$, and main chain of $V232^{Pb}$. When in the intercellular side (c), the urea molecules engage H-bonds with side chains of $Q67^{Pa}$ and $T176^{5a}$, and the main chain of $V68^{Pa}$, $L363^{LICL}$. The H-bonds are shown as red dashed line. (Data cited from ref. [18])

not exactly equivalent: DMU bound to So is positioned to potentially form hydrogen bonds with the first and second oxygen atoms, while selenourea is positioned to interact with the second and third. Similarly, the binding sites are slightly offset in Si as well. This suggests a mechanism for how the selectivity filter could continuously provide at least two hydrogen bonds to a urea molecule migrating stepwise through the So and Si sites.

No electron density corresponding to substrates was observed in the Sm region; however, it remained ambiguous whether this was due to the absence of a stable binding site in this region, or because the larger, impermeable DMU and selenourea
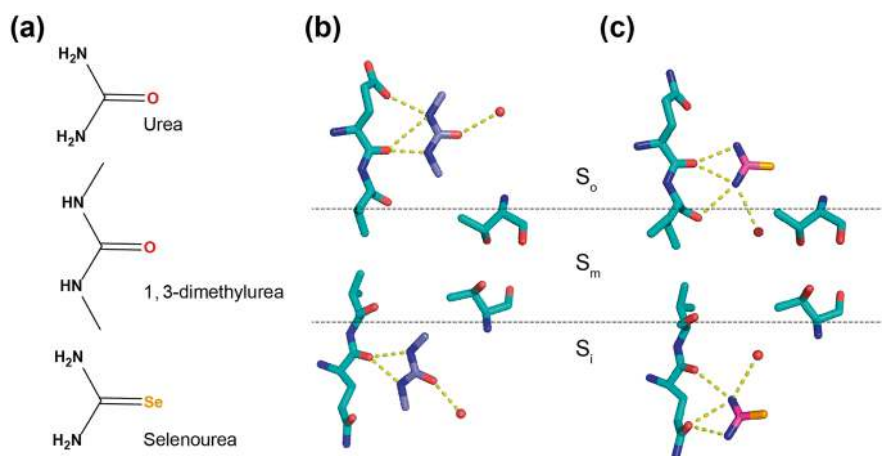
Fig. 2.6 Ligand-binding sites in the urea transporter selectivity filter. (**a**) The chemical structures of urea, dimethylurea (DMU), and selenourea. (**b, c**) The locations of DMU molecules in the dvUT structure (**b**) and selenourea molecules in the bUT-B structure (**c**) are shown relative to the oxygens lining one side of the selectivity filter. The central threonines in the Sm site and ordered water molecules within hydrogen bonding distance to the bound substrates are shown as well. (Data cited from ref. [15, 16])

analogs could not enter the narrowest region of the pore. To gain additional information on the interaction between urea and the pore, particularly in the Sm region, molecular dynamics simulations were carried out on bovine UT-B and used to calculate a potential of mean force (PMF) for urea permeation, representing the change in the total energy of the system as a function of the position of urea in the pore [16].

Multiple local energy minima were observed in the So and Si sites, indicating that these regions contain a series of low-affinity urea-binding sites. These minima agree well with the observed positions of urea analogs in the crystal structures. Also, in agreement with the ligand-bound crystal structures, urea in the So and Si sites was still partly solvated and oriented in alignment to the pore helix dipoles. Upon entering the Sm site, urea was completely stripped of hydration waters and the PMF exhibits a large energy barrier, with a maximal ΔG of ~5 kcal/mol. No conformational changes other than thermal fluctuations were required for urea to pass completely through the pore, confirming that UTs are channels, not transporters.

Based on calculation and modeling combined with the Monte Carlo (MC) method, the urea flux in dvUT, the combination of equilibrium urea and dvUT, and the process of urea substitution by DMU in dvUT were simulated [39]. Of the different UTs, the selectivity of UT-B has been the most thoroughly characterized due in part to the early development of assays for measuring substrate flux through UT-B in erythrocytes [40–42]. This approach has been used to test the selectivity of UT-B with a large number of urea analogues [4].

The channel can permeate formamide and acetamide at rates close to those for urea, indicating that loss or substitution of one amide nitrogen is tolerated. Transport

is significantly decreased by changes to the substrate that increase the size and decrease the strength of potential hydrogen bonds, such as substitution of the oxygen atom with sulfur in thiourea, or N-methylation of the amides in DMU; however, both of these compounds are effective inhibitors of UT-B.

The structural data discussed above provide a rationale for this behavior: DMU and thiourea are able to compete with urea for binding to the So and Si sites but have difficulty permeating through the constricted Sm site. In comparison with UT-B, functional data on UT-A are relatively scarce; however, transport through mouse UT-A2 and UT-A3 has been measured in vesicles derived from oocyte plasma membranes [1]. Both homologs exhibited higher selectivity than UT-B and did not permeate any of the tested urea analogs, including formamide and acetamide. The residues forming the selectivity filter in both UT-A domains and UT-B are similar, and the structural basis for this difference in selectivity is not yet understood.

Structural Basis of the Selective Inhibitors of UT-A

Competitive inhibitors competitively bind to the active site, competing with substrates [43]. 25a is a synthetic competitive inhibitor of UT with potency in the micromolar range [44]. In the cryo-EM structure of 25a-hUT-A2, the furan ring of 25a occupies the EUBP and CUBP regions of hUT-A2. This is achieved through a variety of polar and hydrophobic interactions with amino acid residues in the EUBP pocket, including T338[5b], Q231[Pb], L131[3a], F179[5a], V323[4b], F287[3b], and C337[3b]. The interaction mode of 25a with CUBP is symmetrical to that with EUBP. Notably, 25a also occupies two additional pockets on the extracellular side and intracellular side, which are designated as the extracellular blocker binding pocket 1 (EBBP1) and cytoplasmic blocker binding pocket 1 (CBBP1)—on both sides of the cellular membrane. The benzene ring of 25a engages in π-π stacking interactions with F135[3a] in the EBBP or with F120[3a] and F300[3b] in the CBBP, the terminal end of 25a reached the confines of the outer EBBP, touching L202[LECL], A326[4b], and P336[ECL3b], while within CBBP, it encounters a more spacious environment by engaging L363[LICL] (Fig. 2.7). These findings were supported by functional experiments following mutations. These structural and mutational analyses indicated that 25a, as a urea channel blocker, competes with urea to form hydrogen bonds with the conserved Q[Pb]-T[5b]-T[5a]-Q[Pa] motif necessary for urea transport, thereby competitively inhibiting UT activity by binding to both ends of the transmembrane transport channel (EUBP and CUBP) [18].

The aminothiazolone derivative UTA$_{inh}$-B3 (ATB3) is a competitive inhibitor of hUT-A2, with an inhibitory effect approximately six-fold stronger than that on UT-B [45]. In the cryo-EM structure of ATB3-hUT-A2, the benzene ring and thiazole ring of ATB3 have some shifts compared to 25a, forming a new binding pocket composed of F135[3a], L202[LECL], F282[3b], and L284[3b], named EBBP2, a new interaction is formed between ATB3 and F282[3b]. In the EUBP, the nitrogen atoms and carbonyl group of the thiazole ring of ATB3 engage in hydrogen bonding and polar
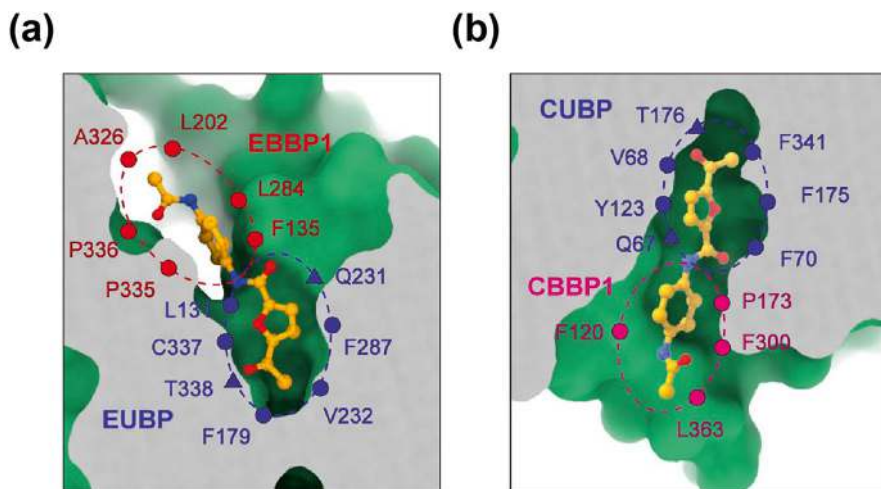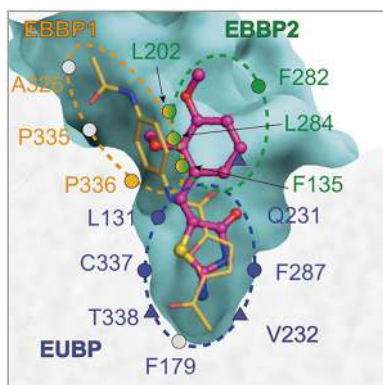
Fig. 2.7 The cutaway view of binding pockets of 25a in extracellular side or cytoplasmic side. (**a**) In the extracellular side, the 25a occupied two subpockets, the EBBP1 and EUBP, represented by red or blue dashed line, respectively. (**b**) On the intracellular side, the 25a occupied CBBP1 (violet) and CUBP (blue). Residues forming polar interactions or hydrogen bonds with 25a are depicted using triangles. Residues only forming hydrophobic or van der Waals interactions are depicted as solid round circles. The 25a is represented by stick-ball and the hUT-A2 is represented by surface. (Data cited from ref. [18])

interactions with Q231[Pb] and T338[5b], the ortho-methoxy group of ATB3 forms hydrophobic interactions with L284[3b] and P336[ECL3b] in EBBP1, while the benzene ring and the meta-methoxy group form π-π stacking and hydrophobic interactions with F135[3a], L202[LECL], F282[3b], and L284[3b] in EBBP2 (Fig. 2.8). On the cytoplasmic side, the thiazole ring is 1.5 Å away from the channel's Sm region and forms polar interactions with Q67[Pa] and T176[3a] in CUBP.

Remarkably, the thiazole ring of ATB3 forms extensive polar interactions with the "Q[Pb]-T[5b]-T[5a]-Q[Pa]" motif in the UT channel, which is crucial for UT transport. Therefore, the mechanism of ATB3 inhibiting UT may be based on competing with urea for interactions with the "Q[Pb]-T[5b]-T[5a]-Q[Pa]" motif [18].

Noncompetitive inhibition, a type of allosteric regulation, is a distinct type of enzyme inhibition wherein the inhibitor binds to an allosteric site rather than the substrate binding site, diminishing the enzyme's efficacy [46]. Research has reported that UTAinh-F11 (CF11) was an uncompetitive inhibitor of UT-A, with an EC$_{50}$ value for UT-A1 approximately 10 times better than that for UT-B [47]. In contrast, in the cryo-EM structure of CF11-hUT-A2, the presence of CF11 is observed only on the intracellular side of hUT-A2, where CF11 is located within a cavity surrounded by helices 3a-4a, Pa, ICL3a, and LICL (Fig. 2.9a). The methoxy group of CF11 inserts into the CUBP, but does not interact with T176[5a], V68 [Pa], and F341 [3b]. Instead, it forms hydrophobic interactions with Q67[Pa] and F70[Pa]. Therefore, CF11 functions differently from competitive inhibitors 25a and ATB3, as it cannot compete with urea molecules for the polar interactions formed by the

Fig. 2.8 The cutaway view of the binding pockets of ATB3 in extracellular side. The ATB3 occupied three subpockets on the extracellular side, the EBBP1, EBBP2 and EUBP, represented by orange, green and blue dashed line, respectively. Residues forming polar interactions or hydrogen bonds with ATB3 are depicted using triangles. Residues only forming hydrophobic or van der Waals interactions are depicted as solid round circles. Additionally, the residues F135, L202, and L284 are shared by both EBBP1 and EBBP2. The 25a and ATB3 were represented by orange stick and magenta stick-ball, respectively. The hUT-A2 is represented by surface. (Data cited from ref. [18])
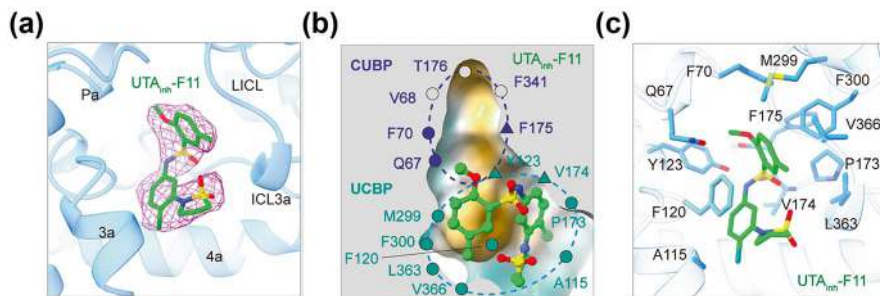

Fig. 2.9 The structural characterization of Compound UTAinh-F11 binding to hUT-A2. (**a**) The cryo-EM density of CF11 (red mesh) contoured at 4.0σlevel is located in a cavity surrounded by helices 3a-4a, Pa, ICL3a, and LICL. (**b**) The cutaway view of the binding pocket of CF11. The CUBP and the UCBP are represented by blue and green dashed lines, respectively. Residues forming polar interactions or hydrogen bonds with CF11 are depicted using triangles. Residues only forming hydrophobic or van der Waals interactions are depicted as solid round circles. The CF11 is represented by stick-ball and the hUT-A2 are represented by surface. (**c**) The key residues of hUT-A2 in CF11 binding pocket are shown by blue sticks. The CF11 is represented by green sticks. (Data cited from ref. [18])

Q231[Pb]-T338[5b]-T176[5a]-Q67[Pa] motif within CUBP. The specific residues containing the uncompetitive inhibitor CF11 are named the uncompetitive binding pocket (UCBP). Within the UCBP, CF11 forms hydrophobic interactions with A115[3a], M299[3b], L363[LICL], and V366[LICL]. The two benzene rings of CF11 form π-π stacking interactions with F120[3a], while the nitrogen-sulfur atoms connecting the two

benzene rings form hydrogen bonds with the hydroxyl group of Y123[3a] and the main chain of V174[5a]-F175[5a]. CF11 also forms π-π stacking interactions with F300[3b] (Fig. 2.9b,c). These observations indicate the uncompetitive inhibition mode of CF11, where urea can still bind to the extracellular side of UT-A2 but cannot be transported to the intracellular side [18].

The 8-hydroxyquinoline derivative UTAinh-A2 (HQA2) acts as a noncompetitive inhibitor of UT-A, exhibits over ten-fold selectivity compared to its interaction with UT-B [45]. In the HQA2-hUT-A2 complex structure, HQA2 binds only to the extracellular side of hUT-A2, with the binding site formed by helices 3a, 3b-4b, and Pb, as well as LECL and ECL3b (Fig. 2.10a). Other competitive and uncompetitive inhibitors often bind perpendicular to the extracellular side of the UT, whereas HQA2 exhibits a novel binding mode—parallel to hUT-A2. Notably, the benzene ring of HQA2 is embedded in EBBP1 and EBBP2. Within EBBP1–2, the benzene ring of HQA2 forms a stable π-π stacking interaction with F135[3a], and it also forms hydrophobic interactions with L202[LECL], L284[3b], P335[ECL3b], and P336[ECL3b]. Specifically, the methoxy group in the benzene ring of HQA2 extends into the EUBP, forming a hydrogen bond with the side chain of Q231[Pb], without occupying the entire EUBP or CUBP. Importantly, HQA2 also occupies a unique side pocket— the SCG pocket, which is composed of 6 residues with small side chains. Within the SCG pocket, the hydroxyquinoline moiety of HQA2 forms hydrogen bonds and van der Waals interactions with residues such as S279[3b], T275[ECL2b], C285[3b], G322[4b], and A323[4b], further stabilizing the binding state of HQA2 (Fig. 2.10b, c). The above structural characteristics not only reveal the deep mechanism of HQA2's noncompetitive inhibition of urea transport but also suggest the potential application
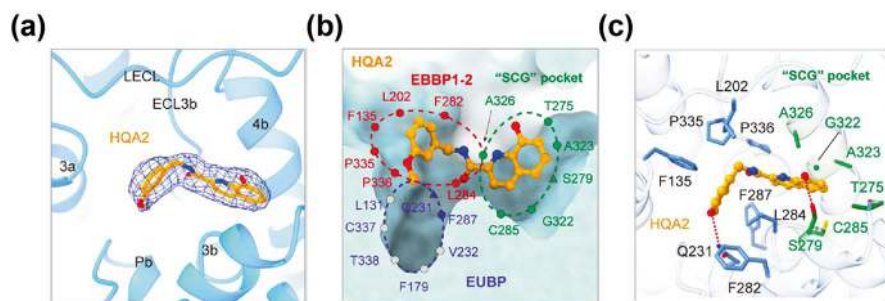
Fig. 2.10 Mechanism of noncompetitive blocking hUT-A2 by HQA2. (**a**) The cryo-EM density (blue mesh) of HQA2 at the 4.0 σ contour level is located in the cavity surrounded by helices 3a, 3b-4b, and Pb, and the LECL, and ECL3b. (**b**) The cutaway view of the binding pocket of HQA2 (orange stick-ball). The EUBP, EBBP1–2 and the noncompetitive "SCG" pocket are represented by blue, red and green dashed lines, respectively. Residues forming polar interactions or hydrogen bonds with HQA2 are depicted using triangles. Residues only forming hydrophobic or van der Waals interactions are depicted as solid round circles. The HQA2 are represented by orange stick-ball and the hUT-A2 are represented by surface. (**c**) The key residues of the HQA2 binding pocket of hUT-A2 are represented by sticks and the residues involved in the "SCG" pocket are colored green. The HQA2 is represented by orange stick-ball. The H-bond is shown as red dashed line. (Data cited from ref. [18])

prospects of the SCG pocket. Given that the region where the SCG pocket is located is completely independent of the urea transport channel of hUT-A2, it may serve as an allosteric pocket, regulating the urea transport process mediated by UT through ligand binding, providing important clues for the development of novel UT inhibitors [18].

Structural Basis of the Selective Inhibition of UT-B

UTBinh-14 is a highly selective inhibitor of UT-B, with selectivity over UT-A thousands of times [48]. In the complex structure of UTB inh-14 and HsUT-B, UTB inh-14 primarily binds to the extracellular side of the HsUT-B channel, with a small-molecule feature similar to UTBinh-14 present on the intracellular side, which is different from the predicted binding mode in previous docking studies [49]. The 2-thienyl group of UTB inh-14 is located at the entrance of the channel, forming hydrophobic interactions with the side chain of Q232 and the main chain carbonyl group of A337 in HsUT-B. Meanwhile, its 4-ethylphenyl group forms hydrophobic interactions with W286, F288, G323, and A327. On the intracellular side, the binding mode of UTBinh-14 to UT-B exhibits C2 symmetry with that on the extracellular side (Fig. 2.11). Further comparison with the structure of HsUT-A3
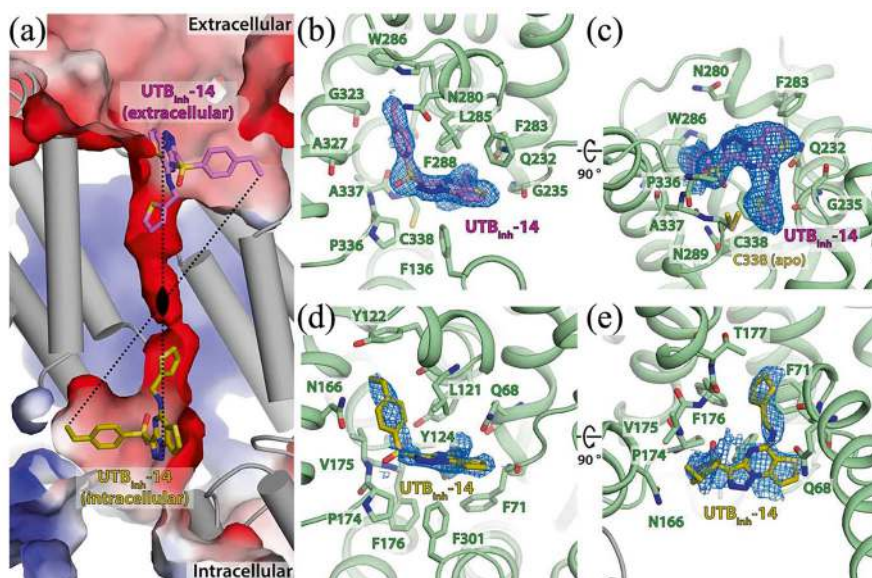
Fig. 2.11 UTBinh-14 inhibits HsUT-B at both extracellular and intracellular sides of its urea channel pore. (**a**) Transsectional view of HsUT-B channel pore showing the locations of UTB inh-14. Black oval denotes the center of C2 pseudosymmetry axis of the inhibitor binding modes. (**b**, **c**) Extracellular view of the primary UTB inh-14 binding mode and its transsectional view. (**d**, **e**) Intracellular view of the secondary UTB inh-14 binding mode and its transsectional view. (Data cited from ref. [17])

reveals that, due to the significantly more negative charge in the binding pocket of HsUT-A3 compared to HsUT-B, UTB inh-14 cannot adapt to the equivalent site of UT-A3. Additionally, the sulfonate group of UTB inh-14 sterically clashes with P397 in HsUT-A (equivalent to A337 in HsUT-B).

Mutating the important binding sites of UT-B to the corresponding amino acids of UT-A3, such as G323E, A327S, and N280T, and performing free energy calculations of in silico binding, show that there is a significant change in free energy, indicating that these amino acid sites participate in the selective binding of the inhibitor to UT-B. Although UTB inh-14 can bind to both the intracellular and extracellular sides of the UT-B, due to the high affinity of UTB >inh-14 and the fact that drug molecules typically have higher bioavailability on the extracellular surface, we hypothesize that UTB inh-14 bound to the extracellular side of UT-B is likely its primary mode of inhibition in vivo [17].

Design of UT-A Selective Inhibitor Based on Structure

Analysis of the precise three-dimensional structure of UT, as an emerging target for diuretic drugs, holds immeasurable value for advancing the process of drug development. Notably, the key subtypes within the UT-A family—UT-A1, UT-A2, UT-A3, and UT-A4, exhibit highly specific expression in renal tissues, whereas UT-B is widely distributed in the body. Knockout of the UT-B gene leads to significant diuretic effects but also causes adverse reactions, such as promoting bladder epithelial cell DNA damage and inducing depressive-like behavior in mice [50–52]. Therefore, we propose that UT-A, rather than UT-B, is a better target for diuretic drugs. Selective inhibitors of UT-A or small molecules with weak inhibitory activity against UT-B will be more beneficial for clinical research.

Structure-based drug discovery (SBDD) is one of the main means of designing and optimizing innovative drugs [53]. Through sequence alignment analysis, we observed that in hUT-A2, the amino acids $L202^{LECL}$ and $P336^{ECL3a}$ in the EBBP region were replaced by $V203^{LECL}$ and $A337^{ECL3a}$ in hUT-B, which directly led to a weakening of the hydrophobic interaction between 25a and UT-B. Additionally, the change from $F120^{3a}$ to $L121^{3a}$ in the CBBP region on the intracellular side disrupted the π-π stacking interaction with the phenyl ring of 25a. Experimental data further confirmed that the allelic mutations L202V and F120L in hUT-A2 significantly reduced its binding affinity. These findings suggest that the non-conserved amino acid sites $F120^{3a}$ and $L202^{LECL}$ in UT provide valuable molecular targets for designing highly effective and selective hUT-A2 inhibitors.

Furthermore, the study of the ATB3-hUT-A2 complex structure has provided insights. Particularly, the two key residues $L202^{LECL}$ and $P336^{ECL3b}$, which interact with the methoxy group of ATB3, are replaced by $V203^{LECL}$ and $A337^{ECL3b}$ in UT-B. Molecular dynamics simulations and mutation analyses collectively reveal how these differences contribute to the selective inhibition of hUT-A2 by ATB3. The differences in the "L-P" pocket between UT-A and UT-B present new ideas for

inhibitor design. Lastly, the SCG pocket in the HQA2 complex with hUT-A2 is also worth noting. The amino acid sequence in this pocket is not conserved among different UT subtypes, particularly the residues S279[3b], C285[3b], and G322[4b]. Importantly, the mutation of SCG pocket residues to structurally equivalent residues found in other UT members, such as S279D or C285W, significantly reduced the activity of HQA2 in blocking urea transport. This finding not only reveals the potential of the SCG pocket in designing selective inhibitors for hUT-A/B, but also suggests it may act as a ligand-binding allosteric site, regulating the urea transport process mediated by UT, opening up a new strategy for drug development.

UT-A1 is located in the apical membrane region of the inner medullary collecting duct principal cells and is an ideal target in the diuretic mechanism of action. Although UT-A1 covers the sequence features of UT-A2 and UT-A3 in terms of gene composition, we speculate that inhibitor molecules targeting UT-A2 and UT-A3 may also exhibit inhibitory activities against UT-A1. However, it is still unclear whether UT-A1 has a protein-folding structure similar to UT-A2 and UT-A3, and its structural complexity may be higher. Therefore, in order to design more selective drug molecules, future studies urgently need to further analyze the precise three-dimensional structure of UT-A1. By then, relying on comprehensive and detailed UT family structure information, we can develop more accurate compounds, which are expected to become efficient and promising diuretic drug candidates.

Interactions with Other Natural Substrates

The permeation of water through UT-B, despite initial controversies [54, 55], has been consistently demonstrated [42, 56–58]. Recent estimates of the rate of water permeation through UT-B are similar to those measured for aquaporins [59]. Given the similarities between the architecture of the aquaporin and UT pores discussed above, this result is not entirely surprising. Molecular dynamics simulations of water permeation through a homology model of human UT-B, based on the bovine UT-B structure, suggest that the magnitude of the energy barrier for water permeation is similar to that observed for aquaporins [59].

The observation that UT-B is an efficient water channel raises the question of how protons are excluded from leaking through the pore. In aquaporins, proton exclusion has been attributed primarily to two electrostatic barriers: one at a constriction formed by positively charged residues and another at the NPA motifs, where the positive ends of two helix dipoles point into the pore [60, 61]. In contrast, the UT selectivity filter lacks any positively charged side chains, and the orientations of the two pore helices are reversed relative to aquaporins, leading to a negative potential at the Sm site rather than a positive one. Interestingly, molecular dynamics simulations predict that water permeating through UT-B undergoes a reversal of the orientation of its dipole moment correlated with passage through the Sm site [59]. A similar change in orientation was predicted by molecular dynamics

simulations in aquaporins [62, 63] and recently gained experimental support from an ultra-high resolution crystal structure of a yeast aquaporin [64]. This re-orientation was proposed to play a role in proton exclusion in aquaporins.

Permeability of human UT-B to ammonia, but not ammonium, has also been reported recently [65]. Molecular dynamics simulations suggest that the ammonia is transported via the same central pore that serves as the urea and water permeation pathway and that the energetics of permeation are similar to those for water, including the location and size of the central energy barrier at the Sm site.

There is also some debate as to whether UT-A has the capacity to facilitate the transport of water and ammonia. Several studies have found that UT-A2, UT-A3 and UT-A5 are impermeable to both compounds [1, 66]. Conversely, groundbreaking research has demonstrated that UT-A2 and UT-A3 are also permeable to water by injecting cRNAs encoding for c-Myc-tagged murine UT-A2 or UT-A3 in *Lithobates* oocytes [56]. Previous structural analyses and amino acid sequence alignments observed that residues located on the selective filters are well conserved between UT-A2, UT-A3, and UT-B [18], including at the Sm site, and we suspect that the mechanism by which UT-A can transport water molecules is reasonable. Considering that the flux through UT-A is one to two orders of magnitude slower than UT-B [1, 2], for a more definitive understanding, further examination into the variations in energy barriers across different UT channels would be invaluable.

Comparison with Other Solute Channels

UTs are one of three unrelated families of proteins of known structure that transport urea via a channel-like mechanism. The other two families include the proton-gated UreI channels, which are renowned for conferring acid resistance to *Helicobacter pylori* [10, 11, 67], and certain members of the aquaporin family, commonly referred to as aquaglyceroporins. These aquaglyceroporins are capable of transporting urea, in addition to water and other small polar molecules, such as glycerol. These proteins play important physiological functions in vivo, especially in maintaining osmotic pressure balance, regulating water and salt balance and acid-base balance [68]. Notably, there is no apparent similarity between the permeation pathways of UTs and UreI, whose selectivity filter is characterized by two constrictions surrounded by aromatic residues [10, 11, 69]. In contrast, the permeation pathways of aquaporins exhibit obvious parallels to the UT pore, particularly in the presence of re-entrant helices and exposed backbone carbonyls that stabilize the permeant water molecules through hydrogen bonds. Furthermore, the aquaporins possess a pseudo-symmetry axis that intersects the center of the permeation pathway. The center of the pore harbors the NPA motifs, containing two pseudosymmetry-related asparagines that are reminiscent of the central threonines in UT and that contribute to selectivity in aquaporins [70–72].

Additionally, there is notable similarity between the UT pore and the permeation pathways of some ion channels. In tetrameric K$^+$ channels, the central permeation

pathway is surrounded by four re-entrant pore helices [73], whose dipole moments are thought to help stabilize K$^+$ within the hydrophobic core of the membrane [74]. Exposed backbone carbonyls are also key features of the K$^+$ channel selectivity filter and provide octahedral coordination to replace the hydration sphere on K$^+$, although these oxygens are located on non-helical segments following the pore helices, rather than being located directly on the helix C-terminal. Tilted re-entrant helices also play a role in permeation of chloride ions in the CLC channels [75].

Interestingly, the spatial organization of the ten transmembrane helices in the UT fold is similar to that of the first ten helices in the ammonia transporters of the Amt/Rh family [26, 76, 77]. Because the ammonia transporters lack equivalents to the UT pore helices, their largely hydrophobic pores bear little resemblance to the pores of the UT proteins. Nevertheless, the similarities in their folds suggest a potential shared evolutionary origin.

Conflicts of Interest The authors have no conflicts of interest.

References

1. B. Maciver et al., Functional characterization of mouse urea transporters UT-A2 and UT-A3 expressed in purified Xenopus laevis oocyte plasma membranes. Am. J. Physiol. Renal Physiol. **294**(4), F956–F964 (2008)
2. L.M. Mannuzzu, M.M. Moronne, R.I. Macey, Estimate of the number of urea transport sites in erythrocyte ghosts using a hydrophobic mercurial. J. Membr. Biol. **133**(1), 85–97 (1993)
3. R.R. Mayrand, D.G. Levitt, Urea and ethylene glycol-facilitated transport systems in the human red cell membrane. Saturation, competition, and asymmetry. J. Gen. Physiol. **81**(2), 221–237 (1983)
4. D. Zhao et al., Comparative transport efficiencies of urea analogues through urea transporter UT-B. Biochim. Biophys. Acta **1768**(7), 1815–1821 (2007)
5. R. Minocha, K. Studley, M.H. Saier Jr., The urea transporter (UT) family: Bioinformatic analyses leading to structural, functional, and evolutionary predictions. Recept. Channels **9**(6), 345–352 (2003)
6. G. Rousselet, P. Ripoche, P. Bailly, Tandem sequence repeats in urea transporters: Identification of an urea transporter signature sequence. Am. J. Phys. **270**(3 Pt 2), F554–F555 (1996)
7. E.A. Marcus et al., The periplasmic alpha-carbonic anhydrase activity of Helicobacter pylori is essential for acid acclimation. J. Bacteriol. **187**(2), 729–738 (2005)
8. G.M. Young, D. Amid, V.L. Miller, A bifunctional urease enhances survival of pathogenic Yersinia enterocolitica and Morganella morganii at low pH. J. Bacteriol. **178**(22), 6487–6495 (1996)
9. F. Sebbane et al., The Yersinia pseudotuberculosis Yut protein, a new type of urea transporter homologous to eukaryotic channels and functionally interchangeable in vitro with the Helicobacter pylori UreI protein. Mol. Microbiol. **45**(4), 1165–1174 (2002)
10. D. Strugatsky et al., Structure of the proton-gated urea channel from the gastric pathogen Helicobacter pylori. Nature **493**(7431), 255–258 (2013)

11. Y. Cui et al., pH-dependent gating mechanism of the Helicobacter pylori urea channel revealed by cryo-EM. Sci. Adv. **5**(3), eaav8423 (2019)
12. G. Godara et al., Functional characterization of Actinobacillus pleuropneumoniae urea transport protein, ApUT. Am. J. Physiol. Regul. Integr. Comp. Physiol. **296**(4), R1268–R1273 (2009)
13. S. Raunser et al., Oligomeric structure and functional characterization of the urea transporter from Actinobacillus pleuropneumoniae. J. Mol. Biol. **387**(3), 619–627 (2009)
14. M.A. Hediger et al., Structure, regulation and physiological roles of urea transporters. Kidney Int. **49**(6), 1615–1623 (1996)
15. E.J. Levin, M. Quick, M. Zhou, Crystal structure of a bacterial homologue of the kidney urea transporter. Nature **462**(7274), 757–761 (2009)
16. E.J. Levin et al., Structure and permeation mechanism of a mammalian urea transporter. Proc. Natl. Acad. Sci. USA **109**(28), 11194–11199 (2012)
17. G. Chi et al., Structural characterization of human urea transporters UT-A and UT-B and their inhibition. Sci. Adv. **9**(39), eadg8229 (2023)
18. S.M. Huang et al., Structural insights into the mechanisms of urea permeation and distinct inhibition modes of urea transporters. Nat. Commun. **15**(1), 10226 (2024)
19. G. von Heijne, Y. Gavel, Topogenic signals in integral membrane proteins. Eur. J. Biochem. **174**(4), 671–678 (1988)
20. H. Tsukaguchi et al., Cloning and characterization of the urea transporter UT3: Localization in rat kidney and testis. J. Clin. Invest. **99**(7), 1506–1515 (1997)
21. G. You et al., Cloning and characterization of the vasopressin-regulated urea transporter. Nature **365**(6449), 844–847 (1993)
22. A.D. Bansal et al., Phosphoproteomic profiling reveals vasopressin-regulated phosphorylation sites in collecting duct. J. Am. Soc. Nephrol. **21**(2), 303–315 (2010)
23. J. Abramson et al., Structure and mechanism of the lactose permease of Escherichia coli. Science **301**(5633), 610–615 (2003)
24. N.J. Hu et al., Crystal structure of a bacterial homologue of the bile acid sodium symporter ASBT. Nature **478**(7369), 408–411 (2011)
25. Y. Huang et al., Structure and mechanism of the glycerol-3-phosphate transporter from Escherichia coli. Science **301**(5633), 616–620 (2003)
26. S. Khademi et al., Mechanism of ammonia transport by Amt/MEP/Rh: Structure of AmtB at 1.35 a. Science **305**(5690), 1587–1594 (2004)
27. J. Liao et al., Structural insight into the ion-exchange mechanism of the sodium/calcium exchanger. Science **335**(6069), 686–690 (2012)
28. A. Yamashita et al., Crystal structure of a bacterial homologue of Na+/Cl--dependent neurotransmitter transporters. Nature **437**(7056), 215–223 (2005)
29. D. Yernool et al., Structure of a glutamate transporter homologue from Pyrococcus horikoshii. Nature **431**(7010), 811–818 (2004)
30. A. Laganowsky et al., Membrane proteins bind lipids selectively to modulate their structure and function. Nature **510**(7503), 172–175 (2014)
31. K. Gupta et al., The role of interfacial lipids in stabilizing membrane protein oligomers. Nature **541**(7637), 421–424 (2017)
32. P. Huang et al., Cryo-EM structure supports a role of AQP7 as a junction protein. Nat. Commun. **14**(1), 600 (2023)
33. J. Ge et al., Molecular mechanism of prestin electromotive signal amplification. Cell **184**(18), 4669–4679 e13 (2021)
34. S. Maeda et al., Structure, lipid scrambling activity and role in autophagosome formation of ATG9A. Nat. Struct. Mol. Biol. **27**(12), 1194–1201 (2020)
35. C. Alvadia et al., Cryo-EM structures and functional characterization of the murine lipid scramblase TMEM16F. elife **8**, e44365 (2019)
36. J.D. Klein, M.A. Blount, J.M. Sands, Urea transport in the kidney. Compr. Physiol. **1**(2), 699–729 (2011)

37. S. Nielsen et al., Cellular and subcellular localization of the vasopressin- regulated urea transporter in rat kidney. Proc. Natl. Acad. Sci. USA **93**(11), 5495–5500 (1996)
38. G.S. Stewart et al., The basolateral expression of mUT-A3 in the mouse kidney. Am. J. Physiol. Renal Physiol. **286**(5), F979–F987 (2004)
39. H.T. Zhang et al., Modeling of flux, binding and substitution of urea molecules in the urea transporter dvUT. J. Mol. Graph. Model. **76**, 504–511 (2017)
40. B. Chasan, A.K. Solomon, Urea reflection coefficient for the human red cell membrane. Biochim. Biophys. Acta **821**(1), 56–62 (1985)
41. D.G. Levitt, H.J. Mlekoday, Reflection coefficient and permeability of urea and ethylene glycol in the human red cell membrane. J. Gen. Physiol. **81**(2), 239–253 (1983)
42. B. Yang, A.S. Verkman, Urea transporter UT3 functions as an efficient water channel. Direct evidence for a common water/urea pathway. J. Biol. Chem. **273**(16), 9369–9372 (1998)
43. S. Zhuo, C. Yuan, Active site competition is the mechanism for the inhibition of lipoprotein-associated phospholipase A(2) by detergent micelles or lipoproteins and for the efficacy reduction of darapladib. Sci. Rep. **10**(1), 17232 (2020)
44. S. Wang et al., N-(4-acetamidophenyl)-5-acetylfuran-2-carboxamide as a novel orally available diuretic that targets urea transporters with improved PD and PK properties. Eur. J. Med. Chem. **226**, 113859 (2021)
45. C. Esteva-Font et al., A small molecule screen identifies selective inhibitors of urea transporter UT-A. Chem. Biol. **20**(10), 1235–1244 (2013)
46. K.P. Delaune, K. Alsayouri, Physiology, noncompetitive inhibitor, in *Disclosure: Khalid Alsayouri declares no relevant financial relationships with ineligible companies*, ed. by StatPearls, (Ineligible Companies, Treasure Island, 2024)
47. C. Esteva-Font et al., Diuresis and reduced urinary osmolality in rats produced by small-molecule UT-A-selective urea transport inhibitors. FASEB J. **28**(9), 3878–3890 (2014)
48. M.O. Anderson et al., Nanomolar potency and metabolically stable inhibitors of kidney urea transporter UT-B. J. Med. Chem. **55**(12), 5942–5950 (2012)
49. Verkman, A.S., et al., Small-molecule inhibitors of urea transporters. Subcell. Biochem., 2014. 73: p. 165–177, Springer Netherlands
50. Z. Dong et al., Urea transporter UT-B deletion induces DNA damage and apoptosis in mouse bladder urothelium. PLoS One **8**(10), e76952 (2013)
51. X. Li et al., Mice lacking urea transporter UT-B display depression-like behavior. J. Mol. Neurosci. **46**(2), 362–372 (2012)
52. H. Wang et al., High urea induces depression and LTP impairment through mTOR signalling suppression caused by carbamylation. EBioMedicine **48**, 478–490 (2019)
53. K.F. Zhu et al., Applications and prospects of cryo-EM in drug discovery. Mil. Med. Res. **10**(1), 10 (2023)
54. S. Martial et al., Functional differentiation of the human red blood cell and kidney urea transporters. Am. J. Phys. **271**(6 Pt 2), F1264–F1268 (1996)
55. F. Sidoux-Walter et al., At physiological expression levels the Kidd blood group/urea transporter protein is not a water channel. J. Biol. Chem. **274**(42), 30228–30235 (1999)
56. J. Kabutomori, N. Pina-Lopes, R. Musa-Aziz, Water transport mediated by murine urea transporters: Implications for urine concentration mechanisms. Biol Open **9**(8) (2020)
57. Y. Meng et al., A novel mutation at the JK locus causing Jk null phenotype in a Chinese family. Sci China C Life Sci **48**(6), 636–640 (2005)
58. B. Yang, A.S. Verkman, Analysis of double knockout mice lacking aquaporin-1 and urea transporter UT-B. Evidence for UT-B-facilitated water transport in erythrocytes. J. Biol. Chem. **277**(39), 36782–36786 (2002)
59. S. Azouzi et al., Energetic and molecular water permeation mechanisms of the human red blood cell urea transporter B. PLoS One **8**(12), e82338 (2013)
60. E. Beitz et al., Point mutations in the aromatic/arginine region in aquaporin 1 allow passage of urea, glycerol, ammonia, and protons. Proc. Natl. Acad. Sci. USA **103**(2), 269–274 (2006)

61. B. Wu et al., Concerted action of two cation filters in the aquaporin water channel. EMBO J. **28**(15), 2188–2194 (2009)
62. B.L. de Groot, H. Grubmuller, Water permeation across biological membranes: Mechanism and dynamics of aquaporin-1 and GlpF. Science **294**(5550), 2353–2357 (2001)
63. E. Tajkhorshid et al., Control of the selectivity of the aquaporin water channel family by global orientational tuning. Science **296**(5567), 525–530 (2002)
64. U.K. Eriksson et al., Subangstrom resolution X-ray structure details aquaporin-water interactions. Science **340**(6138), 1346–1349 (2013)
65. R.R. Geyer et al., Movement of NH(3) through the human urea transporter B: A new gas channel. Am. J. Physiol. Renal Physiol. **304**(12), F1447–F1457 (2013)
66. R.A. Fenton et al., Molecular characterization of a novel UT-A urea transporter isoform (UT-A5) in testis. Am. J. Physiol. Cell Physiol. **279**(5), C1425–C1431 (2000)
67. D.L. Weeks et al., A H+-gated urea channel: The link between Helicobacter pylori urease and gastric colonization. Science **287**(5452), 482–485 (2000)
68. Z.E. Newby et al., Crystal structure of the aquaglyceroporin PfAQP from the malarial parasite Plasmodium falciparum. Nat. Struct. Mol. Biol. **15**(6), 619–625 (2008)
69. R. McNulty et al., Mechanisms of molecular transport through the urea channel of Helicobacter pylori. Nat. Commun. **4**, 2900 (2013)
70. K. Murata et al., Structural determinants of water permeation through aquaporin-1. Nature **407**(6804), 599–605 (2000)
71. Y. Wang, K. Schulten, E. Tajkhorshid, What makes an aquaporin a glycerol channel? A comparative study of AqpZ and GlpF. Structure **13**(8), 1107–1118 (2005)
72. D. Wree et al., Requirement for asparagine in the aquaporin NPA sequence signature motifs for cation exclusion. FEBS J. **278**(5), 740–748 (2011)
73. D.A. Doyle et al., The structure of the potassium channel: Molecular basis of K+ conduction and selectivity. Science **280**(5360), 69–77 (1998)
74. B. Roux, R. MacKinnon, The cavity and pore helices in the KcsA K+ channel: Electrostatic stabilization of monovalent cations. Science **285**(5424), 100–102 (1999)
75. R. Dutzler et al., X-ray structure of a ClC chloride channel at 3.0 A reveals the molecular basis of anion selectivity. Nature **415**(6869), 287–294 (2002)
76. F. Gruswitz et al., Function of human Rh based on structure of RhCG at 2.1 A. Proc. Natl. Acad. Sci. USA **107**(21), 9638–9643 (2010)
77. D. Lupo et al., The 1.3-A resolution structure of Nitrosomonas europaea Rh50 and mechanistic implications for NH3 transport by Rhesus family proteins. Proc. Natl. Acad. Sci. USA **104**(49), 19303–19308 (2007)

Chapter 3
Tissue Distribution, Expression and Regulation of Urea Transporters

Nannan Li, Janet D. Klein, Jeff M. Sands, and Baoxue Yang

Abstract UT-A and UT-B families of urea transporters consist of multiple isoforms with the majority of the isoforms located in the kidney. UT-B (*Slc14A1*) in kidney is primarily located in the descending vasa recta. The UT-A (*Slc14A2*) urea transporter family comprises six distinct isoforms, three of which are predominantly found in the kidney. Specifically, UT-A1 and UT-A3 are located in the inner medullary collecting duct (IMCD), while UT-A2 is situated in the thin descending limb. These transporters play a crucial role in the renal concentration of urine. The regulation of renal urea transporter activity involves acute modifications through phosphorylation and subsequent translocation to the plasma membrane. In response to stimulation by vasopressin or hypertonicity, UT-A1 and UT-A3 accumulate in the IMCD plasma membrane. Chronic regulation of IMCD urea transporters involves hormonal modulation of protein expression levels, such as adrenal steroids, low-protein diets, electrolyte abnormalities, aging or other pathologic conditions. This chapter provides a brief overview of the tissue distribution, expression of the urea transporter isoforms, locations in the kidney, and regulation of urea transporters.

Keywords Urea · Urea transporter · Vasopressin · Phosphorylation · Regulation

N. Li · B. Yang (✉)
State Key Laboratory of Vascular Homeostasis and Remodeling, Department of Pharmacology, School of Basic Medical Sciences, Peking University, Beijing, China
e-mail: baoxue@bjmu.edu.cn

J. D. Klein · J. M. Sands
Renal Division, Department of Medicine, Emory University School of Medicine, Atlanta, GA, USA

Tissue Distribution and Expression of Urea Transporters

Urea transporters (UTs) are a family of membrane channel proteins that mediate the rapid and passive transport of urea across the plasma membrane down its concentration gradient. Two genes *slc14a1* and *slc14a2* encode for UT-B and UT-As, respectively, in mammals.

The *slc14a1* gene encodes UT-B through a conserved UT domain, with protein localization observed in renal descending vasa recta and multiple extrarenal sites including erythrocytes, brain, heart, spleen, colon, bladder, testis, etc. [1]. In contrast, the *slc14a2* (UT-A gene) is large [2–4] and gives rise to at least 6 isoforms (splice variants) due to its two promoters (alternative transcriptional start sites), and differential splicing processes [4–6]. These isoforms, designated UT-A1, UT-A2, UT-A3, UT-A4, UT-A5, and UT-A6, predict 6 UT-A proteins of 929, 397, 460, 466, 323, and 235 amino acids, respectively. Four of these UT-A isoforms have been cloned from kidney; UT-A5 was cloned from mouse testis [7] and UT-A6 from human colon [8]. In kidney, UT-A1 and/or UT-A3 are major contributors to the urinary concentrating mechanism, whereas UT-A2 has a minor role under physiologic conditions. Under basal conditions, the UT-A1 and UT-A1/A3 null mouse has a severe concentrating defect [9–11], whereas the UT-A2 null mouse has a minor defect that is apparent when it is water-deprived and on a low protein diet [12].

UT isoforms exhibit predominant renal localization (Fig. 3.1), with their physiological function in urine concentration dynamics being extensively characterized
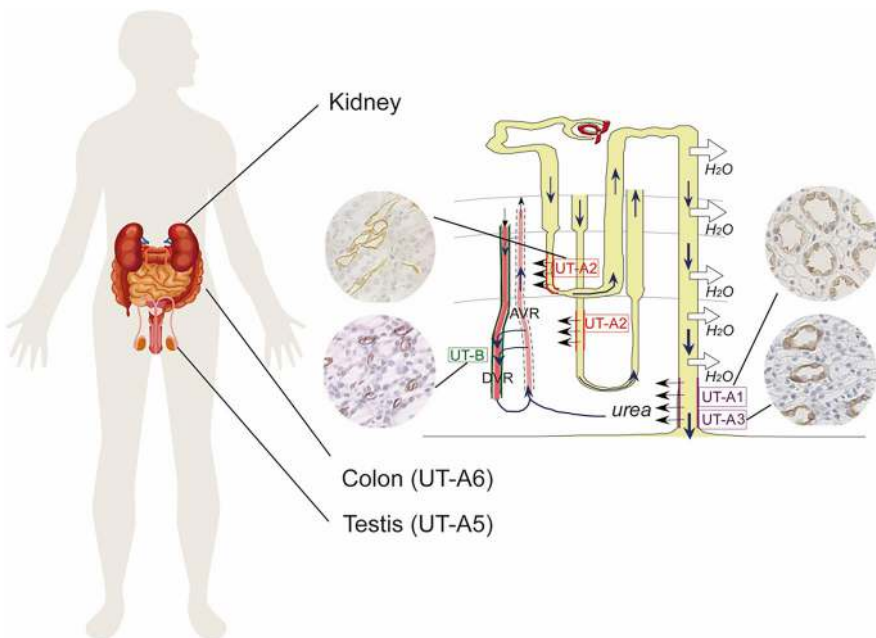
Fig. 3.1 Localization of UT-A isoforms in the body, and UT-B in the kidney

by using knockout mouse models [9–11, 13–15]. UT-A1 is localized to the apical membranes and UT-A3 predominantly resides on the basolateral membranes of principle cells of the terminal inner medullary collecting duct (IMCD), which demonstrates the highest intrinsic urea permeability among renal tubular structures [6, 16, 17]. One study reported that UT-A3 is also localized to the apical membranes of cells in the IMCD after vasopressin administration [18]. UT-A2 shows distinct anatomical distribution along descending thin limbs of short-loop nephrons within outer medullary regions and the terminal portions of long-loop nephrons in inner medullary zones [19]. UT-A4 expression appears species-specific, having been exclusively identified in rat renal medullary tissue, though its detailed subcellular distribution remains uncharacterized [6]. UT-B is expressed in endothelial cells of the descending vasa recta in kidney [20, 21].

UT-B is expressed in multiple tissues (Fig. 3.2) [20, 22]. Immunocytochemical studies reveal UT-B localization in gastrointestinal epithelia (small intestinal villi, gastric glands [1], colonic crypts [23, 24]), brain ependymal cells/astrocytes [25], aortic endothelia [20, 26, 27], and testicular Sertoli cells [28]. While UT-A isoforms show minimal extrarenal expression, UT-A1 [29], -A2 [30], -A3 [29], and -A6 [8] are detected in human non-renal tissues, with species-specific UT-A5 mRNA restricted to murine seminiferous tubule myoid cells [7, 31].
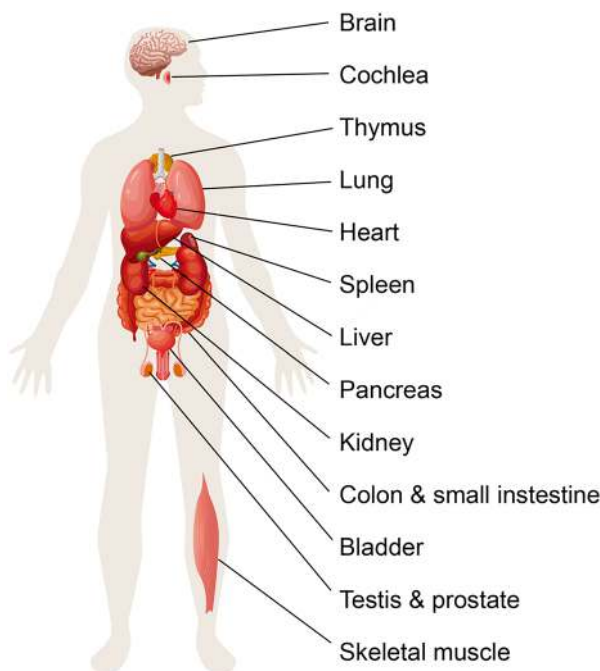
Fig. 3.2 UT-B is widely expressed in multiple tissues in human, including kidney, brain, liver, colon, small intestine, pancreas, testis, prostate, spleen, thymus, heart, skeletal muscle, lung, bladder, and cochlea

Expression Regulation of Urea Transporters

The expression of urea transporters in the kidney is modulated by hormonal signals and adapts to different physiological conditions and disease states (Table 3.1).

Hormones

Vasopressin

Vasopressin's regulation of collecting duct urea permeability (P_{urea}) was established before UT discovery [43–45]. Current evidence confirms its role as the primary modulator of UT-A1/-A3 in the IMCD via phosphorylation and membrane trafficking mechanisms.

The bath application of vasopressin in microperfused rat terminal IMCDs initiates a signaling cascade through V2 receptor activation, triggering sequential biochemical events: [1] activation of adenylyl cyclase with subsequent cAMP generation, [2] protein kinase A (PKA) activation, and [3] enhanced urea transport through increased membrane trafficking of functional transporters rather than altered binding affinity (unchanged K_m value for urea) [46–50]. The time course for vasopressin-increased urea permeability, or the time course after vasopressin

Table 3.1 Expression and regulation of urea transporters in kidney

Conditions	Expression level in the kidney				Regulation	References
	UT-A1	UT-A2	UT-A3	UT-B1		
Vasopressin	↑	↑	↑	↓	Urea reabsorption increased and medullary hypertonicity increased.	[18, 32–34]
Adrenal steroids	↓	–	↓	–	Inhibiting the activity of UT-A promoter I and inhibiting urea transport in the inner medullary collecting duct.	[35, 36]
Hyperosmolality	↑	–	↑	–	Increased urea reabsorption and accumulation in the inner medulla.	[18]
Low-protein diet	↑	↑	–	↑	Presence of urea transport in the initial IMCD after low-protein diet for 4 weeks.	[37, 38]
Hypercalcemia	↓	↓	↓	–	Reduced the urine concentrating ability.	[39, 40]
Hypokalemia	↓	↓	↓	–	Decreased renal medullary interstitial tone, accompanied by a reduction in distal tubular sodium transporter expression.	[41]
Aging	↓	–	↓	↓	The capacity to concentrate urine progressively declines during aging.	[42]

withdrawal, each consist of two distinct phases: an initial 10-min period during which facilitated urea permeability increases or decreases rapidly, followed by a second 10- to 60-min period during which facilitated urea permeability changes back slowly [45, 48, 51].

Experimental evidence from microperfused rat terminal IMCDs reveals compartment-specific vasopressin effects: Luminal administration induces V2 receptor activation and enhances urea transport [52], whereas pre-exposure to basolateral vasopressin followed by luminal application paradoxically reduces transport efficiency, demonstrating an antagonistic regulatory relationship between luminal and basolateral vasopressin signaling pathways [52].

The deduced amino acid sequences for UT-A1 and UT-A3 contain several consensus PKA phosphorylation sites [6]. Proteomic and cDNA array approaches have identified UT-A1 and UT-A3 as proteins that are phosphorylated by vasopressin in the inner medulla [53–58]. Incubating freshly isolated suspensions of rat IMCDs with vasopressin increases the phosphorylation of both the 117 and 97 kDa UT-A1 glycoproteins within 2 min [59] and of the 67 and 44 kDa UT-A3 proteins [32]. Vasopressin also increases the phosphorylation of UT-A1 in UT-A1 MDCK cells [60, 61] and UT-A1 mIMCD3 cells [62]. The time course and dose response for vasopressin-stimulated increases in UT-A1 phosphorylation are consistent with the time course and dose response for vasopressin-stimulated increases in urea permeability in perfused rat terminal IMCDs [45, 48, 51, 59]. Research demonstrates that vasopressin suppresses UT-B expression [18, 34], while therapeutic administration of desmopressin (dDAVP, [deamino-Cys1, D-Arg8] vasopressin) induces a corresponding reduction in renal UT-B protein levels.

cAMP, forskolin, and dDAVP (a V2-selective agonist) also increase UT-A1 phosphorylation. PKA inhibitors block vasopressin- or forskolin-stimulated phosphorylation of UT-A1 in rat IMCD suspensions [59] and UT-A1 MDCK cells [61, 63]. In addition to stimulating PKA, vasopressin/cAMP can stimulate Epac (exchange protein activated by cAMP) [54, 64–67]. Activating Epac increases urea permeability in perfused rat terminal IMCDs and increases UT-A1 phosphorylation in IMCD suspensions [68] (Fig. 3.3).

A phosphoproteomic analysis identified serine 486 as a potential vasopressin stimulated phosphorylation site in UT-A1 [55]. This same serine was identified in a second study that also identified serine 499 as a second potential PKA phosphorylation site [69]. Using site-directed mutagenesis and transient transfection in heterologous expression systems, PKA was shown to phosphorylate UT-A1 at Ser 486 and Ser 499 [69]. Chimera proteins of UT-A that attached the loop region of UT-A1 (aa 460–532) containing Ser 486 and Ser 499 to the UT-A2 protein, which normally lacks this region, showed that this section conferred vasopressin sensitivity to UT-A2 [33]. Ser 486-phosphorylated UT-A1 is detected primarily in the apical plasma membrane in rat IMCDs [70].

A subsequent phosphoproteomic screen showed that Ser 84, which is present in both UT-A1 and UT-A3, could be phosphorylated by PKA [53]. Vasopressin was shown to increase phosphorylation at Ser 84 in rat UT-A1 and UT-A3 [71]; however, the vasopressin-stimulated phosphorylation site in human or mouse UT-A3
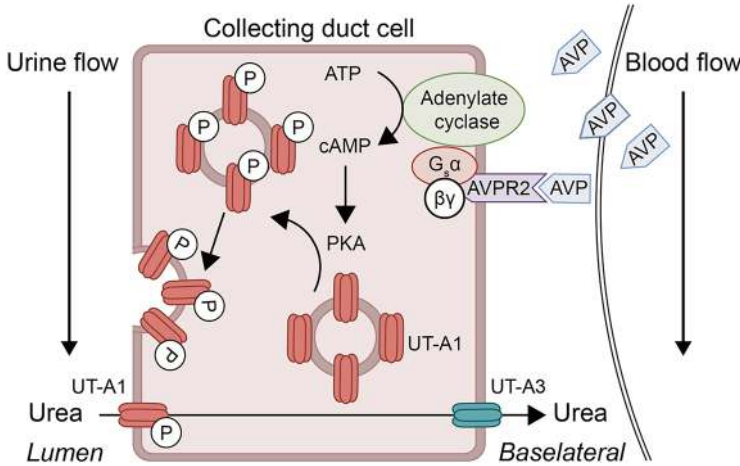
Fig. 3.3 The regulatory pathway mediated by vasopressin

has not been determined, since Ser 84 is not conserved in the human sequence and neither of the two PKA consensus sites in mouse (Ser 85 or Ser 92) are phosphory-lated [8]. There is currently no explanation for the species variation in sites that are phosphorylated.

As well as the PKA-mediated phosphorylation of UT-A1, there are other consen-sus kinase sites on this urea transporter. Protein kinase C (PKC) stimulates urea permeability and the phosphorylation of UT-A1 at serine 494 [72–75]. Specifically, PKCα is involved in the phosphorylation of UT-A1 under hypertonic condi-tions [74].

Stimulation by phosphorylation suggests the importance of dephosphorylation in the regulation of urea transporters. However, there are very limited studies analyz-ing the dephosphorylation of urea transporters. Ilori et al. reported that the phos-phorylation level of UT-A1 is affected by inhibition of calcineurin suggesting that protein phosphatase 2B may be responsible for dephosphorylation of UT-A1, but this account also suggests the possibility that other phosphatases may be involved [76]. A recent study showed that calyculin, which inhibits protein phosphatase 2A, increases IMCD urea permeability and phosphorylated UT-A1 in the inner medulla [77].

Both UT-A1 and UT-A3 proteins can be ubiquitinated based on studies showing that the abundance of these proteins is increased when ubiquitin proteasome proteo-lytic pathways have been inhibited [78, 79]. Only UT-A1, however, has been rigor-ously shown to have ubiquitinated high-molecular weight forms by immunoprecipitation and Western blot analysis [78, 80]. In normal conditions, cyto-solic UT-A1 (including misfolded UT-A1 from the endoplasmic reticulum) and constitutively internalized cell surface UT-A1 is polyubiquitinated and degraded in a proteasome system. However, upon AVP stimulation, UT-A1 is phosphorylated and processed for monoubiquitination at the cell surface. The internalized monou-biquitinated UT-A1 is trafficked to early endosomes, then targeted to the lysosome for degradation [81] (Fig. 3.4).
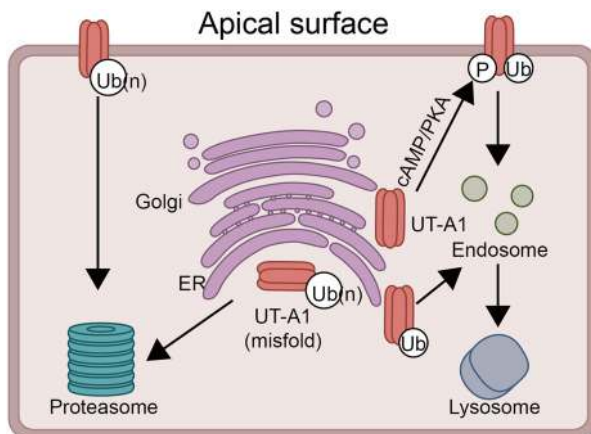
Fig. 3.4 UT-A1 ubiquitination, internalization, and degradation

Adrenal Steroids

Studies demonstrate that glucocorticoids and aldosterone inhibit urea transports in the IMCD by reducing the abundance of the UT-A1 transporter [82–84]. Glucocorticoids suppress the transcription of both UT-A1 and UT-A3 by inhibiting the activity of UT-A promoter I [35]. While the precise molecular pathway has not yet been completely characterized, functional analysis indicates the observed inhibitory effect operates independently of cis-regulatory glucocorticoid response elements within the promoter. Both diabetic patients and streptozotocin-induced diabetic rats demonstrate increased excretion of corticosterone and urea, with elevated glucocorticoid levels in the rodent model observed to suppress early-stage UT-A1 protein expression [85, 86]. The Dahl salt-sensitive rat strain, a genetic model of salt-sensitive hypertension, displayed upregulated UT-A1 and UT-A3 expression in the inner medullary collecting duct (IMCD) compared with salt-resistant counterparts, corresponding to enhanced urea transport' capacity. These animals also manifested elevated 11β-hydroxysteroid dehydrogenase type II (11β-HSD2) levels, the enzyme responsible for glucocorticoid catabolism [36]. Diminished glucocorticoid concentrations in these animals may mechanistically enhance UT-A promoter I activation, driving transcriptional upregulation and subsequent protein abundance of UT-A1/UT-A3 transporters. In contrast, aldosterone-mediated suppression of UT-A1 expression operates through the mineralocorticoid receptor signaling pathway, exhibiting mechanistic independence from transcriptional regulation processes [82]. Research has demonstrated that volume expansion induced by aldosterone administration combined with a high-salt diet leads to significant reductions in UT-A1 and UT-A3 expression levels in rat models.

Renin-angiotensin System

The mRNA for the type 1 angiotensin II (AT1) receptor is present in rat IMCDs [87–89], and radioligand-binding studies show that AT1 receptors are expressed [90]. Angiotensin II does not affect basal (no vasopressin) urea permeability in rat terminal IMCDs [91]. However, it increases both vasopressin-stimulated urea permeability and UT-A1 phosphorylation via PKC-mediated effects [91]. By augmenting the maximal urea permeability response to vasopressin, angiotensin II may play a physiologic role in the urinary concentrating mechanism.

ACE2 transgenic mice lacking the tissue form of angiotensin-converting enzyme (ACE) develop a normal renal medulla but exhibit impaired urine concentrating ability, akin to knockout mice deficient in angiotensinogen and the angiotensin II receptors AT1a and AT1b. This functional defect observed in ACE2 mice is associated with significant reductions in the UT-A1 level in the inner medulla, as well as a decreased abundance of the Na^+–K^+–$2Cl^-$ symporter NKCC2/BSC1. ACE2 transgenic mice deficient in the tissue-specific isoform of angiotensin-converting enzyme exhibit normal renal medullary development but demonstrate impaired urine-concentrating capacity [92]. This phenotype mirrors observations in angiotensinogen knockout mice and those lacking both AT1a and AT1b angiotensin II receptors. The functional impairment in ACE2-deficient mice correlates with two distinct molecular alterations in the inner medullary region: diminished expression of the urea transporter UT-A1 and reduced protein abundance of the Na^+–K^+–$2Cl^-$ cotransporter NKCC2/BSC1.

Physiological studies demonstrate that while glucagon elevates urinary urea excretion by 45% in rats [93, 94], it fails to activate cAMP signaling [95, 96] or modify urea permeability in isolated inner medullary collecting ducts (IMCDs), regardless of vasopressin stimulation [95].

Oxytocin activates V2 receptor-mediated cAMP signaling to enhance phloretin-sensitive urea transport in rat terminal IMCDs [97], with sustained permeability observed despite 48-hour hydration challenges in medullary segment 2 [97].

Hyperosmolality

The osmolality of the renal medulla varies over a wide range, depending on the hydration status of the animal. Increasing the osmolality, either by adding NaCl (as occurs during transition to an antidiuretic state) or mannitol, rapidly increases urea permeability in rat terminal IMCDs, even in the absence of vasopressin [49, 98, 99]. These findings suggest that hyperosmolality is an independent regulator of urea transporters. When vasopressin is present, increasing osmolality has an additive stimulatory effect on urea permeability [49, 97, 99, 100]. Hyperosmolality-stimulated urea permeability is inhibited by phloretin and thiourea [100]. Kinetic

studies show that hyperosmolality, similar to vasopressin, increases urea permeability by increasing V_{max} rather than K_m [47, 100]. However, hyperosmolality stimulates urea permeability via increases in PKC activation and intracellular calcium [91, 92, 101, 102], while vasopressin stimulates urea permeability via increases in adenylyl cyclase (AC) [48]. Hyperosmolality, similar to vasopressin, increases phosphorylation and plasma membrane accumulation both UT-A1 and UT-A3 [18, 32, 59, 103]. Thus, both hyperosmolality and vasopressin rapidly increase urea permeability, but they do so via different signaling pathways with vasopressin dependent on the second messenger cAMP and hypertonicity dependent on intracellular calcium. In a clinical study, treatment of patients with hypertonic saline solution resulted in increased expression of UT-A1, confirming responsiveness in human subjects [104]. Hyperosmolality has also been shown to induce expression of UT-A2 in mouse medullary collecting duct [105].

The collecting duct of the houndshark, Triakis scyllium expresses a urea transporter [106]. Transfer of the shark from 30% sea water to 100% sea water results in a progressive increase in the apical plasma membrane accumulation of its urea transporter in the collecting duct [106].

Low-protein Diets

Modulating the expression of mammalian urea transporters is crucial in response to varying protein intake and urea loads, contributing to overall nitrogen balance. Research on the abundance of urea transporters in the kidneys of rats subjected to a low-protein diet for different durations revealed an upregulation of UT-A2 mRNA and protein after 1 to 2 weeks [37, 107]. Additionally, a 2-week low-protein diet was found to induce increased protein expression of UT-B in the outer medulla [38]. An increase in UT-A1 mRNA abundance was observed following 4 weeks of protein restriction. The upregulation of UT-A and UT-B enhances urea circulation and reabsorption, thereby mitigating urea loss associated with low protein intake.

Observations in UT-A and UT-B knockout mice support the notion that effective regulation of urea excretion, in response to changes in urea load and protein intake, requires modulation of renal urea transporter expression and activity. UT-B knockout mice are unable to adequately eliminate the increased urea load resulting from intraperitoneal injection, leading to significantly elevated plasma urea levels when fed a high-protein diet. Furthermore, they cannot achieve sufficient urea excretion without a substantial increase in urine output [108]. Similarly, in UT-A1/A3 knockout mice, the inability to concentrate urine under normal protein intake (20% protein diet) can be improved by restricting protein intake to a lower level (4% protein diet) [9].

Electrolyte Abnormalities

Hypercalcemia impairs urinary concentration capacity in both humans and rats [39, 40, 109]. While varying the perfusate calcium concentration between 0 and 5 mM did not affect facilitated urea permeability in the terminal IMCD of normocalcemic rats, a significant increase in terminal IMCD urea permeability was observed in hypercalcemic rats [39]. The elevated levels were observed in both baseline and vasopressin-activated urea permeability rates. Moreover, increased concentrations of 97 kDa and 117 kDa UT-A1 proteins were detected in the inner medullary tip region of hypercalcemic rats, corresponding to their enhanced urea-transporting capability [39].

Furthermore, vasopressin significantly increased facilitated urea permeability in terminal IMCDs of hypercalcemic rats [39]. Hypercalcemia also induces active urea reabsorption at the apical membrane of the terminal IMCD, while inhibiting active urea secretion in the IMCD segment 3 [110]. Thus, hypercalcemia and low-protein dietary conditions elicit comparable modifications in both facilitative and active urea transporter proteins localized within this specific IMCD subsegment.

Hypokalemia results in a significant decrease in renal medullary interstitial tone, accompanied by a reduction in distal tubular sodium transporter expression. One study found that the abundance of the tonicity response enhancer-binding protein (TonEBP) was significantly reduced in the outer and inner medulla of hypokalemic rats [41]. The underlying mechanisms appear to differ between outer and inner medulla; specifically, TonEBP mRNA abundance is lower in the outer medulla while remaining unchanged in the inner medulla. TonEBP expression decreased markedly in the collecting ducts of the outer and inner medulla, as well as in the thick ascending limbs and interstitial cells, with a slight decrease observed in the descending and ascending limbs. In the outer medulla, TonEBP translocates to the cytoplasm of the descending limb. As anticipated, transcription of the TonEBP target aldose reductase was diminished, reflecting reduced abundance of both mRNA and protein. Furthermore, downregulation of TonEBP led to decreased expression of aquaporin-2 (AQP2) and UT-A in the renal medulla, while the expression of UT-A1 and UT-A2 was severely impaired in transgenic mice expressing a dominant negative form of TonEBP [111].

Aging

The ability of urine to concentrate diminishes with age. In aged rats, this impairment is linked to a reduced urea concentration in the renal papilla and a decreased abundance of UT-A1, UT-A3, and UT-B in the kidney [42]. Treatment with dDAVP effectively corrects polyuria in aging rats and is associated with an upregulation of

UT-A1 abundance in the terminal IMCD [42]. Notably, UT-B protein abundance is significantly reduced in aged Wag/Rij rats; however, the administration of supraphysiological doses of dDAVP enhances its abundance [112]. Consequently, the decreased levels of UT-B protein represent an additional factor contributing to the diminished urine concentrating ability in aged rats, and potentially in humans [112].

Pathologic Conditions and Iatrogenic Effects

Unilateral and bilateral ureteral obstructions were associated with a reduced expression of medullary UT-A1, UT-A3, and UT-B. Notably, the downregulation of these transporters persisted for two weeks after the obstruction was relieved [113]. Furthermore, a reduction in fibrosis following unilateral ureteral obstruction was observed in UT-A1/A3 knockout mice, indicating that decreased UT activity may mitigate the severity of renal fibrosis after unilateral ureteral obstruction [114].

Studies involving Dahl salt-sensitive hypertensive rats suggest a potential association with hypertension [36], wherein terminal medullary cell colonies stimulate increased urea transport in the IMCD and enhance the protein abundance of UT-A1 and UT-A3 in the inner medulla. However, it remains to be determined whether alterations in urea transporter activity or abundance within the kidney are related to blood pressure regulation.

The use of certain medications may lead to dysregulation of renal urea transport. Angiotensin II type 1 (AT1) blockers may downregulate the renal UT-A transporter [115]. Long-term treatment with the calcineurin inhibitor cyclosporine, an immunosuppressant commonly used in organ transplant recipients, results in impaired urine concentrating ability and a significant decrease in the abundance of UT-A2, UT-A3, and UT-B [116]. In a study involving rats fed lithium for 25 days, a reduction in urine osmolarity was observed alongside a decrease in the abundance of UT-A1 and UT-B in the inner medulla [117]. This finding may explain the diminished urine concentrating ability seen in patients receiving lithium for the treatment of bipolar disorder. Furthermore, prolonged use of the widely utilized antimalarial drug chloroquine can lead to polyuria. Research indicated that chloroquine caused the downregulation of AQP2 and NKCC2; however, in rats treated with chloroquine, the abundance of UT-A1 and UT-A3 remained unaffected. This may be attributed to chloroquine's inhibition of cAMP production in the inner medulla, which likely alters the transport of UT-A1 [118]. Metformin, an AMPK activator, stimulates the phosphorylation of UT-A1 (and AQP2) in rat terminal IMCDs [119]. Metformin also improves urine concentration in rodents with nephrogenic diabetes insipidus [120].

References

1. J.J. Doran, J.D. Klein, Y.H. Kim, T.D. Smith, S.D. Kozlowski, R.B. Gunn, J.M. Sands, Tissue distribution of UT-A and UT-B mRNA and protein in rat. Am. J. Physiol. Regul. Integr. Comp. Physiol. **290**, R1446–R1459 (2006)

2. S.M. Bagnasco, T. Peng, M.G. Janech, A. Karakashian, J.M. Sands, Cloning and characterization of the human urea transporter UT-A1 and mapping of the human Slc14a2 gene. Am. J. Physiol. Renal Physiol. **281**, F400–F406 (2001)

3. R.A. Fenton, C.A. Cottingham, G.S. Stewart, A. Howorth, J.A. Hewitt, C.P. Smith, Structure and characterization of the mouse UT-A gene (Slc14a2). Am. J. Physiol. Renal Physiol. **282**, F630–F638 (2002)

4. Y. Nakayama, M. Naruse, A. Karakashian, T. Peng, J.M. Sands, S.M. Bagnasco, Cloning of the rat Slc14a2 gene and genomic organization of the UT-A urea transporter. Biochim. Biophys. Acta **1518**, 19–26 (2001)

5. S.M. Bagnasco, T. Peng, Y. Nakayama, J.M. Sands, Differential expression of individual UT-A urea transporter isoforms in rat kidney. J. Am. Soc. Nephrol. **11**, 1980–1986 (2000)

6. A. Karakashian, R.T. Timmer, J.D. Klein, R.B. Gunn, J.M. Sands, S.M. Bagnasco, Cloning and characterization of two new isoforms of the rat kidney urea transporter: UT-A3 and UT-A4. J. Am. Soc. Nephrol. **10**, 230–237 (1999)

7. R.A. Fenton, A. Howorth, G.J. Cooper, R. Meccariello, I.D. Morris, C.P. Smith, Molecular characterization of a novel UT-A urea transporter isoform (UT-A5) in testis. Am. J. Physiol. Cell Physiol. **279**, C1425–C1431 (2000)

8. C.P. Smith, E.A. Potter, R.A. Fenton, G.S. Stewart, Characterization of a human colonic cDNA encoding a structurally novel urea transporter, hUT-A6. Am. J. Physiol. Cell Physiol. **287**, C1087–C1093 (2004)

9. R.A. Fenton, C.L. Chou, G.S. Stewart, C.P. Smith, M.A. Knepper, Urinary concentrating defect in mice with selective deletion of phloretin-sensitive urea transporters in the renal collecting duct. Proc. Natl. Acad. Sci. USA **101**, 7469–7474 (2004)

10. T. Jiang, Y. Li, A.T. Layton, W. Wang, Y. Sun, M. Li, H. Zhou, B. Yang, Generation and phenotypic analysis of mice lacking all urea transporters. Kidney Int. **91**, 338–351 (2017)

11. X. Geng, S. Zhang, J. He, A. Ma, Y. Li, M. Li, H. Zhou, G. Chen, B. Yang, The urea transporter UT-A1 plays a predominant role in a urea-dependent urine-concentrating mechanism. J. Biol. Chem. **295**, 9893–9900 (2020)

12. S. Uchida, E. Sohara, T. Rai, M. Ikawa, M. Okabe, S. Sasaki, Impaired urea accumulation in the inner medulla of mice lacking the urea transporter UT-A2. Mol. Cell. Biol. **25**, 7357–7363 (2005)

13. B. Yang, L. Bankir, A. Gillespie, C.J. Epstein, A.S. Verkman, Urea-selective concentrating defect in transgenic mice lacking urea transporter UT-B. J. Biol. Chem. **277**, 10633–10637 (2002)

14. R.A. Fenton, A. Flynn, A. Shodeinde, C.P. Smith, J. Schnermann, M.A. Knepper, Renal phenotype of UT-A urea transporter knockout mice. J. Am. Soc. Nephrol. **16**, 1583–1592 (2005)

15. J.D. Klein, Y. Wang, A. Mistry, L.M. LaRocque, P.A. Molina, R.T. Rogers, M.A. Blount, J.M. Sands, Transgenic restoration of urea transporter A1 confers maximal urinary concentration in the absence of urea transporter A3. J. Am. Soc. Nephrol. **27**, 1448–1455 (2016)

16. G.S. Stewart, R.A. Fenton, W. Wang, T.H. Kwon, S.J. White, V.M. Collins, G. Cooper, S. Nielsen, C.P. Smith, The basolateral expression of mUT-A3 in the mouse kidney. Am. J. Physiol. Renal Physiol. **286**, F979–F987 (2004)

17. J.M. Terris, M.A. Knepper, J.B. Wade, UT-A3: localization and characterization of an additional urea transporter isoform in the IMCD. Am. J. Physiol. Renal Physiol. **280**, F325–F332 (2001)

18. N.W. Blessing, M.A. Blount, J.M. Sands, C.F. Martin, J.D. Klein, Urea transporters UT-A1 and UT-A3 accumulate in the plasma membrane in response to increased hypertonicity. Am. J. Physiol. Renal Physiol. **295**, F1336–F1341 (2008)

19. J.B. Wade, A.J. Lee, J. Liu, C.A. Ecelbarger, C. Mitchell, A.D. Bradford, J. Terris, G.H. Kim, M.A. Knepper, UT-A2: a 55-kDa urea transporter in thin descending limb whose abundance is regulated by vasopressin. Am. J. Physiol. Renal Physiol. **278**, F52–F62 (2000)

20. R.T. Timmer, J.D. Klein, S.M. Bagnasco, J.J. Doran, J.W. Verlander, R.B. Gunn, J.M. Sands, Localization of the urea transporter UT-B protein in human and rat erythrocytes and tissues. Am. J. Physiol. Cell Physiol. **281**, C1318–C1325 (2001)

21. Y. Xu, B. Olives, P. Bailly, E. Fischer, P. Ripoche, P. Ronco, J.P. Cartron, E. Rondeau, Endothelial cells of the kidney vasa recta express the urea transporter HUT11. Kidney Int. **51**, 138–146 (1997)

22. G.S. Stewart, C. Graham, S. Cattell, T.P. Smith, N.L. Simmons, C.P. Smith, UT-B is expressed in bovine rumen: potential role in ruminal urea transport. Am. J. Physiol. Regul. Integr. Comp. Physiol. **289**, R605–R612 (2005)

23. D. Collins, D.C. Winter, A.M. Hogan, L. Schirmer, A.W. Baird, G.S. Stewart, Differential protein abundance and function of UT-B urea transporters in human colon. Am. J. Physiol. Gastrointest. Liver Physiol. **298**, G345–G351 (2010)

24. H. Inoue, S.D. Jackson, T. Vikulina, J.D. Klein, K. Tomita, S.M. Bagnasco, Identification and characterization of a Kidd antigen/UT-B urea transporter expressed in human colon. Am. J. Physiol. Cell Physiol. **287**, C30–C35 (2004)

25. B. Huang, H. Wang, D. Zhong, J. Meng, M. Li, B. Yang, J. Ran, Expression of Urea Transporter B in Normal and Injured Brain. Front. Neuroanat. **15**, 591726 (2021)

26. B. Olives, P. Neau, P. Bailly, M.A. Hediger, G. Rousselet, J.P. Cartron, P. Ripoche, Cloning and functional expression of a urea transporter from human bone marrow cells. J. Biol. Chem. **269**, 31649–31652 (1994)

27. L. Wagner, J.D. Klein, J.M. Sands, C. Baylis, Urea transporters are distributed in endothelial cells and mediate inhibition of L-arginine transport. Am. J. Physiol. Renal Physiol. **283**, F578–F582 (2002)

28. H. Tsukaguchi, C. Shayakul, U.V. Berger, T. Tokui, D. Brown, M.A. Hediger, Cloning and characterization of the urea transporter UT3: localization in rat kidney and testis. J. Clin. Invest. **99**, 1506–1515 (1997)

29. Y.S. Kwun, S.W. Yeo, Y.H. Ahn, S.W. Lim, J.Y. Jung, W.Y. Kim, J.M. Sands, J. Kim, Immunohistochemical localization of urea transporters A and B in the rat cochlea. Hear. Res. **183**, 84–96 (2003)

30. R. Duchesne, J.D. Klein, J.B. Velotta, J.J. Doran, P. Rouillard, B.R. Roberts, A.A. McDonough, J.M. Sands, UT-A urea transporter protein in heart: increased abundance during uremia, hypertension, and heart failure. Circ. Res. **89**, 139–145 (2001)

31. R.A. Fenton, G.J. Cooper, I.D. Morris, C.P. Smith, Coordinated expression of UT-A and UT-B urea transporters in rat testis. Am. J. Physiol. Cell Physiol. **282**, C1492–C1501 (2002)

32. M.A. Blount, J.D. Klein, C.F. Martin, D. Tchapyjnikov, J.M. Sands, Forskolin stimulates phosphorylation and membrane accumulation of UT-A3. Am. J. Physiol. Renal Physiol. **293**, F1308–F1313 (2007)

33. A.C. Mistry, R. Mallick, J.D. Klein, J.M. Sands, O. Frohlich, Functional characterization of the central hydrophilic linker region of the urea transporter UT-A1: cAMP activation and snapin binding. Am. J. Physiol. Cell Physiol. **298**, C1431–C1437 (2010)

34. M.-M. Trinh-Trang-Tan, F. Lasbennes, P. Gane, N. Roudier, P. Ripoche, J.-P. Cartron, P. Bailly, UT-B1 proteins in rat: tissue distribution and regulation by antidiuretic hormone in kidney. Am. J. Physiol. Renal Physiol. **283**, F912–F922 (2002)

35. T. Peng, J.M. Sands, S.M. Bagnasco, Glucocorticoids inhibit transcription and expression of the UT-A urea transporter gene. Am. J. Physiol. Renal Physiol. **282**, F853–F858 (2002)

36. R.A. Fenton, C.L. Chou, S. Ageloff, W. Brandt, J.B. Stokes, M.A. Knepper, Increased collecting duct urea transporter expression in Dahl salt-sensitive rats. Am. J. Physiol. Renal Physiol. **285**, F143–F151 (2003)

37. D. Kim, J.D. Klein, S. Racine, B.P. Murrell, J.M. Sands, Urea may regulate urea transporter protein abundance during osmotic diuresis. Am. J. Physiol. Renal Physiol. **288**, F188–F197 (2005)

38. H. Inoue, S.D. Kozlowski, J.D. Klein, J.L. Bailey, J.M. Sands, S.M. Bagnasco, Regulated expression of renal and intestinal UT-B urea transporter in response to varying urea load. Am. J. Physiol. Renal Physiol. **289**, F451–F458 (2005)

39. J.M. Sands, F.X. Flores, A. Kato, M.A. Baum, E.M. Brown, D.T. Ward, S.C. Hebert, H.W. Harris, Vasopressin-elicited water and urea permeabilities are altered in IMCD in hypercalcemic rats. Am. J. Phys. **274**, F978–F985 (1998)

40. S. Goldfarb, Z.S. Agus, Mechanism of the polyuria of hypercalcemia. Am. J. Nephrol. **4**, 69–76 (1984)

41. U.S. Jeon, K.H. Han, S.H. Park, S.D. Lee, M.R. Sheen, J.Y. Jung, W.Y. Kim, J.M. Sands, J. Kim, H.M. Kwon, Downregulation of renal TonEBP in hypokalemic rats. Am. J. Physiol. Renal Physiol. **293**, F408–F415 (2007)

42. S. Combet, N. Geffroy, V. Berthonaud, B. Dick, L. Teillet, J.M. Verbavatz, B. Corman, M.M. Trinh-Trang-Tan, Correction of age-related polyuria by dDAVP: molecular analysis of aquaporins and urea transporters. Am. J. Physiol. Renal Physiol. **284**, F199–F208 (2003)

43. M.C. Reif, S.L. Troutman, J.A. Schafer, Sustained response to vasopressin in isolated rat cortical collecting tubule. Kidney Int. **26**, 725–732 (1984)

44. A.S. Rocha, L.H. Kudo, Water, urea, sodium, chloride, and potassium transport in the in vitro isolated perfused papillary collecting duct. Kidney Int. **22**, 485–491 (1982)

45. S.M. Wall, J.S. Han, C.L. Chou, M.A. Knepper, Kinetics of urea and water permeability activation by vasopressin in rat terminal IMCD. Am. J. Phys. **262**, F989–F998 (1992)

46. J.M. Sands, H. Nonoguchi, M.A. Knepper, Vasopressin effects on urea and H2O transport in inner medullary collecting duct subsegments. Am. J. Phys. **253**, F823–F832 (1987)

47. C.L. Chou, M.A. Knepper, Inhibition of urea transport in inner medullary collecting duct by phloretin and urea analogues. Am. J. Phys. **257**, F359–F365 (1989)

48. R.A. Star, H. Nonoguchi, R. Balaban, M.A. Knepper, Calcium and cyclic adenosine monophosphate as second messengers for vasopressin in the rat inner medullary collecting duct. J. Clin. Invest. **81**, 1879–1888 (1988)

49. J.M. Sands, D.C. Schrader, An independent effect of osmolality on urea transport in rat terminal inner medullary collecting ducts. J. Clin. Invest. **88**, 137–142 (1991)

50. J.B. Stokes, Potassium secretion by cortical collecting tubule: relation to sodium absorption, luminal sodium concentration, and transepithelial voltage. Am. J. Phys. **241**, F395–F402 (1981)

51. S. Nielsen, M.A. Knepper, Vasopressin activates collecting duct urea transporters and water channels by distinct physical processes. Am. J. Phys. **265**, F204–F213 (1993)

52. H. Nonoguchi, A. Owada, N. Kobayashi, M. Takayama, Y. Terada, J. Koike, K. Ujiie, F. Marumo, T. Sakai, K. Tomita, Immunohistochemical localization of V2 vasopressin receptor along the nephron and functional role of luminal V2 receptor in terminal inner medullary collecting ducts. J. Clin. Invest. **96**, 1768–1778 (1995)

53. A.D. Bansal, J.D. Hoffert, T. Pisitkun, S. Hwang, C.L. Chou, E.S. Boja, G. Wang, M.A. Knepper, Phosphoproteomic profiling reveals vasopressin-regulated phosphorylation sites in collecting duct. J. Am. Soc. Nephrol. **21**, 303–315 (2010)

54. J.L. Bos, Epac: a new cAMP target and new avenues in cAMP research. Nat. Rev. Mol. Cell Biol. **4**, 733–738 (2003)

55. J.D. Hoffert, T. Pisitkun, G. Wang, R.F. Shen, M.A. Knepper, Quantitative phosphoproteomics of vasopressin-sensitive renal cells: regulation of aquaporin-2 phosphorylation at two sites. Proc. Natl. Acad. Sci. USA **103**, 7159–7164 (2006)

56. E.J. Hoorn, J.D. Hoffert, M.A. Knepper, Combined proteomics and pathways analysis of collecting duct reveals a protein regulatory network activated in vasopressin escape. J. Am. Soc. Nephrol. **16**, 2852–2863 (2005)

57. P. Uawithya, T. Pisitkun, B.E. Ruttenberg, M.A. Knepper, Transcriptional profiling of native inner medullary collecting duct cells from rat kidney. Physiol. Genomics **32**, 229–253 (2008)

58. M.J. Yu, T. Pisitkun, G. Wang, J.F. Aranda, P.A. Gonzales, D. Tchapyjnikov, R.F. Shen, M.A. Alonso, M.A. Knepper, Large-scale quantitative LC-MS/MS analysis of detergent-resistant membrane proteins from rat renal collecting duct. Am. J. Physiol. Cell Physiol. **295**, C661–C678 (2008)

59. C. Zhang, J.M. Sands, J.D. Klein, Vasopressin rapidly increases phosphorylation of UT-A1 urea transporter in rat IMCDs through PKA. Am. J. Physiol. Renal Physiol. **282**, F85–F90 (2002)

60. O. Frohlich, J.D. Klein, P.M. Smith, J.M. Sands, R.B. Gunn, Urea transport in MDCK cells that are stably transfected with UT-A1. Am. J. Physiol. Cell Physiol. **286**, C1264–C1270 (2004)

61. O. Frohlich, J.D. Klein, P.M. Smith, J.M. Sands, R.B. Gunn, Regulation of UT-A1-mediated transepithelial urea flux in MDCK cells. Am. J. Physiol. Cell Physiol. **291**, C600–C606 (2006)

62. J.D. Klein, O. Fröhlich, A.C. Mistry, K.J. Kent, C.F. Martin, J.M. Sands, Transgenic mice expressing UT-A1, but lacking UT-A3, have intact urine concentrating ability. FASEB J. **27**, 1111.1117 (2013)

63. H. Su, C.B. Carter, O. Laur, J.M. Sands, G. Chen, Forskolin stimulation promotes urea transporter UT-A1 ubiquitination, endocytosis, and degradation in MDCK cells. Am. J. Physiol. Renal Physiol. **303**, F1325–F1332 (2012)

64. M.N. Helms, X.J. Chen, S. Ramosevac, D.C. Eaton, L. Jain, Dopamine regulation of amiloride-sensitive sodium channels in lung cells. Am. J. Physiol. Lung Cell. Mol. Physiol. **290**, L710–L722 (2006)

65. K.J. Honegger, P. Capuano, C. Winter, D. Bacic, G. Stange, C.A. Wagner, J. Biber, H. Murer, N. Hernando, Regulation of sodium-proton exchanger isoform 3 (NHE3) by PKA and exchange protein directly activated by cAMP (EPAC). Proc. Natl. Acad. Sci. USA **103**, 803–808 (2006)

66. N. Laroche-Joubert, S. Marsy, S. Michelet, M. Imbert-Teboul, A. Doucet, Protein Kinase A-independent Activation of ERK and H,K-ATPase by cAMP in Native Kidney Cells. J. Biol. Chem. **277**, 18598–18604 (2002)

67. S.K. Yang, L. Xiao, J. Li, F. Liu, L. Sun, Y.S. Kanwar, Role of guanine-nucleotide exchange factor Epac in renal physiology and pathophysiology. Am. J. Physiol. Renal Physiol. **304**, F831–F839 (2013)

68. Y. Wang, J.D. Klein, M.A. Blount, C.F. Martin, K.J. Kent, V. Pech, S.M. Wall, J.M. Sands, Epac regulates UT-A1 to increase urea transport in inner medullary collecting ducts. J. Am. Soc. Nephrol. **20**, 2018–2024 (2009)

69. M.A. Blount, A.C. Mistry, O. Frohlich, S.R. Price, G. Chen, J.M. Sands, J.D. Klein, Phosphorylation of UT-A1 urea transporter at serines 486 and 499 is important for vasopressin-regulated activity and membrane accumulation. Am. J. Physiol. Renal Physiol. **295**, F295–F299 (2008)

70. J.D. Klein, M.A. Blount, O. Frohlich, C.E. Denson, X. Tan, J.H. Sim, C.F. Martin, J.M. Sands, Phosphorylation of UT-A1 on serine 486 correlates with membrane accumulation and urea transport activity in both rat IMCDs and cultured cells. Am. J. Physiol. Renal Physiol. **298**, F935–F940 (2010)

71. S. Hwang, R. Gunaratne, M.M. Rinschen, M.J. Yu, T. Pisitkun, J.D. Hoffert, R.A. Fenton, M.A. Knepper, C.L. Chou, Vasopressin increases phosphorylation of Ser84 and Ser486 in Slc14a2 collecting duct urea transporters. Am. J. Physiol. Renal Physiol. **299**, F559–F567 (2010)

72. J.D. Klein, C.F. Martin, K.J. Kent, J.M. Sands, Protein kinase C-alpha mediates hypertonicity-stimulated increase in urea transporter phosphorylation in the inner medullary collecting duct. Am. J. Physiol. Renal Physiol. **302**, F1098–F1103 (2012)

73. T.L. Thai, M.A. Blount, J.D. Klein, J.M. Sands, Lack of protein kinase C-alpha leads to impaired urine concentrating ability and decreased aquaporin-2 in angiotensin II-induced hypertension. Am. J. Physiol. Renal Physiol. **303**, F37–F44 (2012)

74. Y. Wang, J.D. Klein, O. Froehlich, J.M. Sands, Role of protein kinase C-alpha in hypertonicity-stimulated urea permeability in mouse inner medullary collecting ducts. Am. J. Physiol. Renal Physiol. **304**, F233–F238 (2013)

75. M.A. Blount, P. Cipriani, S.K. Redd, R.J. Ordas, L.N. Black, D.L. Gumina, C.A. Hoban, J.D. Klein, J.M. Sands, Activation of protein kinase Cα increases phosphorylation of the UT-A1 urea transporter at serine 494 in the inner medullary collecting duct. Am. J. Physiol. Cell Physiol. **309**, C608–C615 (2015)

76. T.O. Ilori, Y. Wang, M.A. Blount, C.F. Martin, J.M. Sands, J.D. Klein, Acute calcineurin inhibition with tacrolimus increases phosphorylated UT-A1. Am. J. Physiol. Renal Physiol. **302**, F998–F1004 (2012)

77. Y. Wang, J.D. Klein, J.M. Sands, Phosphatases decrease water and urea permeability in rat inner medullary collecting ducts. Int. J. Mol. Sci. **24** (2023)

78. G. Chen, H. Huang, O. Frohlich, Y. Yang, J.D. Klein, S.R. Price, J.M. Sands, MDM2 E3 ubiquitin ligase mediates UT-A1 urea transporter ubiquitination and degradation. Am. J. Physiol. Renal Physiol. **295**, F1528–F1534 (2008)

79. G.S. Stewart, J.H. O'Brien, C.P. Smith, Ubiquitination regulates the plasma membrane expression of renal UT-A urea transporters. Am. J. Physiol. Cell Physiol. **295**, C121–C129 (2008)

80. Klein, J. D. (2014) Expression of urea transporters and their regulation. Subcell. Biochem. 73, 79–107, Springer Netherlands

81. H. Su, M. Chen, J.M. Sands, G. Chen, Activation of the cAMP/PKA pathway induces UT-A1 urea transporter monoubiquitination and targets it for lysosomal degradation. Am. J. Physiol. Renal Physiol. **305**, F1775–F1782 (2013)

82. R.A. Gertner, J.D. Klein, J.L. Bailey, D.U. Kim, X.H. Luo, S.M. Bagnasco, J.M. Sands, Aldosterone decreases UT-A1 urea transporter expression via the mineralocorticoid receptor. J. Am. Soc. Nephrol. **15**, 558–565 (2004)

83. M.A. Knepper, R.A. Danielson, G.M. Saidel, K.H. Johnston, Effects of dietary protein restriction and glucocorticoid administration on urea excretion in rats. Kidney Int. **8**, 303–315 (1975)

84. M. Naruse, J.D. Klein, Z.M. Ashkar, J.D. Jacobs, J.M. Sands, Glucocorticoids downregulate the vasopressin-regulated urea transporter in rat terminal inner medullary collecting ducts. J. Am. Soc. Nephrol. **8**, 517–523 (1997)

85. D. Kim, J.M. Sands, J.D. Klein, Role of vasopressin in diabetes mellitus-induced changes in medullary transport proteins involved in urine concentration in Brattleboro rats. Am. J. Physiol. Renal Physiol. **286**, F760–F766 (2004)

86. J.M. Sands, Renal urea transporters. Curr. Opin. Nephrol. Hypertens. **13**, 525–532 (2004)

87. Y. Kakinuma, A. Fogo, T. Inagami, I. Ichikawa, Intrarenal localization of angiotensin II type 1 receptor mRNA in the rat. Kidney Int. **43**, 1229–1235 (1993)

88. A. Sasaki, O. Kida, T. Kita, J. Kato, S. Nakamura, K. Kodama, A. Miyata, K. Kangawa, H. Matsuo, K. Tanaka, Effects of antiserum against alpha-rat atrial natriuretic polypeptide in spontaneously hypertensive rats. Am. J. Phys. **257**, H1104–H1109 (1989)

89. Y. Terada, K. Tomita, H. Nonoguchi, F. Marumo, PCR localization of angiotensin II receptor and angiotensinogen mRNAs in rat kidney. Kidney Int. **43**, 1251–1259 (1993)

90. Y. Nakayama, T. Peng, J.M. Sands, S.M. Bagnasco, The TonE/TonEBP pathway mediates tonicity-responsive regulation of UT-A urea transporter expression. J. Biol. Chem. **275**, 38275–38280 (2000)

91. A. Kato, J.D. Klein, C. Zhang, J.M. Sands, Angiotensin II increases vasopressin-stimulated facilitated urea permeability in rat terminal IMCDs. Am. J. Physiol. Renal Physiol. **279**, F835–F840 (2000)

92. J.D. Klein, D. Le Quach, J.M. Cole, K. Disher, A.K. Mongiu, X. Wang, K.E. Bernstein, J.M. Sands, Impaired urine concentration and absence of tissue ACE: involvement of medullary transport proteins. Am. J. Physiol. Renal Physiol. **283**, F517–F524 (2002)

93. M.A. Knepper, C.V. Gunter, R.A. Danielson, Effects of glucagon on renal function in protein-deprived rats. Surg. Forum **27**, 29–31 (1976)
94. M. Ahloulay, N. Bouby, F. Machet, M. Kubrusly, C. Coutaud, L. Bankir, Effects of glucagon on glomerular filtration rate and urea and water excretion. Am. J. Phys. **263**, F24–F36 (1992)
95. T. Isozaki, A.G. Gillin, C.E. Swanson, J.M. Sands, Protein restriction sequentially induces new urea transport processes in rat initial IMCD. Am. J. Phys. **266**, F756–F761 (1994)
96. Y. Maeda, Y. Terada, H. Nonoguchi, M.A. Knepper, Hormone and autacoid regulation of cAMP production in rat IMCD subsegments. Am. J. Phys. **263**, F319–F327 (1992)
97. C.L. Chou, S.R. DiGiovanni, A. Luther, S.J. Lolait, M.A. Knepper, Oxytocin as an antidiuretic hormone. II. Role of V2 vasopressin receptor. Am. J. Phys. **269**, F78–F85 (1995)
98. J.H. Galla, B.B. Booker, R.G. Luke, Role of the loop segment in the urinary concentrating defect of hypercalcemia. Kidney Int. **29**, 977–982 (1986)
99. L.H. Kudo, K.R. Cesar, W.C. Ping, A.S. Rocha, Effect of peritubular hypertonicity on water and urea transport of inner medullary collecting duct. Am. J. Phys. **262**, F338–F347 (1992)
100. A.G. Gillin, J.M. Sands, Characteristics of osmolarity-stimulated urea transport in rat IMCD. Am. J. Phys. **262**, F1061–F1067 (1992)
101. A.G. Gillin, R.A. Star, J.M. Sands, Osmolarity-stimulated urea transport in rat terminal IMCD: role of intracellular calcium. Am. J. Phys. **265**, F272–F277 (1993)
102. Y. Wang, J.D. Klein, C.M. Liedtke, J.M. Sands, Protein kinase C regulates urea permeability in the rat inner medullary collecting duct. Am. J. Physiol. Renal Physiol. **299**, F1401–F1406 (2010)
103. J.D. Klein, O. Frohlich, M.A. Blount, C.F. Martin, T.D. Smith, J.M. Sands, Vasopressin increases plasma membrane accumulation of urea transporter UT-A1 in rat inner medullary collecting ducts. J. Am. Soc. Nephrol. **17**, 2680–2686 (2006)
104. V.S. Issa, L. Andrade, S.M. Ayub-Ferreira, F. Bacal, A.C. de Braganca, G.V. Guimaraes, F.G. Marcondes-Braga, F.D. Cruz, P.R. Chizzola, G.E. Conceicao-Souza, I.T. Velasco, E.A. Bocchi, Hypertonic saline solution for prevention of renal dysfunction in patients with decompensated heart failure. Int. J. Cardiol. **167**, 34–40 (2013)
105. W. Jin, X. Yao, T. Wang, Q. Ji, Y. Li, X. Yang, L. Yao, Effects of hyperosmolality on expression of urea transporter A2 and aquaporin 2 in mouse medullary collecting duct cells. J. Huazhong Univ. Sci. Technolog. Med. Sci. **32**, 59–64 (2012)
106. Y. Yamaguchi, S. Takaki, S. Hyodo, Subcellular distribution of urea transporter in the collecting tubule of shark kidney is dependent on environmental salinity. J. Exp. Zool. A Ecol. Genet. Physiol. **311**, 705–718 (2009)
107. Z.M. Ashkar, S. Martial, T. Isozaki, S.R. Price, J.M. Sands, Urea transport in initial IMCD of rats fed a low-protein diet: functional properties and mRNA abundance. Am. J. Phys. **268**, F1218–F1223 (1995)
108. L. Bankir, K. Chen, B. Yang, Lack of UT-B in vasa recta and red blood cells prevents urea-induced improvement of urinary concentrating ability. Am. J. Physiol. Renal Physiol. **286**, F144–F151 (2004)
109. M. Levi, L. Peterson, T. Berl, Mechanism of concentrating defect in hypercalcemia. Role of polydipsia and prostaglandins. Kidney Int. **23**, 489–497 (1983)
110. A. Kato, J.M. Sands, Urea transport processes are induced in rat IMCD subsegments when urine concentrating ability is reduced. Am. J. Phys. **276**, F62–F71 (1999)
111. J.Y. Jung, H.M. Kwon, J. Kim, Regulation of urea transporters by tonicity-responsive enhancer binding protein. Electrolyte Blood Press **5**, 28–33 (2007)
112. J.M. Sands, Urine concentrating and diluting ability during aging. J. Gerontol. A Biol. Sci. Med. Sci. **67**, 1352–1357 (2012)
113. C. Li, J.D. Klein, W. Wang, M.A. Knepper, S. Nielsen, J.M. Sands, J. Frokiaer, Altered expression of urea transporters in response to ureteral obstruction. Am. J. Physiol. Renal Physiol. **286**, F1154–F1162 (2004)
114. F. Rianto, A. Kuma, C.L. Ellis, F. Hassounah, E.L. Rodriguez, X.H. Wang, J.M. Sands, J.D. Klein, UT-A1/A3 knockout mice show reduced fibrosis following unilateral ureteral obstruction. Am. J. Physiol. Renal Physiol. **318**, F1160–F1166 (2020)

115. X.Y. Wang, K. Beutler, J. Nielsen, S. Nielsen, M.A. Knepper, S. Masilamani, Decreased abundance of collecting duct urea transporters UT-A1 and UT-A3 with ECF volume expansion. Am. J. Physiol. Renal Physiol. **282**, F577–F584 (2002)
116. S.W. Lim, C. Li, B.K. Sun, K.H. Han, W.Y. Kim, Y.W. Oh, J.U. Lee, P.F. Kador, M.A. Knepper, J.M. Sands, J. Kim, C.W. Yang, Long-term treatment with cyclosporine decreases aquaporins and urea transporters in the rat kidney. Am. J. Physiol. Renal Physiol. **287**, F139–F151 (2004)
117. J.D. Klein, R.B. Gunn, B.R. Roberts, J.M. Sands, Down-regulation of urea transporters in the renal inner medulla of lithium-fed rats. Kidney Int. **61**, 995–1002 (2002)
118. J.D. Klein, M.A. Blount, J.M. Sands, Molecular mechanisms of urea transport in health and disease. Pflugers Arch. **464**, 561–572 (2012)
119. J.D. Klein, Y. Wang, M.A. Blount, P.A. Molina, L.M. LaRocque, J.A. Ruiz, J.M. Sands, Metformin, an AMPK activator, stimulates the phosphorylation of aquaporin 2 and urea transporter A1 in inner medullary collecting ducts. Am. J. Physiol. Renal Physiol. **310**, F1008–F1012 (2016)
120. O. Efe, J.D. Klein, L.M. LaRocque, H. Ren, J.M. Sands, Metformin improves urine concentration in rodents with nephrogenic diabetes insipidus. JCI Insight **1** (2016)

Chapter 4
Biochemical Modification and Subcellular Trafficking of Urea Transporters

Xuechen Li and Guangping Chen

Abstract Urea and urea transporters (UT) are critical to the production of concentrated urine and hence in maintaining body fluid balance. The UT-A1 urea transporter is the major and most important UT isoform in the kidney. Native UT-A1, expressed in the terminal inner medullary collecting duct (IMCD) epithelial cells, is a glycosylated protein with two glycoforms of 117 and 97 kDa. Vasopressin is the major hormone *in vivo* that rapidly increases urea permeability in the IMCD through increasing the phosphorylation and apical plasma membrane accumulation of UT-A1. The cell signaling pathway for vasopressin-mediated UT-A1 phosphorylation and activity involves two cAMP-dependent signaling pathways: protein kinase A (PKA) and exchange protein activated by cAMP (Epac). UT-A3 is the NH_2-terminal half of UT-A1, exhibiting similarities and dissimilarities with UT-A1. In this chapter, we will discuss UT-A1 and UT-A3 regulation by phosphorylation, ubiquitination and glycosylation.

Keywords Urinary concentration · Vasopressin · Phosphorylation · Ubiquitination · Glycosylation

X. Li (✉)
Institute of Materia Medica, Chinese Academy of Medical Science & Peking Union Medical College, Beijing, China
e-mail: xli@imm.ac.cn

G. Chen
Department of Physiology and Renal Division, Department of Medicine, Emory University, Atlanta, GA, USA

Phosphorylation of Urea Transporters

A tubular perfusion study by Sands et al. [1] in 1987 first demonstrated that the terminal IMCD exhibits a high basal urea permeability. This activity is dramatically increased in the presence of the hormone vasopressin. The first UT-A urea transporter, UT-A2, was cloned by You et al. [2] in 1991 and was characterized as the vasopressin-regulated urea transporter. Vasopressin [AVP; also known as anti-diuretic hormone (ADH)], synthesized in the hypothalamus and stored in vesicles in the posterior pituitary, is the major hormone regulating urine-concentrating ability. Vasopressin increases both osmotic water and urea permeabilities in principal cells in the kidney collecting duct [3–6]. Knockout of UT-A1, or both UT-A1 and UT-A3, results in a significant diuretic effect in mice [7–9]. Using [^{32}P] radioisotope labeling techniques in IMCD suspensions, Zhang et al. [10] in 2002 provided the first experimental evidence that UT-A1 is directly phosphorylated by vasopressin. Subsequently, new technologies, such as proteomic and cDNA array, have identified UT-A1, as well as UT-A3, as the phosphorylated proteins stimulated by vasopressin in the inner medulla [11–16]. Adding vasopressin (or the cAMP stimulator forskolin) to IMCD suspensions rapidly increases the abundance of phosphorylated UT-A1 at 2 min, which peaks at 5~10 min, and remains elevated for up to 30 min [10]. The time course and dose response of UT-A1 phosphorylation are identical to vasopressin-induced stimulation of urea permeability observed by Wall et al. [6] in 1992 in perfused rat terminal IMCDs. Vasopressin also increases the phosphorylation of UT-A1 in UT-A1-MDCK cells [17, 18] and UT-A1-mIMCD3 cells [19]. The role of UT-A1 phosphorylation for vasopressin-stimulated activity and trafficking to the IMCD apical plasma membrane was further emphasized by Blount et al. [20] using phosphomutant forms of UT-A1 heterologously expressed in cultured cells.

Vasopressin Signaling Pathway Mediating UT-A1 Phosphorylation

Star et al. [21] in 1988 used isolated perfused tubules to demonstrate that both vasopressin-regulated urea transport and vasopressin-regulated water transport are dependent on a rise in intracellular cyclic AMP levels. The addition of vasopressin to the basolateral membrane of a rat terminal IMCD stimulates kidney urea permeability via the V2 vasopressin receptor. This is mimicked by a selective V2 agonist, dDAVP, in perfused terminal IMCDs [21]. Vasopressin binds to the IMCD cell V2 receptor in the basolateral plasma membrane, activates the heterotrimeric G protein Gαs, and results in an increased generation of cAMP by at least two adenylyl cyclase isoforms, III and VI [1, 6, 10, 22]. Rat, mouse, and human UT-A1 are stimulated by cAMP when expressed in Xenopus oocytes [23–26]. One important downstream kinase activated by increased cAMP is PKA. A study by Zhang et al. [10] showed that the PKA inhibitor H89 significantly suppresses vasopressin-stimulated UT-A1

phosphorylation. These studies indicate that UT-A1 is phosphorylated, possibly by PKA directly. In vitro assays using synthetic UT-A1 peptides showed that purified PKA can directly phosphorylate UT-A1 [11]. Inhibitors of PKA reduce both the vasopressin-stimulated and basal levels of UT-A1 phosphorylation, showing that PKA can phosphorylate UT-A1, both basally and in response to vasopressin stimulation [10].

Though cyclic AMP is traditionally believed to act through PKA, a study by Fröhlich et al. [18] noticed that the PKA inhibitor H-89 could not completely inhibit forskolin-induced urea flux in UT-A1-MDCK cells. The portion of the non-PKA effect caused by elevated cAMP raises the possibility that vasopressin may have a second cAMP-dependent, but non-PKA-mediated, signaling pathway in rat IMCDs. In addition to acting through PKA, cAMP can activate Epac (exchange protein activated by cAMP) [27–31]. There are two closely related Epac proteins, Epac1 and Epac2, and both have been detected in rat IMCDs [29, 30]. Functional analysis showed that incubation of rat IMCD suspensions with the Epac activator Sp-8-pCPT-2′-O-Me-cAMPS causes an increase in UT-A1 phosphorylation and its accumulation in the plasma membrane [31]. Epac activates Rap1, a Ras-related small molecular weight G protein, which in turn signals through mitogen-activated protein kinase kinase (MEK) and extracellular signal-related kinase (ERK). Inhibition of MEK 1/2 phosphorylation by U0126 decreased the forskolin-stimulated UT-A1 phosphorylation [31]. Thus, as illustrated in Fig. 4.1, UT-A1 phosphorylation is stimulated by vasopressin in the IMCD through at least two cAMP-dependent signaling pathways: PKA-dependent and Epac-MEK-dependent pathways.

UT-A1 Phosphorylation by PKA

The rat UT-A1 amino acid sequence contains multiple consensus PKA phosphorylation motifs (x-(R/K)-(R/K)-x-(S/T)-(^P): 3 phosphorylation sites in the N-terminus, 6 in the large intracellular loop, and 1 in the C-terminus. Mass spectrometry-based phosphoproteomic analysis of rat collecting ducts by Hoffert [13] and later by Bansal [11] suggested several cAMP-PKA sites including Ser10, Ser62, Ser63, Ser84, Ser486,and Ser499. Among these sites, three are highly demonstrated by mass spectrometry to be regulated by vasopressin: Ser84, Ser486, and Ser499 [11]. Although the UT-A1 amino acid sequence possesses many potential PKA phosphorylation sites, including both serine and threonine residues, phosphoproteomic analysis [11, 13] only shows phosphorylation of serine residues. This is in agreement with an early observation by Zhang et al. [10] that vasopressin does not phosphorylate the UT-A1 tyrosine residue. The anti-phosphotyrosine antibody (PY-20) did not recognize any proteins from UT-A1 immunoprecipitated samples from IMCD suspensions.

Serine 486 and serine 499 in the central intracellular loop of UT-A1 have been experimentally reported to serve as cAMP-PKA phosphorylation sites by two independent laboratories [11, 13, 19, 20]. Ser499 is highly evolutionary conserved
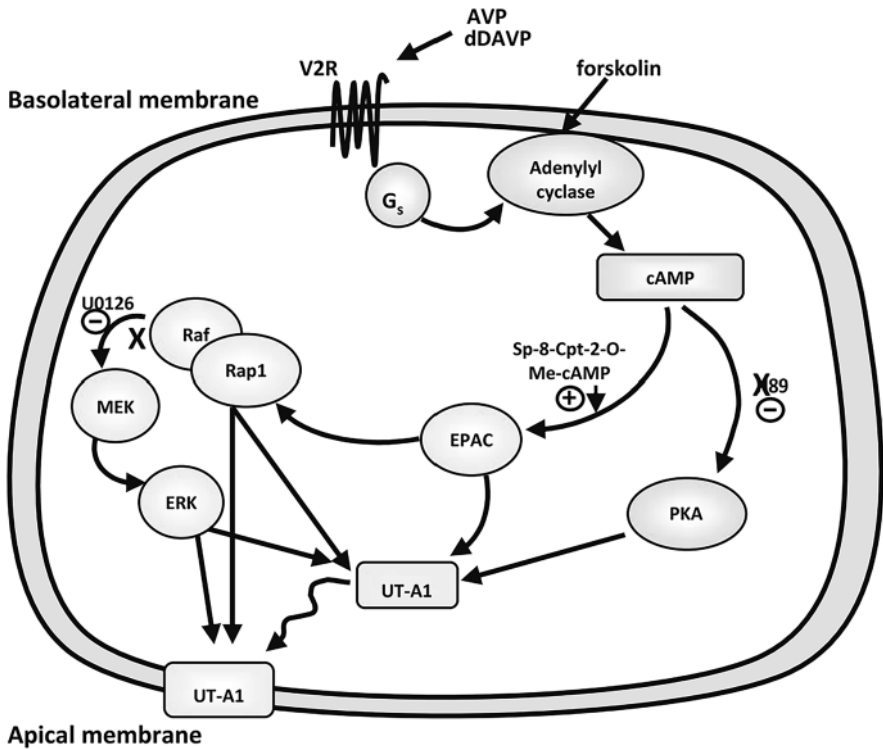
Fig. 4.1 UT-A1 phosphorylation signaling pathways mediated by vasopressin [31]. Protein kinase A (PKA)-dependent and exchange protein activated by cAMP (Epac)-mitogen-activated protein kinase (MEK)-dependent pathways

across rat, mouse, horse, cow, and human UT-A1. Ser486 is also conserved in all of these species except for cows, where it is an asparagine residue. Mutation of both Ser486 and Ser499, but not either one alone, eliminates forskolin's ability to stimulate UT-A1 accumulation in the apical plasma membrane and urea transport, indicating that at least one of these serines must be phosphorylated [20]. The double mutant was unable to traffic to the plasma membrane, showing that phosphorylation of UT-A1 at these sites is critical to urea transport and trafficking [20]. Using phosphosite-specific antibodies at Ser486 and Ser499, the UT-A1 phosphorylation at these two sites in response to vasopressin is found to be similar, which increased at the same rate within 1 min, reached the maximum at 2 min and maintained stable within 20 min [32]. Site-directed mutagenesis confirms that the phosphorylation at these two sites occurs independently. In addition, Ser486-phosphorylated and Ser499-phosphorylated UT-A1 are primarily expressed in the apical plasma membrane in rat IMCDs (Fig. 4.2) [19, 32]. Epac stimulation does not change UT-A1 phosphorylation at Ser486 and Ser499 in mIMCD3 UT-A1 cells [32], further confirming that UT-A1 phosphorylation at these two sites is independent of vasopressin-sensitive Epac pathway.
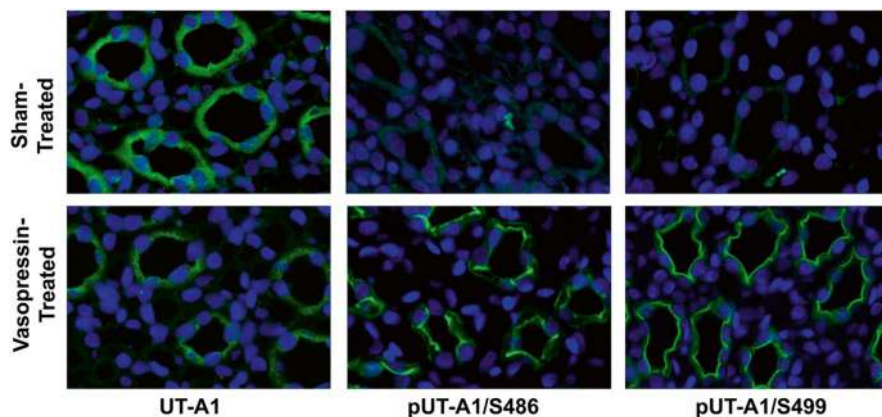
Fig. 4.2 Phosphorylated UT-A1 located in the apical membrane of rat IMCDs [32]. Immunofluorescence was applied to detect phosphorylated UT-A1 at Ser486 or Ser499 in Sprague-Dawley rats injected with 5 nM vasopressin for 45 min

A third vasopressin-stimulated phosphorylation site in rat UT-A1 at Ser84 has been suggested by phosphoproteomic analysis [11, 13] and confirmed by Hwang et al. [33]. However, Ser84 is less conserved among species. In human UT-A1, Ser84 is not preserved but substituted by aspartic acid. Interestingly, the aspartic acid in humans has the same charge (-1) as a phosphorylated serine. Therefore, it probably represents a constitutively activated form [11].

UT-A1 Phosphorylation by PKC

It is well documented that urea permeability is regulated by vasopressin via cAMP-dependent signaling pathways. PKA activated by cAMP is the most important kinase responsible for UT-A1 phosphorylation, particularly in the presence of vasopressin; however, other kinases may also phosphorylate UT-A1. Several early observations demonstrate that urea permeability in perfused IMCDs is activated by hypertonicity (adding NaCl or mannitol) in the absence of vasopressin [34–36].

Interestingly, hypertonicity does not increase intracellular cAMP levels in the IMCD, but it does increase intracellular calcium [37]. Hypertonicity increases urea permeability via changes in intracellular calcium, suggesting involvement of a calcium-dependent protein kinase in the urea transport response [38]. Subsequent studies show that hypertonicity mediates urea permeability through a calcium-dependent PKC signaling pathway independently of vasopressin [36, 37, 39, 40].

PKC is a family of serine/threonine-related protein kinases that plays a key role in many cellular functions and affect many signal transduction pathways. PKC isoforms can be subclassified into three groups: conventional PKC (cPKC) isoforms (PKCα, βI, βII, and λ); novel PKC isoforms (nPKCs) (PKCδ, ε, η, θ, μ); and

atypical PKC isoforms (aPKCs) (PKCι/λ and ζ) [40]. Seven PKC isoforms are present in rat inner medulla, including PKC α, β, γ, δ, ε, θ, τ, and λ [38]. Consistent with putative PKC phosphorylation sites in UT-A1's amino acid sequence, PKC does phosphorylate UT-A1 [39].

The role of PKC in UT-A1 phosphorylation and urea transport activity regulation has been extensively investigated in PKCα knockout mice [39–41]. PKCα is a calcium-dependent PKC isoform and PKCα-deficient mice have a urine-concentrating defect [39, 42]. Direct evidence using metabolic labeling with ^{32}P-orthophosphate shows that inhibiting PKC prevents the hypertonicity-mediated stimulation of UT-A1 phosphorylation. In IMCD suspensions from PKCα-deficient mice, hypertonicity fails to induce UT-A1 phosphorylation [39, 40]. Klein et al. [39] showed that in response to hypertonicity, UT-A1 phosphorylation was increased; however, phosphorylation at Ser486 was not increased, indicating that PKC does not phosphorylate UT-A1 at the same residue as PKA [39]. Blount et at. in 2015 found that PKC activator phorbol dibutyrate (PDBu) induced UT-A1 phosphorylation at Ser494 [43]. Conversely, among the eight possible phosphorylation sites by PKC, site-directed mutagenesis at only Ser494 results in dampened total UT-A1 phosphorylation. cAMP activation by either PKA or Epac does not change UT-A1 phosphorylation at Ser494 [43], indicating no crosstalk with the PKC-activated pathway.

UT-A1 Phosphorylation by Other Kinases

In addition to being phosphorylated by PKA and PKC, analysis of the UT-A1 amino acid sequence reveals various other potential phosphorylation consensus sites, suggesting that UT-A1 may also be susceptible to other kinases. These phosphorylation recognition sites include: casein kinase I, II (CK1, CK2), GSK3, never in mitosis A (NimA)-related kinase (NEK) 2, phosphoinositide-3-OH-kinase-related kinases (PIKKs), and phosphorylase kinase (PK). Proteomic studies by Knepper's group identified over 200 serine/threonine protein kinases in native collecting duct cells [11, 15]. Rinschen et al. [44] reported that vasopressin activates CaM kinase II in collecting duct cells.

The recognized energy sensor, adenosine monophosphate-activated protein kinase (AMPK), is another activator of UT-A1 phosphorylation. Similar to Na-K-2Cl cotransporter (NKCC2) and aquaporin 2 (AQP2), UT-A1 is directly phosphorylated by AMPK both *in vitro* and in rat IMCDs [45]. Metformin, the AMPK activator, increases urea permeability but not UT-A1 membrane accumulation [45], indicating that AMPK activates UT-A1 already present at membrane by inducing its phosphorylation. This finding suggests that by activating UT-A1 and AQP2 phosphorylation, AMPK might be a therapeutic target for congenital X-linked nephrogenic diabetes insipidus (NDI), which results from type 2 vasopressin receptor (V2R) mutation-induced urine concentrating failure.

## Regulation of UT-A1 Phosphorylation by Dephosphorylation Enzymes

Phosphatases act in an opposite way to kinase/phosphorylases. Undoubtedly, the level of protein phosphorylation is also controlled by dephosphorylation enzymes that catalyze the dephosphorylation of UT-A1. Compared to UT-A1 phosphorylation, the specific phosphatases that act on UT-A1 and the role of dephosphorylation in the activation and transport activity of the urea transporter UT-A1 is relatively less explored. Studies by Zhang et al. [10] and Wang et al. [46] showed that treatment of IMCD suspensions with the phosphatase inhibitors calyculin or okadaic acid could increase the level of phosphorylated UT-A1.

Calcineurin is a calcium-calmodulin-dependent serine threonine phosphatase, also known as protein phosphatase 3 (PPP3CA). It was previously referred to as protein phosphatase 2B (PP2B) [47]. Calcineurin activity is detected in the kidney inner medulla. Ilori et al. [47] investigated the effect of calcineurin and protein phosphatase PP1 and PP2A on the dephosphorylation of UT-A1. Inhibition of these two phosphatases increases phosphorylation of the UT-A1 urea transporter without the use of vasopressin. In vitro perfusion of IMCDs shows that incubation with the calcineurin inhibitor tacrolimus increases urea permeability [47]. Interestingly, inhibition of calcineurin by tacrolimus shows an increase in UT-A1 phosphorylation at Ser486, while inhibition of PP1 and PP2A with calyculin increases total phosphorylated UT-A1 but does not increase Ser486-phosphorylated UT-A1. These results suggest that UT-A1 might be dephosphorylated by multiple phosphatases (like PP2A and calcineurin) and that the PKA-mediated phosphorylation at serine 486 is dephosphorylated by calcineurin.

Regulation of UT-A3 Phosphorylation

UT-A3 is a variant of UT-A1. As illustrated in Fig. 4.3, UT-A3 is the NH$_2$ terminal-half of UT-A1, while UT-A2 be the COOH terminal-half of UT-A1. Out of 929 aa in rUT-A1, UT-A3 consists of 460 aa, with a COOH-terminal domain consisting of 52 aa in the cytoplasm [48]. However, neither UT-A3 nor UT-A2 shares the cytoplasmic central hydrophilic linker region (Lc) of UT-A1, which includes the PKA phosphorylation sites of UT-A1, Ser486 and Ser499.

Unlike UT-A1, UT-A3 is a basolateral membrane transporter expressed in the kidney IMCDs, especially in the IM tip [49–51]. Similar to UT-A1, UT-A3 is activated in response to both vasopressin and hypertonicity (adding sucrose or sodium chloride) stimulation, including increased basolateral membrane accumulation, phosphorylation and urea permeability [33, 52, 53]. There are two phases of UT-A3 trafficking to the basolateral membrane in response to vasopressin (Fig. 4.4). At first, vasopressin increases the cAMP level by activating the V2R and adenylyl cyclase. Then, a rapid activation of UT-A3 occurs within 5–10 min through the
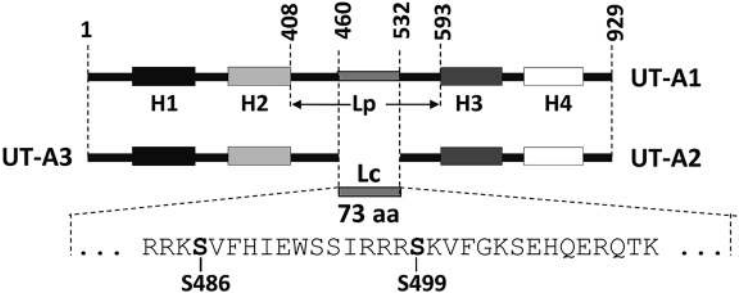
Fig. 4.3 UT-A3 as a variant of UT-A1 [48]. UT-A3 is the NH$_2$-terminal half of UT-A1, consisting of 466 aa with a 52 aa- cytoplasmic COOH-terminal domain
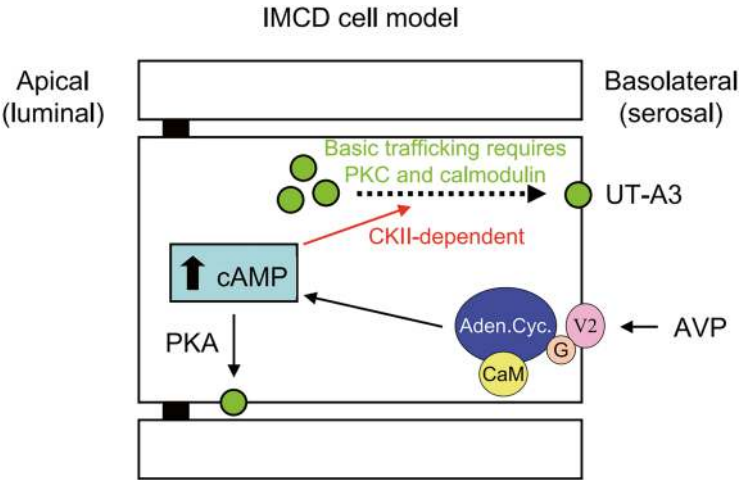
Fig. 4.4 UT-A3 trafficking regulated by vasopressin in IMCDs [54]. Vasopressin increases the cAMP level and activates UT-A3 membrane trafficking through PKA and CK2-dependent pathways

cAMP-PKA pathway. Finally, a slower activation of UT-A3 occurs within 1 h, which is mediated by a CK2-dependent pathway, requiring PKC and calmodulin [54]. However, whether hypertonicity-stimulated UT-A3 activation is mediated by PKC, like UT-A1, requires further investigation.

Although the two PKA phosphorylation sites of UT-A1, Ser486 and Ser499, are not shared in UT-A3, the phosphorylation of UT-A3 is significantly increased in response to vasopressin. Phosphoproteomic profiling has reported that Ser84 is the vasopressin-regulated phosphorylation site present in UT-A3 [11], which is further confirmed in rat IMCDs using phospho-specific antibodies [33].

Ubiquitination of Urea Transporters

Protein degradation is an important mechanism by which cells control the levels of cellular proteins. Eukaryotic cells contain two major proteolytic systems, the lysosome and the 26S proteasome systems, which mediate protein degradation. Membrane proteins are capable of being degraded by the proteasomal and/ or lysosomal pathways, depending on the type of ubiquitination (i.e., monoubiquitin vs. polyubiquitin) and the state of the protein complex (e.g., phosphorylation). Different types of ubiquitin modification of proteins often yield different consequences. Monoubiquitination, which chiefly occurs on the plasma membrane, often involves the trafficking and lysosomal degradation of membrane proteins. In contrast, polyubiquitinated proteins in the cytosol are usually targeted to the proteasome for degradation. Evidence indicates that the ubiquitination process plays an important role in regulating renal transepithelial urea transport [55–58].

UT-A1 Degradation by the Ubiquitin-Proteasome Pathway

An in silico analysis of UT-A1 reveals a consensus MDM2-binding sequence in the intracellular loop, suggesting that ubiquitination/degradation may serve as an important mechanism for UT-A1 regulation. Indeed, studies from Smith's group and our group [55, 56] show that inhibition of ubiquitin-proteasome activity by MG132 or lactacystin decreases UT-A1 degradation and increases cell-surface expression, with a concurrent rise in urea transport activity [55, 56]. Inhibition of the lysosome pathway, however, does not affect UT-A1 degradation [55]. These findings demonstrate that UT-A1 undergoes ubiquitination and is degraded through the proteasome but not the lysosomal proteolytic pathway.

Activation of PKA/cAMP Promotes UT-A1 Ubiquitination and Degradation

Vasopressin regulates urea permeability in the IMCD through increases in UT-A1 phosphorylation and apical plasma-membrane accumulation [10, 19, 20]. Interestingly, forskolin treatment also promotes UT-A1 ubiquitination in UT-A1-MDCK cells [57]. In freshly isolated IMCD suspensions, extended vasopressin treatment (4 h) stimulates UT-A1 ubiquitination and protein degradation [58]. Pretreatment with the PKA inhibitor H89 significantly inhibits forskolin-induced UT-A1 ubiquitination [58]. This indicates that activation of the cAMP/PKA pathway, resulting in UT-A1 phosphorylation, may also trigger the ubiquitination and protein degradation machinery for UT-A1. The resulting ubiquitination of membrane proteins after activation by PKA eventually leads to the attenuation of

signaling processes. This could be the general mechanism for many membrane protein ubiquitination processes, particularly for ligand-induced tyrosine kinase receptor ubiquitination [59–61]. Upon epidermal growth factor (EGF) stimulation, the EGF receptor (EGFR) undergoes rapid dimerization, activation of its intrinsic tyrosine kinase activity, and autophosphorylation at multiple tyrosine sites within its cytoplasmic tail. Tyrosine phosphorylation then recruits the ubiquitin ligase C-Cbl to the EGFR and results in ubiquitination of the EGFR. Ubiquitinated EGFR is then rapidly internalized and degraded [61]. In fact, early studies by Kim [62] and Terris [63] have noted that administering vasopressin to Brattleboro rats (which lack vasopressin) for 5 days decreases UT-A1 protein abundance in the inner medulla. The negative feedback loop of UT-A1 activation and ubiquitination acts as an important mechanism *in vivo* to attenuate the hormonal response by promoting UT-A1 ubiquitination and endocytosis, and facilitating protein degradation, thereby allowing the cell to return to the basal condition.

UT-A1 Monoubiquitination and Lysosomal Degradation

Mature membrane proteins on the cell surface can be modified by the addition of either monoubiquitin or polyubiquitin chains. Interestingly, when compared to ubiquitinated UT-A1 induced by proteasome inhibitor treatment, we observed the much smaller size of ubiquitinated UT-A1 induced by forskolin treatment. This encouraged us to investigate whether forskolin-induced UT-A1 ubiquitination is different. We took the advantage of two specific ubiquitin antibodies for this study: FK1 recognizes only polyubiquitinated proteins, while FK2 detects both monoubiquitinated and polyubiquitinated proteins [58]. Forskolin stimulation induces UT-A1 ubiquitination [57]. However, forskolin-induced UT-A1 ubiquitination is not detected by the FK1 antibody (which only recognizes polyubiquitin) but by the FK2 antibody (which recognizes both mono- and polyubiquitin). This indicates that forskolin-induced UT-A1 ubiquitination is monoubiquitination. Further study showed that the two major PKA phosphorylation sites of UT-A1, at Ser486 and Ser499, are required for forskolin-induced UT-A1 monoubiquitination, since the double mutation of Ser486 and Ser499 reduces forskolin-induced UT-A1 ubiquitination [58]. In contrast, the two PKA phosphorylation sites do not influence UT-A1 ubiquitination caused by the proteasome inhibitor MG132 [58].

By isolating cell plasma membranes using a sucrose-gradient ultracentrifugation or by immune-labeling cell surface UT-A1, we found that forskolin-induced UT-A1 monoubiquitination mainly occurs on the cell membrane [58]. Early studies [55, 56] showed that UT-A1 is ubiquitinated and degraded by the proteasome but not the lysosome proteolytic pathway. However, the proteasome inhibitor MG132 and lactacystin do not block forskolin-induced UT-A1 degradation; on the contrary, forskolin-induced UT-A1 degradation is prevented by the lysosome inhibitor chloroquine [58]. Double immunostaining of UT-A1 and a lysosomal marker confirms

that forskolin-induced UT-A1 enters the lysosome compartment for degradation, which is different from the degradation of non-stimulated UT-A1.

Ubiquitination Regulates UT-A1 Membrane Expression

As a membrane protein, UT-A1 transport activity relies on its presence in the plasma membrane, which is determined by both endocytosis and exocytosis. The importance of ubiquitination in the endocytosis of various membrane proteins has been appreciated in recent years [64–66]. Both monoubiquitination and polyubiquitination can serve as efficient internalization signals [64–66]. Under non-stimulated conditions, inhibition of proteasome activity increases the amount of UT-A1 protein on the cell surface, as reported by Smith et al. [56] and by us [55], indicating that polyubiquitination affects UT-A1 membrane expression.

Although some membrane protein endocytosis is mediated by polyubiquitination or even in an ubiquitination independent manner [67–69], a body of evidence shows that monoubiquitin is an efficient signal for the internalization of membrane proteins such as GPCR, RTKs, hERG, and skAE1 [70–73]. UT-A1 internalization occurs through both caveolae- and clathrin-coated pits (CCP) under non-stimulated conditions [74]. Forskolin-induced UT-A1 monoubiquitination and its endocytosis are blocked by chlorpromazine, as well as K^+ depletion, but not by filipin and nystatin [58]. This indicates that the monoubiquitination-induced UT-A1 internalization is predominantly through a clathrin-mediated route and is subsequently targeted to the lysosome for degradation.
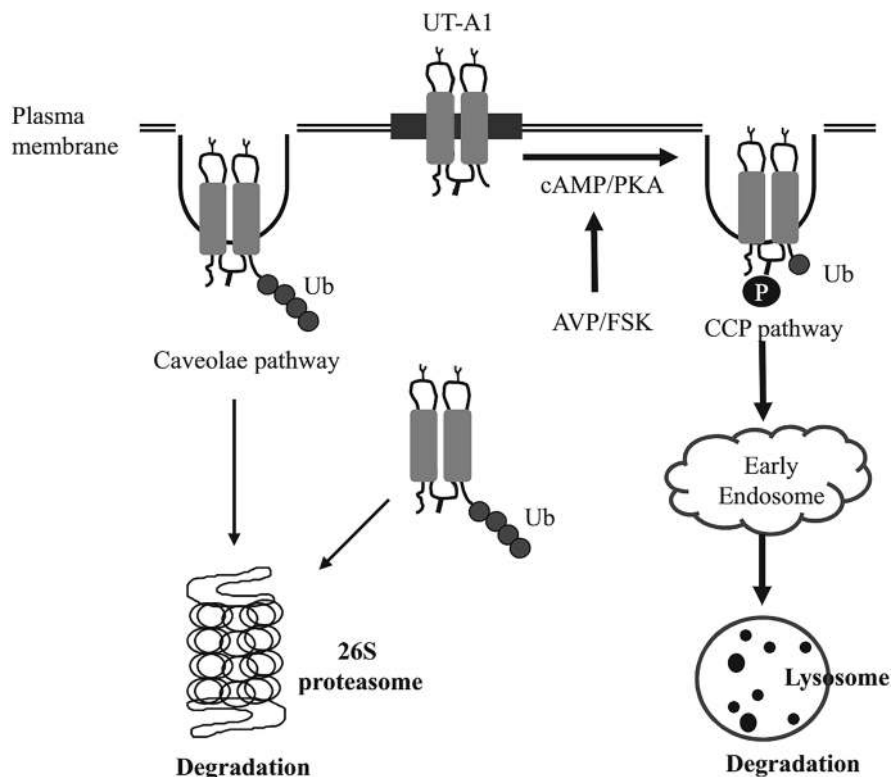
MDM2-Mediated UT-A1 Ubiquitination

Ubiquitination is a posttranslational modification carried out by a cascade of three enzymes: an E1, ubiquitin-activating enzyme, which binds to ubiquitin to generate a high-energy E1-ubiquitin intermediate; an E2, ubiquitin-conjugating enzyme, which is a ubiquitin carrier protein; and an E3, ubiquitin ligase, which transfers ubiquitin to a target protein [75]. UT-A1 has a consensus binding site (FxxxWxx[LIV]) in its intracellular loop for MDM2, a RING finger E3 ligase that ubiquitinates p53 and many other proteins [76]. This sequence is highly conserved among rats, humans, mice, dogs, cattle, and platypuses. Protein binding experiments confirm that UT-A1 can directly interact with MDM2; the binding site is located in the NH2-terminal p53-binding region of MDM2 (30). Functionally, MDM2 mediates UT-A1 ubiquitination in an *in vitro* ubiquitination assay. Overexpression of MDM2 promotes UT-A1 ubiquitination and increases the degradation of UT-A1 protein in HEK293 cells (30). Feng et al. reported that the 14-3-3γ isoform in the 14-3-3 protein family directly interacted with both UT-A1 and MDM2, and cAMP/PKA activation by forskolin improved the interaction, as well as MDM2-mediated UT-A1

ubiquitination [77]. Furthermore, high glucose and angiotensin II also enhances the interaction between UT-A1 and MDM2 [78], therefore boosting MDM2-mediated UT-A1 ubiquitination. However, all of these data come from in vitro studies. It is not clear whether UT-A1 ubiquitination is mediated by MDM2 in tissues and whether other E3 ligases are also involved in UT-A1 ubiquitination. Another important unsolved issue is determining the ubiquitin conjugation sites. UT-A1 possesses a number of lysines dispersed in the intracellular N-terminus, intracellular C-terminus, and the large intracellular loop. However, the lysines that could serve as ubiquitin conjugation sites in UT-A1 have not yet been determined. Further studies are required to identify which lysines are ubiquitinated and whether mutation of these residues affects UT-A1 ubiquitination, protein stability, and membrane accumulation.

In summary, UT-A1 can be polyubiquitinated and degraded through a proteasome pathway and can also be monoubiquitinated and degraded in a lysosome system. The different pathways of UT-A1 ubiquitination and degradation depend on the state of the protein and play distinct roles in response to different physiological situations. Figure 4.5 illustrates UT-A1 ubiquitination, endocytosis, and protein degradation under basal and stimulated conditions. UT-A1 has two endocytic pathways [74] and two protein degradation pathways [55, 56, 58]. The detailed regulatory mechanisms of how UT-A1 is routed to these two different endocytic pathways and the two different degradation systems could be very complicated; however, ubiquitination could be a key regulator of UT-A1 sorting, trafficking, and protein turnover. The caveolin-mediated pathway is responsible for constitutive UT-A1 internalization, whereas the clathrin-coated pit pathway may regulate UT-A1 endocytosis stimulated by vasopressin in vivo (by forskolin in vitro), and the latter pathway is accelerated by monoubiquitination. The monoubiquitinated UT-A1 is trafficked to the lysosome for degradation. In contrast, cytosolic UT-A1, misfolded UT-A1 from the endoplasmic reticulum, and constitutively internalized cell-surface UT-A1 (mostly from the caveolae-mediated endocytic pathway) is polyubiquitinated and targeted to the proteasome for degradation. Needless to say, both endocytic pathways, both ubiquitination processes, and both protein degradation systems are important and required for proper cell functions. They cooperate in concert to maintain the cell in perfect homeostasis under both normal and stimulated conditions.

UT-A3 Ubiquitination

Stewart et al. [56] reported that inhibition of the ubiquitin-proteasome pathway also increased urea transport activity of mouse (m) UT-A3, heterologously expressed in MDCK cells, in a concentration-dependent manner, indicating that UT-A3 is also regulated by ubiquitination and the ubiquitin-proteasome pathway.

Fig. 4.5 UT-A1 ubiquitination, internalization, and degradation [58]. Under normal conditions, cytosolic UT-A1 (including misfolded UT-A1 from the ER) and constitutively internalized cell-surface UT-A1 (mostly from the caveolae-mediated endocytic pathway) are polyubiquitinated and degraded in the 26S proteasome system. However, upon AVP/FSK stimulation, UT-A1 is phosphorylated and processed for monoubiquitination at the cell surface and internalized via a CCP pathway. The internalized monoubiquitinated UT-A1 is trafficked to the early endosome, then targeted to the lysosome for degradation. CCP clathrin-coated pits, AVP arginine vasopressin, FSK forskolin, PKA protein kinase A

Glycosylation of Urea Transporters

UT-A1 Is a Highly Glycosylated Protein

Immunoblotting studies of normal rat renal inner medulla (IM) demonstrate that the native UT-A1 urea transporter is a glycoprotein with two glycoforms of 117 and 97 kDa [79, 80]. These two forms are not caused by gene splicing but by different degrees of posttranslational glycosylation. Both of the 97- and 117-kDa bands disappear and yield a single 88-kDa deglycosylated UT-A1 after deglycosylation treatment by PNGase F [79].
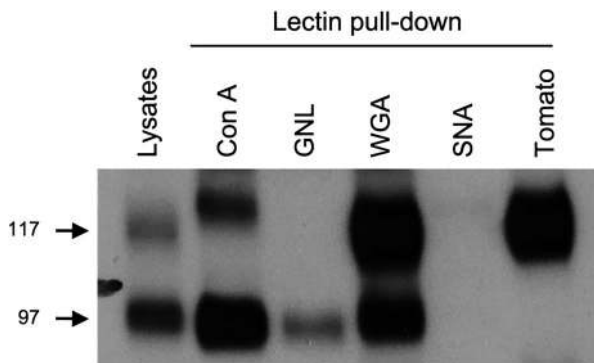
Fig. 4.6 Glycosylation analysis of 97- and 117-kDa UT-A1 by lectin pull-down assay [81]. Normal rat kidney inner medullary lysates were incubated with the indicated agarose bound lectins at 4 °C overnight. The lectin precipitated samples were analyzed by immunoblotting with UT-A1 antibody

It has been believed that the two glycoforms of UT-A1 are the mature glycosylation forms, since they are both insensitive to endoglycosidase H treatment [79]. Experiments using differential centrifugation to fractionate inner medullary membranes also show that both the 97- and 117-kDa glycoforms of UT-A1 are expressed in the cell plasma membrane [79]. Furthermore, both of the two UT-A1 glycoforms are phosphorylated in response to vasopressin stimulation [10, 19, 33]. However, by using different lectins that recognize different structural determinants in glycans, we recently clarified the difference in glycosylation structure between 97- and 117-kDa forms of UT-A1 [81]. Tomato lectin, which is specific for poly-N-acetyllactosamine (poly-LacNAc) on the terminal ends of glycans, only binds to the 117-kDa UT-A1. Conversely, GNL, which binds to mannose, only pulled down the 97-kDa UT-A1. Therefore, the higher molecular mass form, the 117-kDa UT-A1, is a complex N-glycan with heavier glycosylation. The 97-kDa UT-A1 is a hybrid glycan form with low content of terminal N-acetylglucosamine (GlcNAc) residues but high content of mannose glycans (Fig. 4.6).

Interestingly, the relative protein abundance of the two forms varies under different conditions. The 117-kDa form increases dramatically in several states associated with decreased urine concentration, such as streptozotocin (STZ)-induced diabetes mellitus (DM) [80], a low-protein diet [63], hypercalcemia [82], water diuresis [63], and furosemide administration [63]. A tubule perfusion study of initial IMCDs from rats with STZ-induced DM shows that the appearance of the 117-kDa form in the inner medullary base is associated with increased urea transport activity [83]. Therefore, changes in the relative abundance of the 97- and 117-kDa forms of UT-A1 may have important roles in regulating UT-A1 function.

Role of Glycosylation in UT-A1 Membrane Expression and Protein Stability

N-Glycosylation is a key posttranslational modification and is required for the functional activity of many membrane transporters. N-Glycosylation can play an important role in modulating protein biological activity, directing protein folding, regulating cell-surface expression and membrane localization, or increasing protein stability. The amino acid sequence of rat UT-A1 contains four consensus N-linked glycosylation sites (NX(S/T), where X ≠ proline) at Asn-13, −279, −544 and −742. By site-directed mutagenesis, we determined that two sites (Asn-279 and Asn-742) are involved in N-linked glycosylation of UT-A1. Interestingly, these two sites make different contributions to the glycosylation of UT-A1. The Asn-742 site in the second extracellular loop appears to have a greater extent of glycosylation than the Asn-279 site in the first extracellular loop, suggesting differential glycan synthesis and trimming among these two sites [84]. It is not clear whether and how the two glycosylation sites play different roles in urea transport activity.

In MDCK cells expressing wild-type UT-A1, urea flux was stimulated by either vasopressin or forskolin. However, the cells expressing mutant forms of UT-A1 lacking these two N-glycosylation sites had a delayed and significantly reduced maximal urea flux [84]. In many cases, N-linked glycosylation is critical for membrane protein intracellular movement and its eventual delivery to the cell surface. Indeed, most membrane proteins targeted to the plasma membrane possess N-linked glycosylation. Hendriks et al. [85] reported that the glycan mutant of AQP2 was unable to exit the Golgi apparatus and failed to be delivered to the cell membrane. By fractional ultracentrifugation, we found that unglycosylated UT-A1 is mainly trapped in the Golgi apparatus, and it significantly lost its ability to move to the cell surface in response to vasopressin and forskolin. This indicates that loss of glycosylation affects UT-A1 exiting both the ER and Golgi, especially when moving from the Golgi to the cell surface.

For many glycoproteins, deletion of glycosylation increases protein turnover. Removal of the glycosylation site in AQP2 produces a protein with a reduced half-life [85]. Pulse-chase experiments show that UT-A1 half-life is reduced when the two glycosylation sites are eliminated. Immature unglycosylated proteins often stay longer in the ER [84]. The prolonged residence may facilitate UT-A1 breakdown by the ER quality control mechanisms. Additionally, even when an unglycosylated protein escapes from the ER, it is more susceptible to proteolytic attack and has a greater chance of being degraded before being inserted into the plasma membrane [86]. Thus, by affecting UT-A1 trafficking to the plasma membrane and protein stability, glycosylation actively participates in the regulation of UT-A1 function.

Role of Glycosylation in UT-A1 Lipid Raft Targeting

The cell plasma membrane contains many specialized microdomains, referred to as lipid rafts, floating in the membrane. The lipid raft is a highly ordered membrane structure enriched in cholesterol and sphingolipids [87]. The activity of many membrane proteins can be modulated by its specific localization within different microdomains at the plasma membrane [88]. Being associated with lipid rafts becomes an important regulatory mechanism for some proteins. Some membrane protein (channel) activities are higher outside of lipid raft microdomains, as seen in TRPM8 [89]. However, NKCC1 is strongly activated when it is moved into lipid rafts [90].

Protein partitioning to membrane rafts occurs either via protein–protein interactions or by a variety of posttranslational modifications, such as palmitoylation, myristoylation, acylation, or glycosylphosphatidylinositol modification [90–93]. Glycosylation serves as an important apical plasma-membrane trafficking signal that has been well acknowledged [84, 85, 94]. The role for glycosylation as a lipid raft sorting signal has been appreciated in several reports. Xiong et al. [95] reported that differential partitioning in lipid raft microdomains determines the apical versus basolateral localization of the PMCA2w and 2z splice variants. Therefore, directing membrane protein into lipid rafts by glycosylation is of particular importance in the control of membrane protein apical trafficking.

The UT-A1 urea transporter is associated with lipid rafts, both in stably expressing UT-A1-HEK-293 cells [74, 96] and in freshly isolated rat kidney IMCD suspensions [74, 81]. The highly glycosylated 117-kDa form of UT-A1 prefers to reside in less buoyant lipid rafts (fractions 1–3). Loss of glycosylation impairs UT-A1 trafficking to lipid rafts [81]. Interestingly, unlike in IMCD and HEK293 cells, UT-A1 in transfected MDCK cells has a much wider distribution, both in the lipid raft fractions and in the non-raft fractions. By using sugar-specific binding lectins, we compared UT-A1 trafficking to lipid raft versus non-raft subdomains and found that the UT-A1 in non-lipid rafts contains a higher amount of mannose, as detected by concanavalin A. In contrast, UT-A1 in lipid rafts is the mature N-acetylglucosamine-containing form, as detected by wheat germ agglutinin. Differential N-glycosylation influences UT-A1 distribution in lipid rafts. The mature glycosylation acts as a targeting signal, facilitating UT-A1 trafficking into membrane lipid raft subdomains. In polarized epithelial cells, lipid rafts are believed to be in the apical membrane [87]. Thus, association with lipid rafts mediated by glycosylation represents an important mechanism for UT-A1 targeting to the apical plasma membrane in polarized epithelial cells.

UT-A1 Glycosylation in Streptozotocin-Induced Diabetic Rats

Diabetes mellitus (DM) is a metabolic disease characterized by increased blood glucose. The elevated glucose and its metabolic derivatives affect many aspects of cellular function including the sophisticated protein glycosylation mechanisms. In diabetes, the kidney has elevated urea reabsorption activity, which plays a critical role in ameliorating the osmotic diuresis caused by glucosuria [62, 80]. In streptozotocin (STZ) -induced diabetic rats, which have uncontrolled type 1 DM, UT-A1 urea transporter protein abundance in the inner medullary (IM) tip was 55% of control in 5-day diabetic rats but increased to 170, 220, and 280% at 10, 14, and 20 days of DM, respectively. Interestingly, the two glycosylated UT-A1 forms increase differentially. Diabetes causes an increase in the 117-kDa rather than 97-kDa glycoprotein in both the IM tip and base [80]. Analysis of the lipid rafts shows an increase of 117-kDa UT-A1 in lipid rafts in STZ diabetic rat IM. The increased 117-kDa UT-A1 in lipid rafts may contribute to the enhanced urea permeability in IMCDs in diabetic rats [62, 80].

Glycosylation, an extremely complicated posttranslational process, is initially started in the ER, as early as during protein synthesis. The maturation of a glycan is mainly processed in the Golgi complex by trimming and adding different sugars, such as fucose, sialic acid, iduronic acid, xylose, etc. More recently, studies examined the structural change of glycan sugars on UT-A1 [81, 97]. These studies demonstrate that diabetes not only causes an increase of UT-A1 protein abundance, but also results in UT-A1 glycan changes, including an increase of sialic acid content [81]. Since sialic acid (N-acetylneuraminic acid) is a negatively charged large sugar that caps the terminal galactose in the carbohydrate chains on the cell surface, sialylation modification often affects glycoproteins in many aspects, like changing the protein's overall conformation, ligand binding, and galectin binding [98, 99]. We found that increased sialylation, reflecting glycan maturation, is linked to an increase in UT-A1 urea transport activity as well as membrane accumulation under diabetic conditions, and these effects are mediated by PKCα-Src pathway [100]. In addition, the amount of fucose content in UT-A1 is increased and the glycan becomes more branched under diabetic conditions [101]. Future studies should investigate more deeply the structural features of UT-A1 N-glycosylation, particularly under diabetic conditions. In terms of this question, the new technology of glycomics will be helpful to decipher the specific oligosaccharide structures and this information will be helpful to dissect how glycan changes regulate UT-A1 apical membrane trafficking, lipid raft association, protein stability, and functional activity.

UT-A3 Glycosylation

UT-A3 is also a glycoprotein and has two types of glycosylation forms of 67 kDa and 44 kDa [102]. By removing the N-glycans with PNGnase, UT-A3 yields a single band at 40 kDa. Lectin pull-down analysis shows that the 67-kDa UT-A3 contains higher content of poly-LacNAc, which is mainly accumulated in the lipid raft domain. Interestingly, although only a half of UT-A1 in structure, UT-A3 exhibits higher urea transport activity than UT-A1 in Xenopus oocytes. The maturation of UT-A3 glycosylation with poly-LacNAc may contribute to the increased protein stability and urea transport activity of UT-A3 [97]. In addition, the mature form of 67-kDa UT-A3 is also highly sialylated, which is catalyzed by the sialyltransferase ST6GalI. PKC activation promotes UT-A3 sialylation and accumulation in the plasma membrane, eventually increases urea transport activity of UT-A3 [103].

Conflicts of interest The authors have no conflicts of interest.

References

1. J.M. Sands, H. Nonoguchi, M.A. Knepper, Vasopressin effects on urea and H_2O transport in inner medullary collecting duct subsegments. Am. J. Phys. **253**(5 Pt 2), F823–F832 (1987)
2. G. You, C.P. Smith, Y. Kanai, W.S. Lee, M. Stelzner, M.A. Hediger, Cloning and characterization of the vasopressin-regulated urea transporter. Nature **365**(6449), 844–847 (1993)
3. S. Nielsen, J. Terris, C.P. Smith, M.A. Hediger, C.A. Ecelbarger, M.A. Knepper, Cellular and subcellular localization of the vasopressin-regulated urea transporter in rat kidney. Proc. Natl. Acad. Sci. USA **93**(11), 5495–5500 (1996)
4. J.M. Sands, M.A. Blount, J.D. Klein, Regulation of renal urea transport by vasopressin. Trans. Am. Clin. Climatol. Assoc. **122**, 82–92 (2011)
5. J.M. Sands, H.E. Layton, Advances in understanding the urine-concentrating mechanism. Annu. Rev. Physiol. **76**, 387–409 (2014)
6. S.M. Wall, J.S. Han, C.L. Chou, M.A. Knepper, Kinetics of urea and water permeability activation by vasopressin in rat terminal IMCD. Am. J. Phys. **262**(6 Pt 2), F989–F998 (1992)
7. N. Li, H. Zhang, S. Wang, Y. Xu, Y. Ying, J. Li, et al., Urea transporter UT-A1 as a novel drug target for hyponatremia. FASEB J. **38**(13), e23760 (2024)
8. X. Geng, S. Zhang, J. He, A. Ma, Y. Li, M. Li, et al., The urea transporter UT-A1 plays a predominant role in a urea-dependent urine-concentrating mechanism. J. Biol. Chem. **295**(29), 9893–9900 (2020)
9. A. Kuma, X.H. Wang, J.D. Klein, L. Tan, N. Naqvi, F. Rianto, et al., Inhibition of urea transporter ameliorates uremic cardiomyopathy in chronic kidney disease. FASEB J. **34**(6), 8296–8309 (2020)
10. C. Zhang, J.M. Sands, J.D. Klein, Vasopressin rapidly increases phosphorylation of UT-A1 urea transporter in rat IMCDs through PKA. Am. J. Physiol. Renal Physiol. **282**(1), F85–F90 (2002)

11. A.D. Bansal, J.D. Hoffert, T. Pisitkun, S. Hwang, C.L. Chou, E.S. Boja, et al., Phosphoproteomic profiling reveals vasopressin-regulated phosphorylation sites in collecting duct. J. Am. Soc. Nephrol. **21**(2), 303–315 (2010)

12. H.L. Brooks, S. Ageloff, T.H. Kwon, W. Brandt, J.M. Terris, A. Seth, et al., cDNA array identification of genes regulated in rat renal medulla in response to vasopressin infusion. Am. J. Physiol. Renal Physiol. **284**(1), F218–F228 (2003)

13. J.D. Hoffert, T. Pisitkun, G. Wang, R.F. Shen, M.A. Knepper, Quantitative phosphoproteomics of vasopressin-sensitive renal cells: regulation of aquaporin-2 phosphorylation at two sites. Proc. Natl. Acad. Sci. USA **103**(18), 7159–7164 (2006)

14. E.J. Hoorn, J.D. Hoffert, M.A. Knepper, Combined proteomics and pathways analysis of collecting duct reveals a protein regulatory network activated in vasopressin escape. J. Am. Soc. Nephrol. **16**(10), 2852–2863 (2005)

15. P. Uawithya, T. Pisitkun, B.E. Ruttenberg, M.A. Knepper, Transcriptional profiling of native inner medullary collecting duct cells from rat kidney. Physiol. Genomics **32**(2), 229–253 (2008)

16. M.J. Yu, T. Pisitkun, G. Wang, R.F. Shen, M.A. Knepper, LC-MS/MS analysis of apical and basolateral plasma membranes of rat renal collecting duct cells. Mol. Cell. Proteomics **5**(11), 2131–2145 (2006)

17. O. Frohlich, J.D. Klein, P.M. Smith, J.M. Sands, R.B. Gunn, Urea transport in MDCK cells that are stably transfected with UT-A1. Am. J. Physiol. Cell Physiol. **286**(6), C1264–C1270 (2004)

18. O. Frohlich, J.D. Klein, P.M. Smith, J.M. Sands, R.B. Gunn, Regulation of UT-A1-mediated transepithelial urea flux in MDCK cells. Am. J. Physiol. Cell Physiol. **291**(4), C600–C606 (2006)

19. J.D. Klein, M.A. Blount, O. Frohlich, C.E. Denson, X. Tan, J.H. Sim, et al., Phosphorylation of UT-A1 on serine 486 correlates with membrane accumulation and urea transport activity in both rat IMCDs and cultured cells. Am. J. Physiol. Renal Physiol. **298**(4), F935–F940 (2010)

20. M.A. Blount, A.C. Mistry, O. Frohlich, S.R. Price, G. Chen, J.M. Sands, et al., Phosphorylation of UT-A1 urea transporter at serines 486 and 499 is important for vasopressin-regulated activity and membrane accumulation. Am. J. Physiol. Renal Physiol. **295**(1), F295–F299 (2008)

21. R.A. Star, H. Nonoguchi, R. Balaban, M.A. Knepper, Calcium and cyclic adenosine monophosphate as second messengers for vasopressin in the rat inner medullary collecting duct. J. Clin. Invest. **81**(6), 1879–1888 (1988)

22. S. Nielsen, M.A. Knepper, Vasopressin activates collecting duct urea transporters and water channels by distinct physical processes. Am. J. Phys. **265**(2 Pt 2), F204–F213 (1993)

23. S.M. Bagnasco, T. Peng, Y. Nakayama, J.M. Sands, Differential expression of individual UT-A urea transporter isoforms in rat kidney. J. Am. Soc. Nephrol. **11**(11), 1980–1986 (2000)

24. R.A. Fenton, G.S. Stewart, B. Carpenter, A. Howorth, E.A. Potter, G.J. Cooper, et al., Characterization of mouse urea transporters UT-A1 and UT-A2. Am. J. Physiol. Renal Physiol. **283**(4), F817–F825 (2002)

25. C. Shayakul, M.A. Knepper, C.P. Smith, S.R. DiGiovanni, M.A. Hediger, Segmental localization of urea transporter mRNAs in rat kidney. Am. J. Phys. **272**(5 Pt 2), F654–F660 (1997)

26. C. Shayakul, A. Steel, M.A. Hediger, Molecular cloning and characterization of the vasopressin-regulated urea transporter of rat kidney collecting ducts. J. Clin. Invest. **98**(11), 2580–2587 (1996)

27. J.L. Bos, Epac: a new cAMP target and new avenues in cAMP research. Nat. Rev. Mol. Cell Biol. **4**(9), 733–738 (2003)

28. K.J. Honegger, P. Capuano, C. Winter, D. Bacic, G. Stange, C.A. Wagner, et al., Regulation of sodium-proton exchanger isoform 3 (NHE3) by PKA and exchange protein directly activated by cAMP (EPAC). Proc. Natl. Acad. Sci. USA **103**(3), 803–808 (2006)

29. N. Laroche-Joubert, S. Marsy, S. Michelet, M. Imbert-Teboul, A. Doucet, Protein kinase A-independent activation of ERK and H, K-ATPase by cAMP in native kidney cells: role of Epac I. J. Biol. Chem. **277**(21), 18598–18604 (2002)

30. Y. Li, I.B. Konings, J. Zhao, L.S. Price, E. de Heer, P.M. Deen, Renal expression of exchange protein directly activated by cAMP (Epac) 1 and 2. Am. J. Physiol. Renal Physiol. **295**(2), F525–F533 (2008)

31. Y. Wang, J.D. Klein, M.A. Blount, C.F. Martin, K.J. Kent, V. Pech, et al., Epac regulates UT-A1 to increase urea transport in inner medullary collecting ducts. J. Am. Soc. Nephrol. **20**(9), 2018–2024 (2009)

32. C.A. Hoban, L.N. Black, R.J. Ordas, D.L. Gumina, F.E. Pulous, J.H. Sim, et al., Vasopressin regulation of multisite phosphorylation of UT-A1 in the inner medullary collecting duct. Am. J. Physiol. Renal Physiol. **308**(1), F49–F55 (2015)

33. S. Hwang, R. Gunaratne, M.M. Rinschen, M.J. Yu, T. Pisitkun, J.D. Hoffert, et al., Vasopressin increases phosphorylation of Ser84 and Ser486 in Slc14a2 collecting duct urea transporters. Am. J. Physiol. Renal Physiol. **299**(3), F559–F567 (2010)

34. A.G. Gillin, J.M. Sands, Characteristics of osmolarity-stimulated urea transport in rat IMCD. Am. J. Phys. **262**(6 Pt 2), F1061–F1067 (1992)

35. L.H. Kudo, K.R. Cesar, W.C. Ping, A.S. Rocha, Effect of peritubular hypertonicity on water and urea transport of inner medullary collecting duct. Am. J. Phys. **262**(3 Pt 2), F338–F347 (1992)

36. J.M. Sands, D.C. Schrader, An independent effect of osmolality on urea transport in rat terminal inner medullary collecting ducts. J. Clin. Invest. **88**(1), 137–142 (1991)

37. A.G. Gillin, R.A. Star, J.M. Sands, Osmolarity-stimulated urea transport in rat terminal IMCD: role of intracellular calcium. Am. J. Phys. **265**(2 Pt 2), F272–F277 (1993)

38. Y. Wang, J.D. Klein, C.M. Liedtke, J.M. Sands, Protein kinase C regulates urea permeability in the rat inner medullary collecting duct. Am. J. Physiol. Renal Physiol. **299**(6), F1401–F1406 (2010)

39. J.D. Klein, C.F. Martin, K.J. Kent, J.M. Sands, Protein kinase C-alpha mediates hypertonicity-stimulated increase in urea transporter phosphorylation in the inner medullary collecting duct. Am. J. Physiol. Renal Physiol. **302**(9), F1098–F1103 (2012)

40. Y. Wang, J.D. Klein, O. Froehlich, J.M. Sands, Role of protein kinase C-alpha in hypertonicity-stimulated urea permeability in mouse inner medullary collecting ducts. Am. J. Physiol. Renal Physiol. **304**(2), F233–F238 (2013)

41. T.L. Thai, M.A. Blount, J.D. Klein, J.M. Sands, Lack of protein kinase C-alpha leads to impaired urine concentrating ability and decreased aquaporin-2 in angiotensin II-induced hypertension. Am. J. Physiol. Renal Physiol. **303**(1), F37–F44 (2012)

42. L. Yao, D.Y. Huang, I.L. Pfaff, X. Nie, M. Leitges, V. Vallon, Evidence for a role of protein kinase C-alpha in urine concentration. Am. J. Physiol. Renal Physiol. **287**(2), F299–F304 (2004)

43. M.A. Blount, P. Cipriani, S.K. Redd, R.J. Ordas, L.N. Black, D.L. Gumina, et al., Activation of protein kinase C alpha increases phosphorylation of the UT-A1 urea transporter at serine 494 in the inner medullary collecting duct. Am. J. Physiol. Cell Physiol. **309**(9), C608–C615 (2015)

44. M.M. Rinschen, M.J. Yu, G. Wang, E.S. Boja, J.D. Hoffert, T. Pisitkun, et al., Quantitative phosphoproteomic analysis reveals vasopressin V2-receptor-dependent signaling pathways in renal collecting duct cells. Proc. Natl. Acad. Sci. USA **107**(8), 3882–3887 (2010)

45. J.D. Klein, Y. Wang, M.A. Blount, P.A. Molina, L.M. LaRocque, J.A. Ruiz, et al., Metformin, an AMPK activator, stimulates the phosphorylation of aquaporin 2 and urea transporter A1 in inner medullary collecting ducts. Am. J. Physiol. Renal Physiol. **310**(10), F1008–F1012 (2016)

46. Y. Wang, J.D. Klein, J.M. Sands, Phosphatases decrease water and urea permeability in rat inner medullary collecting ducts. Int. J. Mol. Sci. **24**(7) (2023)

47. T.O. Ilori, Y. Wang, M.A. Blount, C.F. Martin, J.M. Sands, J.D. Klein, Acute calcineurin inhibition with tacrolimus increases phosphorylated UT-A1. Am. J. Physiol. Renal Physiol. **302**(8), F998–F1004 (2012)

48. A.C. Mistry, R. Mallick, J.D. Klein, J.M. Sands, O. Frohlich, Functional characterization of the central hydrophilic linker region of the urea transporter UT-A1: cAMP activation and snapin binding. Am. J. Physiol. Cell Physiol. **298**(6), C1431–C1437 (2010)

49. G.S. Stewart, R.A. Fenton, W. Wang, T.H. Kwon, S.J. White, V.M. Collins, et al., The basolateral expression of mUT-A3 in the mouse kidney. Am. J. Physiol. Renal Physiol. **286**(5), F979–F987 (2004)

50. S. Nandi, S. Sanyal, S.A. Amin, S.K. Kashaw, T. Jha, S. Gayen, Urea transporter and its specific and nonspecific inhibitors: State of the art and pharmacological perspective. Eur. J. Pharmacol. **911**, 174508 (2021)

51. M. Li, S. Zhang, B. Yang, Urea transporters identified as novel diuretic drug targets. Curr. Drug Targets **21**(3), 279–287 (2020)

52. M.A. Blount, J.D. Klein, C.F. Martin, D. Tchapyjnikov, J.M. Sands, Forskolin stimulates phosphorylation and membrane accumulation of UT-A3. Am. J. Physiol. Renal Physiol. **293**(4), F1308–F1313 (2007)

53. G.S. Stewart, S.L. King, E.A. Potter, C.P. Smith, Acute regulation of mUT-A3 urea transporter expressed in a MDCK cell line. Am. J. Physiol. Renal Physiol. **292**(4), F1157–F1163 (2007)

54. G.S. Stewart, A. Thistlethwaite, H. Lees, G.J. Cooper, C. Smith, Vasopressin regulation of the renal UT-A3 urea transporter. Am. J. Physiol. Renal Physiol. **296**(3), F642–F648 (2009)

55. G. Chen, H. Huang, O. Frohlich, Y. Yang, J.D. Klein, S.R. Price, et al., MDM2 E3 ubiquitin ligase mediates UT-A1 urea transporter ubiquitination and degradation. Am. J. Physiol. Renal Physiol. **295**(5), F1528–F1534 (2008)

56. G.S. Stewart, J.H. O'Brien, C.P. Smith, Ubiquitination regulates the plasma membrane expression of renal UT-A urea transporters. Am. J. Physiol. Cell Physiol. **295**(1), C121–C129 (2008)

57. H. Su, C.B. Carter, O. Laur, J.M. Sands, G. Chen, Forskolin stimulation promotes urea transporter UT-A1 ubiquitination, endocytosis, and degradation in MDCK cells. Am. J. Physiol. Renal Physiol. **303**(9), F1325–F1332 (2012)

58. H. Su, M. Chen, J.M. Sands, G. Chen, Activation of the cAMP/PKA pathway induces UT-A1 urea transporter monoubiquitination and targets it for lysosomal degradation. Am. J. Physiol. Renal Physiol. **305**(12), F1775–FF178 (2013)

59. F. Huang, D. Kirkpatrick, X. Jiang, S. Gygi, A. Sorkin, Differential regulation of EGF receptor internalization and degradation by multiubiquitination within the kinase domain. Mol. Cell **21**(6), 737–748 (2006)

60. Y. Mao, Y. Shang, V.C. Pham, J.A. Ernst, J.R. Lill, S.J. Scales, et al., Polyubiquitination of insulin-like growth factor I receptor (IGF-IR) activation loop promotes antibody-induced receptor internalization and down-regulation. J. Biol. Chem. **286**(48), 41852–41861 (2011)

61. K. Umebayashi, H. Stenmark, T. Yoshimori, Ubc4/5 and c-Cbl continue to ubiquitinate EGF receptor after internalization to facilitate polyubiquitination and degradation. Mol. Biol. Cell **19**(8), 3454–3462 (2008)

62. D. Kim, J.M. Sands, J.D. Klein, Role of vasopressin in diabetes mellitus-induced changes in medullary transport proteins involved in urine concentration in Brattleboro rats. Am. J. Physiol. Renal Physiol. **286**(4), F760–F766 (2004)

63. A. Kato, M. Naruse, M.A. Knepper, J.M. Sands, Long-term regulation of inner medullary collecting duct urea transport in rat. J. Am. Soc. Nephrol. **9**(5), 737–745 (1998)

64. J. de Juan-Sanz, F. Zafra, B. Lopez-Corcuera, C. Aragon, Endocytosis of the neuronal glycine transporter GLYT2: role of membrane rafts and protein kinase C-dependent ubiquitination. Traffic **12**(12), 1850–1867 (2011)

65. E.J. Kamsteeg, G. Hendriks, M. Boone, I.B. Konings, V. Oorschot, P. van der Sluijs, et al., Short-chain ubiquitination mediates the regulated endocytosis of the aquaporin-2 water channel. Proc. Natl. Acad. Sci. USA **103**(48), 18344–18349 (2006)

66. D.H. Lin, P. Yue, C.Y. Pan, P. Sun, X. Zhang, Z. Han, et al., POSH stimulates the ubiquitination and the clathrin-independent endocytosis of ROMK1 channels. J. Biol. Chem. **284**(43), 29614–29624 (2009)

67. J. Eriksen, W.E. Bjorn-Yoshimoto, T.N. Jorgensen, A.H. Newman, U. Gether, Postendocytic sorting of constitutively internalized dopamine transporter in cell lines and dopaminergic neurons. J. Biol. Chem. **285**(35), 27289–27301 (2010)

68. B. Varghese, H. Barriere, C.J. Carbone, A. Banerjee, G. Swaminathan, A. Plotnikov, et al., Polyubiquitination of prolactin receptor stimulates its internalization, postinternalization sorting, and degradation via the lysosomal pathway. Mol. Cell. Biol. **28**(17), 5275–5287 (2008)

69. S. Ye, K. Cihil, D.B. Stolz, J.M. Pilewski, B.A. Stanton, A. Swiatecka-Urban, c-Cbl facilitates endocytosis and lysosomal degradation of cystic fibrosis transmembrane conductance regulator in human airway epithelial cells. J. Biol. Chem. **285**(35), 27008–27018 (2010)

70. K. Haglund, S. Sigismund, S. Polo, I. Szymkiewicz, P.P. Di Fiore, I. Dikic, Multiple monoubiquitination of RTKs is sufficient for their endocytosis and degradation. Nat. Cell Biol. **5**(5), 461–466 (2003)

71. M.W. Musch, A.B. Puffer, L. Goldstein, Volume expansion stimulates monoubiquitination and endocytosis of surface-expressed skate anion-exchanger isoform. Am. J. Physiol. Regul. Integr. Comp. Physiol. **294**(5), R1657–R1665 (2008)

72. T. Sun, J. Guo, H. Shallow, T. Yang, J. Xu, W. Li, et al., The role of monoubiquitination in endocytic degradation of human ether-a-go-go-related gene (hERG) channels under low K$^+$ conditions. J. Biol. Chem. **286**(8), 6751–6759 (2011)

73. J. Terrell, S. Shih, R. Dunn, L. Hicke, A function for monoubiquitination in the internalization of a G protein-coupled receptor. Mol. Cell **1**(2), 193–202 (1998)

74. H. Huang, X. Feng, J. Zhuang, O. Frohlich, J.D. Klein, H. Cai, et al., Internalization of UT-A1 urea transporter is dynamin dependent and mediated by both caveolae- and clathrin-coated pit pathways. Am. J. Physiol. Renal Physiol. **299**(6), F1389–F1395 (2010)

75. R. Debigare, S.R. Price, Proteolysis, the ubiquitin-proteasome system, and renal diseases. Am. J. Physiol. Renal Physiol. **285**(1), F1–F8 (2003)

76. M. Li, D. Chen, A. Shiloh, J. Luo, A.Y. Nikolaev, J. Qin, et al., Deubiquitination of p53 by HAUSP is an important pathway for p53 stabilization. Nature **416**(6881), 648–653 (2002)

77. X. Feng, Z. Li, Y. Du, H. Fu, J.D. Klein, H. Cai, et al., Downregulation of urea transporter UT-A1 activity by 14-3-3 protein. Am. J. Physiol. Renal Physiol. **309**(1), F71–F78 (2015)

78. H. Su, C. Ye, J.M. Sands, C. Zhang, E3 ligase MDM2 mediates urea transporter-A1 ubiquitination under either constitutive or stimulatory conditions. Am. J. Physiol. Renal Physiol. **317**(5), F1331–F1341 (2019)

79. A.D. Bradford, J.M. Terris, C.A. Ecelbarger, J.D. Klein, J.M. Sands, C.L. Chou, et al., 97- and 117-kDa forms of collecting duct urea transporter UT-A1 are due to different states of glycosylation. Am. J. Physiol. Renal Physiol. **281**(1), F133–F143 (2001)

80. D. Kim, J.M. Sands, J.D. Klein, Changes in renal medullary transport proteins during uncontrolled diabetes mellitus in rats. Am. J. Physiol. Renal Physiol. **285**(2), F303–F309 (2003)

81. G. Chen, A.G. Howe, G. Xu, O. Frohlich, J.D. Klein, J.M. Sands, Mature N-linked glycans facilitate UT-A1 urea transporter lipid raft compartmentalization. FASEB J. **25**(12), 4531–4539 (2011)

82. J.M. Sands, F.X. Flores, A. Kato, M.A. Baum, E.M. Brown, D.T. Ward, et al., Vasopressin-elicited water and urea permeabilities are altered in IMCD in hypercalcemic rats. Am. J. Phys. **274**(5 Pt 2), F978–F985 (1998)

83. V. Pech, J.D. Klein, S.D. Kozlowski, S.M. Wall, J.M. Sands, Vasopressin increases urea permeability in the initial IMCD from diabetic rats. Am. J. Physiol. Renal Physiol. **289**(3), F531–F535 (2005)

84. G. Chen, O. Frohlich, Y. Yang, J.D. Klein, J.M. Sands, Loss of N-linked glycosylation reduces urea transporter UT-A1 response to vasopressin. J. Biol. Chem. **281**(37), 27436–27442 (2006)

85. G. Hendriks, M. Koudijs, B.W. van Balkom, V. Oorschot, J. Klumperman, P.M. Deen, et al., Glycosylationis important for cell surface expression of the water channel aquaporin-2 but

is not essential for tetramerization in the endoplasmic reticulum. J. Biol. Chem. **279**(4), 2975–2983 (2004)

86. L.B. Li, N. Chen, S. Ramamoorthy, L. Chi, X.N. Cui, L.C. Wang, et al., The role of N-glycosylation in function and surface trafficking of the human dopamine transporter. J. Biol. Chem. **279**(20), 21012–21020 (2004)

87. K. Simons, M.J. Gerl, Revitalizing membrane rafts: new tools and insights. Nat. Rev. Mol. Cell Biol. **11**(10), 688–699 (2010)

88. C. Dart, Lipid microdomains and the regulation of ion channel function. J. Physiol. **588**(Pt 17), 3169–3178 (2010)

89. C. Morenilla-Palao, M. Pertusa, V. Meseguer, H. Cabedo, F. Viana, Lipid raft segregation modulates TRPM8 channel activity. J. Biol. Chem. **284**(14), 9215–9224 (2009)

90. P. Welker, A. Bohlick, K. Mutig, M. Salanova, T. Kahl, H. Schluter, et al., Renal Na⁺-K⁺-Cl⁻ cotransporter activity and vasopressin-induced trafficking are lipid raft-dependent. Am. J. Physiol. Renal Physiol. **295**(3), F789–F802 (2008)

91. D.A. Brown, E. London, Functions of lipid rafts in biological membranes. Annu. Rev. Cell Dev. Biol. **14**, 111–136 (1998)

92. A.M. Hartmann, P. Blaesse, T. Kranz, M. Wenz, J. Schindler, K. Kaila, et al., Opposite effect of membrane raft perturbation on transport activity of KCC2 and NKCC1. J. Neurochem. **111**(2), 321–331 (2009)

93. D. Lingwood, K. Simons, Lipid rafts as a membrane-organizing principle. Science **327**(5961), 46–50 (2010)

94. R.S. Hoover, E. Poch, A. Monroy, N. Vazquez, T. Nishio, G. Gamba, et al., N-Glycosylation at two sites critically alters thiazide binding and activity of the rat thiazide-sensitive Na(⁺):Cl(⁻) cotransporter. J. Am. Soc. Nephrol. **14**(2), 271–282 (2003)

95. Y. Xiong, G. Antalffy, A. Enyedi, E.E. Strehler, Apical localization of PMCA2w/b is lipid raft-dependent. Biochem. Biophys. Res. Commun. **384**(1), 32–36 (2009)

96. X. Feng, H. Huang, Y. Yang, O. Frohlich, J.D. Klein, J.M. Sands, et al., Caveolin-1 directly interacts with UT-A1 urea transporter: the role of caveolae/lipid rafts in UT-A1 regulation at the cell membrane. Am. J. Physiol. Renal Physiol. **296**(6), F1514–F1520 (2009)

97. H. Su, C.B. Carter, O. Frohlich, R.D. Cummings, G. Chen, Glycoforms of UT-A3 urea transporter with poly-N-acetyllactosamine glycosylation have enhanced transport activity. Am. J. Physiol. Renal Physiol. **303**(2), F201–F208 (2012)

98. S.K. Cha, B. Ortega, H. Kurosu, K.P. Rosenblatt, O.M. Kuro, C.L. Huang, Removal of sialic acid involving Klotho causes cell-surface retention of TRPV5 channel via binding to galectin-1. Proc. Natl. Acad. Sci. USA **105**(28), 9805–9810 (2008)

99. Y. Zhuo, S.L. Bellis, Emerging role of alpha2, 6-sialic acid as a negative regulator of galectin binding and function. J. Biol. Chem. **286**(8), 5935–5941 (2011)

100. X. Li, B. Yang, M. Chen, J.D. Klein, J.M. Sands, G. Chen, Activation of protein kinase C-α and Src kinase increases urea transporter A1 α-2, 6 sialylation. J. Am. Soc. Nephrol. **26**(4), 926–934 (2015)

101. X. Qian, X. Li, Ilori TO, J.D. Klein, R.P. Hughey, C.J. Li, et al., RNA-seq analysis of glycosylation related gene expression in STZ-induced diabetic rat kidney inner medulla. Front. Physiol. **6**, 274 (2015)

102. J.M. Terris, M.A. Knepper, J.B. Wade, UT-A3: localization and characterization of an additional urea transporter isoform in the IMCD. Am. J. Physiol. Renal Physiol. **280**(2), F325–F332 (2001)

103. X. Qian, J.M. Sands, X. Song, G. Chen, Modulation of kidney urea transporter UT-A3 activity by alpha2,6-sialylation. Pflugers Arch. **468**(7), 1161–1170 (2016)

Chapter 5
Transport Characteristics of Urea Transporters

Zhizhen Huang and Baoxue Yang

Abstract Rapid urea permeation mediated by urea transporters (UTs) is crucial for maintaining normal physiological processes in organisms. UTs not only facilitate urea transport but also water transport, further underscoring their role in maintaining fluid balance. Advances in structural biology have led to the elucidation of high-resolution three-dimensional structures of various UTs, offering critical insights into the molecular mechanisms underlying their efficiency in transporting urea and water. UT-B displays high permeability to urea analogs, which can competitively inhibit urea permeation by obstructing the channel. However, whether UT-A is capable of transporting urea analogs remains contentious. Additionally, further investigation is required to determine if UTs can facilitate ammonia transport. Urea permeability (P_{urea}) in erythrocytes differs between different mammals. Carnivores exhibit high P_{urea}. In contrast, herbivores show much lower P_{urea}. Erythrocyte P_{urea} in omnivores was intermediate. Rodents and lagomorphs have P_{urea} intermediate between carnivores and omnivores. This chapter provides information about the transporter characteristics of UTs.

Keywords Urea transport · Water transport · Urea analogues · Ammonia · Species

Urea Transport Mediated by Urea Transporters

Urea Transport Efficiency

Urea is one of the most ubiquitous organic compounds in nature, serving as the final product of amino acid metabolism in both human and animal bodies. Research in the 1970s confirmed the permeability of mammalian erythrocyte membranes to urea

Z. Huang · B. Yang (✉)
State Key Laboratory of Vascular Homeostasis and Remodeling, Department of
Pharmacology, School of Basic Medical Sciences, Peking University, Beijing, China
e-mail: baoxue@bjmu.edu.cn

[1, 2]. Subsequent studies reported that the inner medullary collecting ducts (IMCD) regulate urea permeability under the influence of vasopressin [3–5], and individuals with Jk(a-b-) erythrocytes exhibit impaired urea permeability [6], suggesting the presence of urea transporter proteins. Ultimately, two families of urea transporter (UT) proteins, UT-A and UT-B, were discovered in mammals, encoded by the independent genes *Slc14a2* and *Slc14a1*, respectively [7–10].

Xenopus oocytes injected with human UT-B (hUT-B) cRNA resulted in a P_{urea} (urea permeability) of 2.5×10^{-5} cm/s, significantly higher than the control group injected with water, which had a P_{urea} of $1.2 \sim 2 \times 10^{-6}$ cm/s [8]. Based on the quantity of UT-B protein in human erythrocytes and urea permeability calculations, the turnover rate of hUT-B is estimated to be approximately $20 \sim 60 \times 10^{5}$ urea molecules per second, highlighting its crucial role in rapid urea transport [11]. The ability of hUT-B to transport urea can be inhibited by phloretin, purachloromercuribenzene sulfonate (pCMBS), and urea analogs. Phloretin (0.1 mM) inhibited P_{urea} by 54%, while complete inhibition was observed at 0.2 mM phloretin. Additionally, 0.5 mM pCMBS reduced urea transport by 65%. Furthermore, thiourea at 50 mM, nitrophenylthiourea (NPTU) at 0.1 mM, and (3,4-dichlorophenyl)-2-thiourea (DCPTU) at 0.1 mM inhibited urea transport by 88%, 35%, and 54%, respectively [8].

Expression of rat UT-B (rUT-B) in oocytes increases urea uptake by approximately 50-fold. Urea transport mediated by rUT-B is inhibited by 57%, 21%, and 86% with 150 mM urea analogs thiourea, 1,1-dimethylthiourea (DMT), and 1,3-DMT, respectively [12]. In UT-B deficient mice, red blood cell permeability is 45-fold lower compared to wild-type mice [13]. Urea flux in mouse red blood cells is inhibited by 98%, 93%, 87%, 72%, and 64% with 200 mM urea analogs dimethylurea, acrylamide, methylurea, thiourea, and formamide, respectively [14]. Phloretin at 0.7 mM completely inhibits hUT-B and mUT-B, but only inhibits rUT-B by 55% [12, 14]. In the presence of 0.5 mM pCMBS, urea uptake by rUT-B is inhibited by 32%, while hUT-B is inhibited by 61% [12]. These results highlight species-specific differences in UT-B function.

Expression of hUT-A1 in *Xenopus* oocytes increases uptake of ^{14}C-urea by $15 \sim 20$ times compared to control. The uptake of ^{14}C-urea by hUT-A1 is reduced by 55% and 73% with 0.5 mM phloretin and 150 mM thiourea, respectively [15]. However, injection of hUT-A6 cRNA into oocytes increased urea uptake only fourfold, and urea permeability was completely inhibited by 0.5 mM phloretin [16], suggesting differential urea transport capabilities and sensitivities to phloretin among UT-A subtypes.

Similar to hUT-A1, expression of rUT-A1 in *Xenopus* oocytes enhances uptake of ^{14}C-urea by $15 \sim 20$ times compared to control. 0.7 mM phloretin, 150 mM thiourea, and 150 mM dimethylurea almost completely inhibit the increase in urea uptake mediated by rUT-A1, whereas 1 mM pCMBS does not affect urea transport rates in oocytes expressing rUT-A1 [9]. In perfused rat IMCDs, the transporter rUT-A1 has been quantified using an ELISA-based method, revealing a transport rate of $0.3 \sim 1 \times 10^{5}$ urea molecules per second [17]. Expression of rUT-A2 in oocytes increased urea uptake by $7 \sim 11$ times compared to water-injected oocytes. Urea

absorption by rUT-A2 was inhibited by 71% with 0.35 mM phloretin and completely inhibited by 0.70 mM phloretin; 150 mM thiourea inhibited it by 62% [18]. rUT-A3 and rUT-A4 exhibit similar urea transport capabilities to rUT-A1 and rUT-A2 [19].

The urea uptake by oocytes expressing mUT-A1, mUT-A2, mUT-A3, or mUT-A5 increased by only three-fold, two-fold, five-fold, and three-fold, respectively, compared to water-injected oocytes [20, 21], indicating that the urea permeability of mUT-As is much lower than that of rUT-As. The urea permeability of mUT-A1 and mUT-A2 was completely inhibited by 0.5 mM phloretin [20], while the inhibition rates for urea permeability of mUT-A3 and mUT-A5 were 75% and 53%, respectively [21]. The turnover rates of mUT-A2 and mUT-A3 are 0.46×10^5 and 0.59×10^5 urea molecules per second, respectively [22], similar to rUT-A1. These findings suggest that the reduced urea permeability observed in experiments with mUT-As compared to rUT-As is due to lower expression levels of mUT-As proteins.

Urea Transport Mechanism

In recent years, advancements in structural biology techniques, such as X-ray crystallography and cryo-electron microscopy, have led to the elucidation of high-resolution structures of several UT family members, including *Desulfovibrio vulgaris* UT (dvUT), bovine UT-B, human UT-A2, UT-A3, UT-B, and zebrafish UT [23–26]. These structural analyses have revealed a high degree of conservation in both structure and function within the UT family, providing critical insights into the urea transport mechanism. The resolved structures of UT family members exhibit significant structural similarities. All UTs exist as trimers, with each monomer containing an independent urea channel. This trimeric assembly allows for independent urea transport by each UT monomer, while the overall trimeric structure enhances the stability of the channels (Fig. 5.1).

Each UT monomer comprises ten complete transmembrane helices and two half-transmembrane helices. These helices are symmetrically distributed on either side of the urea channel, with the complete transmembrane helices designated as 1a-5a and 1b-5b, and the half-transmembrane helices referred to as Pa and Pb. Helices 3a, 3b, 5a, 5b, Pa, and Pb collectively envelop the urea channel, forming a continuous
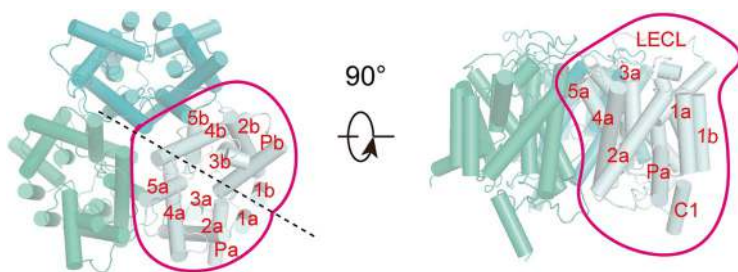

Fig. 5.1 Overall structure of hUT-A2

conduit (Fig. 5.1). The structure of the urea channel exhibits a characteristic "wide-end narrow-middle" morphology, with wider openings at both ends and a narrower selective filter region in the central section. The constricted region of the channel is composed of several conserved amino acid residues that provide hydrogen bonding interactions with urea, facilitating its transport in a dehydrated state.

Recently, Huang et al. captured transient structures of urea passage through UTs, obtaining crystal structures of human UT-A2 and zebrafish UT in complex with urea. Based on these high-resolution structures and molecular dynamics simulations, they elucidated the detailed mechanism of urea transport by UTs. The selective filter in the channel can be divided into three regions: So, Sm, and Si, traversing from the extracellular side to the cytoplasmic side. Free urea molecules from the extracellular space are first captured by forming hydrogen bonds with the side chain of Q231[Pb], entering the So region. The subsequent swinging of the T338[5b] side chain guides the urea molecule into the Sm region, where it alternately forms hydrogen bonds with T338[5b] and T176[5a], effectively reorienting the oxygen atoms of urea. The movement of the T176[5a] side chain may facilitate the transfer of the urea molecule from the Sm to the Si region. Finally, urea forms hydrogen bonds with the side chain of Q67[Pa] and is released into the cytoplasm, completing the transport process from extracellular to intracellular environments. The movement of urea within the channel is constrained by pairs of hydrophobic amino acids on either side, ensuring that only one urea molecule can pass through specific positions within the channel at a time. This mechanism guarantees unidirectional transport of urea across the membrane. Sequence alignment and mutational analyses demonstrate that different UTs possess a conserved transport mechanism, with the polar network formed by Q231[Pb], T338[5b], T176[5a], and Q67[Pa] being critical for the recognition and transport of urea (Fig. 5.2) [26].

In previous studies, although the protein structure with the urea-bound state had not been determined, researchers utilized the apo state of the protein structure to perform molecular dynamics simulations in order to investigate the mechanism of
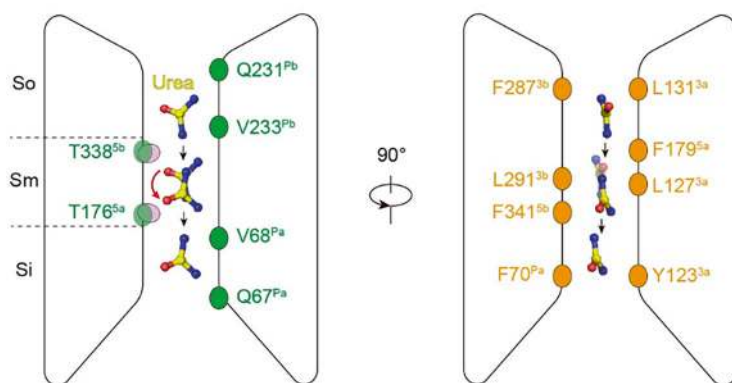
Fig. 5.2 Urea permeation mechanism of the human urea transporter hUT-A2 [26]

urea permeation through urea channels. During this process, it was widely accepted that the "oxygen ladder" structure played a critical role in the selective permeation of urea. The selective filter region is surrounded by a series of linearly arranged oxygen atoms, forming the so-called "oxygen ladder." Urea molecules gradually move through the channel by forming hydrogen bonds with these oxygen atoms, facilitating rapid permeation [23, 24, 27] (Fig. 5.3). However, in the study by Huang et al., the polar motif Q231[Pb]-T338[5b]-T176[5a]-Q67[Pa] was accurately identified for the first time, providing deeper insights into the selective mechanism of urea transport.

It is interesting that water molecules play a crucial role in the process of urea permeation through urea channels. As urea molecules traverse the channel, they are accompanied by water molecules, which form hydrogen bonds with urea and facilitate its passage. However, when urea enters the narrow Sm region, it must undergo
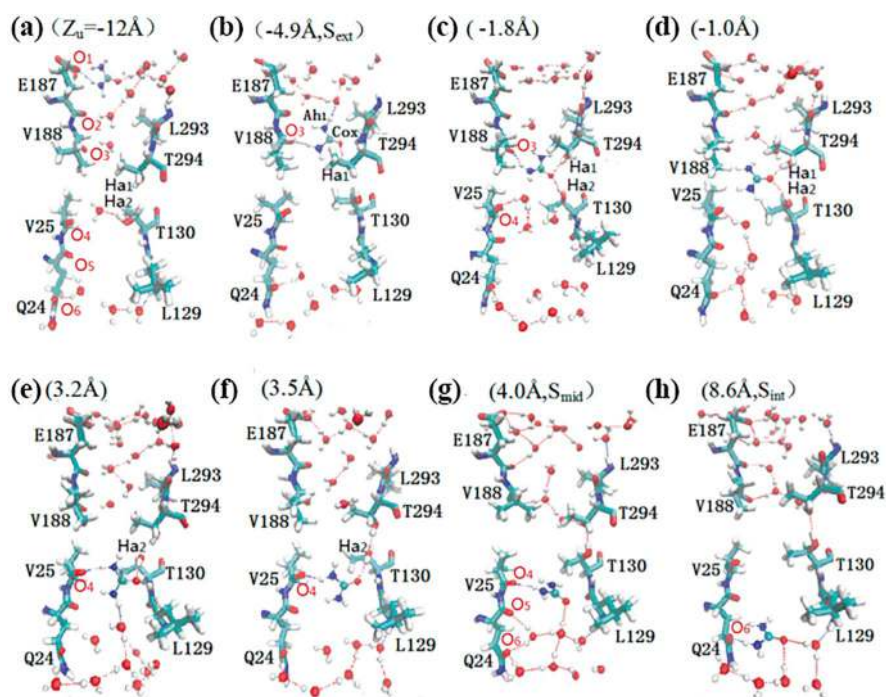
Fig. 5.3 Snapshots describing the transport process of urea in the pore. Z_u represents the Z-coordinate of the carbon atom in the urea molecule. The hydrogen bonds are represented by dashed lines. (**a**) A urea molecule enters the entrance of the pore from the extracellular side. (**b**) At the external resident site (S_{ext}), the urea forms hydrogen bonds with O_3, water, and T294. (**c**) The hydroxyl arm of T294, Ha1, drags the urea to the middle region of the pore. (**d**) The urea is located at the unstable equilibrium site near the center of the pore. (**e**) In the transitional configuration, the hydroxyl arm of T130, Ha2, is dragging the urea to O_4. (**f**) The process of dragging the urea from the middle region to O_4 has been completed. (**g**) At the middle resident site (S_{mid}), urea forms a hydrogen bond with O_4 and can be bridged with O_5 and/or O_6 via water. (**h**) At the internal resident site (S_{int}), the urea forms a hydrogen bond with O_6 and can interact with the amide hydrogen of L129 via a bridging water molecule [27]

complete dehydration and overcome an energy barrier of approximately 5.0 kcal/mol to continue through the channel. The energy loss due to dehydration is partially compensated by the formation of consecutive hydrogen bonds between the urea and oxygen atoms within the channel. This mechanism helps to explain the efficient permeation of urea through the channel [23, 24, 26, 27].

It is noteworthy that there is ongoing debate regarding whether urea molecules rotate while passing through the channel. Huang et al., using molecular dynamics simulations based on the urea-bound hUT-A2 structure, observed that urea molecules undergo rotation as they pass through the polar motif ($Q231^{Pb}$-$T338^{5b}$-$T176^{5a}$-$Q67^{Pa}$), a process considered crucial for urea transport through the channel [26]. In contrast, Elena J. Levin et al., using molecular dynamics simulations based on the apo state structure of bovine UT-B, observed that urea molecules exhibit minimal rotation within the channel [24]. However, it should be noted that since Elena J. Levin's study did not capture the transient structure of urea permeation through UT, the reliability of their molecular dynamics results is relatively lower, limiting their explanation of the urea transport mechanism to some extent.

Additionally, Zhang et al. developed a cooperative binding model using the structure of dvUT, indicating that binding at one site can enhance the binding ability of other unoccupied sites, revealing a positive cooperative effect. As binding sites become progressively occupied, the movement of urea within the channel becomes more efficient [28].

## Water Transport Mediated by Urea Transporters

Water Transport Efficiency

By measuring osmotic water permeability (P_f) in *Xenopus* oocytes expressing UTs, it is clear that UT-B functions as an efficient water channel [29–32]. Quantitative measurement of single-channel P_f of UT-B gives a value of 1.4 cm^3/s. UT-B-mediated water permeability is weakly temperature dependent (activation energy <4 kcal/mol), inhibited >75% by the urea transport inhibitor 1,3-dimethylthiourea, but not inhibited by the water channel (aquaporin) inhibitor $HgCl_2$ [29]. These results indicate that UT-B functions as a urea/water channel utilizing a common aqueous pathway (Fig. 5.4).

The significant intrinsic water permeability of UT-B suggests the existence of a continuous aqueous channel through the UT-B protein that permits passage of both water and urea. A study of temperature dependence shows a weak temperature dependence for UT-B-mediated transport of both water and urea. The low Arrhenius activation energy (<4 kcal/mol) is consistent with an aqueous pore pathway and is in agreement with the low activation energies found for several of the aquaporin-type water channels. UT-B-mediated water and urea transport were each strongly inhibited by the urea analogue 1,3-dimethylthiourea and by phloretin. Neither water nor urea transport was inhibited by $HgCl_2$, a potent inhibitor of most aquaporin-type

Fig. 5.4 Schematic diagram of UT-B as a urea/water channel utilizing a common aqueous pathway
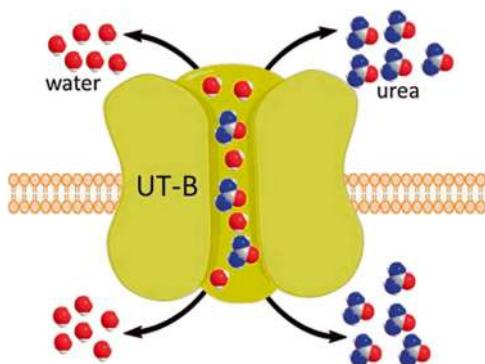
water channels. HgCl$_2$, but not the urea transport inhibitors, strongly inhibit water permeability in oocytes expressing the water channel aquaporin-1 (AQP1). These results support a common aqueous route for water and urea transport through UT-B.

Increased water permeability in *Xenopus* oocytes expressing UT-B was subsequently confirmed by Sidoux-Walter et al. [32] However, they concluded that UT-B-facilitated water transport does not occur under physiological conditions. They proposed, based on water versus urea permeability measurements in oocytes expressing different levels of UT-B, that UT-B-associated water permeability occurs only when UT-B is expressed at non-physiological, high levels.

To quantify UT-B-mediated water transport, Yang et al. generated double knock-out mice lacking UT-B and the major erythrocyte water channel AQP1 [13]. Osmotic water permeability in erythrocytes from mice lacking both AQP1 and UT-B is 4.2-fold lower in the double knockout mice than in erythrocytes from mice lacking AQP1 alone. A similar low water permeability was found in erythrocytes from AQP1 null mice after UT-B inhibition by phloretin and in erythrocytes from UT-B null mice after inhibition of AQP1 by HgCl$_2$. UT-B-facilitated water transport was weakly temperature dependent. These results explain why the activation energy of erythrocyte water transport after mercurial inhibition or AQP1 deletion is substantially lower than expected for lipid-mediated water transport [33]. The experimental results also provide a molecular basis for the conclusion of Dix and Solomon [34], which were based on studies of membrane perturbing agents, showing that the mercurial-insensitive water permeability in erythrocytes involves, in large part, a protein pathway.

Figure 5.5 summarizes the contributions of protein and lipid pathways for water and urea transport in mouse erythrocytes. At 10 °C, ~90% of water is transported through AQP1, 8% through UT-B, and the remainder through the lipid membrane. The vast majority of urea is transported through UT-B. At 37 °C, ~79% of water is transported through AQP1, 6% through UT-B, and the remainder through the lipid membrane.

It is interesting to compare the intrinsic (single channel) water permeabilities of AQP1 versus UT-B. Assuming, as in human erythrocytes, that there are 14,000 copies of UT-B and 200,000 copies of AQP1 [36] per mouse erythrocyte plasma
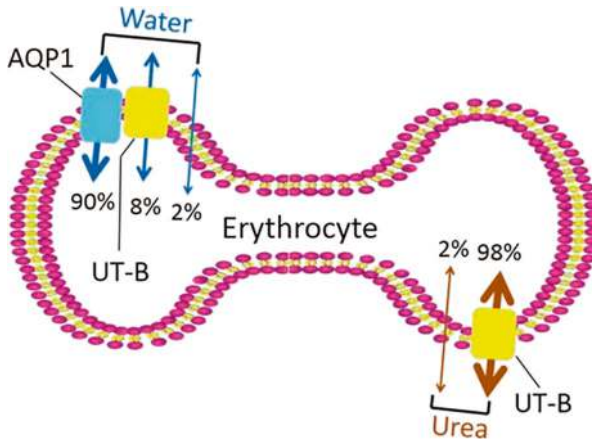
Fig. 5.5 Schematic diagram of relative contributions of AQP1, UT-B, and the lipid bilayer to erythrocyte water and urea permeability [35]

membrane, then there is ~1 UT-B molecule per 14 AQP1 molecules. Yang and Verkman [35] showed that AQP1 contributes 13 times more than UT-B to erythrocyte water permeability. Thus, the single-channel (per molecule) water permeability of UT-B in erythrocytes is very similar to that of AQP1 (7.5×10^{-14} cm³/s). The presence of a continuous aqueous pathway through UT-B that efficiently facilitates osmosis is an interesting observation that may account for the exceptionally high transport turnover rate of UT-B ($2 \sim 6 \times 10^6$ molecules/s) [11], as high as that of ion channels and $> 2 \sim 3$ orders of magnitude greater than that of classic carriers and active transporters. A recent functional study of human erythrocyte variants and MD simulations clearly demonstrates that urea and water share the same pathway through the pore of UT-B [31]. Geyer et al. [30] also confirmed that human UT-B is a water channel in *Xenopus* oocytes.

A recent study has proposed that the UT-B protein may not facilitate water permeability. The researchers collected blood samples from healthy volunteers and hospital blood banks, observing significant variability in urea permeability among red blood cells from different donors, while water diffusion permeability remained relatively constant. Inhibition experiments further demonstrated that urea permeability could be effectively reduced by specific inhibitors, whereas water permeability was not significantly affected under the same conditions [37]. However, this phenomenon may be attributed to the high expression of aquaporins in red blood cells, which could mask the potential water permeability function of the UT-B protein, thereby explaining the lack of significant water permeability observed in the study.

There is some controversy regarding the water permeability of UT-A subtypes. Studies have reported that UT-A2, UT-A3, and UT-A5 do not possess water permeability [21, 22, 29]. Yang & Verkman first explored whether UT-A exhibits water permeability, finding that oocytes expressing rUT-A2 showed no statistically significant difference in water permeability compared to the control group [29].

Subsequently, another study reported that expression of mUT-A3 or mUT-A5 had no effect on oocyte osmotic water permeability [21]. Maciver et al. reported that oocytes expressing mUT-A2 had a P_f of $2.85 \pm 0.26 \times 10^{-4}$ cm/s, while those expressing mUT-A3 had a P_f of $4.38 \pm 0.41 \times 10^{-4}$ cm/s, both showing no statistically significant difference compared to control oocytes with a P_f of $4.34 \pm 0.40 \times 10^{-4}$ cm/s [22].

However, one study [38] indicated that oocytes injected with mUT-A2 and mUT-A3 cRNA show significantly increased mean P_f values compared to oocytes injected with water. Furthermore, the addition of 0.5 mM phloretin significantly reduces the mean P_f values of the mUT-A2 and mUT-A3 injection groups, while the control group injected with water remains unaffected by phloretin. The significant differences in results among different studies may partly be attributed to variations in experimental conditions, leading to biased assessments of the water permeability of UT-A subtypes.

Water Transport Mechanism

Exploring the ability of UTs to permeate water is crucial, not only relying on experimental validation but also through structural biology analysis. Researchers constructed a three-dimensional model of human UT-B based on the structure of bovine UT-B using homology modeling and conducted molecular dynamics simulations. The simulation results indicated that water molecules in the UT-B protein rapidly traverse the channel in a single-file manner, primarily facilitated by the rapid exchange of hydrogen bonds between water molecules, particularly involving key threonine residues: Thr177 and Thr339. The dynamic exchange of these hydrogen bonds significantly enhances water conduction. In the central region of the channel, water molecules undergo polar reorientation, a process closely related to hydrogen bond exchange, especially around the threonine-rich residues. As water molecules move through the channel, they encounter an energy barrier located in the reorientation region. Despite this barrier, water molecules are able to overcome it through thermodynamic fluctuations, successfully completing their passage. This mechanism highlights the complexity of water movement within UT channels and its reliance on the hydrogen bond network [31] (Fig. 5.6).

Interestingly, the mechanism by which UT-B facilitates water transport is very similar to that of aquaporin 1 (AQP1), further suggesting that UT-B possesses water permeability. Both AQP1 and UT-B conduct water in a single-file arrangement, where water molecules rapidly move through the channel via hydrogen bond exchange. In both channels, water molecules experience reorientation of their dipole moments, a phenomenon associated with critical amino acid residues in the channel. In AQP1, water molecules reorient in the NPA (asparagine-proline-alanine) region, while in UT-B, this reorientation occurs near the two key threonine residues (Thr177 and Thr339) [31].
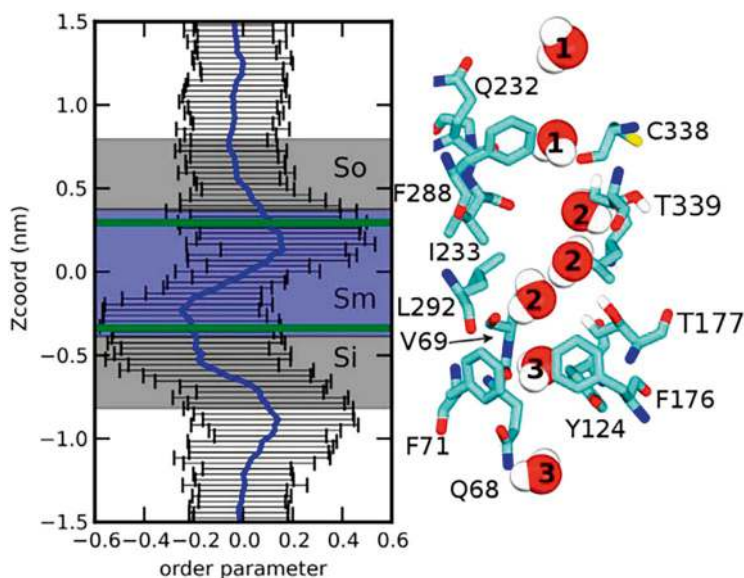
Fig. 5.6 Orientation of water molecules through the pore [31]

Although direct experimental data indicating whether dvUT can permeate water are currently lacking, molecular dynamics simulation results demonstrate that water molecules can enter and traverse the dvUT channel. During this process, water molecules typically move in a discrete manner, occasionally forming continuous water chains, thereby constructing a hydrogen bond network. At the midsection of the dvUT channel ($Z = -1.0$ Å), water molecules exhibit polar inversion, resembling the mechanism of urea transport [27].

Overall, the water transport mechanisms of both dvUT and bovine UT-B are highly similar to that of urea, suggesting a conservation of water permeability and mechanisms among UT family members. Although most laboratories have yet to observe water transport in UT-A, this may relate to experimental conditions such as expression levels. Future studies need to further validate the water permeability of the UT-A family through additional experiments and molecular dynamics simulations.

Urea Analogues Transport Mediated by Urea Transporters

The mechanism of small solute transport in erythrocytes has been a subject of long-standing interest [1, 39, 40]. It was previously reported that human erythrocytes are highly permeable to small non-electrolytes such as formamide and acetamide, implying the presence of a hydrophilic pathway(s) [1, 41]. The UT-B knockout mouse model makes it possible to determine transport rates of urea analogues [14].

Formamide, acetamide, and urea permeabilities were inhibited >80% by UT-B deletion or 0.7 mM phloretin in wild-type erythrocytes. These solutes showed identical permeabilities in UT-B-null and wild-type erythrocytes, both in the absence and presence of phloretin. UT-B-attributable P_s (solute permeability) for urea, formamide, acetamide, methylurea, methylformamide, ammonium carbamate, and acrylamide ranged from 0.5 to 3.2×10^{-5} cm/s. UT-B had a lower permeability to glycolamide, hydroxyurea, and carbohydrazide (P_s of 0.6–1.5×10^{-6} cm/s). Phloretin treatment did not reduce butyramide or isobutyramide permeabilities in either wild-type or UT-B-null erythrocytes (P_s of 9×10^{-6} cm/s and 6×10^{-6} cm/s, respectively), demonstrating that UT-B does not transport butyramide or isobutyramide. In contrast, UT-B conferred >70% of total erythrocyte urea, formamide, acetamide, methylurea, hydroxyurea, and ammonium carbamate transport (Fig. 5.7).

Measurements of solute permeabilities across UT-B-null erythrocytes showed that urea, methylurea, dimethylurea, hydroxyurea, and thiourea permeabilities were low ($<8 \times 10^{-7}$ cm/s) at temperatures between 10 °C and 37 °C, and weakly temperature dependent, which suggests that UT-B is the specific transporter for these solutes. In contrast, formamide, acetamide, acrylamide, and butyramide permeabilities were strongly temperature dependent, ninefold, 11-fold, sevenfold, and sevenfold higher, respectively, at 37 °C compared to 10 °C. Transport of the amides formamide, acetamide, methylformamide, acrylamide, butyramide, and isobutyramide was strongly temperature dependent, indicative of diffusion across the erythrocyte lipid bilayer.

UT-B-mediated transport requires at least one primary amide, i.e. carbonylfunction, attached to a primary unsubstituted amino group. Indeed, UT-B mediates efficient transport of formamide, acetamide, carbamate, and acrylamide, all of which contain primary amide functions. N-methylated amides are poorly transported by UT-B, as evidenced by the relative threefold and 15-fold lower transmembrane flux of methylurea and dimethylurea, respectively. Methylation decreases amide hydrogen-bond capacity and increases lipophilicity and molecular size. Compounds lacking amide functionalities altogether, such as glycine and acetic acid, are not transported by UT-B.

Acetamide and urea have similar molecular sizes, with both also possessing an oxygen to accept hydrogen bonding. Replacement of this oxygen by sulphur, as in thioacetamide and thiourea, results in reduced UT-B-facilitated transport. This could be attributed to loss of hydrogen-bonding capacity of sulphur versus oxygen. In addition, molecular volumes and polar surface are as large or greater as in sulphur-containing compounds compared to their oxygen-containing counterparts. Similarly, guanidine, which has comparable physicochemical properties as urea, was not transported by UT-B, as it replaces urea carbonyl byimine function ($C=N - H$). More lipophilic, less polar analogues such as butyramide, isobutyramide, and acetone tend to rely upon membrane diffusion rather than UT-B facilitated transport. In hydrophilic transport pathways, hydrogen-bond formation is one of the essential processes conferring transport specificity.

Urea is a highly polar molecule with significant hydrogen-bonding capacity, and it seems likely that UT-B-facilitated transport relies on hydrogen bonding. UT-B
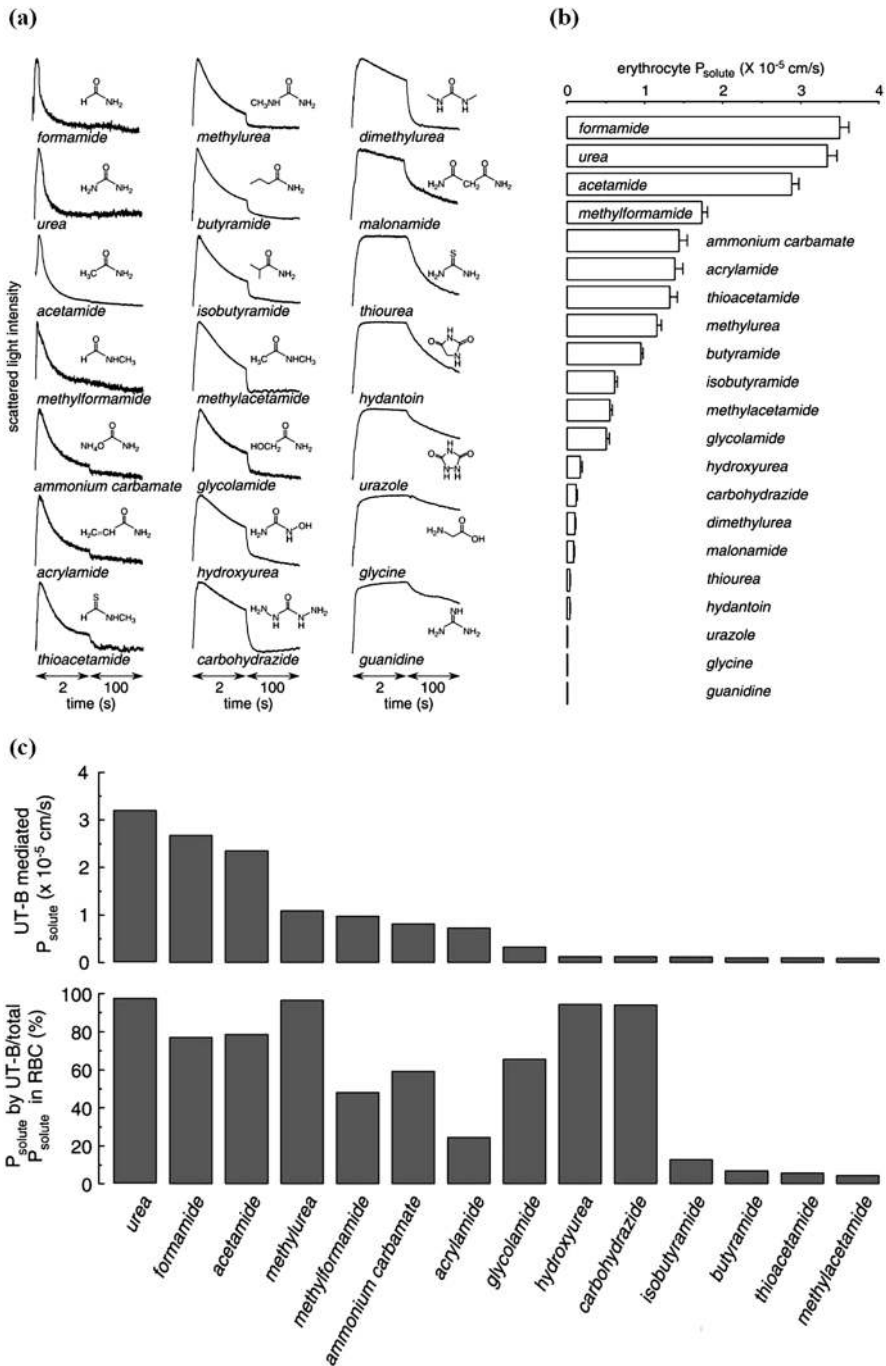
Fig. 5.7 Erythrocyte solute permeability. (**a**) Representative curves for the time course of scattered light intensity at 10 °C in response to a 250 mM inwardly directed gradient of urea analogues. (**b**) Averaged solute permeability coefficients (P_s) for experiments done as in panel A. (**c**) UT-B mediated P_s calculated from $P_s^{wildtype}$ versus $P_s^{UT-B-null}$ (top) and percentage of UT-B mediated P_s in total P_s in erythrocytes (bottom) [14]

prefers to transport neutral, more hydrophilic, urea and primary amides that have more H-bonding capacity and selectively retard transport of lipophilic molecules. Large analogues with less hydrogen-bonding capacity tend to have less permeability. This suggests that UT-B provides a unique type of narrow hydrophilic pathway for transport of urea and that transport specificity/selectivity may largely be governed by H-bonding capacity, size, and the hydrophilic nature of solute. Since urea analogues such as thiourea and acetamide are similar to urea in structure, they were suggested to inhibit urea transport by interacting competitively at transport sites [11, 42].

The transport characteristics of UT-A proteins towards urea analogs have been investigated in limited depth. Only one study has been documented in the literature, which reports that purified *Xenopus* laevis oocyte plasma membrane vesicles expressing mUT-A2 or mUT-A3 exhibit no statistically significant differences in the transport rates of formamide, acetamide, methylurea, or dimethylurea compared to control vesicles. These findings suggest that UT-As demonstrate a high specificity for urea, excluding molecules of similar size and structural resemblance (such as formamide). However, further research is warranted to comprehensively understand these observations [22].

Although structural biology studies on the transport of urea analogs by UT proteins are currently lacking, existing research shows that the transport mechanisms of urea and water are highly conserved within the UT family [23, 24, 27, 28, 31]. These processes rely on the hydrogen bond network and critical polar residues within the channel, particularly threonine residues, to achieve rapid and efficient transport. Furthermore, both urea and water molecules undergo dipole reorientation as they pass through the channel, a phenomenon closely associated with hydrogen bond exchange. This evidence suggests that UT proteins may follow similar molecular mechanisms for transporting urea analogs as they do for urea and water. Therefore, different members of the UT family may possess similar capacities for transporting urea analogs. However, no transport ability for urea analogs has been observed in mUT-A2 and mUT-A3, which may be related to factors such as insufficient expression levels. Further research is needed to determine whether UT-A can transport urea analogs, including molecular dynamics simulations and experimental validations.

Ammonia Transport Mediated by Urea Transporters

Geyer et al. explored the NH_3 permeability of human UT-B expressed in *Xenopus* oocytes [30]. They monitored gas permeability using microelectrodes to record the maximum transient change in surface pH (ΔpHS) caused by exposing oocytes to 5% CO_2/33 mM HCO_3^- (pHS increase) or 0.5 mM NH_3/NH_4^+ (pHS decrease). UT-B expression had no effect on the CO_2-induced ΔpHS but doubled the NH_3-induced ΔpHS. Phloretin reduced UT-B-dependent ($-\Delta pHS^*$) NH_3 by 70%. p-Chloromerc uribenzenesulphonate (pCMBS) reduced (ΔpHS^*) NH_3 by 100%. Molecular

dynamics (MD) simulations of membrane-embedded models of UT-B identified the monomeric UT-B pores as the main conduction pathway for NH_3. These data suggest that UT-B has significant NH_3 permeability.

However, a subsequent study showed that UT-B seems not to be involved in NH_3 transport in human erythrocytes, although the erythrocyte variants used in the same study gave evidence of water permeation through UT-B [31]. These authors think that the measurement of ammonia transport across UT-B might be limited by the high erythrocyte lipid ammonia diffusion and/or by the weak NH_3 unit permeability of UT-B.

Maciver et al. divided *Xenopus* laevis oocyte plasma membrane vesicles expressing either mUT-A2 or mUT-A3 into two groups: one for measuring ammonia permeability and the other for urea permeability. Their study revealed that both UT-A isoforms facilitated urea transport but did not demonstrate permeability to ammonia. These findings suggest that further in-depth research is necessary to determine their permeability characteristics towards ammonia.

UT-B-Mediated Urea Transport in Different Species

Urea permeability was measured in erythrocytes from 11 mammals using the stopped flow technique. The results show that P_{urea} of erythrocytes differs greatly among species. Erythrocytes from dog exhibited the highest P_{urea} (5.3×10^{-5} cm/s), followed by that from fox (3.8×10^{-5} cm/s) > mouse (3.3×10^{-5} cm/s) > cat (2.8×10^{-5} cm/s) > rat (2.5×10^{-5} cm/s) > rabbit (2.4×10^{-5} cm/s) > pig (1.5×10^{-5} cm/s) > human (1.1×10^{-5} cm/s) > sheep (1.0×10^{-5} cm/s) > cow (0.8×10^{-5} cm/s) > donkey (0.7×10^{-5} cm/s). The range of variation of P_{urea} among species spans more than a 7.5-fold difference between the donkey and the dog. Purea was significantly inhibited by 0.7 mM phloretin in all species indicating that urea transport through the erythrocyte membrane is mediated by selective urea transporter proteins.

Osmotic water permeability was measured in erythrocytes from the same 11 mammals. The lowest value was observed in the human (in $\times 10^{-3}$ cm/s, 2.9 ± 0.4) and the highest value in the rabbit (5.2 ± 0.3), only 1.8-fold higher than that in human. Water permeability in erythrocytes is thus relatively similar in all species tested.

Cell membrane urea permeability resulting from simple diffusion across the lipid bilayer is strongly temperature dependent, contrary to that occurring through facilitated transporters. Comparing P_{urea} observed at different temperatures (10, 22, and 27 °C) thus provides information about how much urea transport occurs by simple diffusion. In cat, fox, dog, rat, and mouse, P_{urea} was high at all three temperatures, and only weakly temperature dependent. In contrast, there was a stronger influence of temperature on P_{urea} in cow, donkey, sheep, human, pig, and rabbit. The high activation energy (E_a) of urea transport in herbivores and omnivores suggests that most of the urea transported through the erythrocyte membrane moves through the

lipid bilayer by simple diffusion, with only a moderate amount of urea transported through UT-B. In contrast, in three carnivores and two rodents, only a small fraction of the total urea transport occurs by simple diffusion, and the majority occurs through UT-B. A very significant inverse relationship was observed between E_a and P_{urea}. Only the rabbit departs somewhat from the general trend. It exhibits the same P_{urea} as that of the rat and mouse while its E_a is similar to that of the other herbivores. The urea flux through UT-B in the rabbit is probably much smaller than the UT-B-mediated urea flux in rat and mouse.

The urea and water permeabilities were also measured in erythrocytes from 5 species of birds. In goose, duck, pigeon, and quail, P_{urea} ranged from 0.04 to 0.07×10^{-5} cm/s, i.e. 10 ~ 20-fold lower than in mammals. In chicken, the value of P_{urea} was not available due to the P_f (0.05×10^{-3} cm/s) being too low to measure urea flux-driven volume change in erythrocytes with the stopped flow technique. In goose, duck, pigeon, and quail, erythrocytes showed an osmotic water permeability that was modestly higher than that observed in mammals ($6.1 \sim 7.3 \times 10^{-3}$ cm/s).

The urea permeability of erythrocytes in mammals is obviously related to their ability to concentrate urea. The high P_{urea} allows fast equilibration of urea in erythrocytes during their transit in the renal medulla, where the urea concentration may reach values 50 ~ 200-fold higher than in peripheral blood. Because of their high (AQP1-dependent) water permeability, erythrocytes would undergo severe shrinkage when exposed to the high urea concentration of the inner medulla, if their membrane was not also highly permeable to urea. They would shrink during their transit in the hyperosmotic medulla and subsequently swell on leaving the medulla if they did not possess a high urea permeability [33]. Birds, which concentrate urine to some extent (up to 2.5 times more than plasma in the quail) but excrete their nitrogen wastes as uric acid rather than as urea, do not exhibit facilitated urea transport in their erythrocytes and show a very low P_{urea}, as already described in the literature [33, 43], and as shown in five different birds [44].

Conflicts of Interest The authors have no conflicts of interest.

References

1. P. Naccache, R.I. Sha'afi, Patterns of nonelectrolyte permeability in human red blood cell membrane. J. Gen. Physiol. **62**, 714–736 (1973). https://doi.org/10.1085/jgp.62.6.714
2. R.I. Sha'afi, C.M. Gary-Bobo, Water and nonelectrolytes permeability in mammalian red cell membranes. Prog. Biophys. Mol. Biol. **26**, 103–146 (1973). https://doi.org/10.1016/0079-6107(73)90018-7
3. J.M. Sands, H. Nonoguchi, M.A. Knepper, Vasopressin effects on urea and H2O transport in inner medullary collecting duct subsegments. Am. J. Phys. **253**, F823–F832 (1987). https://doi.org/10.1152/ajprenal.1987.253.5.F823

4. M.A. Knepper, R.A. Star, The vasopressin-regulated urea transporter in renal inner med-
   ullary collecting duct. Am. J. Phys. **259**, F393–F401 (1990). https://doi.org/10.1152/
   ajprenal.1990.259.3.F393
5. S.M. Wall, J.S. Han, C.L. Chou, M.A. Knepper, Kinetics of urea and water permeability acti-
   vation by vasopressin in rat terminal IMCD. Am. J. Phys. **262**, F989–F998 (1992). https://doi.
   org/10.1152/ajprenal.1992.262.6.F989
6. O. Fröhlich, R.I. Macey, J. Edwards-Moulds, J.J. Gargus, R.B. Gunn, Urea transport defi-
   ciency in Jk(a-b-) erythrocytes. Am. J. Phys. **260**, C778–C783 (1991). https://doi.org/10.1152/
   ajpcell.1991.260.4.C778
7. G. You et al., Cloning and characterization of the vasopressin-regulated urea transporter.
   Nature **365**, 844–847 (1993). https://doi.org/10.1038/365844a0
8. B. Olives et al., Cloning and functional expression of a urea transporter from human bone mar-
   row cells. J. Biol. Chem. **269**, 31649–31652 (1994)
9. C. Shayakul, A. Steel, M.A. Hediger, Molecular cloning and characterization of the
   vasopressin-regulated urea transporter of rat kidney collecting ducts. J. Clin. Invest. **98**,
   2580–2587 (1996). https://doi.org/10.1172/JCI119077
10. J.M. Sands, R.T. Timmer, R.B. Gunn, Urea transporters in kidney and erythrocytes. Am.
    J. Phys. **273**, F321–F339 (1997). https://doi.org/10.1152/ajprenal.1997.273.3.F321
11. L.M. Mannuzzu, M.M. Moronne, R.I. Macey, Estimate of the number of urea transport sites in
    erythrocyte ghosts using a hydrophobic mercurial. J. Membr. Biol. **133**, 85–97 (1993). https://
    doi.org/10.1007/BF00231880
12. H. Tsukaguchi et al., Cloning and characterization of the urea transporter UT3: Localization in
    rat kidney and testis. J. Clin. Invest. **99**, 1506–1515 (1997). https://doi.org/10.1172/JCI119313
13. B. Yang, L. Bankir, A. Gillespie, C.J. Epstein, A.S. Verkman, Urea-selective concentrating
    defect in transgenic mice lacking urea transporter UT-B. J. Biol. Chem. **277**, 10633–10637
    (2002). https://doi.org/10.1074/jbc.M200207200
14. D. Zhao, N.D. Sonawane, M.H. Levin, B. Yang, Comparative transport efficiencies of urea
    analogues through urea transporter UT-B. Biochim. Biophys. Acta **1768**, 1815–1821 (2007).
    https://doi.org/10.1016/j.bbamem.2007.04.010
15. S.M. Bagnasco, T. Peng, M.G. Janech, A. Karakashian, J.M. Sands, Cloning and char-
    acterization of the human urea transporter UT-A1 and mapping of the human Slc14a2
    gene. Am. J. Physiol. Renal Physiol. **281**, F400–F406 (2001). https://doi.org/10.1152/
    ajprenal.2001.281.3.F400
16. C.P. Smith, E.A. Potter, R.A. Fenton, G.S. Stewart, Characterization of a human colonic cDNA
    encoding a structurally novel urea transporter, hUT-A6. Am. J. Physiol. Cell Physiol. **287**,
    C1087–C1093 (2004). https://doi.org/10.1152/ajpcell.00363.2003
17. B.K. Kishore, J. Terris, P. Fernández-Llama, M.A. Knepper, Ultramicrodetermination of
    vasopressin-regulated urea transporter protein in microdissected renal tubules. Am. J. Phys.
    272, F531–F537 (1997). https://doi.org/10.1152/ajprenal.1997.272.4.F531
18. C.P. Smith et al., Cloning and regulation of expression of the rat kidney urea transporter
    (rUT2). J. Clin. Invest. **96**, 1556–1563 (1995). https://doi.org/10.1172/JCI118194
19. A. Karakashian et al., Cloning and characterization of two new isoforms of the rat kidney
    urea transporter: UT-A3 and UT-A4. J. Am. Soc. Nephrol. **10**, 230–237 (1999). https://doi.
    org/10.1681/ASN.V102230
20. R.A. Fenton et al., Characterization of mouse urea transporters UT-A1 and UT-A2. Am.
    J. Physiol. Renal Physiol. **283**, F817–F825 (2002). https://doi.org/10.1152/ajprenal.00263.2001
21. R.A. Fenton et al., Molecular characterization of a novel UT-A urea transporter isoform (UT-
    A5) in testis. Am. J. Physiol. Cell Physiol. **279**, C1425–C1431 (2000). https://doi.org/10.1152/
    ajpcell.2000.279.5.C1425
22. B. Maciver, C.P. Smith, W.G. Hill, M.L. Zeidel, Functional characterization of mouse urea
    transporters UT-A2 and UT-A3 expressed in purified Xenopus laevis oocyte plasma mem-
    branes. Am. J. Physiol. Renal Physiol. **294**, F956–F964 (2008). https://doi.org/10.1152/
    ajprenal.00229.2007

23. E.J. Levin, M. Quick, M. Zhou, Crystal structure of a bacterial homologue of the kidney urea transporter. Nature **462**, 757–761 (2009). https://doi.org/10.1038/nature08558
24. E.J. Levin et al., Structure and permeation mechanism of a mammalian urea transporter. Proc. Natl. Acad. Sci. USA **109**, 11194–11199 (2012). https://doi.org/10.1073/pnas.1207362109
25. G. Chi et al., Structural characterization of human urea transporters UT-A and UT-B and their inhibition. Sci. Adv. **9**, eadg8229 (2023). https://doi.org/10.1126/sciadv.adg8229
26. S.M. Huang et al., Structural insights into the mechanisms of urea permeation and distinct inhibition modes of urea transporters. Nat. Commun. **15**, 10226 (2024). https://doi.org/10.1038/s41467-024-54305-y
27. Z. Wang et al., Computation and simulation of the structural characteristics of the kidney urea transporter and behaviors of urea transport. J. Phys. Chem. B **119**, 5124–5131 (2015). https://doi.org/10.1021/jp511300u
28. H.T. Zhang et al., Modeling of flux, binding and substitution of urea molecules in the urea transporter dvUT. J. Mol. Graph. Model. **76**, 504–511 (2017). https://doi.org/10.1016/j.jmgm.2017.04.022
29. B. Yang, A.S. Verkman, Urea transporter UT3 functions as an efficient water channel. Direct evidence for a common water/urea pathway. J. Biol. Chem. **273**, 9369–9372 (1998). https://doi.org/10.1074/jbc.273.16.9369
30. R.R. Geyer et al., Movement of NH3 through the human urea transporter B: A new gas channel. Am. J. Physiol. Renal Physiol. **304**, F1447–F1457 (2013). https://doi.org/10.1152/ajprenal.00609.2012
31. S. Azouzi et al., Energetic and molecular water permeation mechanisms of the human red blood cell urea transporter B. PLoS One **8**, e82338 (2013). https://doi.org/10.1371/journal.pone.0082338
32. F. Sidoux-Walter et al., At physiological expression levels the Kidd blood group/urea transporter protein is not a water channel. J. Biol. Chem. **274**, 30228–30235 (1999). https://doi.org/10.1074/jbc.274.42.30228
33. R.I. Macey, Transport of water and urea in red blood cells. Am. J. Phys. **246**, C195–C203 (1984). https://doi.org/10.1152/ajpcell.1984.246.3.C195
34. J.A. Dix, A.K. Solomon, Role of membrane proteins and lipids in water diffusion across red cell membranes. Biochim. Biophys. Acta **773**, 219–230 (1984). https://doi.org/10.1016/0005-2736(84)90085-3
35. B. Yang, A.S. Verkman, Analysis of double knockout mice lacking aquaporin-1 and urea transporter UT-B. Evidence for UT-B-facilitated water transport in erythrocytes. J. Biol. Chem. **277**, 36782–36786 (2002). https://doi.org/10.1074/jbc.M206948200
36. N. Lucien et al., Antigenic and functional properties of the human red blood cell urea transporter hUT-B1. J. Biol. Chem. **277**, 34101–34108 (2002). https://doi.org/10.1074/jbc.M205073200
37. J. Brahm, M.H. Dziegiel, J. Leifelt, Urea and water are transported through different pathways in the red blood cell membrane. J. Gen. Physiol. **155** (2023). https://doi.org/10.1085/jgp.202213322
38. J. Kabutomori, N. Pina-Lopes, R. Musa-Aziz, Water transport mediated by murine urea transporters: Implications for urine concentration mechanisms. Biol Open **9** (2020). https://doi.org/10.1242/bio.051805
39. W.R. Galey, J.D. Owen, A.K. Solomon, Temperature dependence of nonelectrolyte permeation across red cell membranes. J. Gen. Physiol. **61**, 727–746 (1973). https://doi.org/10.1085/jgp.61.6.727
40. R.R. Mayrand, D.G. Levitt, Urea and ethylene glycol-facilitated transport systems in the human red cell membrane. Saturation, competition, and asymmetry. J. Gen. Physiol. **81**, 221–237 (1983). https://doi.org/10.1085/jgp.81.2.221
41. R.I. Sha'afi, A. Dakkuri, G. To'mey, Solute and solvent flow across mammalian red cell membrane. How to test for Onsager reciprocal relation. Biochim. Biophys. Acta **249**, 260–265 (1971). https://doi.org/10.1016/0005-2736(71)90103-9

42. C.L. Chou, M.A. Knepper, Inhibition of urea transport in inner medullary collecting duct by phloretin and urea analogues. Am. J. Phys. **257**, F359–F365 (1989). https://doi.org/10.1152/ajprenal.1989.257.3.F359
43. F.R. Hunter, Facilitated diffusion in pigeon erythrocytes. Am. J. Phys. **218**, 1765–1772 (1970). https://doi.org/10.1152/ajplegacy.1970.218.6.1765
44. L. Liu et al., Erythrocyte permeability to urea and water: Comparative study in rodents, ruminants, carnivores, humans, and birds. J. Comp. Physiol. B **181**, 65–72 (2011). https://doi.org/10.1007/s00360-010-0515-5

Chapter 6
Physiological Functions of Urea Transporters

Zhiwei Qiu, Tao Jiang, Guangying Shao, and Baoxue Yang

Abstract Urea transporters (UTs) are a group of membrane channel proteins that specifically facilitate the permeation of urea, which play an essential role in urea reabsorption and water conservation. There are 4 isoforms, UT-A1, UT-A2, UT-A3, UT-B, that are expressed in the kidney to maintain the urea recycle and establish the urea concentration gradient in the medulla, which is essential for the urinary concentration capacity of the kidney. Outside the kidney, widely distributed UT-B and some UT-A isoforms directly participate in regulating signaling transduction and determining cell fate by regulating osmotic pressure, arginine metabolism, and protein carbamylation in various systems. In recent years, studies on different UT knockout mouse models revealed multiple physiological roles of UTs. This chapter summarizes the physiological functions of UTs, including the blood system, urinary system, nervous system, circulatory system, digestive system, auditory system, visual system, reproductive system, and skeletal system.

Keywords Urine concentration · Urea transporter · Osmotic pressure · Arginine metabolism · Protein carbamylation

Z. Qiu (✉)
Institute of Clinical Pharmacology, Peking University First Hospital, Beijing, China
e-mail: 11067@pkufh.com

T. Jiang
College of Basic Medicine, Beihua University, Jilin, China

G. Shao
Department of Cardiology, Beijing Hospital, National Center of Gerontology, Institute of Geriatric Medicine, Chinese Academy of Medical Sciences, Beijing, China

B. Yang (✉)
Department of Pharmacology, State Key Laboratory of Vascular Homeostasis and Remodeling, School of Basic Medical Sciences, Peking University, Beijing, China
e-mail: baoxue@bjmu.edu.cn

Introduction

Urea transporters (UTs) are a class of transmembrane proteins specifically permeable to urea, playing a pivotal role in the transport of urea across cellular membranes [1]. UTs are categorized into two subfamilies: UT-A and UT-B. The UT-A subfamily includes 6 members (UT-A1 to UT-A6), primarily expressed in the kidney, testis and colon (Fig. 6.1) [1, 2]. While the UT-B subfamily consists solely of UT-B [3, 4], which is expressed in various tissues, such as erythrocyte, kidney, brain, heart, intestine, bladder, testis, bone marrow, vascular endothelium, etc. (Fig. 6.1) [1, 2, 4].

UTs play physiological roles in the organs that are related to urea metabolism [4]. By mediating rapid urea transport across membranes driven by concentration gradients, they facilitate efficient urine concentration in the kidney [4]. Furthermore, UT-B is also involved in multiple physiological functions, such as the regulation of bladder homeostasis, sperm development, and maintenance of cardiac electrophysiological activity [4–19].
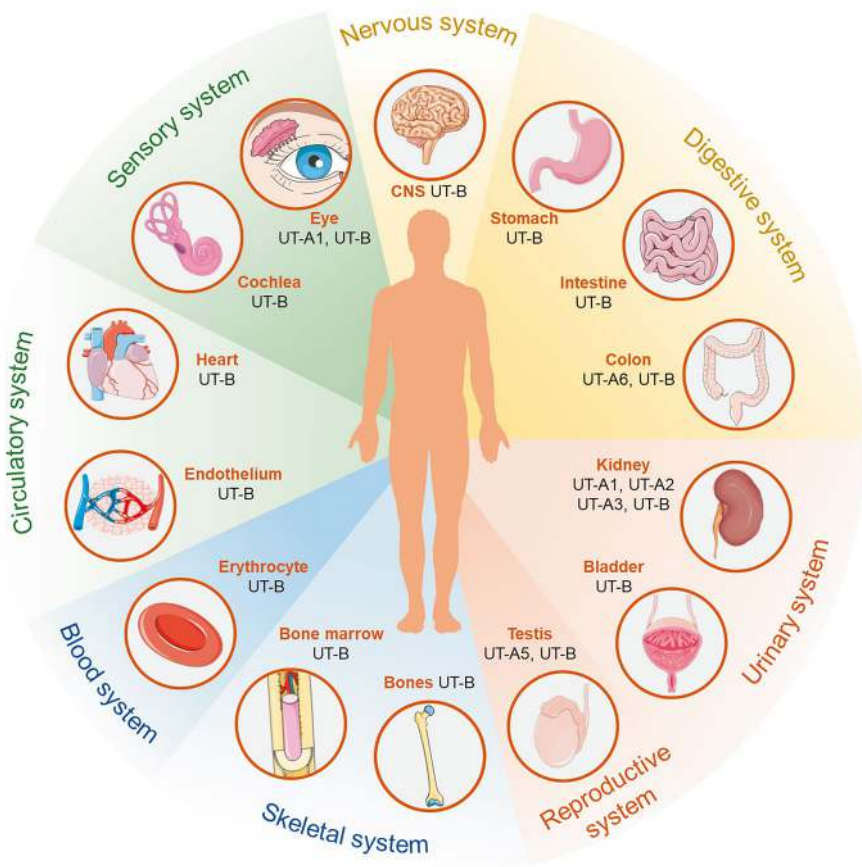
Fig. 6.1 Distribution of urea transporters in human
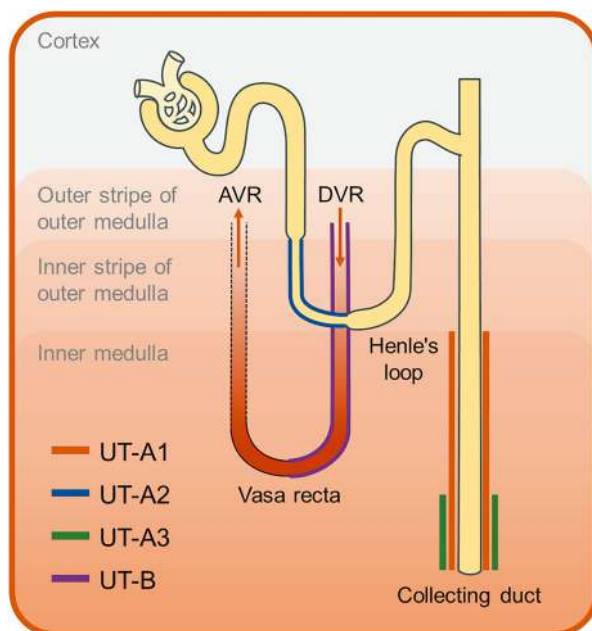
Fig. 6.2 Localization of urea transporters in the kidney

Physiological Function of UTs in the Kidney

Both human and mouse kidneys express UT-A1, UT-A2, UT-A3, and UT-B, which localize to certain parts in the kidney (Fig. 6.2) [4, 20–23]. Over past 30 years, studies on UT knockout mouse models have provided crucial insights into the physiological functions of UT in the urine concentrating mechanism and intrarenal urea recycling [24].

Role of UT-B in the Urine Concentrating Mechanism

UT-B is predominantly expressed on the endothelial cells of the descending vasa recta in the kidney [1, 4, 19, 25]. UT-B facilitates urea transport from the vascular lumen to the interstitial fluid depending on the urea concentration gradient difference trans-endothelia, which in turn enhances the urea concentration gradient in the medullary tissue [4, 19]. In 2002, Yang et al. generated the UT-B knockout mouse model [26]. Daily urine output was 1.5-fold greater and urine osmolarity was lower in UT-B knockout mice than wildtype mice (Table 6.1) [26]. Urine urea concentration was 35% lower in UT-B knockout mice than in wildtype mice (Table 6.1) [26]. It was also found that there was a disproportionate reduction in the concentration of urea compared with salt in homogenized renal inner medullas of UT-B knockout

mice, defining a novel "urea selective" urinary concentrating defect in UT-B knockout mice [26]. These data directly reflect the pivotal role of UT-B in maintaining the high urea concentration gradient and osmolarity gradient in the renal inner medulla [26].

The role of UT-B in the urine concentrating mechanism was also studied in normal conditions and after acute or chronic alterations in urea excretion (acute urea loading or variations in protein intake, respectively) with the UT-B knockout mouse model [26]. Acute urea loading induced a progressive increase in urinary urea concentrating ability in wildtype mice and a subsequent improvement in their urine concentrating ability in contrast to UT-B knockout mice, in which urinary osmolality and urine urea concentration did not rise, due to the failure to accumulate urea in the medulla [26]. With increasing protein intake (from 10% to 40% protein in the diet, leading to a five-fold increase in urea excretion), UT-B knockout mice were not able to increase urea in urine as did wildtype mice [26]. These data suggest that UT-B in renal medullary vessels plays an important role in urine concentrating ability and in renal urea handling during high-protein intake.

To deeply understand the physiological role of UT-B in urine concentration, particularly its synergy with UT-A2, Lei et al. established a UT-A2 and UT-B double knockout mouse model (UT-A2/B knockout) and conducted a series of physiological and molecular biological analyses [27]. Although UT-A2/B knockout mice also had higher urine volumes than wildtype mice, their urine output were less than those of UT-B knockout mice, and their urine osmolality fell between those of UT-B knockout and wildtype mice (Table 6.1) [27]. Further studies revealed that after 18 h of water deprivation, urine osmolarities in wildtype, UT-B knockout, and UT-A2/B knockout mice all increased significantly, but UT-B knockout mice maintained the lowest urine osmolarity, while UT-A2/B double knockout mice exhibited intermediate levels [27]. The experiment of acute urea loading or chronic changes in protein intake also detected an intermediate urinary concentration capacity in UT-A2/B knockout mice.

The experimental data from both UT-B knockout mice and UT-A2/B knockout mice indicate that UT-B plays a more important role than UT-A2 in maintaining the

Table 6.1 Parameters of urine concentrating ability of mice with different UT genotypes

Genotype	Urine output (mL/day)	Urinary osmolality (mOsm/L)	Urinary urea (mmol/L)	Urinary non-urea solutes (mmol/L)	Medulla osmolality (mOsm/L)
Wildtype	1.5	2288	1472	816	340
UT-B$^{-/-}$	2.4	1318	797	521	171
UT-B/A2$^{-/-}$	1.8	1775	1205	570	302
UT-A2$^{-/-}$	1.5	2052	No data	No data	No data
UT-A1/A3$^{-/-}$	5.0	861	799	62	86
UT-A1$^{-/-}$	No data	No data	No data	No data	No data
UT-A3$^{-/-}$	1.8	2246	1286	960	No data
All-UT$^{-/-}$	6.4	941	797	144	77

hyperosmotic state of the inner medulla and in the urine concentrating mechanism. While the presence of UT-A2 can partially compensate for UT-B deficiency [27]. These results revealed the synergistic action of UT-A2 and UT-B in urine concentration [27, 28].

Moreover, UT-B not only specifically permeates urea but also exhibits a degree of water permeability [29, 30]. This dual transport function endows UT-B with a crucial role in both urea and water metabolism in the kidney. By facilitating the transport of urea from the vascular lumen to the interstitial fluid, UT-B indirectly promotes water reabsorption, contributing to urine concentration [29, 30]. Simultaneously, the water permeability of UT-B enables it to directly participate in the regulation of renal water transport [29, 30].

Role of UT-As in the Urine Concentrating Mechanism

UT-A1 is a vasopressin regulated urea transporter and expressed in the apical plasma membrane of principal cells at the end part of inner medullary collecting ducts (IMCD) [21]. Single UT-A1 knock mice are a good model to study the function of UT-A1. However, since UT-A1 and UT-A3 are expressed at the same location, share the same promoter and the same sequence of the first nine exons in *Slc14a2*, it is difficult to knockout UT-A1 without affecting UT-A3 [21, 31]. In 2004, the Knepper group generated a UT-A1 and UT-A3 double (UT-A1/3) knockout mouse model. UT-A1/3 knockout mice exhibited a severe urine-concentrating deficiency and urea-selective diuresis (Table 6.1) [32]. However, this model did not clearly distinguish the functionality of UT-A1 and UT-A3 in the kidney.

Basing on a unique sequence at the 3′-coding regions of UT-A3 that was located in the intron of UT-A1 [33], the Yang group creatively designed an ingenious point synonymous mutation of the consensus splice site of UT-A1 mRNA to disrupt the gene transcription process without any influence on the expression of UT-A3, and successfully generated an UT-A1 knockout mouse model [21]. These mice exhibited a marked increase in daily urine output, approximately 3 times that of wildtype mice, accompanied by a significant decrease in urine osmolality [21]. Even under the conditions such as 24 h water restriction, acute urea loading, or high-protein diet, UT-A1 knockout mice failed to effectively enhance urine concentration, confirming the key role of UT-A1 in urea concentration in inner medulla and urine concentrating mechanism [21].

UT-A2 is expressed in the lower half of the thin descending limb of Henle's loops (TDL) in short-looped nephrons, and in the initial inner medullary segments of the TDL in long-looped nephrons. Unlike UT-A1, UT-A2 does not share a promoter with any of the other UT-A isoforms [34]. Consequently, construction of UT-A2 knockout mice is relatively simple. As early as 2005, Uchida et al. accomplished this work by deleting the promoter of UT-A2 [34]. However, UT-A2 knockout mice did not display overt physiological abnormalities under basal conditions, with normal urine concentrating ability (Table 6.1) [34]. When subjected to a

low-protein diet, UT-A2 knockout mice exhibited slightly deficient urine concentration ability, but their urine volume and osmolality remained comparable to those of wildtype mice under normal and high-protein diets [34]. These data suggest that UT-A2 contributes relatively little to maintaining urine concentrating ability under basal conditions but may play a role under specific conditions, such as a low-protein diet.

UT-A3 is expressed in the basal plasma membrane of principal cells, which express UT-A1 in apical plasma membrane, at the end part of inner medullary collecting ducts. Due to the particularity of the *slc14a2* gene structure, it is impossible to directly create UT-A3 knockout mice by gene targeting or editing. In 2016, the Sands group successfully restored UT-A1 expression in UT-A1/A3 knockout mouse, equivalently creating a UT-A3 deficient mouse model [35]. UT-A3 deficient mice displayed urine volume and osmolality levels close to those of wildtype mice, significantly outperforming UT-A1/A3 double knockout mice (Table 6.1) [35]. This finding indicates that within the UT-A family, UT-A1 plays a more crucial role in maintaining the urea concentration gradient and urine-concentrating function in the renal inner medulla. Nevertheless, UT-A3 also participates to some extent in this process, and its absence leads to a moderate decline in urine-concentrating ability.

In 2017, the Yang group generated an all-UT knockout mouse model [24], in which there is not any UT expression. All-UT knockout mice exhibited no significant phenotype in growth, development, or overt behavior compared to wildtype mice, indicating that the absence of UT-A and UT-B does not directly affect their basic life activities [24]. However, these mice displayed prominent polyuria, with daily urine output approximately 3.5 times that of wildtype mice, accompanied by a significantly decreased urine osmolality (Table 6.1) [24]. Following water deprivation, wildtype mice were capable of markedly elevating their urine osmolality to cope with water restriction, whereas the increase in urine osmolality was significantly defective in all-UT knockout mice, further reinforcing the central role of UT in urine concentration mechanisms [24]. All-UT knockout mice were not able to increase urinary urea concentration and osmolality after acute urea loading or high protein intake either. No significant histological abnormalities were observed in the renal cortex and outer medulla of all-UT knockout mice, but their inner medulla exhibited dilation of the collecting ducts, significantly lower urea concentration and osmolarity compared to wildtype mice and other single UT knockout mice. These data directly underscored the importance of UTs in regulating urine concentrating ability.

All-UT knockout mice showed greater urine output than other UT knockout mice. The reason is that less urea was reabsorbed at the end of IMCD (by UT-A1 and UT-A3), less urea was returned to the IM by DVR (by UT-B), and more urea was taken up by AVR into circulation, which led to a lower urea concentration in the IM of all-UT knockout mice than in wildtype mice. However, the experimental results from different UT knockout mice showed that UT-A1 played the most dominant role in urine concentrating mechanism. All data from different UT knockout mouse models and mathematical simulations suggest that UT-A1 is a good diuretic target and that UT-A1 inhibitors might be developed into a novel class of diuretics [1, 36–38].

UT Mediated Intrarenal Urea Recycling

Recycling of urea within the renal medulla is known to play an important role in the capacity of the kidney to concentrate urine. This recycling occurs simultaneously through a tubular and a vascular route (i.e., through the loops of Henle and vasa recta, respectively). Intrarenal urea recycling represents a crucial mechanism for maintaining the hyperosmotic environment in the renal inner medulla and facilitating urine concentrating ability [25]. Drawing upon the findings from studies on UT knockout mouse models, researchers have elucidated the regulatory role of UT in the renal urea recycling (Fig. 6.3) [21, 24, 25, 27, 29, 30, 32, 34, 35, 39].

When urine flows through the collecting ducts, water is efficiently reabsorbed via aquaporins, driven by the osmotic pressure gradient across the ducts, a process that gradually elevates the urea concentration within the lumen [40]. Subsequently, at the terminal end of the collecting ducts, high concentrations of urea are efficiently transported into the interstitium via UT-A1 and UT-A3, promoting the accumulation of urea in the apical region of the inner medulla [23, 41–44]. This high concentration urea, under the influence of concentration gradients, permeates into the ascending limbs of the vasa recta through microporous structures [45–48]. Subsequently, urea undergoes countercurrent exchange within the vasa recta system, facilitated by UT-B, being transported from the ascending limbs to the descending limbs and recirculated back to the inner medulla region via the bloodstream [45–48], which forms intrarenal urea recycling.

The intrarenal urea recycling maintains the urea concentration gradient within the renal inner medullary tissue, constituting the core physiological mechanism of the urine concentrating mechanism [25]. Additionally, UT-A2 plays a pivotal role in the thin descending limb of the loop of Henle, delicately modulating the balance of urea concentrations between the lumen and interstitium in response to changes in their respective concentrations [28, 33, 34, 49, 50]. Therefore, the urea concentration gradient and osmotic pressure gradient in the renal inner medullary tissue are intricately dependent on the complex urea cycling processes mediated by various UTs.

Physiological Functions of UTs in Extrarenal Tissues

Blood System

UT-B is highly expressed in the plasma membrane of erythrocytes, primarily responsible for the transmembrane transport of urea and exhibiting some water channel functions [6, 51]. In recent years, with the intensification of research on UT-B, its crucial role in the blood system has gradually been uncovered (Fig. 6.5).

The primary function of UT-B in erythrocytes is to transport urea, which is vital for maintaining the balance of urea concentrations inside and outside the cells [7, 11, 17, 52]. Given the strong dipole moment of urea, it does not directly traverse
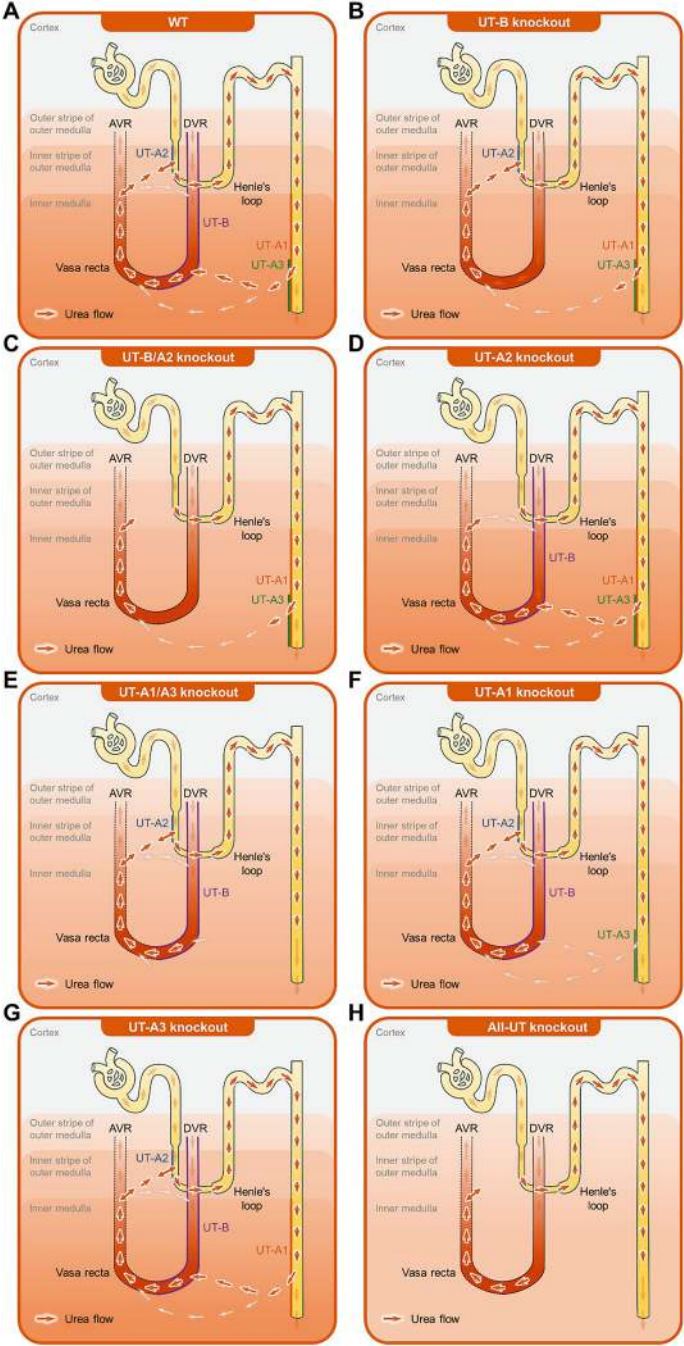
Fig. 6.3 Intrarenal urea cycle of mice with different UT genotypes. (**a**) Diagrams of intrarenal urea cycle of wildtype (WT) mice. (**b**) Diagrams of intrarenal urea cycle of UT-B knockout mice. (**c**) Diagrams of intrarenal urea cycle of UT-B/A2 double knockout mice. (**d**) Diagrams of intrarenal urea cycle of UT-A2 knockout mice. (**e**) Diagrams of intrarenal urea cycle of UT-A1/A3 double knockout mice. (**f**) Diagrams of intrarenal urea cycle of UT-A1 knockout mice. (**g**) Diagrams of intrarenal urea cycle of UT-A3 knockout mice. (**h**) Diagrams of intrarenal urea cycle of all-UT knockout mice

non-polar lipid membranes, necessitating UT-B for its transmembrane transport [17]. The urea transport capacity of UT-B in erythrocytes safeguards the cells from osmotic pressure changes by maintaining the osmotic balance between the intracellular and extracellular environments [11, 17, 52]. In high-urea regions, such as the renal inner medulla, UT-B collaborates with AQP1 to regulate the balance of water and urea transport across erythrocyte membranes, preventing damage from high urea concentrations [11, 17, 52]. Additionally, the rapid urea transport mediated by UT-B facilitates the establishment of a urea concentration gradient between erythrocytes and their surroundings, enhancing effective urea excretion in the body [11, 17, 52].

UT-B also plays a pivotal role in regulating blood rheology [7]. Knockout or inhibition of UT-B improved erythrocyte deformability, reduced osmotic fragility, and affected hematological parameters such as whole blood viscosity [7]. These changes suggest that UT-B may modulate erythrocyte membrane permeability and stability, influencing their fluidity and function within the circulation. Consequently, UT-B might be developed as a potential therapeutic target for improving blood rheology in certain metabolic and genetic disorders.

Notably, UT-B is identical to the Jk antigen in the Kidd blood group system [12, 53–56]. Kidd blood group incompatibility can lead to severe neonatal hemolytic transfusion reactions, underscoring its significance in transfusion safety [12, 53–56]. The JK-null phenotype arises from mutations in UT-B splicing sites, resulting in the absence of functional UT-B protein [12, 53–56]. While UT-B deficiency does not cause severe pathological phenotypes in humans, it may threaten transfusion safety in certain ethnic groups or under specific conditions, such as increased erythrocyte sensitivity to urea-induced hemolysis [12, 53–56]. Thus, screening and identifying Kidd blood group antigens before transfusion is of utmost importance.

Circulation System

The expression of UT-B in the heart is crucial for maintaining normal cardiac electrophysiological activities. Studies have demonstrated that UT-B knockout mice exhibited significantly prolonged ECG P-R intervals, with elderly UT-B knockout mice even presenting with grade II-III atrioventricular block [4, 16]. These phenomena suggest that the absence of UT-B may impair the cardiac conduction system, leading to delayed or obstructed electrical signal propagation (Fig. 6.5).

Further proteomic analysis has shed light on the effects of UT-B deficiency on the cardiac proteome. Multiple proteins related to cardiac function, cellular energy metabolism, ion channel function, and oxidative stress exhibit abnormal expression patterns in the hearts of UT-B knockout mice [17, 57]. Notably, atrial natriuretic peptide, a vital cardiac hormone involved in regulating blood pressure, cardiac function, and responding to cardiovascular diseases such as cardiac hypertrophy, showed a marked elevation [2, 4, 57]. These changes may reflect the adaptive response of

heart to stress load following UT-B deficiency and potentially portend structural and functional alterations in the heart.

Moreover, UT-B knockout mice were prone to cardiac oxidative stress and myocardial hypertrophy, accompanied by elevated urea concentrations and aberrant glucose-lipid metabolism in cardiomyocytes [58]. These observations indicated that UT-B played a pivotal role in maintaining cardiomyocyte energy metabolism and redox balance. UT-B deficiency may lead to urea accumulation within cardiomyocytes, disrupting the arginine-nitric oxide (NO) pathway, affecting NO production and vasodilation [58, 59]. Concurrently, urea accumulation may foster the generation of reactive oxygen species (ROS), exacerbating oxidative stress and further compromising cardiomyocyte structure and function [58].

In addition, although direct studies on the function of UT-B in vessels are relatively scarce, existing evidence suggested that UT-B may indirectly regulate vascular function by influencing urea transport and metabolism [59]. Changes in urea concentrations associated with UT-B can modulate the arginine-NOS-NO pathway, thereby regulating the contraction and relaxation of vascular smooth muscle cells [59].

Digestive System

UT-B is expressed in the human small intestine, colon, and colonic crypts, playing a pivotal role in maintaining intestinal health and microbial balance (Fig. 6.5) [60–63]. It was reported that the regulation of UT-B on gut microbiota may be linked to its modulation of the intestinal urea nitrogen salvage (UNS) process [64]. During UNS, urea is broken down by intestinal bacterial ureases, releasing ammonia and carbon dioxide [64, 65]. The resulting ammonia is then utilized by bacteria to synthesize amino acids and peptides, which are absorbed through intestinal epithelial transport systems, contributing to nutrition and fostering a healthy microbial balance [64, 65]. By facilitating UNS, UT-B indirectly influenced the metabolic activities and ecological equilibrium of the gut microbiota [64, 65]. As alterations in gut microbiota are implicated in the development of various diseases, such as diabetes, inflammatory bowel diseases, and obesity, the regulation of UT-B on gut microbiota may exert an influence on these conditions.

Furthermore, the promotion of UT-B on UNS in the gut reduced urea accumulation and lower intestinal ammonia concentrations, mitigating the toxic effects of ammonia on intestinal mucosa [64]. Additionally, UT-B may regulate the transport functions of intestinal epithelial cells, impacting nutrient absorption and metabolite excretion, further safeguarding intestinal health [4].

Although UT-A6 has been shown to be expressed along the human gastrointestinal tract and Caco-2 cell line [66, 67], its specific physiological function has not been clarified. The current evidence only shows that hyperosmotic stimulation significantly up-regulated UT-A6 expression in Caco-2 cells, and this process was

regulated by protein kinase C and calcium [66], suggesting that UT-A6 may play a role in intestinal adaptation to a hypertonic environment. More work is needed in the future to uncover the physiological function of UT-A6 in the gut.

Urinary System

Current research evidence indicates that UT-B is highly expressed in bladder epithelial cells [4, 5, 19]. The concentration of urea is high in bladder urine, suggesting that the overexpression of UT-B may be closely related to its role in maintaining bladder epithelial cell homeostasis and preventing urea toxicity (Fig. 6.5).

Studies utilizing UT-B knockout mouse models have revealed a significant impact on bladder epithelial structure and function following UT-B deficiency [18]. While optical microscopy failed to discern notable differences in bladder tissue architecture between UT-B knockout mice and wildtype mice, transmission electron microscopy revealed abnormalities such as increased myelination, mitochondrial swelling, and lysosome formation in bladder epithelial cells of UT-B knockout mice, indicating compromised cellular function [18]. Further investigation demonstrated early apoptosis in the bladder epithelium of UT-B knockout mice, manifested by increased cytoplasmic density, nuclear chromatin condensation, and elevated TUNEL-positive cell counts [4, 18].

The bladder epithelial apoptosis caused by UT-B knockout is multifaceted. Firstly, the absence of UT-B significantly elevated urea concentration within bladder epithelial cells [18]. High urea levels disrupt protein hydrophobic regions or carbamylate proteins, altering their bioactivity and thereby inducing apoptosis [18]. Secondly, UT-B knockout altered the expression of genes associated with apoptosis and DNA damage in bladder epithelia, with upregulation of genes like *Dcaf11*, *MCM2-4*, and downregulation of *Uch-L1*, *Bnip3* [18]. These changes further promoted cellular apoptosis and DNA damage. Additionally, UT-B deficiency disrupted arginine metabolism, leading to reduced polyamine production and increased NO levels, with excessive NO exacerbating DNA damage and apoptosis [18]. This cascade of pathological changes triggered by UT-B knockout not only affected normal bladder function but also elevated the risk of bladder cancer [18].

Nervous System

UT-B is broadly expressed in the central nervous system (CNS) of mice, encompassing crucial brain regions such as the olfactory bulb, cortex, caudate nucleus, hippocampus, and hypothalamus [4, 13]. Additionally, UT-B is present in astrocytes, co-localizing with the astrocyte marker GFAP in brain slices, suggesting its vital physiological functions within the glial network of the CNS [4, 13]. Recent advancements in the study of UT-B functions in the CNS have gradually unveiled its

roles in maintaining urea concentrations, modulating neurotransmitter levels, influencing cerebral blood flow (CBF), and participating in cerebrospinal fluid (CSF) sodium and water homeostasis (Fig. 6.5) [4, 68, 69].

By facilitating urea transport, UT-B plays a pivotal role in maintaining urea concentrations within the brain [4]. Although the urea cycle in the CNS is incomplete, UT-B regulates urea distribution and balance [4]. UT-B deficiency led to increased urea content in the cerebral cortex and hypothalamus of mice, potentially impacting neuronal function [13]. This alteration in urea concentration is closely tied to the role of UT-B in preserving the microenvironmental stability of the brain [13].

UT-B was intricately linked to NO levels and CBF [68]. UT-B deficiency reduced NO content in the mouse hippocampus while enhancing neuronal nitric oxide synthase (nNOS) expression [70, 71]. This decrease in NO levels may stem from urea competitively inhibiting L-arginine transport into endothelial cells via UT-B [4, 17]. As NO functions as a crucial neurotransmitter and vasodilator, regulating CBF and neuronal function, UT-B deficiency-induced NO reduction could further decrease CBF, elevating the risk of neuronal degeneration and damage [4, 68].

Furthermore, UT-B may be vital for sodium and water balance in the CSF [4, 69]. Long-term high-salt diets significantly elevated Na^+ concentrations in the CSF of salt-sensitive rats and markedly reduced UT-B expression in choroid plexus epithelial cells [69]. This finding indicates the importance of UT-B in regulating Na^+ concentration and maintaining water balance in CSF. High-salt diets may downregulate UT-B expression by increasing arginine vasopressin levels, thereby affecting urea and Na^+ transport and distribution in CSF. This regulatory mechanism is crucial for maintaining CNS homeostasis.

Notably, UT-B-deficient mice exhibited depressive-like behaviors from an early age [13]. This behavioral change may result from the combined effects of increased urea concentrations, decreased NO levels, and reduced CBF caused by UT-B deficiency [13]. These alterations could ultimately lead to depressive-like behaviors in mice by influencing neuronal excitability and synaptic plasticity [13]. This finding provided new insights into the pathogenesis of neuropsychiatric disorders such as depression.

Auditory System

UT-B is expressed in pillar cells, hair cells, and Boettcher cells of both the inner and outer ear, where these cells play pivotal roles in ear structure and function (Fig. 6.5) [72]. For instance, the inner ear is responsible for sound conduction and balance maintenance, while the outer ear participates in sound collection and conduction [73]. The presence of UT-B in these cells suggests its potential involvement in specific physiological processes within the ear.

The stability of endolymphatic volume, pressure, and chemical composition is crucial for electromechanical sound transduction within the ear [4]. As a diagnostic marker for endolymphatic hydrops, content and transport of urea are vital for

maintaining endolymphatic homeostasis [4]. The expression of UT-B in the supporting cell system of the inner ear, such as Boettcher cells interfacing with endolymph, the reticular layer, and perilymph, could play a pivotal role in urea transport between endolymph and perilymph [4]. By regulating urea transport between these two compartments, UT-B contributed to maintaining endolymphatic volume and pressure, thereby ensuring the normalcy of sound conduction [4].

Visual System

Both UT-A1 and UT-B are expressed in the eyes of various species, including humans, pigs, and mice. UTs are primarily localized in corneal epithelial and endothelial cells, conjunctival epithelial cells, the terminal ends and excretory ducts of lacrimal glands, meibomian glands, as well as Moll and Zeis glands [74, 75]. Interestingly, the similar pattern of UT expression across different species suggested a conserved physiological role of urea transporter in the eye [74, 75]. Research has demonstrated that UTs not only participate in the transport of urea in tears, aqueous humor, and vitreous humor but also significantly impact the maintenance of tear film homeostasis and ocular surface health (Fig. 6.5) [74–76].

The concentration of urea in tears is crucial for preserving tear film stability and ocular surface health [74]. Notably, a significant decrease in urea concentration in tears from patients with dry eye syndrome (DES) indicated that UTs may be involved in regulating urea homeostasis in tears [74]. As the primary transporters of urea, alterations in UT-B and UT-A1 expression in lacrimal glands and ocular surface tissues can affect urea transport and distribution in tears, subsequently influencing tear composition and stability [74]. Thus, abnormal expression of UTs may be intimately linked to the pathogenesis of DES [74].

In the tear film, urea serves not only as an osmolarity regulator but also contributes to maintaining the lipid-water interface, playing a vital role in tear film stability [76]. Through its hydrating properties, urea helps retain moisture in the tear film, reducing evaporation and protecting the ocular surface from osmotic stress [76]. Furthermore, urea may participate in corneal epithelial repair processes, facilitating the healing of corneal injuries [76]. In patients with evaporative dry eye, reduced urea levels in tears may exacerbate tear film instability, affecting ocular surface health [76]. These facts indicated that UTs expressed in the eye may also play crucial roles in maintaining the stability of tear film.

Reproductive System

The expression of UT-B in the testis exhibits a specific temporal and spatial pattern. UT-B is primarily localized in the Sertoli cells of seminiferous tubules, particularly during stages II-III of spermatogenesis [55, 77, 78]. Sertoli cells provide essential

nutrients and growth factors to developing spermatids while also modulating the intratesticular microenvironment [79, 80]. The presence of UT-B in Sertoli cells suggests its potential involvement in regulating urea transport and metabolism within the testis, thereby influencing spermatogenesis and sperm maturation (Fig. 6.5).

Urea in the testis primarily arises from arginine metabolism, catalyzed by arginase, yielding urea and ornithine [17]. High concentrations of urea have been observed in the testis of UT-B knockout mice, particularly in aged animals, indicating that UT-B may regulate urea transport and metabolism in the testis [9]. Elevated urea levels may impact the intratesticular microenvironment, though the specific mechanisms remain to be elucidated.

Notably, UT-B knockout mice exhibited accelerated spermatogenesis and reproductive system maturation compared to wildtype mice [9]. Although UT-B deficiency did not result in macrostructural abnormalities in spermatogenic epithelium integrity, sperm morphology or distribution, seminiferous tubule and lumen diameters, its potential role in regulating testicular development and spermatogenesis cannot be overlooked.

Further research has revealed significantly increased expression levels of follicle-stimulating hormone receptor (FSHR) and androgen-binding protein (ABP) in the testis of UT-B knockout mice [9]. FSHR, the receptor for follicle-stimulating hormone (FSH), stimulates ABP expression in Sertoli cells, crucial for maintaining sperm count [81, 82]. ABP, on the other hand, binds androgens, modulating their bioactivity within the testis. The elevated expression of FSHR and ABP in UT-B knockout mice may reflect an adaptive response to the high urea environment or constitute one of the molecular mechanisms underlying accelerated testicular development and spermatogenesis following UT-B deficiency [9].

At present, there are few studies on the function of UT-A5 in testis. Current evidence only shows that UT-A5 mRNA is distributed in the peritubular myoid cells forming the outermost layer of the seminiferous tubules in the testis [83]. UT-A5 mRNA levels are coordinated with the stage of testis development and increase 15 days postpartum [83], suggesting that it may be related to development of the testis. More research is needed to uncover the physiological function of UT-A5 in the testis.

Skeletal System

UT-B is expressed in both bone and bone marrow, intimately linked to bone metabolism, osteoporosis, and the formation of bone marrow adipose tissue (Fig. 6.5) [4, 84, 85]. The dynamic equilibrium between adipose and bone tissues within the bone marrow is significantly influenced by UT-B [4]. Studies demonstrate that during bone marrow adipogenesis, UT-B expression is downregulated, whereas the expression of the nuclear hormone receptor peroxisome proliferator-activated receptor γ2

(PPARγ2) is upregulated [85]. The downregulation of UT-B potentially fostered the development of bone marrow adipose tissue, which was further enhanced by the upregulation of PPARγ2 [85].

UT-B expression in osteoblasts may be closely associated with the increased adipogenesis in bone marrow during osteoporosis [86]. Both osteoblasts and adipocytes derive from bone marrow mesenchymal stem cells (MSCs), and their differentiation is orchestrated by a myriad of signaling molecules [86–88]. By modulating urea concentrations, UT-B may indirectly affect the activities of these signaling molecules, thereby influencing the differentiation fate of MSCs [86]. Furthermore, metabolites in the urea cycle, such as NO and polyamines, were also implicated in this process, modulating the biochemical processes of osteoblasts, chondrocytes, and adipocytes, and consequently influencing the composition and function of bone marrow [86].

Recent research highlighted that UT-B was not solely involved in bone marrow adipogenesis but also regulated bone metabolism and inflammatory processes [86]. In bone cells of osteoporosis patients, expression of UT-B was notably decreased, potentially correlated with high levels of cytokines [86]. The presence of cytokines suppressed UT-B expression, subsequently impacting the differentiation patterns of cells in the bone marrow [86]. Moreover, downregulating UT-B expression augmented the expression of inflammatory factors like interleukin-6 and interleukin-1β, exacerbating bone metabolic disorders [86].

In human MSCs and their derivative cell lines, UT-B expression levels correlated with cellular differentiation status [86]. Undifferentiated MSCs exhibited the highest UT-B expression, whereas its expression significantly decreases during osteogenic or adipogenic differentiation [86]. This indicates that UT-B might participate in the early differentiation control of MSCs. UT-B knockdown promoted the expression of adipogenic markers while inhibiting osteogenic markers, further substantiating the pivotal role of UT-B in hMSC differentiation [86].

In conclusion, UT-B plays diverse and crucial roles in bone and bone marrow. By modulating urea concentration and the activities of its metabolic products, UT-B indirectly impacts the differentiation directions and functional states of cells in the bone marrow. Consequently, UT-B may be a potential therapeutic target for bone metabolic disorders such as osteoporosis.

Prospect

In recent years, significant advances have been made in the study of UTs' structures, functions, and relationships with diseases, thanks to the rapid development in molecular biology, cellular biology, and computational simulation techniques. Current studies suggest that UTs play different physiological functions in different organs by regulating osmotic pressure, arginine metabolism, or protein carbamylation (Fig. 6.4).
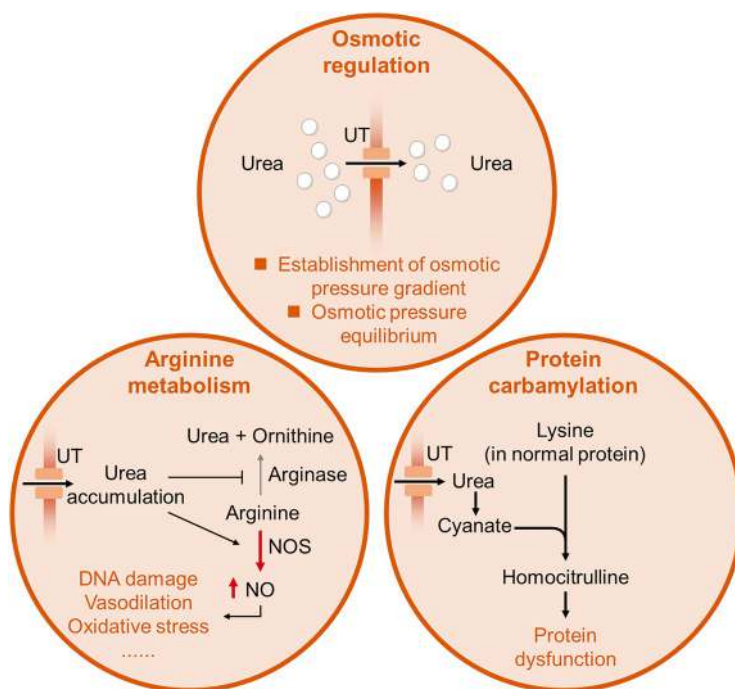
Fig. 6.4 The mechanism by which urea transporter exerts physiological functions

However, it should be noted that the study of the physiological functions of UTs in many organs (such as the function of UT-B in the lungs, liver, pancreas, and spleen, the function of UT-A6 in the colon, and the function of UT-A5 in the testis) were still limited to the observation of phenotypes (Fig. 6.5), and the specific physiological mechanisms have not been fully elucidated. In addition, the cell composition of organs is complex. Study of the expression and function of UTs should be accurate to the cellular level, so as to reduce research defects and avoid misunderstandings. With the widespread application of single cell sequencing, proteomics, and computer simulations, we anticipate a more comprehensive understanding of the biological characteristics of UTs. Concurrently, the development of drugs targeted to UTs will emerge as a research hotspot, offering novel perspectives and strategies for the prevention and treatment of related diseases.

In summary, UTs play vital physiological roles within organisms and are intimately linked to various diseases. As research progresses, we can expect to uncover more secrets about UTs, thereby contributing to the prevention and treatment of related diseases.
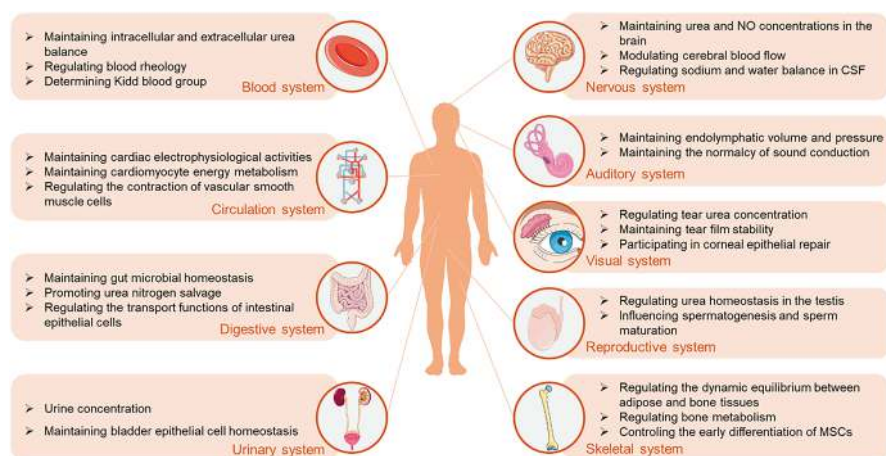
Fig. 6.5 Physiological functions of UTs in different system

Conflicts of Interest The authors have no conflicts of interest.

References

1. M. Li, S. Zhang, B. Yang, Urea transporters identified as novel diuretic drug targets. Curr. Drug Targets **21**, 279–287 (2020)
2. S. Tavoulari, D. Lacabanne, C. Thangaratnarajah, E.R.S. Kunji, Pathogenic variants of the mitochondrial aspartate/glutamate carrier causing citrin deficiency. Trends Endocrinol. Metab. **33**, 539–553 (2022)
3. G.S. Stewart, C. Graham, S. Cattell, T.P. Smith, N.L. Simmons, C.P. Smith, UT-B is expressed in bovine rumen: Potential role in ruminal urea transport. Am. J. Physiol. Regul. Integr. Comp. Physiol. **289**, R605–R612 (2005)
4. L. Yu, T. Liu, S. Fu, L. Li, X. Meng, X. Su, Z. Xie, J. Ren, Y. Meng, X. Lv, Y. Du, Physiological functions of urea transporter B. Pflugers Arch. **471**, 1359–1368 (2019)
5. C. Walpole, A. Farrell, A. McGrane, G.S. Stewart, Expression and localization of a UT-B urea transporter in the human bladder. Am. J. Physiol. Renal Physiol. **307**, F1088–F1094 (2014)
6. J. Leifelt, M.H. Dziegiel, J. Brahm, Functional asymmetry of the urea transporter UT-B in human red blood cells. Am. J. Physiol. Cell Physiol. **326**, C905–C916 (2024)
7. X. Geng, T. Lei, H. Zhou, W. Yao, W. Xin, B. Yang, The knockout of urea transporter-B improves the hemorheological properties of erythrocyte. Clin. Hemorheol. Microcirc. **65**, 249–257 (2017)
8. A.C. Jones, F. Pinki, G.S. Stewart, D.A. Costello, Inhibition of urea transporter (UT)-B modulates LPS-induced inflammatory responses in BV2 microglia and N2a neuroblastoma cells. Neurochem. Res. **46**, 1322–1329 (2021)

9. L. Guo, D. Zhao, Y. Song, Y. Meng, H. Zhao, X. Zhao, B. Yang, Reduced urea flux across the blood-testis barrier and early maturation in the male reproductive system in UT-B-null mice. Am. J. Physiol. Cell Physiol. **293**, C305–C312 (2007)

10. X.X. Zhang, Y. Meng, W.J. Zhang, Electrophysiological change of heart in UT-B gene knockout. Zhongguo Ying Yong Sheng Li Xue Za Zhi **24**(390–392), 438 (2008)

11. S.M. Bagnasco, The erythrocyte urea transporter UT-B. J. Membr. Biol. **212**, 133–138 (2006)

12. S. Lawicki, R.B. Covin, A.A. Powers, The Kidd (JK) blood group system. Transfus. Med. Rev. **31**, 165–172 (2017)

13. X. Li, J. Ran, H. Zhou, T. Lei, L. Zhou, J. Han, B. Yang, Mice lacking urea transporter UT-B display depression-like behavior. J. Mol. Neurosci. **46**, 362–372 (2012)

14. B. Huang, H. Wang, D. Zhong, J. Meng, M. Li, B. Yang, J. Ran, Expression of urea transporter B in normal and injured brain. Front. Neuroanat. **15**, 591726 (2021)

15. C. Shayakul, B. Clemencon, M.A. Hediger, The urea transporter family (SLC14): Physiological, pathological and structural aspects. Mol. Asp. Med. **34**, 313–322 (2013)

16. Y. Meng, C. Zhao, X. Zhang, H. Zhao, L. Guo, B. Lu, X. Zhao, B. Yang, Surface electrocardiogram and action potential in mice lacking urea transporter UT-B. Sci China C Life Sci **52**, 474–478 (2009)

17. B. Yang, X. Li, L. Guo, Y. Meng, Z. Dong, X. Zhao, Extrarenal phenotypes of the UT-B knockout mouse. Subcell. Biochem. **73**, 153–164 (2014)

18. Z. Dong, J. Ran, H. Zhou, J. Chen, T. Lei, W. Wang, Y. Sun, G. Lin, L. Bankir, B. Yang, Urea transporter UT-B deletion induces DNA damage and apoptosis in mouse bladder urothelium. PLoS One **8**, e76952 (2013)

19. D.A. Spector, Q. Yang, J. Liu, J.B. Wade, Expression, localization, and regulation of urea transporter B in rat urothelia. Am. J. Physiol. Renal Physiol. **287**, F102–F108 (2004)

20. R.A. Fenton, B. Yang, Urea transporter knockout mice and their renal phenotypes. Subcell. Biochem. **73**, 137–152 (2014)

21. X. Geng, S. Zhang, J. He, A. Ma, Y. Li, M. Li, H. Zhou, G. Chen, B. Yang, The urea transporter UT-A1 plays a predominant role in a urea-dependent urine-concentrating mechanism. J. Biol. Chem. **295**, 9893–9900 (2020)

22. C. Esteva-Font, M.O. Anderson, A.S. Verkman, Urea transporter proteins as targets for small-molecule diuretics. Nat. Rev. Nephrol. **11**, 113–123 (2015)

23. J.D. Klein, M.A. Blount, J.M. Sands, Urea transport in the kidney. Compr. Physiol. **1**, 699–729 (2011)

24. T. Jiang, Y. Li, A.T. Layton, W. Wang, Y. Sun, M. Li, H. Zhou, B. Yang, Generation and phenotypic analysis of mice lacking all urea transporters. Kidney Int. **91**, 338–351 (2017)

25. C.M. Nawata, T.L. Pannabecker, Mammalian urine concentration: A review of renal medullary architecture and membrane transporters. J. Comp. Physiol. B **188**, 899–918 (2018)

26. B. Yang, L. Bankir, A. Gillespie, C.J. Epstein, A.S. Verkman, Urea-selective concentrating defect in transgenic mice lacking urea transporter UT-B. J. Biol. Chem. **277**, 10633–10637 (2002)

27. T. Lei, L. Zhou, A.T. Layton, H. Zhou, X. Zhao, L. Bankir, B. Yang, Role of thin descending limb urea transport in renal urea handling and the urine concentrating mechanism. Am. J. Physiol. Renal Physiol. **301**, F1251–F1259 (2011)

28. J.D. Klein, J.M. Sands, L. Qian, X. Wang, B. Yang, Upregulation of urea transporter UT-A2 and water channels AQP2 and AQP3 in mice lacking urea transporter UT-B. J. Am. Soc. Nephrol. **15**, 1161–1167 (2004)

29. B. Yang, A.S. Verkman, Urea transporter UT3 functions as an efficient water channel. Direct evidence for a common water/urea pathway. J. Biol. Chem. **273**, 9369–9372 (1998)

30. J. Kabutomori, N. Pina-Lopes, R. Musa-Aziz, Water transport mediated by murine urea transporters: Implications for urine concentration mechanisms. Biol Open **9** (2020)

31. J.M. Sands, M.A. Blount, Genes and proteins of urea transporters. Subcell. Biochem. **73**, 45–63 (2014)

32. R.A. Fenton, C.L. Chou, G.S. Stewart, C.P. Smith, M.A. Knepper, Urinary concentrating defect in mice with selective deletion of phloretin-sensitive urea transporters in the renal collecting duct. Proc. Natl. Acad. Sci. USA **101**, 7469–7474 (2004)

33. R.A. Fenton, G.S. Stewart, B. Carpenter, A. Howorth, E.A. Potter, G.J. Cooper, C.P. Smith, Characterization of mouse urea transporters UT-A1 and UT-A2. Am. J. Physiol. Renal Physiol. **283**, F817–F825 (2002)

34. S. Uchida, E. Sohara, T. Rai, M. Ikawa, M. Okabe, S. Sasaki, Impaired urea accumulation in the inner medulla of mice lacking the urea transporter UT-A2. Mol. Cell. Biol. **25**, 7357–7363 (2005)

35. J.D. Klein, Y. Wang, A. Mistry, L.M. LaRocque, P.A. Molina, R.T. Rogers, M.A. Blount, J.M. Sands, Transgenic restoration of urea transporter A1 confers maximal urinary concentration in the absence of urea transporter A3. J. Am. Soc. Nephrol. **27**, 1448–1455 (2016)

36. S. Zhang, Y. Zhao, S. Wang, M. Li, Y. Xu, J. Ran, X. Geng, J. He, J. Meng, G. Shao, H. Zhou, Z. Ge, G. Chen, R. Li, B. Yang, Discovery of novel diarylamides as orally active diuretics targeting urea transporters. Acta Pharm. Sin. B **11**, 181–202 (2021)

37. N. Li, H. Zhang, S. Wang, Y. Xu, Y. Ying, J. Li, X. Li, M. Li, B. Yang, Urea transporter UT-A1 as a novel drug target for hyponatremia. FASEB J. **38**, e23760 (2024)

38. Y. Ying, N. Li, S. Wang, H. Zhang, Y. Zuo, Y. Tang, P. Qiao, Y. Quan, M. Li, B. Yang, Urea transporter inhibitor 25a reduces ascites in cirrhotic rats. Biomedicines **11** (2023)

39. B. Yang, A.S. Verkman, Analysis of double knockout mice lacking aquaporin-1 and urea transporter UT-B. Evidence for UT-B-facilitated water transport in erythrocytes. J. Biol. Chem. **277**, 36782–36786 (2002)

40. F.H. Login, L.N. Nejsum, Aquaporin water channels: Roles beyond renal water handling. Nat. Rev. Nephrol. **19**, 604–618 (2023)

41. F. Rianto, A. Kuma, C.L. Ellis, F. Hassounah, E.L. Rodriguez, X.H. Wang, J.M. Sands, J.D. Klein, UT-A1/A3 knockout mice show reduced fibrosis following unilateral ureteral obstruction. Am. J. Physiol. Renal Physiol. **318**, F1160–F1166 (2020)

42. C. Li, W. Wang, S.N. Summer, S. Falk, R.W. Schrier, Downregulation of UT-A1/UT-A3 is associated with urinary concentrating defect in glucocorticoid-excess state. J. Am. Soc. Nephrol. **19**, 1975–1981 (2008)

43. Q. Cai, S.K. Nelson, M.R. McReynolds, M.K. Diamond-Stanic, D. Elliott, H.L. Brooks, Vasopressin increases expression of UT-A1, UT-A3, and ER chaperone GRP78 in the renal medulla of mice with a urinary concentrating defect. Am. J. Physiol. Renal Physiol. **299**, F712–F719 (2010)

44. C.L. Chou, G. Hwang, D.J. Hageman, L. Han, P. Agrawal, T. Pisitkun, M.A. Knepper, Identification of UT-A1- and AQP2-interacting proteins in rat inner medullary collecting duct. Am. J. Physiol. Cell Physiol. **314**, C99–C117 (2018)

45. R.J. Hogg, J.P. Kokko, Renal countercurrent multiplication system. Rev. Physiol. Biochem. Pharmacol. **86**, 95–135 (1979)

46. J.M. Sands, J.P. Kokko, Current concepts of the countercurrent multiplication system. Kidney Int. Suppl. **57**, S93–S99 (1996)

47. S.Y. Kuang, A better explanation of countercurrent multiplication in the formation of the corticopapillary osmotic gradient in the outer medulla. Adv. Physiol. Educ. **47**, 665–671 (2023)

48. Y. Nakagawa, R. Kaseda, Y. Suzuki, H. Watanabe, T. Otsuka, S. Yamamoto, Y. Kaneko, S. Goto, Y. Terada, T. Haishi, S. Sasaki, I. Narita, Sodium magnetic resonance imaging shows impairment of the counter-current multiplication system in diabetic mice kidney. Kidney **360**(4), 582–590 (2023)

49. J.B. Wade, A.J. Lee, J. Liu, C.A. Ecelbarger, C. Mitchell, A.D. Bradford, J. Terris, G.H. Kim, M.A. Knepper, UT-A2: A 55-kDa urea transporter in thin descending limb whose abundance is regulated by vasopressin. Am. J. Physiol. Renal Physiol. **278**, F52–F62 (2000)

50. B. Maciver, C.P. Smith, W.G. Hill, M.L. Zeidel, Functional characterization of mouse urea transporters UT-A2 and UT-A3 expressed in purified Xenopus laevis oocyte plasma membranes. Am. J. Physiol. Renal Physiol. **294**, F956–F964 (2008)

51. J. Brahm, M.H. Dziegiel, J. Leifelt, Urea and water are transported through different pathways in the red blood cell membrane. J. Gen. Physiol. **155** (2023)

52. B. Yang, Transport characteristics of urea transporter-B. Subcell. Biochem. **73**, 127–135 (2014)

53. J. Ran, H. Wang, T. Hu, Clinical aspects of urea transporters. Subcell. Biochem. **73**, 179–191 (2014)
54. J.R. Hamilton, Kidd blood group system: a review. Immunohematology **31**, 29–35 (2015)
55. R.T. Timmer, J.D. Klein, S.M. Bagnasco, J.J. Doran, J.W. Verlander, R.B. Gunn, J.M. Sands, Localization of the urea transporter UT-B protein in human and rat erythrocytes and tissues. Am. J. Physiol. Cell Physiol. **281**, C1318–C1325 (2001)
56. J. Leifelt, M.H. Dziegiel, J. Brahm, Urea transport in human red blood cells: Donor variation compared to chloride, glucose, and water transport. J. Gen. Physiol. **155** (2023)
57. H. Yu, Y. Meng, L.S. Wang, X. Jin, L.F. Gao, L. Zhou, K. Ji, Y. Li, L.J. Zhao, G.Q. Chen, X.J. Zhao, B. Yang, Differential protein expression in heart in UT-B null mice with cardiac conduction defects. Proteomics **9**, 504–511 (2009)
58. Y. Du, Y. Meng, J. Zhu, L. Kang, X. Jia, L. Guo, L. Zhang, M. Ye, L. Hu, X. Zhao, J. Gu, B. Yang, H. Zou, Quantitative proteomic study of myocardial mitochondria in urea transporter B knockout mice. Proteomics **14**, 2072–2083 (2014)
59. Y. Sun, C.W. Lau, Y. Jia, Y. Li, W. Wang, J. Ran, F. Li, Y. Huang, H. Zhou, B. Yang, Functional inhibition of urea transporter UT-B enhances endothelial-dependent vasodilatation and lowers blood pressure via L-arginine-endothelial nitric oxide synthase-nitric oxide pathway. Sci. Rep. **6**, 18697 (2016)
60. H. Inoue, S.D. Kozlowski, J.D. Klein, J.L. Bailey, J.M. Sands, S.M. Bagnasco, Regulated expression of renal and intestinal UT-B urea transporter in response to varying urea load. Am. J. Physiol. Renal Physiol. **289**, F451–F458 (2005)
61. A. Ritzhaupt, I.S. Wood, A.A. Jackson, B.J. Moran, S.P. Shirazi-Beechey, Isolation of a RT-PCR fragment from human colon and sheep rumen RNA with nucleotide sequence similarity to human and rat urea transporter isoforms. Biochem. Soc. Trans. **26**, S122 (1998)
62. D. Collins, D.C. Winter, A.M. Hogan, L. Schirmer, A.W. Baird, G.S. Stewart, Differential protein abundance and function of UT-B urea transporters in human colon. Am. J. Physiol. Gastrointest. Liver Physiol. **298**, G345–G351 (2010)
63. C. Walpole, A. McGrane, H. Al-Mousawi, D. Winter, A. Baird, G. Stewart, Investigation of facilitative urea transporters in the human gastrointestinal tract. Physiol. Rep. **6**, e13826 (2018)
64. G.S. Stewart, C.P. Smith, Urea nitrogen salvage mechanisms and their relevance to ruminants, non-ruminants and man. Nutr. Res. Rev. **18**, 49–62 (2005)
65. C. Zhong, R. Long, G.S. Stewart, The role of rumen epithelial urea transport proteins in urea nitrogen salvage: A review. Anim Nutr **9**, 304–313 (2022)
66. A. McGrane, G. Stewart, Hyperosmolality regulates UT-A6 urea transporter expression in the Caco-2 cell line. Physiol. Rep. **4**, e12984 (2016)
67. C.P. Smith, E.A. Potter, R.A. Fenton, G.S. Stewart, Characterization of a human colonic cDNA encoding a structurally novel urea transporter, hUT-A6. Am. J. Physiol. Cell Physiol. **287**, C1087–C1093 (2004)
68. A.J. Thomas, J.T. O'Brien, S. Davis, C. Ballard, R. Barber, R.N. Kalaria, R.H. Perry, Ischemic basis for deep white matter hyperintensities in major depression: A neuropathological study. Arch. Gen. Psychiatry **59**, 785–792 (2002)
69. L. Guo, J. Meng, C. Xuan, J. Ge, W. Sun, S.T. O'Rourke, C. Sun, High salt-diet reduces SLC14A1 gene expression in the choroid plexus of Dahl salt sensitive rats. Biochem. Biophys. Res. Commun. **461**, 254–259 (2015)
70. B. Chanrion, C. Mannoury la Cour, F. Bertaso, M. Lerner-Natoli, M. Freissmuth, M.J. Millan, J. Bockaert, P. Marin, Physical interaction between the serotonin transporter and neuronal nitric oxide synthase underlies reciprocal modulation of their activity. Proc. Natl. Acad. Sci. USA **104**, 8119–8124 (2007)
71. J. Garthwaite, Neuronal nitric oxide synthase and the serotonin transporter get harmonious. Proc. Natl. Acad. Sci. USA **104**, 7739–7740 (2007)
72. Y.S. Kwun, S.W. Yeo, Y.H. Ahn, S.W. Lim, J.Y. Jung, W.Y. Kim, J.M. Sands, J. Kim, Immunohistochemical localization of urea transporters A and B in the rat cochlea. Hear. Res. **183**, 84–96 (2003)

73. J.W. Hall 3rd, Development of the ear and hearing. J. Perinatol. **20**, S12–S20 (2000)

74. F. Jager, F. Paulsen, A. Bergua, R. Jungbauer, C.M. Hammer, Urea transporter-B expression on the ocular surface and in the lacrimal glands. Ann. Anat. **243**, 151954 (2022)

75. F. Jager, F. Paulsen, A. Bergua, R. Jungbauer, C.M. Hammer, Immunohistochemical detection of urea transporter-A in the tear-producing part of the lacrimal system. Ann. Anat. **244**, 151991 (2022)

76. S. Singh, C.M. Hammer, F. Paulsen, Urea and ocular surface: synthesis, secretion and its role in tear film homeostasis. Ocul. Surf. **27**, 41–47 (2023)

77. R.A. Fenton, G.J. Cooper, I.D. Morris, C.P. Smith, Coordinated expression of UT-A and UT-B urea transporters in rat testis. Am. J. Physiol. Cell Physiol. **282**, C1492–C1501 (2002)

78. H. Tsukaguchi, C. Shayakul, U.V. Berger, T. Tokui, D. Brown, M.A. Hediger, Cloning and characterization of the urea transporter UT3: Localization in rat kidney and testis. J. Clin. Invest. **99**, 1506–1515 (1997)

79. M.D. Griswold, The central role of Sertoli cells in spermatogenesis. Semin. Cell Dev. Biol. **9**, 411–416 (1998)

80. Y. Gao, Z. Wang, Y. Long, L. Yang, Y. Jiang, D. Ding, B. Teng, M. Chen, J. Yuan, F. Gao, Unveiling the roles of Sertoli cells lineage differentiation in reproductive development and disorders: A review. Front Endocrinol (Lausanne) **15**, 1357594 (2024)

81. F. De Pascali, A. Trefier, F. Landomiel, V. Bozon, G. Bruneau, R. Yvinec, A. Poupon, P. Crepieux, E. Reiter, Follicle-stimulating hormone receptor: Advances and remaining challenges. Int. Rev. Cell Mol. Biol. **338**, 1–58 (2018)

82. L. Casarini, M. Simoni, Membrane estrogen receptor and follicle-stimulating hormone receptor. Vitam. Horm. **123**, 555–585 (2023)

83. R.A. Fenton, A. Howorth, G.J. Cooper, R. Meccariello, I.D. Morris, C.P. Smith, Molecular characterization of a novel UT-A urea transporter isoform (UT-A5) in testis. Am. J. Physiol. Cell Physiol. **279**, C1425–C1431 (2000)

84. B. Olives, P. Neau, P. Bailly, M.A. Hediger, G. Rousselet, J.P. Cartron, P. Ripoche, Cloning and functional expression of a urea transporter from human bone marrow cells. J. Biol. Chem. **269**, 31649–31652 (1994)

85. W.P. Prichett, A.J. Patton, J.A. Field, K.A. Brun, J.G. Emery, K.B. Tan, D.J. Rieman, H.A. McClung, D.P. Nadeau, J.L. Mooney, L.J. Suva, M. Gowen, M.E. Nuttall, Identification and cloning of a human urea transporter HUT11, which is downregulated during adipogenesis of explant cultures of human bone. J. Cell. Biochem. **76**, 639–650 (2000)

86. M. Komrakova, M. Blaschke, M.L. Ponce, A. Kluver, R. Kopp, M. Hufner, M. Schieker, N. Miosge, H. Siggelkow, Decreased expression of the human urea transporter SLC14A1 in bone is induced by cytokines and stimulates adipogenesis of mesenchymal progenitor cells. Exp. Clin. Endocrinol. Diabetes **128**, 582–595 (2020)

87. Q. Chen, P. Shou, C. Zheng, M. Jiang, G. Cao, Q. Yang, J. Cao, N. Xie, T. Velletri, X. Zhang, C. Xu, L. Zhang, H. Yang, J. Hou, Y. Wang, Y. Shi, Fate decision of mesenchymal stem cells: Adipocytes or osteoblasts? Cell Death Differ. **23**, 1128–1139 (2016)

88. C. Wang, H. Meng, X. Wang, C. Zhao, J. Peng, Y. Wang, Differentiation of bone marrow mesenchymal stem cells in osteoblasts and adipocytes and its role in treatment of osteoporosis. Med. Sci. Monit. **22**, 226–233 (2016)

Chapter 7
Urea Transporters and Their Gene Mutations in Diseases

Boyue Huang, Hongkai Wang, Jiaoyu Hou, and Jianhua Ran

Abstract Urea transporters (UTs) UT-As (encoded by *Slc14A2*) and UT-B (encoded by *Slc14A1*), are important members of the solute carrier family. They are a group of membrane channel proteins that are selectively permeable to urea. *Slc14A1* is considered the key gene determining the Kidd blood group system, and its variants can lead to the loss of Jk antigens, resulting in transfusion-related complications. Additionally, studies have shown that *Slc14A1* is closely associated with cancer development and progression, with its expression level and promoter methylation status potentially serving as biomarkers for cancer progression and prognosis. Recent research suggests that UT-B functional deficiency may cause neurodegenerative diseases by accumulating urea in the brain, thereby affecting neuronal function and viability. Mutations of *Slc14A2* are linked to hypertension and metabolic syndrome, due to its essential role in maintaining urea homeostasis. This chapter aims to introduce the clinical significance of UT-B and UT-A and highlight their potential roles as diagnostic and therapeutic targets.

Keywords Urea transporter · UT-A · UT-B · Kidd blood group · Jk antigens

Urea transporters (UTs), a group of membrane channel proteins responsible for selective permeability to urea across cellular membranes, belong to the members of the solute carrier (SLC) family. UTs include 6 UT-A isoforms and a UT-B isoform,

B. Huang (✉) · J. Ran (✉)
Department of Anatomy, and Laboratory of Neuroscience and Tissue Engineering, Basic Medical College, Chongqing Medical University, Chongqing, China
e-mail: boyue960521@cqmu.edu.cn; ranjianhua@cqmu.edu.cn

H. Wang
Laboratory of Regenerative Rehabilitation, Shirley Ryan Ability Lab, Department of Physical Medicine and Rehabilitation, Northwestern University Feinberg School of Medicine, Chicago, IL, USA

J. Hou
Department of Geriatrics, The First Hospital of Jilin University, Changchun, China

which are coded by genes *Slc14A2* and *Slc14A1,* respectively. *Slc14A1* and *Slc14A1* are linked on chromosome 18. UTs are primarily known for their roles in urea transport, a critical process for maintaining nitrogen balance in the body. Recent research has highlighted that UT abnormalities and their gene mutation are involved in a variety of diseases, including blood group, tumors, neurodegenerative diseases, and renal pathologies. This chapter aims to provide a comprehensive overview of the current understanding of UTs and their genes in diverse disease mechanisms, and their potential as diagnostic and therapeutic targets.

UT-B in Hemolytic Transfusion Reaction

UT-B, which is expressed in erythrocytes, has been identified as the genetic determinant of the Kidd (Jk) blood group system. Mutations in *Slc14A1* can lead to the absence of Jk antigens. This condition, known as the Jk(a−b−) phenotype, poses a significant risk in transfusion medicine due to potential hemolytic transfusion reactions and challenges in blood cross-matching.

The discovery of the Kidd blood group system is an important milestone in the fields of transfusion medicine and immunohematology. This system was identified in 1951 when a woman named Kidd in Boston, USA, gave birth to her sixth child, John Kidd, who exhibited symptoms of Hemolytic Disease of the Newborn. The physician responsible for the transfusion, Dr. Allen, discovered a new antibody in Mrs. Kidd's serum that reacted with a new antigen on the infant's red blood cells, leading to hemolytic jaundice. In honor of this discovery, the new blood group was named the Kidd blood group, and the corresponding antibody was designated as the Jk(a)antigen [1]. Subsequently, in 1953, Plaut and colleagues in the UK discovered the antibody Jk(b) corresponding to the Jk(a) antigen [2]. Both Jk(a) and Jk(b) contribute to the three common phenotypes: Jk(a + b−), Jk(a − b+), and Jk(a + b+). The Jk(a − b−) (or JK^{null}) phenotype was identified in 1959 following a post-transfusion hemolytic disease in a Filipina with Spanish and Chinese ancestry [3]. In 1959, Pinkerton and others identified a third antigen of the Kidd blood group system, Jk3, which is present on all red blood cells except those with the Jk(a-b-) phenotype [4]. The distribution of the Kidd blood group antigens Jk(a), Jk(b), and Jk^3 varies among different ethnic groups. The frequency of the Jk(a) gene is higher in Caucasians and Black populations, while the Jk^b gene is somewhat less prevalent. In East Asian populations, the Jk^b gene is generally more common than the Jk^a gene. The Jk(a-b-) phenotype is extremely rare, primarily found among Polynesians in the Pacific Islands, Finns, and certain Asian populations, such as those in Thailand and Japan. In China, the prevalence of Jk(a-b-) is less than one in ten thousand, making it a very rare blood type [5–7].

The functional discovery of glycoproteins containing Kidd antigens preceded the isolation of the protein or gene, as an incidental finding occurred in a Samoan patient suffering from aplastic anemia [8]. His red blood cells were resistant to lysis in 2 mol/L urea. It was found that he had elevated platelet counts in an automated

system dependent on thyroid cell urea dissolution, while peripheral blood smear examination showed no evidence of platelet excess [9]. His red blood cells were not effectively lysed, leading the automated system to count them as platelets. He was discovered to have the JK(a-b-) phenotype, suggesting that the Kidd glycoprotein has urea transport functions.

In 1987, the first isolation of the Kidd glycoprotein was achieved using affinity-purified IgG antibodies against Jk(a), Jk(b), and Jk3 in a dot blot assay, yielding a 45-kDa protein [10]. In 1991, the impermeability of Jk(a-b-) red blood cells to urea was confirmed, coinciding with previous findings that urea flux across artificial lipid bilayers was relatively low [11]. This characteristic of Jk(a-b-) red blood cells strongly suggested a correlation between Jk antigens and transmembrane urea transport. In the same year, scientists first detected a urea transporter protein in the Xenopus oocytes, which facilitates the passage of urea across the cell membrane [12, 13].

In 1993, the direct discovery of a protein of approximately 40 kDa, possibly related to the Kidd antigen and associated with urea transport, was made through photolabeling [14]. That same year, rabbit renal medulla cDNA was microinjected into frog oocytes, successfully cloning UT-2 (later renamed UT-A2) through functional expression [15]. In 1994, scientists reported the isolation of a cDNA encoding the UT-3 protein (later renamed UT-B) from human bone marrow, with sequences showing extensive similarity to UT-A2 [16]. The same research group found that, in addition to red blood cells with the JK(a-b-) phenotype, a 45–60 kDa glycoprotein was isolated from all red blood cells using immunoprecipitation with anti-Jk3. After removing N-glycosylation with N-glycosidase, the molecular weight decreased to 36 kDa [17].

Benefiting from the rapid development of molecular technology, an increasing number of alleles have been identified. The two antigens Jk(a) and Jk(b) are inherited as products of co-dominant alleles. The expression of the Jk(a) and/or Jk(b) antigens is determined by a single nucleotide polymorphism (SNP) within the *Slc14A1* gene, which confers a single amino acid difference between the alleles. The expression sequence of the Jk^b antigen is considered to correspond to the reference allele JK*B or JK*02, featuring adenine at nucleotide 838 and asparagine at position 280. The Jk^a antigen arises from a substitution of guanine for adenine at nucleotide 838,
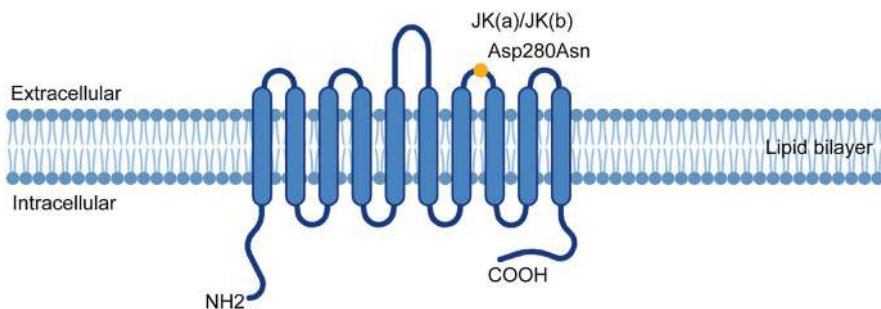
Fig. 7.1 JK glycoprotein composed of 389 amino acids

resulting in an aspartic acid at that position instead of asparagine (Fig. 7.1) [18]. This amino acid difference at position 280 is located on the fourth extracellular loop of the JK protein, which is considered to correspond to the reference allele JK*A or JK*01.

Although the Kidd blood group system is considered relatively simple due to the normal expression of only two different alleles, multiple mutations in these alleles can lead to weak or modified expression profiles of the antigens. As of December 2023, the International Society of Blood Transfusion (ISBT) Working Party on Red Cell Immunogenetics and Blood Group Terminology has acknowledged a total of 26 null alleles for the JK01 and JK02 antigens, 12 weak alleles for the JK01 antigen, and 6 weak alleles for the JK02 antigen [19]. Frequencies of the Jk(a−b−) phenotype in different ethnic groups is dissimilar, while several diverse mutations of the *Slc14A1* gene with Jk(a−b−) phenotype are also associated with different ethnic lineages [20] (Table 7.1).

The Kidd blood group system is frequently involved in transfusion reactions and hemolytic disease of the newborn (HDN) [33–35]. Kidd antibodies, such as anti-Jka and anti-Jkb, are of particular clinical concern due to their potential to cause delayed hemolytic transfusion reactions (DHTRs). These antibodies are typically formed after exposure to incompatible blood, either through transfusion or pregnancy, and may not be detectable in routine screening. However, upon subsequent exposure to the corresponding antigen, these antibodies can cause a severe immune response that leads to hemolysis. The delayed nature of the reaction often complicates diagnosis, as hemolysis can occur days or even weeks post-transfusion. This characteristic makes Kidd antibodies a significant concern in transfusion medicine, as they can lead to acute renal failure and other severe complications if not properly managed. Moreover, the Kidd system is implicated in HDN, although its involvement is less frequent compared to Rh or ABO incompatibilities [36–39]. HDN due to anti-Jka or anti-Jkb antibodies can range from mild to severe, depending on the antibody titer and the density of antigens expressed on the fetal red blood cells. In severe cases, it can lead to fetal anemia, jaundice, and even hydrops fetalis, necessitating careful prenatal monitoring and potential intervention. Given these risks, accurate prenatal screening for Kidd antibodies is essential, particularly in pregnant women with a history of transfusion or previous pregnancies.

UT-B in Transplanted Kidney Rejection

Since UT-B is expressed in renal descending vasa recta endothelial cells and other tissues, the antibodies in transplant recipients may attack Jk alloantigens (UT-B) as minor histocompatibility antigens expressed on the donor's organs after transplantation [40, 41]. It has been reported that the Jk(b) antigen is able to cause acute rejection of a transplanted kidney [41–43].

A recent study by Ramsey et al. shed light on the outcomes of renal transplant patients who possess JK alloantibodies. They found that among five patients with existing JK antibodies and a history of graft loss of uncertain JK antigen status,

Table 7.1 Mutations of *Slc14A1*

	Mutation	Amino acid change	Population	References
Jk(a)	C582G	Tyr194Stop	Swiss	[21]
	C202T	Gln68Stop	Hispanic-American, Caucasian	[22]
	G327del	Leu109Phe	Japanese	[23]
	G432A	Trp144Stop	Japanese	[23]
	757–759delTCC	Ser253del	Japanese	[23]
	G893A	Gly298Glu	Japanese	[23]
	C956T	Thr319Met	African-American, Indian, Thai, Pakistani	[6, 22]
	C561A	Tyr187Stop	African-American	[24]
	del(exon 4 and 5)	protein not expressed	English, Tunisian, Bosnian	[21]
	IVS8 + 5 g > a	skipping of exon 8	Chinese	[25]
	IVS5–1 g > a	skipping of exon 6	Polynesian	[26]
Jk(b)	G130A	Glu44Lys	Caucasian, Thai	[6, 21]
	G191A	Arg64Gln	African-American, Japanese	[23]
	G194A	Gly65Asp	French-Canadian	[27]
	C222A	Asn74Lys	Taiwanese	[28]
	T437C	Leu146Pro	Chinese	[25]
	G512A	Trp171Stop	Chinese	[25]
	C536G	Pro179Arg	Chinese	[25]
	C561A	Tyr187Stop	Japanese	[23]
	647-648delAC	Asp216Ala	Japanese	[23]
	G719A	Trp240Stop	Japanese	[23]
	T871C	Ser291Pro	Finn	[20]
	G896A	Gly299Glu	Taiwanese, Polynesian, Thai	[6, 28]
	C956T	Thr319Met	African-American, Indian, Thai, Pakistani	[6, 22]
	A723del	Ile262Stop	Hispanic-American	[22]
	IVS5–1 g > c	skipping of exon 6	Chinese	[29]
	IVS5–1 g > a	skipping of exon 6	Taiwanese, Chinese, Filipino, Indonesian, Polynesian, Vietnamese, Japanese	[22, 23, 30–32]
	IVS7 + 1 g > t	skipping of exon 7	French	[31]

there was also the presence of human leukocyte antigen (HLA) antibodies that could potentially account for the graft loss. In contrast, seven patients who received a kidney that was knowingly incompatible with JK did not experience any rejection episodes that could be solely attributed to JK antibodies; however, two of these patients did have rejection episodes that were consistent with HLA antibodies [44]. Additionally, a case was reported by Subramaniyan of a patient with pre-transplant anti-Jka who received a Jk(a+) kidney and maintained graft survival for at least five months [45].

In only one reported case, a patient harboring pre-transplant anti-Jka antibodies in the absence of HLA donor-specific antibodies underwent transplantation with a Jk(a+) kidney, and suffered graft loss [46]. These findings imply that the presence of JK antibodies does not necessarily preclude a patient from being a candidate for kidney transplantation, yet it may be linked to an increased risk of complications in certain individuals. We recommend that surgeons pay attention to the Kidd blood group when they meet a hard-to-explain rejection episode.

Genetic Variation of UT-B in Tumor

Growing evidence suggests that *Slc14A1* mutations are involved in tumor development, where its altered expression and promoter methylation status are associated with tumor progression and poor prognosis in several cancer types. Urinary bladder cancer ranks eighth in worldwide tumor incidence and the thirteenth most numerous cause of death from cancer. It is the sixth most common malignancy in men and eighteenth in women, and its frequent recurrence requires regular screening and interventions [47, 48]. Urinary bladder cancer stands out as a huge burden all over the world, particularly in developing countries [49]. The risk factors associated with the development of bladder cancer include cigarette-smoking, exposure to chemicals such as aromatic amines, chronic bladder inflammation, and age [50, 51]. Most tumors are transitional cell carcinomas (95%), which occur in industrialized countries. Bladder cancer has historically not been treated as a tumor with a genetic background though a family history of bladder cancer is associated with an approximately two-fold increase in risk [52].

Multistage genome-wide association studies (GWAS) have found several genes, TP63, MYC, TERT, PSCA, CLPTMIL, TMEM129, TACC3-FGFR3, APOBEC3A, CBX6, CCNE1, UGT1A, NAT2, GSTM1, that are linked to bladder cancer [53–57]. In 2011, a new urinary bladder cancer susceptibility locus was discovered from an extension of the European urinary bladder cancer genome-wide association studies—a single-nucleotide polymorphism (SNP) in intron 3, rs17674580, of the UT-B gene *Slc14A1*. It is hypothesized that sequence variants in the *Slc14A1* gene indirectly modify urinary bladder cancer risk by affecting the urine concentration or frequency of urination that affects the time that carcinogens are contacting the urothelium (urogenous contact hypothesis, set in 1987) [58, 59]. Interestingly, at the same time, a meta-analysis of existing GWAS data [56, 57] also identified a novel susceptibility locus that mapped to a region of 18q12.3, marked by rs7238033 and two highly correlated SNPs, rs10775480/rs10853535, localized to the UT-B gene *Slc14A1*. They found no evidence of modification of the 18q12.3 locus risk association by smoking status [60]. Coincidently, the latter study group speculated that variations in urine volumes and concentration could modify exposure of bladder epithelium to carcinogens in the urine, which is similar with the urogenous contact hypothesis.

To search for more evidence, in 2013, a further study was designed to seek differences between phenotypes that are T allele versus C allele at rs10775480 [61]. Specific gravity was measured representing urine concentration. The results showed that carriage of the bladder cancer risk allele resulted in a significant decrease in urinary specific gravity after controlling for all available predictors. The data suggest that UT-B expressed in the bladder has the ability to influence urine concentration, which might explain the increased bladder cancer susceptibility associated with rs10775480. However, recent studies in rats found evidence that expression of UT-B in urothelium may be associated with bladder cancer directly.

As we introduced previously, UT-B distributes in urothelium so that urea is continuously reabsorbed from the urine across the urothelium via UT-B, and urine is thus altered in its passage through the urinary tract [62]. Additionally, in UT-B null mice, DNA damage and apoptosis were markedly increased, which resulted from urea accumulation, an upregulated expression of iNOS and a downregulation of arginase I expression in urothelial cells induced by deletion of UT-B [63].

In a case-control series of bladder cancer patients, variations in the *Slc14A1* gene were identified as a high-risk factor for bladder cancer, especially among non-smokers [64]. Another study identified a type of cancer-associated fibroblast (CAFs) driven by interferon signaling and overexpression of UT-B through single-cell sequencing in the bladder. Patients with a higher proportion of *Slc14A1*+ CAFs in bladder cancer exhibited a poor prognosis, independent of cancer staging, and had a poor response rate to neoadjuvant chemotherapy or immunotherapy [65]. However, there is research indicating that UT-B is a potential new tumor suppressor in urothelial carcinomas, since reduced levels of UT-B correlate with poorer outcomes in patients with urothelial carcinoma of the bladder, including disease-specific survival and metastasis-free survival.

Epigenetic alterations, such as hypermethylation of DNA at the *Slc14A1* promoter and methylation of histones H3K27 and H3K9, result in reduced *Slc14A1* gene expression and subsequent protein synthesis. The total and membrane-bound forms of UT-B mitigate the buildup of urea and arginine by modulating the mTOR signaling pathway. Furthermore, UT-B within the nucleus interacts with HDAC1 to suppress the expression of genes involved in oncogenic metabolism [66]. Further studies are desired to reveal the precise mechanism.

The expression of the *Slc14A1* gene in humans was affected by castration, in addition to differential expression in the benign and malignant prostate, which suggested that UT-B might also contribute to prostate cancer [67]. Studies show that the expression levels of UT-B are markedly decreased in prostate cancer cells and tissues when compared to normal prostatic epithelial cells and peritumoral tissue, and its downregulation is associated with shorter survival time in patients. *Slc14A1* has emerged as a significant gene linked to the occurrence of biochemical recurrence in prostate cancer [68, 69]. Through bioinformatics and public database analyses, researchers have found that hypermethylation of the promoter region of the *Slc14A1* gene is correlated with its downregulated expression, which may be one of the critical factors contributing to the silencing of *Slc14A1* [69]. Furthermore, DNA

methyltransferase DNMT3B may mediate the methylation of the *Slc14A1* promoter region, thereby leading to its decreased expression.

Even in cancers outside of the urinary system, UT-B stands out unexpectedly. Downregulation of UT-B in noninvolved tissue of pulmonary adenocarcinoma may be a biomarker for a higher clinical stage [70]. In primary colorectal cancer lesions, upregulation of UT-B activates the TGF-β pathway, enhancing the metastatic capability of colorectal tumor cells. The upregulation of UT-B is closely associated with synchronous liver metastasis and poor prognosis in colorectal cancer (CRC) patients, suggesting its potential as a predictive marker for postoperative synchronous liver metastasis in these patients [71]. Emerging research suggests that UT-B plays a significant role in the progression of renal cell carcinoma and may serve as a novel biomarker for this disease [72].These findings highlight the prospective application of *Slc14A1* as a predictive indicator and therapeutic target.

Research progress on the *Slc14A1* gene in cancer suggests that its expression level and promoter methylation status may serve as novel indicators for tumor progression and prognosis. UT-B may inhibit cancer progression by suppressing cell proliferation and metastasis. These findings provide new molecular targets and biomarkers for the diagnosis, treatment, and prognosis evaluation of tumors.

UT-B in Neurodegenerative and Psychiatric Disorders

UT-B has been reported as a marker for neurodegenerative diseases. Researchers have identified increased expression levels of UT-B in the Huntington's disease sheep model [73], and UT-B could serve as a biomarker to distinguish Parkinson's disease and progressive supranuclear palsy, with its expression levels correlating with the Unified Parkinson's disease rating scale total and its part III scores [74]. A noteworthy finding suggests that a significant proportion (81%) of individuals with the JK[null] phenotype in Spanish populations meet the criteria for mood and/or anxiety disorders, coupled with a substantially increased familial risk of suicide, which is seven times higher than in the general population [75]. The strong association between the JK[null] phenotype and increased suicide risk highlights the potential role of *Slc14A1* as a genetic risk factor for suicidality. The mechanisms underlying this association remain unclear but may involve disruptions in cerebral urea transport, leading to altered neurotransmitter levels and neuroinflammation. Further studies are needed to determine whether *Slc14A1* variants can serve as predictive biomarkers for suicide risk and to explore potential interventions aimed at modulating UT-B function in at-risk individuals.

UT-B knockout mice exhibit significant depressive-like and anxiety-like behaviors. The potential mechanism may involve the excessive accumulation of urea in the brain, which induces the loss of synaptic structure in neurons, impairs long-term

potentiation [76], triggers abnormal proliferation of oligodendrocytes, and disrupts the dynamic maintenance of myelin [77].

Gender-Specific Blood Pressure Variations and Metabolic Syndrome Associated with *Slc14A2* Polymorphisms

Apart from *Slc14A1* (discussed above), variations in *Slc14A2* are not negligible. In persons of Asian origin, it has been found through genome scan that Val227Ile (rs1123617, G → A) and Ala357Thr (rs3745009, G → A) are significantly associated with blood pressure variation in men but not women [78]. Both Ile227 and Ala357 alleles exhibit a modest protective effect, but mechanisms for the difference between genders remain vague. How these polymorphisms contribute to blood pressure variation is considered to be by decreasing the activity of UT-A. Then, the reduction in the re-absorption of urea and water leads to lower blood pressure. Moreover, subjects carrying both the Ala357/Ala357 genotype in the Ala357Thr polymorphism and either Val227/Ile227 or Ile227/Ile227 genotypes in the Val227Ile polymorphism had the highest mean change in both systolic and diastolic blood pressure after treatment of hypertension by the nifedipine gastrointestinal therapeutic system [79]. Interestingly, expression of UT-A is up-regulated in hearts and down-regulated in kidneys in rats after hypertension is induced [80, 81].

A genetic study of persons of Asian origin showed that G465C in *Slc14A2* is related to a low risk of metabolic syndrome, revealing a significant difference in triglyceride level [82]. But another study suggested that the *Slc14A2* gene contributes to metabolic syndrome by regulating albumin directly [83]. Based on the above, further studies can delve into the relationship between UT-A and common chronic diseases.

In addition, studies have shown that *Slc14A2* gene polymorphism is associated with urea nitrogen levels in chronic kidney disease [84, 85]. And *Slc14A2* has also been reported to be associated with refractive abnormalities of European ancestry in individuals [86].

Summary

Slc14A1 and *Slc14A2* play crucial roles in the pathogenesis of multiple diseases (Fig. 7.2). Their mutations are associated with disease progression and clinical outcomes, highlighting their potential use as biomarkers or therapeutic targets. Further research into their mechanisms will be essential for developing novel strategies in disease diagnosis and treatment.
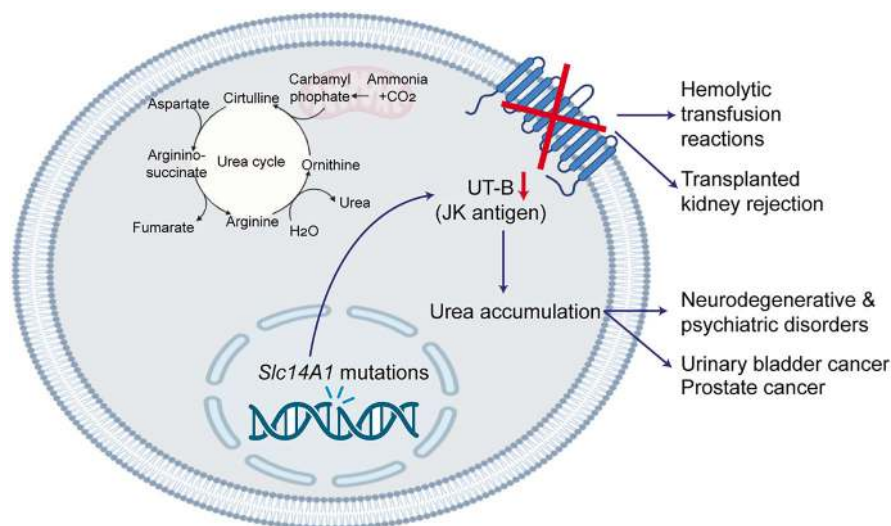
Fig. 7.2 Illustration of the relationship between UT-B abnormality and disease development

References

1. R.R. Race et al., Inheritance of the human blood group antigen JKa. Nature **168**, 207–208 (1951). https://doi.org/10.1038/168207a0
2. G. Plaut et al., A new blood-group antibody, anti Jkb. Nature **171**, 431 (1953). https://doi.org/10.1038/171431a0
3. F.J. Pinkerton et al., The phenotype Jk(a-b-) in the Kidd blood group system. Vox Sang. **4**, 155–160 (1959). https://doi.org/10.1111/j.1423-0410.1959.tb04031.x
4. C.S. Marshall et al., Severe hemolytic reaction due to anti-JK3. Arch. Pathol. Lab Med. **123**, 949–951 (1999). https://doi.org/10.5858/1999-123-0949-shrdta
5. Y. Okubo et al., Heterogeneity of the phenotype Jk(a-b-) found in Japanese. Transfusion **26**, 237–239 (1986). https://doi.org/10.1046/j.1537-2995.1986.26386209377.x
6. P. Sriwanitchrak et al., Genomic characterisation of the Jk(a-b-) phenotype in Thai blood donors. Blood Transfus. **10**, 181–185 (2012). https://doi.org/10.2450/2011.0038-11
7. D.G. Woodfield et al., The Jk(a-b-) phenotype in New Zealand Polynesians. Transfusion **22**, 276–278 (1982). https://doi.org/10.1046/j.1537-2995.1982.22482251206.x
8. O. Fröhlich et al., Urea transport deficiency in Jk(a-b-) erythrocytes. Am. J. Phys. **260**, C778–C783 (1991). https://doi.org/10.1152/ajpcell.1991.260.4.C778
9. D.C. Heaton, K. McLoughlin, Jk(a-b-) red blood cells resist urea lysis. Transfusion **22**, 70–71 (1982). https://doi.org/10.1046/j.1537-2995.1982.22182154224.x
10. L.T. Sinor, K.L. Eastwood, F.V. Plapp, Dot-blot purification of the Kidd blood group antigen. Med. Lab. Sci. **44**, 294–296 (1987)

11. E. Gallucci, S. Micelli, C. Lippe, Non-electrolyte permeability across thin lipid membranes. Arch. Int. Physiol. Biochim. **79**, 881–887 (1971). https://doi.org/10.3109/13813457109104847

12. S. Martial, P. Ripoche, C. Ibarra, Functional expression of urea channels in amphibian oocytes injected with frog urinary bladder mRNA. Biochim. Biophys. Acta **1090**, 86–90 (1991). https://doi.org/10.1016/0167-4781(91)90040-s

13. R.B. Zhang, A.S. Verkman, Water and urea permeability properties of Xenopus oocytes: expression of mRNA from toad urinary bladder. Am. J. Phys. **260**, C26–C34 (1991). https://doi.org/10.1152/ajpcell.1991.260.1.C26

14. P. Neau et al., Photoaffinity labeling of the human red-blood-cell urea-transporter polypeptide components. Possible homology with the Kidd blood group antigen. Eur. J. Biochem. **218**, 447–455 (1993). https://doi.org/10.1111/j.1432-1033.1993.tb18395.x

15. G. You et al., Cloning and characterization of the vasopressin-regulated urea transporter. Nature **365**, 844–847 (1993). https://doi.org/10.1038/365844a0

16. B. Olives et al., Cloning and functional expression of a urea transporter from human bone marrow cells. J. Biol. Chem. **269**, 31649–31652 (1994)

17. B. Olivès et al., Kidd blood group and urea transport function of human erythrocytes are carried by the same protein. J. Biol. Chem. **270**, 15607–15610 (1995). https://doi.org/10.1074/jbc.270.26.15607

18. B. Olivès et al., The molecular basis of the Kidd blood group polymorphism and its lack of association with type 1 diabetes susceptibility. Hum. Mol. Genet. **6**, 1017–1020 (1997). https://doi.org/10.1093/hmg/6.7.1017

19. J.R. Hamilton, An update to Kidd blood group system. Immunohematology **40**, 28–33 (2024). https://doi.org/10.2478/immunohematology-2024-005

20. N.M. Irshaid, S.M. Henry, M.L. Olsson, Genomic characterization of the kidd blood group gene: different molecular basis of the Jk(a-b-) phenotype in Polynesians and Finns. Transfusion **40**, 69–74 (2000). https://doi.org/10.1046/j.1537-2995.2000.40010069.x

21. N.M. Irshaid et al., Novel alleles at the JK blood group locus explain the absence of the erythrocyte urea transporter in European families. Br. J. Haematol. **116**, 445–453 (2002). https://doi.org/10.1046/j.1365-2141.2002.03238.x

22. E.S. Wester et al., Erythroid urea transporter deficiency due to novel JKnull alleles. Transfusion **48**, 365–372 (2008). https://doi.org/10.1111/j.1537-2995.2007.01532.x

23. T. Onodera et al., JK null alleles identified from Japanese individuals with Jk(a−b−) phenotype. Vox Sang. **106**, 382–384 (2014). https://doi.org/10.1111/vox.12117

24. T. Horn et al., A novel JKA allele, nt561C>A, associated with silencing of Kidd expression. Transfusion **52**, 1092–1096 (2012). https://doi.org/10.1111/j.1537-2995.2011.03399.x

25. Z. Guo et al., The mutation spectrum of the JK-null phenotype in the Chinese population. Transfusion **53**, 545–553 (2013). https://doi.org/10.1111/j.1537-2995.2012.03750.x

26. G.C. Ekman, M.J. Hessner, Screening of six racial groups for the intron 5 G→A 3′ splice acceptor mutation responsible for the polynesian kidd (a-b-) phenotype: the null mutation is not always associated with the JKB allele. Transfusion **40**, 888–889 (2000). https://doi.org/10.1046/j.1537-2995.2000.40070888.x

27. M. St-Louis et al., A novel JK*02 allele in a French Canadian family. Transfusion **53**, 3024 (2013). https://doi.org/10.1111/trf.12266

28. H.M. Liu et al., Two novel Jk(null) alleles derived from 222C>A in Exon 5 and 896G>A in Exon 9 of the JK gene. Transfusion **49**, 259–264 (2009). https://doi.org/10.1111/j.1537-2995.2008.01958.x

29. Y. Meng et al., A novel mutation at the JK locus causing Jk null phenotype in a Chinese family. Sci China C Life Sci **48**, 636–640 (2005). https://doi.org/10.1360/062005-127

30. M. Lin, L.C. Yu, Frequencies of the JKnull (IVS5-1g>a) allele in Taiwanese, Fujian, Filipino, and Indonesian populations. Transfusion **48**, 1768–1769 (2008). https://doi.org/10.1111/j.1537-2995.2008.01819.x

31. N. Lucien et al., Characterization of the gene encoding the human Kidd blood group/urea transporter protein. Evidence for splice site mutations in Jknull individuals. J. Biol. Chem. **273**, 12973–12980 (1998). https://doi.org/10.1074/jbc.273.21.12973

32. L. Yan, F. Zhu, Q. Fu, Jk(a-b-) and Kidd blood group genotypes in Chinese people. Transfusion **43**, 289–291 (2003). https://doi.org/10.1046/j.1537-2995.2003.t01-1-00362.x

33. S.S. Hussain et al., Delayed haemolytic transfusion reaction due to anti-Jkb in a patient with non-Hodgkin's lymphoma-transient nature of anti-Jkb and the importance of early serological diagnosis. Transfus. Med. **17**, 197–199 (2007). https://doi.org/10.1111/j.1365-3148.2007.00745.x

34. V. Tomar et al., Hemolytic disease of the newborn due to maternal anti-Kidd (anti-Jkb). Indian Pediatr. **35**, 1251–1253 (1998)

35. D. Vucelic, N. Savic, R. Djordjevic, Delayed hemolytic transfusion reaction due to anti-Jk(a). Acta Chir. Iugosl. **52**, 111–115 (2005). https://doi.org/10.2298/aci0503111v

36. E.J. Baek et al., Haemolytic disease of newborn due to anti-Jka and the duration of antibody persistence. J. Paediatr. Child Health **49**, E101–E102 (2013). https://doi.org/10.1111/jpc.12063

37. M. Ferrando et al., Severe hemolytic disease of the fetus due to anti-Jkb. Transfusion **48**, 402–404 (2008). https://doi.org/10.1111/j.1537-2995.2007.01609.x

38. B. Thakral et al., Hemolytic disease of newborn due to anti-Jk b in a woman with high risk pregnancy. Transfus. Apher. Sci. **43**, 41–43 (2010). https://doi.org/10.1016/j.transci.2010.05.007

39. W.D. Kim, Y.H. Lee, A fatal case of severe hemolytic disease of newborn associated with anti-Jk(b). J. Korean Med. Sci. **21**, 151–154 (2006). https://doi.org/10.3346/jkms.2006.21.1.151

40. A. Rourk, J.E. Squires, Implications of the Kidd blood group system in renal transplantation. Immunohematology **28**, 90–94 (2012)

41. E. Lerut et al., Duffy and Kidd blood group antigens: minor histocompatibility antigens involved in renal allograft rejection? Transfusion **47**, 28–40 (2007). https://doi.org/10.1111/j.1537-2995.2007.01060.x

42. M.S. Hamilton, V. Singh, B.A. Warady, Plasma cell-rich acute cellular rejection of a transplanted kidney associated with antibody to the red cell Kidd antigen. Pediatr. Transplant. **10**, 974–977 (2006). https://doi.org/10.1111/j.1399-3046.2006.00608.x

43. M.S. Hamilton, V. Singh, B.A. Warady, Additional case of acute cellular kidney rejection associated with the presence of antibodies to the red blood cell Kidd antigen. Pediatr. Transplant. **12**, 918–919 (2008). https://doi.org/10.1111/j.1399-3046.2008.00954.x

44. R. Subramaniyan, Occurrence of five distinct red cell alloantibodies in a renal transplant recipient: Diagnostic and therapeutic implications of minor histocompatibility antigens (Kidd and Duffy) for renal allograft outcome. APMIS **125**, 1129–1132 (2017)

45. G. Ramsey et al., *Kidney transplant outcomes in patients with anti-donor kidd blood group antibodies. in 2017 AABB annual meeting* (AABB, 2017)

46. E. Lee et al., Renal allograft rejection with thrombotic microangiopathy associated with a Kidd blood group system alloantibody. Am. J. Clin. Pathol. **156**, S159–S160 (2021)

47. J. Ferlay et al., Estimates of worldwide burden of cancer in 2008: GLOBOCAN 2008. Int. J. Cancer **127**, 2893–2917 (2010). https://doi.org/10.1002/ijc.25516

48. D.M. Parkin, The global burden of urinary bladder cancer. Scand. J. Urol. Nephrol. Suppl. **12**, 12–20 (2008). https://doi.org/10.1080/03008880802285032

49. M. Ploeg, K.K. Aben, L.A. Kiemeney, The present and future burden of urinary bladder cancer in the world. World. J. Urol. **27**, 289–293 (2009). https://doi.org/10.1007/s00345-009-0383-3

50. B.L. Jacobs, C.T. Lee, J.E. Montie, Bladder cancer in 2010: how far have we come? CA Cancer J. Clin. **60**, 244–272 (2010). https://doi.org/10.3322/caac.20077

51. E.M. Wolff, G. Liang, P.A. Jones, Mechanisms of disease: genetic and epigenetic alterations that drive bladder cancer. Nat. Clin. Pract. Urol. **2**, 502–510 (2005). https://doi.org/10.1038/ncpuro0318

52. C. Murta-Nascimento et al., Risk of bladder cancer associated with family history of cancer: do low-penetrance polymorphisms account for the increase in risk? Cancer Epidemiol. Biomarkers Prev. **16**, 1595–1600 (2007). https://doi.org/10.1158/1055-9965.Epi-06-0743

53. L.A. Kiemeney et al., A sequence variant at 4p16.3 confers susceptibility to urinary bladder cancer. Nat. Genet. **42**, 415–419 (2010). https://doi.org/10.1038/ng.558
54. L.A. Kiemeney et al., Sequence variant on 8q24 confers susceptibility to urinary bladder cancer. Nat. Genet. **40**, 1307–1312 (2008). https://doi.org/10.1038/ng.229
55. T. Rafnar et al., Sequence variants at the TERT-CLPTM1L locus associate with many cancer types. Nat. Genet. **41**, 221–227 (2009). https://doi.org/10.1038/ng.296
56. N. Rothman et al., A multi-stage genome-wide association study of bladder cancer identifies multiple susceptibility loci. Nat. Genet. **42**, 978–984 (2010). https://doi.org/10.1038/ng.687
57. X. Wu et al., Genetic variation in the prostate stem cell antigen gene PSCA confers susceptibility to urinary bladder cancer. Nat. Genet. **41**, 991–995 (2009). https://doi.org/10.1038/ng.421
58. D.J. Braver et al., Drinking, micturition habits, and urine concentration as potential risk factors in urinary bladder cancer. J. Natl. Cancer Inst. **78**, 437–440 (1987)
59. T. Rafnar et al., European genome-wide association study identifies SLC14A1 as a new urinary bladder cancer susceptibility gene. Hum. Mol. Genet. **20**, 4268–4281 (2011). https://doi.org/10.1093/hmg/ddr303
60. M. Garcia-Closas et al., A genome-wide association study of bladder cancer identifies a new susceptibility locus within SLC14A1, a urea transporter gene on chromosome 18q12.3. Hum. Mol. Genet. **20**, 4282–4289 (2011). https://doi.org/10.1093/hmg/ddr342
61. S. Koutros et al., Differential urinary specific gravity as a molecular phenotype of the bladder cancer genetic association in the urea transporter gene, SLC14A1. Int. J. Cancer **133**, 3008–3013 (2013). https://doi.org/10.1002/ijc.28325
62. D.A. Spector, Q. Yang, J.B. Wade, High urea and creatinine concentrations and urea transporter B in mammalian urinary tract tissues. Am. J. Physiol. Renal Physiol. **292**, F467–F474 (2007). https://doi.org/10.1152/ajprenal.00181.2006
63. Z. Dong et al., Urea transporter UT-B deletion induces DNA damage and apoptosis in mouse bladder urothelium. PLoS One **8**, e76952 (2013). https://doi.org/10.1371/journal.pone.0076952
64. S. Selinski et al., Identification and replication of the interplay of four genetic high-risk variants for urinary bladder cancer. Carcinogenesis **38**, 1167–1179 (2017). https://doi.org/10.1093/carcin/bgx102
65. Z. Ma et al., Interferon-dependent SLC14A1(+) cancer-associated fibroblasts promote cancer stemness via WNT5A in bladder cancer. Cancer Cell **40**, 1550–1565.e7 (2022). https://doi.org/10.1016/j.ccell.2022.11.005
66. T.C. Chan et al., SLC14A1 prevents oncometabolite accumulation and recruits HDAC1 to transrepress oncometabolite genes in urothelial carcinoma. Theranostics **10**, 11775–11793 (2020). https://doi.org/10.7150/thno.51655
67. M.H. Vaarala et al., Identification of androgen-regulated genes in human prostate. Mol. Med. Rep. **6**, 466–472 (2012). https://doi.org/10.3892/mmr.2012.956
68. B. Ye et al., Study on the role of SLC14A1 gene in biochemical recurrence of prostate cancer. Sci. Rep. **12**, 17064 (2022). https://doi.org/10.1038/s41598-022-20775-7
69. J. Ma et al., Down-regulation of SLC14A1 in prostate cancer activates CDK1/CCNB1 and mTOR pathways and promotes tumor progression. Sci. Rep. **14**, 14914 (2024). https://doi.org/10.1038/s41598-024-66020-1
70. E. Frullanti et al., Association of lung adenocarcinoma clinical stage with gene expression pattern in noninvolved lung tissue. Int. J. Cancer **131**, E643–E648 (2012). https://doi.org/10.1002/ijc.27426
71. Y. Zhang et al., SLC14A1 and TGF-β signaling: a feedback loop driving EMT and colorectal cancer metachronous liver metastasis. J. Exp. Clin. Cancer Res. **43**, 208 (2024). https://doi.org/10.1186/s13046-024-03114-8
72. Z. Wan et al., SLC14A1 is a new biomarker in renal cancer. Clin. Transl. Oncol. **25**, 2607–2623 (2023). https://doi.org/10.1007/s12094-023-03140-6
73. R.R. Handley et al., Brain urea increase is an early Huntington's disease pathogenic event observed in a prodromal transgenic sheep model and HD cases. Proc. Natl. Acad. Sci. USA **114**, E11293–e11302 (2017). https://doi.org/10.1073/pnas.1711243115

74. J.A. Santiago, V. Bottero, J.A. Potashkin, Evaluation of RNA blood biomarkers in the Parkinson's disease biomarkers program. Front. Aging Neurosci. **10**, 157 (2018). https://doi.org/10.3389/fnagi.2018.00157

75. F. Garcia-Sanchez, D. Krause, D. Perez-Garcia, A zincfinger deletion at ZFN850 defines the dominant Kidd-null red blood cell phenotype (InJK) with familiar mood disorder. Vox Sang. **112**, 53 (2017)

76. H. Wang et al., High urea induces depression and LTP impairment through mTOR signalling suppression caused by carbamylation. EBioMedicine **48**, 478–490 (2019). https://doi.org/10.1016/j.ebiom.2019.09.049

77. B. Huang et al., High urea induces anxiety disorders associated with chronic kidney disease by promoting abnormal proliferation of OPC in amygdala. Eur. J. Pharmacol. **957**, 175905 (2023). https://doi.org/10.1016/j.ejphar.2023.175905

78. K. Ranade et al., Genetic variation in the human urea transporter-2 is associated with variation in blood pressure. Hum. Mol. Genet. **10**, 2157–2164 (2001). https://doi.org/10.1093/hmg/10.19.2157

79. X. Hong et al., Genetic polymorphisms of the urea transporter gene are associated with antihypertensive response to nifedipine GITS. Methods Find. Exp. Clin. Pharmacol. **29**, 3–10 (2007). https://doi.org/10.1358/mf.2007.29.1.1063490

80. R. Duchesne et al., UT-A urea transporter protein in heart: increased abundance during uremia, hypertension, and heart failure. Circ. Res. **89**, 139–145 (2001). https://doi.org/10.1161/hh1401.093293

81. J.D. Klein et al., Urea transporter UT-A1 and aquaporin-2 proteins decrease in response to angiotensin II or norepinephrine-induced acute hypertension. Am. J. Physiol. Renal Physiol. **291**, F952–F959 (2006). https://doi.org/10.1152/ajprenal.00173.2006

82. H.J. Tsai et al., Genetic variants of human urea transporter-2 are associated with metabolic syndrome in Asian population. Clin. Chim. Acta **411**, 2009–2013 (2010). https://doi.org/10.1016/j.cca.2010.08.025

83. T. Zemunik et al., Genome-wide association study of biochemical traits in Korcula Island, Croatia. Croat Med J **50**, 23–33 (2009). https://doi.org/10.3325/cmj.2009.50.23

84. J. Lee et al., Genome-wide association analysis identifies multiple loci associated with kidney disease-related traits in Korean populations. PLoS One **13**, e0194044 (2018). https://doi.org/10.1371/journal.pone.0194044

85. A.J. Osborne et al., Multivariate canonical correlation analysis identifies additional genetic variants for chronic kidney disease. NPJ Syst Biol Appl **10**, 28 (2024). https://doi.org/10.1038/s41540-024-00350-8

86. Q. Fan et al., Meta-analysis of gene-environment-wide association scans accounting for education level identifies additional loci for refractive error. Nat. Commun. **7**, 11008 (2016). https://doi.org/10.1038/ncomms11008

Chapter 8
Small-Molecule Inhibitors and Drug Discovery of Urea Transporters

Hang Zhang, Min Li, and Baoxue Yang

Abstract Urea transporters (UT) in renal tubule epithelial cells (UT-A) and vasa recta endothelial cells (UT-B) play an important role in the urine concentrating mechanism. Therefore, UTs are regarded as a potential target for diuretics, or 'urearetics', with unique mechanisms of action and clinical indications. UT inhibitors have a diuretic effect without causing disorders of electrolyte balance like classical diuretics that induce diuresis by natriuresis. This chapter delves into the screening and evaluation methods used for discovering UT inhibitors, the small molecule UT inhibitors that have been identified to date, and UT inhibitors' therapeutic effect in hyponatremic animal models. The studies on UT inhibitors as diuretics show promise for treating dilutional hyponatremia associated with conditions like congestive heart failure, cirrhosis, ascites, and nephrotic syndrome, as well as the syndrome of inappropriate antidiuretic hormone (SIADH) secretion.

Keywords Urea transporters · Diuretic · Small molecule inhibitors · Structural optimization

Urea transporters (UT) are a group of membrane channel proteins that specifically permeate urea and can promote the passive passage of urea across the cell membrane [1–5]. UTs are mainly divided into two subtypes: UT-As and UT-B [6–8]. UT-As include six members from UT-A1 to UT-A6, among which UT-A1, UT-A3, and UT-A4 (only in rat) are expressed in inner medullary collecting duct (IMCD), with UT-A1 at the apical membrane and UT-A3 at the basolateral membrane. UT-A2 is expressed in the thin descending limb of the loop of Henle. UT-A5 is expressed in the testis and UT-A6 is expressed in the colon. UT-B is a protein highly expressed mainly in endothelial cells in renal vasa recta [9]. The urine concentrating mechanism in kidney depends on both the NaCl concentration gradient from the cortex to the medulla and the urea concentration gradient from the extramedullary to the

H. Zhang · M. Li · B. Yang (✉)
Department of Pharmacology, State Key Laboratory of Vascular Homeostasis and Remodeling, School of Basic Medical Sciences, Peking University, Beijing, China
e-mail: baoxue@bjmu.edu.cn

intramedullary [10]. UTs regulate the urea concentration gradient and play an important role in the urine concentration mechanism.

Previous studies show that the UT-B knockout mouse model, UT-A1 knockout mouse model, UT-A1/A3 knockout mouse model, and all-UT knockout mouse model, have varying degrees of impairment in urine concentration ability [3, 9, 11–15]. It manifests as increased urine output and decreased osmotic pressure, but the excretion of non-urea solutes (such as Na^+, K^+, Cl^-) is not affected [16–19]. Therefore, UTs are regarded as a novel diuretic target, and UT inhibitors have the potential to be developed into new diuretics [20–23]. In addition, since the diuretic effect of inhibiting UT-A1 is significantly better than that of inhibiting UT-B, and inhibiting UT-B may produce side effects such as depression-like symptoms, UT-A1 is more suitable as a diuretic target than UT-B. UT-A1 selective inhibitors are more likely to be developed into good diuretics [24].

This chapter reviews the theoretical basis of UT as a diuretic target, the screening and evaluation methods of UT inhibitors, and the currently discovered small molecule UT inhibitors, aiming to provide a reference for the subsequent development of new diuretics targeting UT. Recently, available UT inhibitors are classified as thiourea, diarylamide, 8-hydroxyquinoline, aminothiazolone, triazine, thienoquinoline, triazolothienopyrimidine, phenylphthalazine, thienopyridine, phenylsulphoxyoxazole, benzenesulfoanilide, phthalazinamine, aminobenzimidazole, etc. The discovery and characterization of nanomolar-potency small-molecule UT inhibitors is reviewed in this chapter.

Methods to Assay Urea Transport

Erythrocyte Osmotic Lysis Assay

Mammalian erythrocytes are readily available and naturally express UT-B and the water channel protein aquaporin 1 (AQP1) on their membranes, facilitating rapid permeation of urea and water [25–27]. Erythrocytes are ideal for high-throughput screening of UT inhibitors due to their ability to change volume or rupture under varying osmotic pressures. As diagramed in Fig. 8.1a, the experimental procedure involves incubating freshly prepared erythrocytes in a phosphate buffer solution with a high urea concentration to increase the urea concentration within the cells [28]. Subsequently, the erythrocytes are transferred to an isotonic phosphate buffer solution. As AQP1 is present on the cell membrane, the high osmotic pressure inside the cells drives water in through AQP1 while urea moves out through UT-B, maintaining osmotic balance. When a UT-B inhibitor is introduced, urea is trapped inside the cell, leading to an influx of water through AQP1 and eventual cell lysis. Detection of hemoglobin at 720 nm can identify UT inhibitors by measuring the hemoglobin released from ruptured erythrocytes. This method offers an efficient way to screen for UT-B inhibitors.
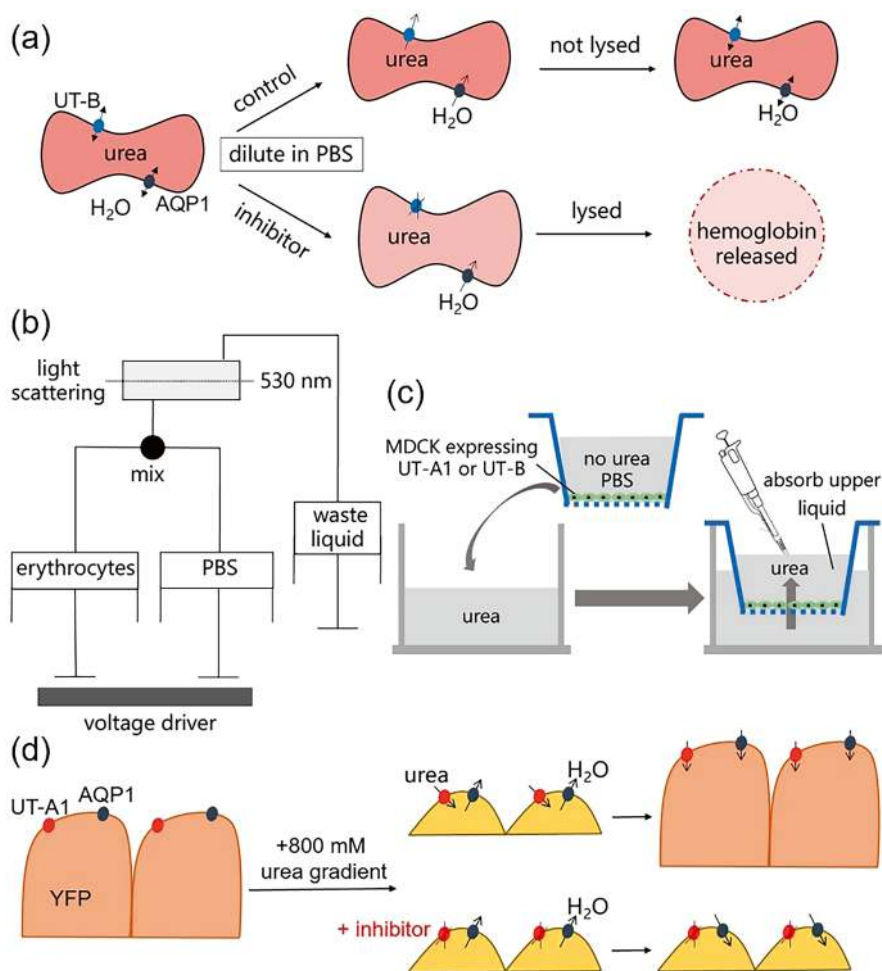
Fig. 8.1 Methods to assay urea transport. (**a**) Erythrocyte osmotic lysis assay. (**b**) Stopped-flow light scattering. (**c**) Transwell assay. (**d**) Fluorescence indicator

Stopped-Flow Light Scattering

The stopped-flow assay is a valuable tool for studying millisecond-level kinetic processes in solution systems, commonly used to assess the efficacy of UT inhibitors [9]. In this assay, as diagramed in Fig. 8.1b, an erythrocyte suspension is quickly mixed with a high-concentration urea solution in the mixing chamber of the stopped-flow instrument. The high osmotic pressure created by the external urea concentration causes rapid water efflux from the cells through AQP1, leading to cell shrinkage. Subsequently, urea enters the cells due to the concentration difference, causing a reversal in osmotic pressure inside and outside the cells, leading to water influx and

cell swelling. The change in erythrocyte volume affects the amount of scattered light passing through the mixing chamber. By measuring the intensity of 90° scattered light at 530 nm, the volume change of the cells can be quantitatively analyzed to calculate the permeability of the erythrocyte membrane to urea.

Transwell Assay

The transwell assay is commonly used to screen UT-A1 inhibitors, involving the use of MDCK cell lines stably transfected with UT-A1 [29]. As diagramed in Fig. 8.1c, these cells are seeded at a specific density in collagen-coated transwell chambers, and cell resistance is monitored until a resistance of around 1 kΩ·cm^2 is reached, indicating the formation of a compact monolayer of cells on the membrane. The compound to be tested, dissolved in PBS containing forskolin (FSK, an adenylyl cyclase activator, induces UT-A1 transport from the cytoplasm to the cell membrane), is applied to both the top and bottom membranes of the transwell. Following incubation with the test compound, high-concentration urea is added to the lower side of the transwell chamber, and the urea concentration in the upper liquid is measured at various time points to assess the inhibitory activity of the test compound on the urea permeability of the MDCK cell membrane UT-A1 [30].

Fluorescence Indicator

The UT-A1 is deemed more suitable as a diuretic target compared to UT-B. Therefore, as diagramed in Fig. 8.1d, a high-throughput screening model for UT-A1 inhibitors is required. Frohlich et al. subcloned the UT-A1 cDNA into the pcDNA5/FRT plasmid and transfected it into Madin-Darby canine kidney (MDCK) cells [31]. Forskolin and arginine vasopressin were shown to increase the phosphorylation of UT-A1, facilitating its transfer from intracellular vesicles to the plasma membrane and enhancing the transmembrane permeability of urea. By utilizing ^{14}C-labeled urea molecules to monitor the permeability rate of MDCK cells expressing UT-A1 to urea, the inhibitory effect of UT inhibitors on UT-A1 can be identified. Following a similar approach, yellow fluorescent protein YFP-H148Q/V163S, AQP1, and UT-A1 or UT-B genes were stably transfected into the MDCK cell line. These cells were cultured in black-walled 96-well culture plates, with YFP-H148Q/V163S, sensitive to Cl$^-$, serving as an indicator of changes in cell volume. A decrease in cell volume leads to an increase in intracellular Cl$^-$ concentration, resulting in reduced YFP fluorescence. When exposed to a urea solution, the osmotic pressure changes caused by extracellular urea drive water out of the cells, causing them to shrink. Subsequently, urea and water enter the cells to restore their normal volume. By analyzing changes in fluorescence signal intensity under varying urea gradients, the

rate of cell volume change can be calculated, membrane permeability to urea can be assessed, and the efficacy of UT-A1 inhibitors can be screened and evaluated [32, 33].

Discovered UT Inhibitors

The names of each type of compound, the structures of representative compounds, and IC$_{50}$ are shown in Table 8.1.
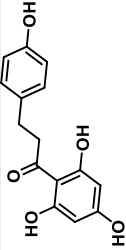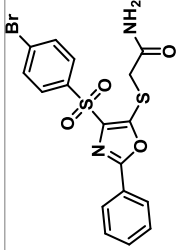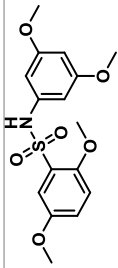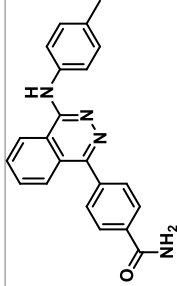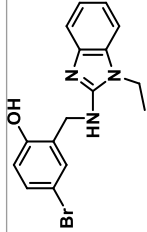
Urea Analogues

In 1970, Macey and Farmer discovered that phloretin could inhibit the permeability coefficient of urea without significantly altering the water permeability coefficient [34, 35]. They also found that urea analogues like thioureas can alter the permeability rate of erythrocytes to urea at 50 ~ 100 mM and inhibit the permeability of isolated inner medullary collecting ducts (IMCD) to urea. However, the effective doses of these UT inhibitors are too large, limiting their potential as drugs.
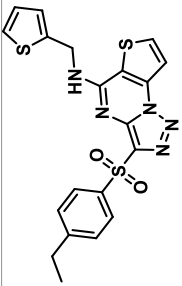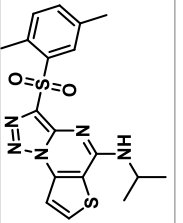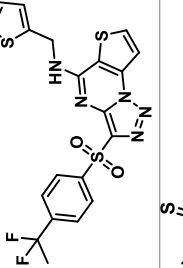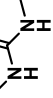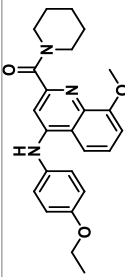
Phenylsulfoxyoxazoles

In 2007, A.S. Verkman et al. employed high-throughput screening to identify high-affinity, small molecule inhibitors of the urea transporter [27]. The primary screening resulted in the discovery of approximately 30 UT-B inhibitors, utilizing a human erythrocyte lysis assay, which were categorized into the phenylsulfoxyoxazole, benzenesulfonanilide, phthalazinamine, and aminobenzimidazole chemical classes.

The first class of phenylsulfoxyoxazoles compounds demonstrates high inhibitory potency against both human and mouse UT-B, exhibiting favorable activity in structure-activity relationship (SAR) analyses. The representative compound within this class is urea$_{inh}$-101, which has an EC$_{50}$ of 0.03 μM in human UT-B and approximately 0.2 μM in mouse UT-B. It shows good selectivity for UT-B and UT-A, with the EC$_{50}$ approximately 1.2 μM for rat UT-A1. Urea$_{inh}$-101 has minimal impact on water transport in the erythrocytes of wildtype mice, as AQP1 serves as the primary water transport channel. However, urea$_{inh}$-101 significantly inhibited water permeability in AQP1-deficient erythrocytes, providing compelling evidence that UT-B facilitates water transport.
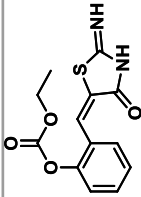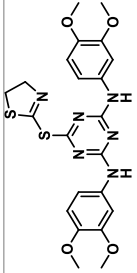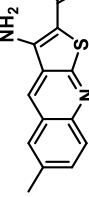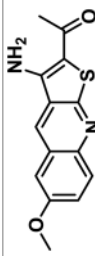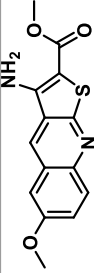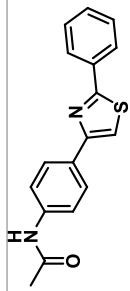
Table 8.1 Chemical structures of UT inhibitors
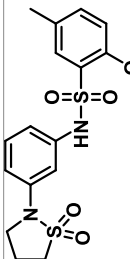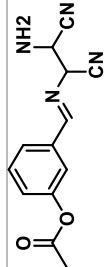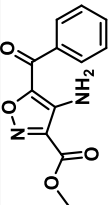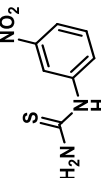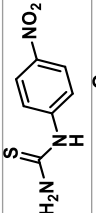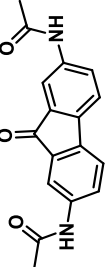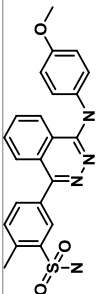
Name		Structure	IC$_{50}$(µM)
2.1	Phloretin	Phloretin		–
2.2	Phenylsulfoxyoxazole	Urea$_{inh}$-101		hUT-B 0.03 mUT-B 0.2 rUT-A1 1.2
2.3	Benzenesulfonanilides	Urea$_{inh}$-201		hUT-B 0.3 mUT-B >25 rUT-B >25 rUT-A1 >25
2.4	Phthalazinamines	Urea$_{inh}$-302		hUT-B 0.2 mUT-B 0.2 rUT-A1 15
2.5	Aminobenzimidazole	Urea$_{inh}$-404		hUT-B 0.4 rUT-A1 >25

2.6	Triazolothienopyrimidines	UTB$_{inh}$-14		hUT-B 10 rUT-B 25
		UTA$_{inh}$-D01		rUT-B 15 rUT-A1 3.8
		3 k		hUT-B 0.015 mUT-B 0.023
2.7	Dimethylthiourea	DMTU		rUT-B 2000 ~ 3000 rUT-A1 2000 ~ 3000
2.8	8-hydroxyquinolin	UTA$_{inh}$-A01		rUT-B 16 rUT-A1 3.3

Table 8.1 (continued)
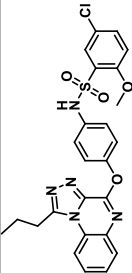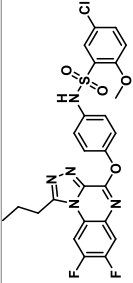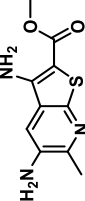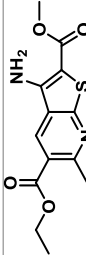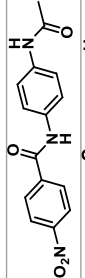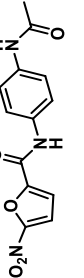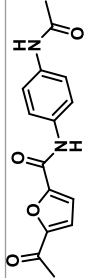
Name		Structure	IC$_{50}$(μM)
2.9	Aminothiazolone	UTA$_{inh}$-B01	rUT-B 4.8 rUT-A1 3.7
2.10	Benzo-[1,3,5]-triazine	UTA$_{inh}$-C01	rUT-B >50 rUT-A1 4.2
2.11	Thienoquinoline	PU-14	hUT-B 1.7 mUT-B 5.2 rUT-B 3.5
2.12	Aryl-thiazole	UTA$_{inh}$-E01	rUT-B 50 rUT-A1 3

	Name	Code	Structure	Activity
2.13	γ-sultambenzosulfonamide	UTA$_{inh}$-F01		rUT-B 6 rUT-A1 1
2.14	Aminocarbonitrile butene	UTA$_{inh}$-G01	NH2, CN, CN	–
2.15	Isoxazole	UTA$_{inh}$-H01	NH$_2$	–
2.16	Nitrophenyl-thiourea	3-nitrophenylthiourea	NO$_2$, H$_2$N	rUT-B 200 rUT-A1 200
		4-nitrophenylthiourea	NO$_2$, H$_2$N	rUT-B 10000 rUT-A1 1300
2.17	2,7-bisacetamido fluorenone	3	NH, HN	rUT-B 1.5 rUT-A1 1
2.18	Phenylphthalazines	PU-1424		hUT-B 0.02 mUT-B 0.69

Table 8.1 (continued)

Name		Structure	$IC_{50}(\mu M)$
2.19	Triazoloquinoxaline	8ay	rUT-B 2 rUT-A1 0.15
		8bl	rUT-B 0.8 rUT-A1 0.3
2.20	Thienopyridine	8n	rUT-B 0.54
		CB-20	hUT-B 1.29 mUT-B 2.01 rUT-B 0.47
2.21	Diarylamide	E04	hUT-B 5.37
		1H	hUT-B 0.13 mUT-B 1.6 rUT-B 0.64 rUT-A1 0.09
		25a	mUT-B 0.48 rUT-B 0.14

hUT-B, human UT-B; mUT-B, mice UT-B; rUT-B, rat UT-B; rUT-A1, rat UT-A1

Benzenesulfonanilides

Benesulfonanilides, compound $urea_{inh}$-201, exhibited micromolar-level inhibitory activity on human UT-B, with an IC_{50} of 0.3 μM [27]. However, $urea_{inh}$-201 demonstrates weak inhibitory effects on mouse and rat UT-B, with no inhibition observed at a concentration of 25 μM. Additionally, $urea_{inh}$-201 did not inhibit rat UT-A1 at 25 μM, indicating a lack of significant inhibitory activity on UT-A1. These limitations may hinder its application in further animal experimental studies.

Phthalazinamines

The representative compound of phthalazinamins, $urea_{inh}$-302, exhibits a strong inhibitory effect on UT-B, with an EC_{50} of approximately 0.2 μM for human UT-B; it also has similar activity against mouse UT-B, with an EC_{50} of around 0.2 μM [27]. This compound displays high inhibitory potency against UT-B, rendering it valuable for use in chemical knockout studies. Additionally, it has an IC_{50} of approximately 15 μM for rat UT-A1, indicating a high selectivity for UT-B. Furthermore, research has revealed that $urea_{inh}$-302 can also inhibit the transport of water by UT-B.

Aminobenzimidazoles

The representative compound of aminobenzimidazoles is $urea_{inh}$-404, with an IC_{50} of approximately 0.4 μM [27]. At a concentration of 25 μM, $urea_{inh}$-404 did not exhibit a significant inhibitory effect on rat UT-A1. Although this class of compounds is not the most potent, they demonstrate specific structural requirements in structure–activity relationship (SAR) analysis, which provides a foundation for further optimization.

Triazolothienopyrimidine

In 2012, Yao et al. identified triazolothienopyrimidine compounds with significant UT-B inhibitory activity among a screening of 100,000 compounds using an erythrocyte lysis model [36]. UTB_{inh}-14, the most potent compound, exhibits IC_{50} values of 10 μM and 25 μM for human and rat UT-B, respectively, completely and reversibly inhibiting urea transport. This compound competitively inhibits urea transport by targeting the intracellular site of the UT-B channel and demonstrates high selectivity for UT-B, showing no inhibitory effects on UT-A1 even at higher concentrations. Intraperitoneal administration of UTB_{inh}-14 in mice decreased urine

osmolality post-administration of 1-deamino-8-D-arginine-vasopressin (dDAVP, Desmopressin). However, UTB_{inh}-14 is unsuitable for clinical diuretic use due to its rapid metabolism in hepatic microsomes and lack of activity against UT-A1.

Another representative compound of triazolothienopyrimidine, $UTA1_{inh}$-D1, features structural characteristics that include 2,5-dimethyl and isopropyl groups [32]. Following structural optimization of triazolothienopyrimidine compounds that competitively inhibit urea transport, $UTA1_{inh}$-D1 was developed with high selectivity for UT-A1, displaying IC_{50} values of 3.8 μM for UT-A1 and 15 μM for UT-B. This compound demonstrates good UT-A1 inhibitory activity and selectivity, and the structures of such compounds provide a basis for further optimization to enhance their pharmacological properties.

After analyzing 273 commercially available analogues of compound 1 to establish a structure–activity relationship, and synthesizing a targeted library of 11 analogues to identify potent, metabolically stable UT-B inhibitors, Anderson et al. discovered that the representative compound triazolothienopyrimidine, designated as 3 k, exhibited IC_{50} values of 23 nM and 15 nM for the inhibition of urea transport by mouse and human UT-B, respectively [37]. Additionally, 3 k demonstrated good *in vitro* metabolic stability in liver microsomes, with a half-life ($t_{1/2}$) of approximately 120 min. In vivo studies in mice revealed that 3 k accumulated in the kidney and urine, leading to a reduction in maximum urinary concentration and urine osmolality. This decrease in urine osmolality is comparable to that observed in UT-B gene knockout mice.

Dimethylthiourea

In 2012, Cil et al. determined that the IC_{50} values of the urea analogue dimethylthiourea (DMTU), when intraperitoneally injected, significantly increased urine output, decreased urine osmolarity, and enhanced free water clearance in female rats [38].

Subsequent research has found that DMTU completely and reversibly inhibits rat UT-A1 and UT-B via a non-competitive mechanism, with an IC_{50} of 2 ~ 3 mM [39]. Homology modeling and docking calculations indicate the presence of a DMTU binding site on rat UT-A1. Following a single intraperitoneal injection of 500 mg/kg DMTU, the peak plasma concentration reached 9 mM, with a half-life ($t_{1/2}$) of approximately 10 h, and urine concentrations ranged from 20 to 40 mM. Rats subjected to long-term DMTU treatment exhibited a sustained and reversible decrease in urine osmolarity from 1800 to 600 mOsm, along with a threefold increase in urine output and mild hypokalemia. Importantly, DMTU did not impair the urine concentrating function in rats fed a low-protein diet. Compared to furosemide-treated rats, DMTU-treated rats demonstrated greater diuresis and reduced urinary salt loss.

In a model of inappropriate antidiuretic hormone secretion syndrome (SIADH), DMTU treatment effectively prevented hyponatremia and water retention induced by water loading in dDAVP-treated rats. Furthermore, it was observed that slight

changes in the symmetry of DMTU resulted in a loss of activity; specifically, the replacement of the sulfur atom in thiourea with oxygen led to a significant reduction in the inhibitory activity of UT-A1 and UT-B, highlighting the importance of this functional group. These findings suggest that DMTU can serve as a tool to confirm UT as a diuretic target; however, the effective dose is excessively large, rendering it unsuitable for the development of new diuretics.

8-Hydroxyquinoline

In 2013, Verkman et al. screened approximately 90,000 synthetic small molecules through YFP-H148Q/V163S fluorescence monitoring experiments, producing four classes of UT-A1 inhibitors with low micromolar half maximal inhibitory concentrations that completely and reversibly inhibit urea transport through non-competitive mechanisms [32].

In the realm of urea transport inhibition, unsubstituted 8-hydroxyquinoline(8-HQ) analogs demonstrated selectivity for UT-A1 over UT-B, indicating a specific interaction with this transporter isoform. The binding mechanism of these 8-HQ inhibitors suggests non-competitive inhibition with respect to urea, as evidenced by comparable inhibition percentages across varying urea concentrations. Furthermore, the reversibility of UT-A1 inhibition by 8-HQ compounds has been confirmed, highlighting their potential utility in modulating urea transport activity in a controlled manner. The representative compound, $UTA1_{inh}$-A1, possesses structural characteristics that include a piperidinyl group and a 4-ethoxyanilinyl group, with UT-A1 IC_{50} at 3.3 μM and UT-B IC_{50} at 16 μM. The application value of these class A inhibitors lies in their high selectivity for UT-A1, which could regulate urea transport and influence the renal capacity to concentrate urine. This provides a novel mechanism of action for the development of new diuretics, termed "urearetics", which may prove effective in treating fluid-retaining conditions where conventional diuretics are less effective.

Aminothiazolone

Aminothiazolones are characterized by a reversible, non-competitive binding mechanism to UT-A1, a significant pharmacological property [32]. The inhibitory potency of aminothiazolones is influenced by the nature and position of substituents on the aniline ring. The representative compound, $UTA1_{inh}$-B1, has an IC_{50} of 3.7 μM for UT-A1 and 4.8 μM for UT-B. Aminothiazolone inhibitors exhibit good inhibitory effects on both UT-A1 and UT-B; however, their selectivity is relatively low. Despite this, aminothiazolones possess drug-like properties and favorable pharmacokinetic profiles, making them an exciting avenue for exploration and optimization in medicinal chemistry. Given the critical role of urea transporters in the

renal concentrating mechanism, aminothiazolones and their analogs may play a pivotal role in developing therapeutics for edema and related conditions. In summary, aminothiazolones have emerged as a potent class of UT-A1 inhibitors with significant potential for the development of new diuretic agents. Their inhibitory activity, selectivity, and structure-activity relationships underscore their value in medicinal chemistry and drug discovery for treating fluid retention disorders.

Benzo-[1,3,5]-Triazine

The inhibition observed with this compound was fully reversible and occurred through a non-competitive mechanism, indicating that Benzo-[1,3,5]-triazine does not directly compete with urea for binding at the active site [32]. The representative compound, UTA1$_{inh}$-C1, contains a 3,4-dimethoxyanilino group and a 2-thio(4,5-dihydrothiazole) group; its IC$_{50}$ values are 4.2 μM for UT-A1 and > 50 μM for UT-B. This class of inhibitors demonstrates high selectivity for UT-A1 but exhibits weaker inhibitory effects on UT-B. Although their larger molecular polar surface area may limit their potential as ideal drug candidates, structural optimization can enhance their drug properties, including binding position (inside or outside the pore).

Functional studies, alongside homology modeling and docking computations, revealed that 8-hydroxyquinoline and aminothiazolone were docked to the cytoplasmic pore region of UT-A1, while benzo-[1,3,5]-triazine was docked to the extracellular pore. Research has established the following order of inhibition by UT-A1 inhibitors: 8-hydroxyquinoline > aminothiazolone > [1,3,5]-triazine > triazolothienopyrimidine.

Thienoquinoline

The Yang group identified that the thienoquinoline compound PU-21 had inhibitory effects on UT-B by computational virtual screening [21]. Computational molecular docking analysis revealed that PU-21 establishes hydrogen bonds with ASN289 of the UT-B molecule, and engages in robust van der Waals forces and hydrophobic interactions with LEU285 and ALA327. Molecular dynamics simulations suggest that PU-21 binds to the functional docking site of UT-B through rivets, thereby inhibiting urea permeability and exerting its inhibitory effects.

In 2013, Li et al. screened thienoquinoline analogs and optimized the chemical structures to discover the active compounds. Compound PU-14 was found to have potent inhibition activity on human, rabbit, rat, and mouse UT-B [40]. The half-maximal inhibitory concentration of PU-14 on rat UT-B-mediated urea transport was ~0.8 μM. PU-14 did not affect urea transport in mouse erythrocytes lacking UT-B. PU-14 significantly inhibited UT-A1 mediated urea permeability by 36% at 4 μM. PU-14 showed no significant cellular toxicity at concentrations up to its

solubility limit of 80 μM. Subcutaneous delivery of PU-14 (at 12.5, 50, and 100 mg/kg) to rats increased urine output and decreased the urine urea concentration and subsequent osmolality without electrolyte disturbances, or liver or renal damage. These experimental results suggest that PU-14 does not alter levels of Na^+, K^+, and Cl^- in the blood, indicating maintenance of electrolyte balance while exerting diuretic effects.

To identify more potent UT inhibitors that effectively inhibit UT-A isoforms, the structure of thienoquinolin was optimized by Ren et al. [41]. Following this optimization, the efficient UT inhibitor PU-48 was identified through structure-activity optimization. PU-48 exhibited potent UT-A1 inhibition activity with an IC_{50} of 0.32 μM. PU-48 significantly inhibited urea transport in perfused rat terminal inner medullary collecting duct (IMCD). PU-48 caused significant diuresis in UT-B null mice, which indicates that UT-A1 is the target of PU-48. The diuresis caused by PU-48 did not change blood Na^+, K^+, or Cl^- levels or nonurea solute excretion in rats and mice. The results suggest that thienoquinolins may have the potential to be developed as a novel class of diuretics. However, the development of PU-48 is hindered by its low bioavailability and lack of oral diuretic activity in rats [42].

Aryl-Thiazole

In 2014, Verkman et al. identified UT-A inhibitors of aryl-thiazole, γ-sultambenzosulfonamide, aminocarbonitrile butene, and 4-isoxazolamide chemical classes from 50,000 synthetic small molecules by a high-throughput assay [43]. The representative compound of aryl-thiazole is UTA_{inh}-E02, whose UT-A1 IC_{50} is 1 μM and UT-B IC_{50} is 50 μM, showing excellent selectivity for UT-A1 [43]. UTA_{inh}-E02 significantly increased urine volume and decreased urine osmolality within the 0–3 h timeframe in rats. Both urine volume and osmolality returned to near baseline levels during the 3–6 h collection period. The selection of a vehicle for the administration of UTA_{inh}-E02 presented challenges due to its limited solubility. Various combinations of vehicles resulted in low plasma and urine concentrations (≪1 μM) following intraperitoneal, subcutaneous, or oral administration of doses up to 100 mg/kg. However, it was found that intravenous administration of 20 mg/kg of UTA_{inh}-E02 (5 mg/ml in saline, 20% dimethylacetamide, 40% 2-hydroxypropyl γ-cyclodextrin) to rats initially yielded plasma levels of approximately 6 μM and urine levels of about 3 μM, with a plasma elimination half-life ($t_{1/2}$) of approximately 4.5 h.

γ-Sultambenzosulfonamide

The representative compound of γ-sultambenzosulfonamide is UTA_{inh}-F11, which exhibits an IC_{50} of 1 μM for UT-A1 and 10 μM for UT-B, indicating a greater selectivity for UT-A1 [43]. The kinetics of the original (nonmetabolized) inhibitors,

UTA$_{inh}$-F11, show approximately 50% metabolism at 60 minutes. The minimal toxicity of UTA$_{inh}$-F11 was at concentrations up to 25 μM, which is close to its solubility limits. Intravenous administration of UTA$_{inh}$-F11 at a dosage of 20 mg/kg resulted in a three- to five-fold increase in urine output and a two-fold decrease in urine osmolality compared to vehicle control rats, even under conditions of maximal antidiuresis induced by 1-deamino-8-D-arginine vasopressin (dDAVP). UTA$_{inh}$-F11 is highly soluble in saline containing 20% dimethylacetamide and 0.6 mg/mL NaOH. Intravenous injection of 20 mg/kg UTAinh-F11 into rats resulted in initial plasma levels that were higher than UTA$_{inh}$-E02 but lower from t$_{1/2}$ to 1 h. Urinary levels of UTAinh-F11 are above 3 μM.

Aminocarbonitrile

One of the identified compounds from this class, UTA$_{inh}$-G01, belongs to the aminocarbonitrile butene class and exhibits significant inhibitory activity against UT-A [43]. The aminocarbonitrile butene compounds inhibit UT-A through a noncompetitive mechanism, suggesting that they do not directly compete with urea for binding at the active site of the transporter. The IC$_{50}$ values for these compounds fall within the low micromolar range, highlighting their potency in inhibiting UT-A-mediated urea transport. Given the role of UT-A in the kidney's ability to concentrate urine, aminocarbonitrile butene inhibitors may hold promise as novel diuretics.

4-Isoxazolamide

The 4-isoxazolamide class of compounds, exemplified by UTA$_{inh}$-H01, demonstrates potent inhibitory activity against UT-A1 [43]. The UTA$_{inh}$-H01 compound, in particularly, exhibits a noncompetitive inhibition mechanism with an IC$_{50}$ also in the low micromolar range. This finding indicates that the 4-isoxazolamide compounds can bind to UT-A1 at a site distinct from the urea binding site, effectively reducing UT-A1-mediated urea transport.

Nitrophenyl-Thiourea

In 2015, Verkman et al. measured UT-A1 and UT-B inhibition activity of 36 thiourea analogs, with the goal of identifying more potent and isoform-selective inhibitors, and establishing structure-activity relationships [44]. The analog set systematically explored modifications of substituents on the thiourea including alkyl, heterocycles and phenyl rings, with different steric and electronic features. The analogs had a wide range of inhibition activities and selectivities. The most

potent inhibitor, 3-nitrophenyl-thiourea, had an IC_{50} of ~0.2 mM for inhibition of both UT-A1 and UT-B. Some analogs such as 4-nitrophenyl-thiourea were relatively UT-A1 selective (IC_{50} 1.3 vs. 10 mM), and others such as thioisonicotinamide were UT-B selective (IC_{50} > 15 vs. 2.8 mM). Despite these findings, it was observed that these compounds demonstrate poor pharmacological properties, including low concentrations in urine and plasma as well as low solubility, rendering them unsuitable for further clinical development as potential new diuretics.

2,7-Bisacetamido Fluorenone

Verkman et al. found that 2,7-bisacetamido fluorenone functions as a novel inhibitor of UT-A (IC_{50} = 1 µM) and UT-B (UT-B IC_{50} = 1.5 µM) [45]. The compound's structure features a symmetrical, rigid crescent shape with carbonyl and bisacetamido groups, which are crucial for its inhibitory effect. These inhibitors specifically bind to UT-A1 in the cytoplasmic region, leading to non-competitive and reversible inhibition of UT-A1 activity. The computational docking to a homology model of UT-A1 suggested that the UT inhibitor binds to the UT cytoplasmic domain at a site distinct from the presumed urea binding site, supporting a noncompetitive inhibition mechanism. Finally, analysis of inhibitor metabolism indicated carbonyl reduction by reductase and subsequent base-catalyzed elimination. Although the aforementioned inhibitors exhibit inhibitory activity *in vitro*, they do not demonstrate a clear diuretic effect *in vivo*.

Phenylphthalazines

In 2016, Yang et al. discovered a potent small-molecule UT-B inhibitor, Phenylphthalazines PU-1424, using an erythrocyte osmotic lysis assay [46]. PU-1424 exhibited inhibition activity on both human and mouse UT-B. The inhibition activity of PU-1424 was much stronger on human UT-B(0.02 µM) than on mouse UT-B(0.69 µM). The inhibitory effect targets the So site of UT-B and is reversible. However, PU-1424 did not display diuretic activity *in vivo*.

1,2,4-Triazoloquinoxaline

In 2018, Lee et al. discovered potent UT-A1 selective inhibitor 1,2,4-triazoloquinoxaline compounds through high-throughput screening [47]. These compounds, particularly compound 8ay, rapidly and reversibly inhibited UT-A1 urea transport through a noncompetitive mechanism, with an IC_{50} of approximately 150 nM; in contrast, the IC_{50} for UT-B is around 2 µM. The inhibition of

UT-A1-mediated urea transport was rapid, reversible, and noncompetitive, suggesting an inhibitor binding site at the cytoplasmic surface of UT-A1, near but distinct from the urea binding site.

Metabolism experiments demonstrated that the epoxidation of quinoxaline compound 8ay yields a metabolically stable 7,8-difluoroquinoxaline analogue, 8bl, with an UT-A1 IC_{50} of approximately 300 nM and an UT-B IC_{50} of 0.8 μM. Intravenous administration of 8bl at a dosage of 4 mg/kg in rats resulted in increased urine output and a decrease in urine osmotic pressure. Consequently, 8bl exhibited favorable pharmacokinetics in rats and elicited a diuretic response.

Thienopyridine

Zhao et al. modified the thienoquinoline structure to obtain new thienopyridine compounds that act as specific UT inhibitors. Through structural optimization, compound 8n was synthesized [48, 49]. Compound 8n has an IC_{50} of 0.54 μM for rat UT-B [48]. The rats that were administered 8n subcutaneously at a dosage of 100 mg/kg showed significantly increased urine output. 8n demonstrates favorable water solubility and an appropriate Log P value. However, 8n only produced diuretic effects when it was administered subcutaneously, without oral diuretic activity, which limits further research.

The Thienoquinoline compound CB-20 was identified through high-throughput virtual screening in conjunction with the erythrocyte osmotic lysis assay [49]. Molecular docking was employed to predict the potential binding modes of CB-20 with human UT-B. CB-20 exhibited comparable inhibitory activity on both UT-A1 and UT-B. Following subcutaneous administration of CB-20, the animals exhibited polyuria without any signs of electrolyte imbalance or abnormal metabolism. Further experiments suggest that CB-20 is unsuitable for further drug development due to its low oral bioavailability.

Diarylamides

Oral administration is very important for long-term use of diuretics. To discover novel UT inhibitors as oral diuretics, the Yang research group screened more than 1000 urea analogs containing hydrophobic structures and found that a series of compounds containing diarylamide cores have strong inhibitory activity against UT-B. The IC_{50} of diarylamide compound E04 is 5.4 μM [29]. Subsequently, a series of structural modifications basing on E04 produced a good diarylamide UT inhibitor 1H with oral diuretic activity. IC_{50} of 1H for human, rat and mouse UT-B were 0.19, 0.56 and 1.60 μM, respectively. After intragastric administration of 100 mg/kg, urine output increased significantly within 2 hours, up to more than 1.5 times (Fig. 8.2a), while urine osmotic pressure decreased significantly (Fig. 8.2b),
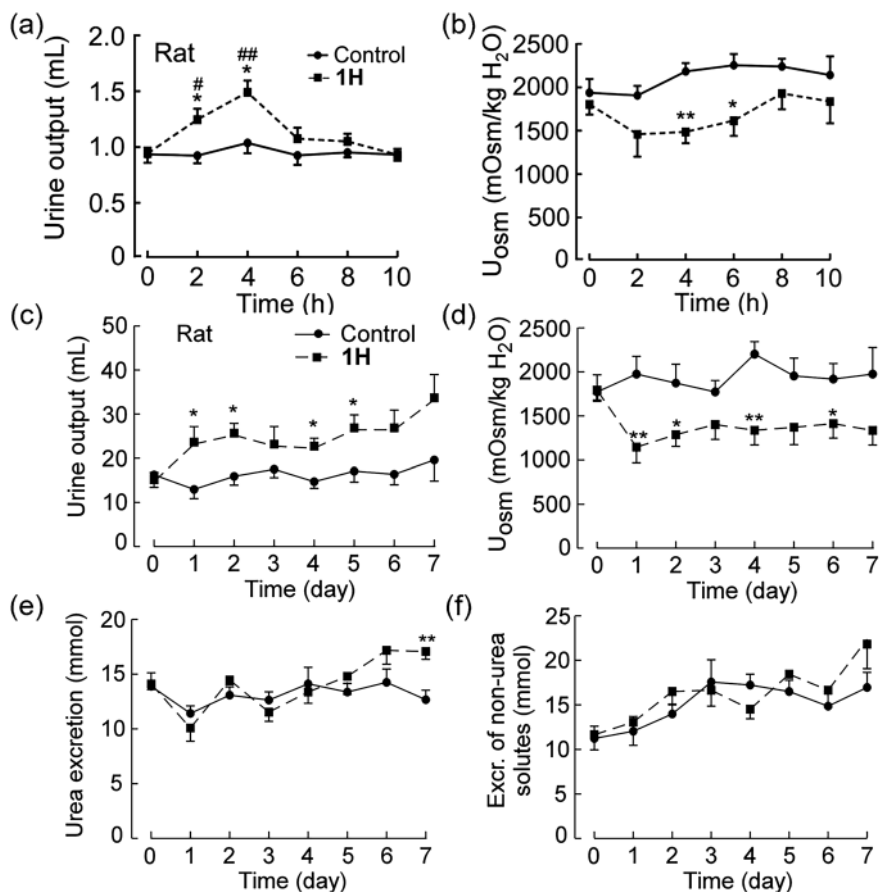
Fig. 8.2 Diuretic effect of intragastric administration of 1H in rats. (**a**) Urine output. Rats were adapted in metabolic cages for three days. After collecting 2-h basal urine output (time 0), 1H with a dose of 100 mg/kg was administrated intragastrically, and then urine samples were collected every 2 h. (**b**) Urine osmolality of rats. (**c**) Urine output of rats. Long-term diuretic effect of 1H in rats. Rats were adapted in metabolic cages for three days, and then urine was collected for 1 day as the basal level. 1H with a dose of 100 mg/kg was given to the experimental group by gavage 3 times a day (the first dose was doubled) for consecutive 7 days. (**d**) Urine osmolality of rats. (**e**) Urea excretion of rats. (**f**) Excretion of non-urea solutes of rats

and there was no significant difference in the excretion of non-urea solutes. The continuous administration of 1H could increase daily urine output and decrease urine osmolality in rats without affecting blood Na^+, K^+, and Cl^- (Fig. 8.2c–f).

In the MDCK cell model, the IC_{50} against rat UT-A1 of 1H was 0.097 μM, significantly lower than the IC_{50} against UT-B (0.64 μM), demonstrating a strong preference for UT-A1 (Fig. 8.3a). Following administration of 100 mg/kg to UT-A1 knockout mice and UT-B knockout mice for 1 h, it was found that the urine output increased and urine osmolality decreased significantly in UT-B knockout mice,
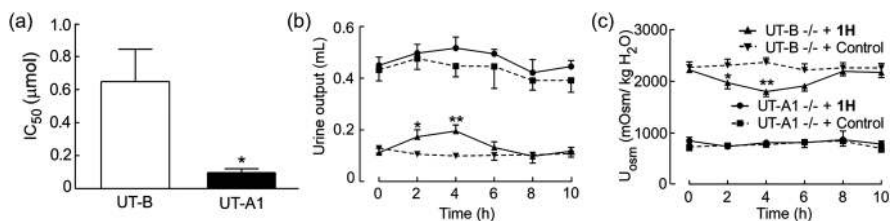
Fig. 8.3 Selective inhibition activity of 1H on UT-A1. (**a**) IC_{50} of 1H on rat UT-B and UT-A1. (**b**) Urine output in UT-A1 and UT-B knockout mice. Mice were adapted in metabolic cages for three days. After collecting 2-h basal urine output (time 0), 1H with a dose of 100 mg/kg was administrated intragastrically, and then urine samples were collected every 2 h. (**c**) Urine osmolality in UT-A1 and UT-B knockout mice
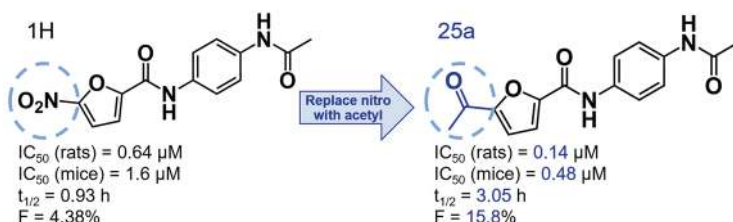
Fig. 8.4 1H structural optimization leads to compound 25a with better UT inhibition activity

while there was no significant change in urine output or urine osmolality in UT-A1 knockout mice, confirming the selectivity of 1H towards UT-A1 (Fig. 8.3b, c).

Subsequent evaluation of the pharmacokinetic properties of 1H revealed good membrane permeability and absorption in the human gastrointestinal tract using the Caco-2 cell model. Further experiments *in vivo* in rats indicated that 1H had low oral bioavailability (approximately 4.4%), which suggests that further enhancement of 1H's drug ability is necessary through structure optimization.

Based on 1H, Wang et al. replaced the nitro group on the furan side of 1H with an acetyl group and obtained compound 25a (Fig. 8.4) [50]. The IC_{50} of 25a for mouse and rat UT-B was 0.48 and 0.14 μM respectively. Also, 25a exhibited stronger inhibition of UT-A1 than 1H. In order to study the binding interaction between the UT-A1 protein and 25a, a molecular docking model was utilized. UT-A1 protein was prepared using a previously described homology model [47]. 25a can be bound to a hydrophobic pocket (Fig. 8.5a, b) with a strong interaction at the intracellular part of the UT-A1 protein. Compound 25a established two hydrogen bonds with the peptide carbonyl of ASP101 and the amino group of ARG106. Additionally, the furan ring underwent π-stacking interactions with the benzene ring of PHE 361 (Fig. 8.5c).

Following oral administration for 7 consecutive days, 25a consistently increased urine volume in mice without causing electrolyte imbalance. 25a inhibits UT-A1 and UT-B in the kidneys, leading to disruption of renal urea circulation and
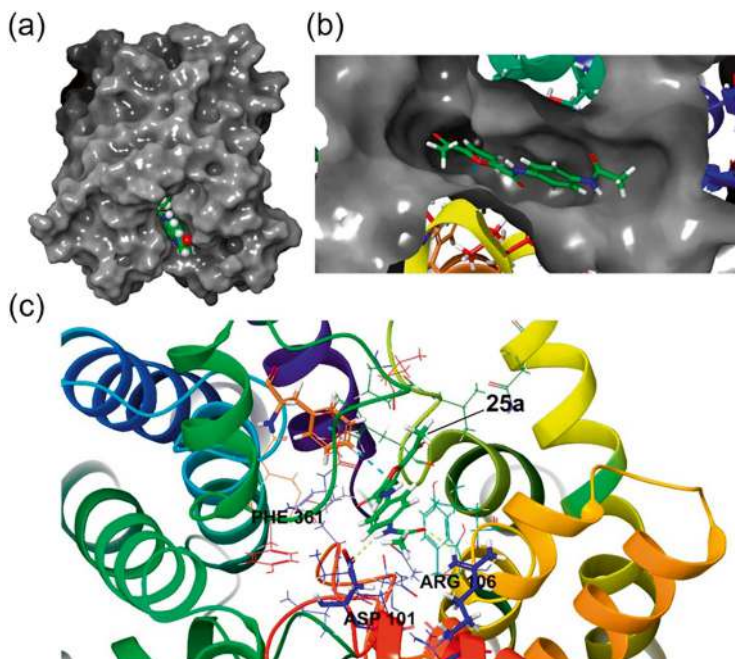
Fig. 8.5 Docking model of 25a and UT-A1. (**a**) The computational model of 25a bound to a homology model of rat UT-A. Grey represents the surface of UT-A. 25a is presented as balls. (**b**) The binding pocket of UT-A and 25a. (**c**) The interaction of Compound 25a with the UT-A protein. Yellow: hydrogen bond; blue: π-π interaction

reduction in urine concentration function, thereby inducing diuretic effects, as illustrated in Fig. 8.6.

Subsequently, by assessing metabolic stability, Xu found that 25a exhibited significantly higher stability than 1H in rat liver microsomes and rat plasma [51]. The $t_{1/2}$ of 25a by oral administration was 3 hours. Distribution studies showed that 25a was widely distributed in various rat tissues, especially in those with rich blood perfusion such as kidneys, heart, lungs, and spleen. Cumulative excretion after oral administration indicated that 25a was predominantly excreted in urine, with smaller fractions in feces and bile. In vitro pharmacokinetic studies demonstrated good stability of 25a in rat, mouse, and human plasma, albeit with more degradation in whole blood and species differences. 25a demonstrates good stability in simulated artificial gastric juice, artificial intestinal juice, and animal intestinal flora. 25a exhibits high metabolic stability in human, dog, rat, and mouse liver microsomes, showing resistance to five major CYP450 enzyme subtypes (1A2, 2C9, 2C19, 2D6, 3A4/5) without significant inhibitory effects. The binding rate of inhibitor 25a to rat, mouse, and human plasma proteins is approximately 40%, indicating relatively low binding. In safety evaluations, a test on mice at 2000 mg/kg revealed no obvious toxicity with no fatalities.
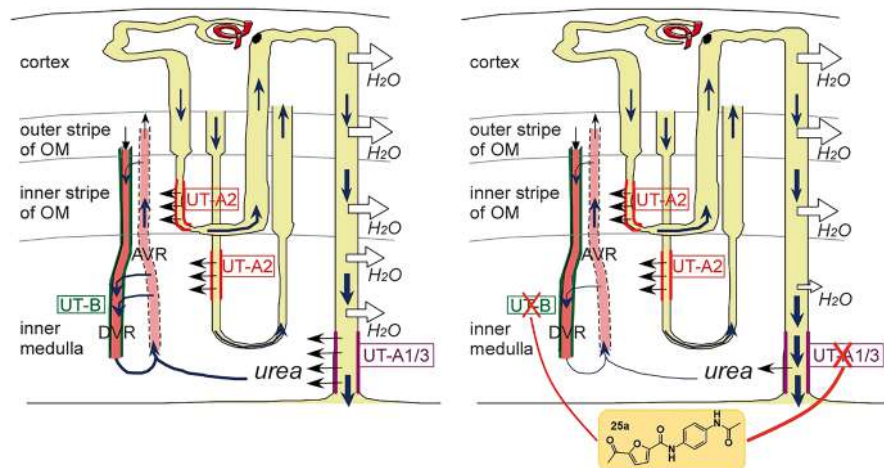
Fig. 8.6 Diagram of urea recycling in the kidney without *(left)* or with 25a treatment *(right)*. Urea flows are indicated by black arrows. Water flows are indicated by white arrows

The Therapeutic Effect of UT Inhibitors on Hyponatremia in Animal Models

In a rat model of acute hyponatremia, during the 24 h of water loading the rats were treated with the UT inhibitor DMTU intraperitoneally at 500 mg/kg initially and 125 mg/kg ten hours later [39]. Compared with the vehicle group, rats treated with DMTU maintained normonatremia and did not retain water, and their urine osmolality was lower than before the water load. This study suggests that DMTU, as a UT inhibitor, has a relieving effect on hyponatremia, but the cumbersome administration method and too large dosage limit further development of DMTU.

Ying et al. determined the therapeutic effect of the UT inhibitor 25a on ascites in a dimethylnitrosamine (DMN)-induced cirrhotic rat model (Fig. 8.7a) [52]. A dosage of 100 mg/kg of 25a significantly increased daily urine output and reduced the abdominal circumference in cirrhotic rats under water intake restrictions (Fig. 8.7b, c). Serum osmolality, as well as sodium and potassium concentrations, were markedly reduced in cirrhotic rats compared to control rats, with the administration of compound 25a effectively reversing these alterations (Fig. 8.7d). Histological analysis and biochemical examinations indicated that 25a did not alter the degree of cirrhosis and liver function in cirrhotic rats. This study suggests that 25a significantly reduces ascites through diuresis without causing electrolyte imbalances in cirrhotic rats.

Li et al. constructed models of inappropriate secretion of antidiuretic hormone (SIADH) in rats and mice to confirm whether the UT inhibitor 25a can treat hyponatremia (Fig. 8.8a, b) [53]. As shown in Fig. 8.8, 100 mg/kg 25a significantly increased serum osmolality (from 249.83 ± 5.95 to 294.33 ± 3.90 mOsm/kg) and serum sodium (from 114 ± 2.07 to 136.67 ± 3.82 mM), respectively, in hyponatremic rats by diuresis (Fig. 8.8c, d). In the SIADH mouse model, serum osmolality
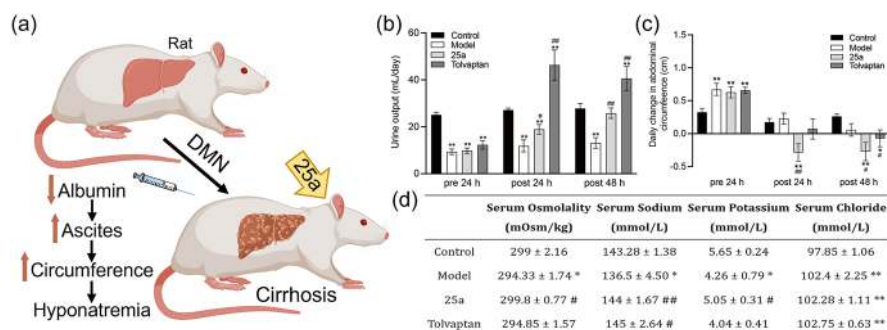
Fig. 8.7 25a reduces ascites in a DMN-induced cirrhotic rat model depending on its diuretic effect. (**a**) Diagram of pharmacological effect of 25a on DMN induced cirrhotic rat model. (**b**) Daily urine output after 25a administration. (**c**) Daily change in abdominal circumference. (**d**) Serum osmolality and electrolyte concentrations in rats
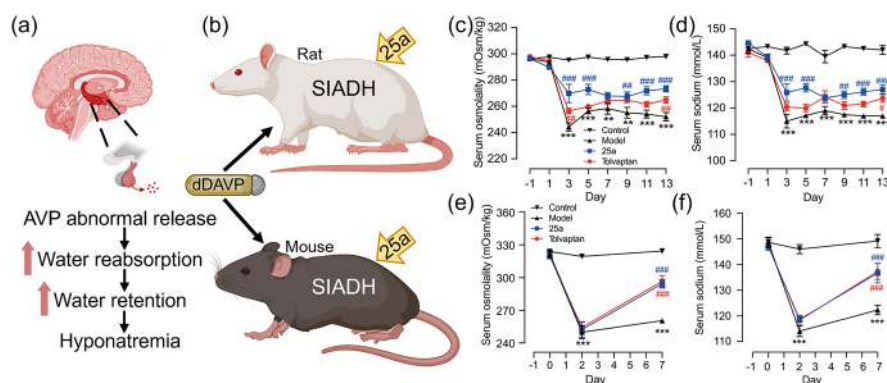
Fig. 8.8 25a improves hyponatremia in Syndrome of inappropriate antidiuretic hormone secretion (SIADH) models. (**a**) Diagram of hyponatremia development in SIADH. (**b**) Diagram of SIADH rat and mouse models. (**c**) Serum osmolality in rats. (**d**) Serum sodium concentration in rats. (**e**) Serum osmolality in mice. (**f**) Serum sodium concentration in mice

and sodium were also significantly increased by 25a (Fig. 8.8e, f). These data suggest 25a has a therapeutic effect on hyponatremia.

These studies provide proof of concept that UT-A1 is a diuretic target for hyponatremia and that UT-A1 inhibitors might be good diuretics to treat hyponatremia.

Summary and Future Directions

Currently, commonly used diuretics in clinical practice often lead to adverse reactions like electrolyte imbalance [54–56]. In response, researchers are exploring development of new diuretics targeting UT-A1. However, there are currently no

approved UT-A1 inhibitors for clinical use. Several challenges exist in the research and development of UT inhibitors. The structural similarity between UT-B and UT-A1 poses difficulties in finding highly selective UT-A1 inhibitors. Additionally, the lack of a resolved crystal structure for UT-A1 hampers the development of structure-based UT-A1 inhibitors. The search for orally active UT inhibitors with high bioavailability presents a bottleneck in new diuretic development. In the future, with advancements in the structural analysis of UT-A1, structure-based drug screening, and compound optimization techniques, along with progress in pharmacology, medicinal chemistry, pharmacokinetics, and pharmaceutics, the successful development of a new class of diuretics targeting UT-A1 is imminent. Novel UT-A1 inhibitors as diuretics hold promise for treating hyponatremic edema-related conditions such as congestive heart failure, cirrhosis, ascites, and nephrotic syndrome.

Conflicts of Interest   The authors have no conflicts of interest.

References

1. A.S. Verkman et al., Small-molecule inhibitors of urea transporters. Subcell. Biochem. **73**, 165–177 (2014)
2. J.M. Sands, Renal urea transporters. Curr. Opin. Nephrol. Hypertens. **13**(5), 525–532 (2004)
3. X. Li, G. Chen, B. Yang, Urea transporter physiology studied in knockout mice. Front. Physiol. **3**, 217 (2012)
4. R.A. Fenton, B. Yang, Urea transporter knockout mice and their renal phenotypes. Subcell. Biochem. **73**, 137–152 (2014)
5. T. Lei et al., Role of thin descending limb urea transport in renal urea handling and the urine concentrating mechanism. Am. J. Physiol. Renal Physiol. **301**(6), F1251–F1259 (2011)
6. C. Shayakul, B. Clemencon, M.A. Hediger, The urea transporter family (SLC14): Physiological, pathological and structural aspects. Mol. Asp. Med. **34**(2–3), 313–322 (2013)
7. C.P. Smith, Mammalian urea transporters. Exp. Physiol. **94**(2), 180–185 (2009)
8. R.A. Fenton et al., Structure and characterization of the mouse UT-A gene (Slc14a2). Am. J. Physiol. Renal Physiol. **282**(4), F630–F638 (2002)
9. B. Yang et al., Urea-selective concentrating defect in transgenic mice lacking urea transporter UT-B. J. Biol. Chem. **277**(12), 10633–10637 (2002)
10. M. Li, S. Zhang, B. Yang, Urea transporters identified as novel diuretic drug targets. Curr. Drug Targets **21**(3), 279–287 (2020)
11. X. Geng et al., The urea transporter UT-A1 plays a predominant role in a urea-dependent urine-concentrating mechanism. J. Biol. Chem. **295**(29), 9893–9900 (2020)
12. T. Jiang et al., Generation and phenotypic analysis of mice lacking all urea transporters. Kidney Int. **91**(2), 338–351 (2017)
13. S. Uchida et al., Impaired urea accumulation in the inner medulla of mice lacking the urea transporter UT-A2. Mol. Cell. Biol. **25**(16), 7357–7363 (2005)
14. R.A. Fenton et al., Renal phenotype of UT-A urea transporter knockout mice. J. Am. Soc. Nephrol. **16**(6), 1583–1592 (2005)

15. R.A. Fenton et al., Urinary concentrating defect in mice with selective deletion of phloretin-sensitive urea transporters in the renal collecting duct. Proc. Natl. Acad. Sci. USA **101**(19), 7469–7474 (2004)
16. R.A. Fenton, Urea transporters and renal function: Lessons from knockout mice. Curr. Opin. Nephrol. Hypertens. **17**(5), 513–518 (2008)
17. J.M. Sands, Critical role of urea in the urine-concentrating mechanism. J. Am. Soc. Nephrol. **18**(3), 670–671 (2007)
18. R.A. Fenton, Essential role of vasopressin-regulated urea transport processes in the mammalian kidney. Pflugers Arch. **458**(1), 169–177 (2009)
19. B. Yang, A.S. Verkman, Urea transporter UT3 functions as an efficient water channel. Direct evidence for a common water/urea pathway. J. Biol. Chem. **273**(16), 9369–9372 (1998)
20. J.D. Klein, J.M. Sands, Urea transport and clinical potential of urearetics. Curr. Opin. Nephrol. Hypertens. **25**(5), 444–451 (2016)
21. M. Li et al., Developing hypothetical inhibition mechanism of novel urea transporter B inhibitor. Sci. Rep. **4**, 5775 (2014)
22. C. Esteva-Font, M.O. Anderson, A.S. Verkman, Urea transporter proteins as targets for small-molecule diuretics. Nat. Rev. Nephrol. **11**(2), 113–123 (2015)
23. B. Yang, L. Bankir, Urea and urine concentrating ability: New insights from studies in mice. Am. J. Physiol. Renal Physiol. **288**(5), F881–F896 (2005)
24. T. Titko et al., Modern trends in diuretics development. Eur. J. Med. Chem. **208**, 112855 (2020)
25. N.A. Saffioti et al., Interactive dynamics of cell volume and cell death in human erythrocytes exposed to alpha-hemolysin from Escherichia coli. Int. J. Mol. Sci. **23**(2) (2022)
26. M.S. Kuo et al., Different involvement of band 3 in red cell deformability and osmotic fragility-a comparative GP.Mur erythrocyte study. Cells **10**(12) (2021)
27. M.H. Levin, R. de la Fuente, A.S. Verkman, Urearetics: A small molecule screen yields nanomolar potency inhibitors of urea transporter UT-B. FASEB J. **21**(2), 551–563 (2007)
28. D. Zhao et al., Comparative transport efficiencies of urea analogues through urea transporter UT-B. Biochim. Biophys. Acta **1768**(7), 1815–1821 (2007)
29. S. Zhang et al., Discovery of novel diarylamides as orally active diuretics targeting urea transporters. Acta Pharm. Sin. B **11**(1), 181–202 (2021)
30. X. Li et al., Activation of protein kinase C-alpha and Src kinase increases urea transporter A1 alpha-2, 6 sialylation. J. Am. Soc. Nephrol. **26**(4), 926–934 (2015)
31. O. Frohlich et al., Urea transport in MDCK cells that are stably transfected with UT-A1. Am. J. Physiol. Cell Physiol. **286**(6), C1264–C1270 (2004)
32. C. Esteva-Font et al., A small molecule screen identifies selective inhibitors of urea transporter UT-A. Chem. Biol. **20**(10), 1235–1244 (2013)
33. O. Frohlich et al., Regulation of UT-A1-mediated transepithelial urea flux in MDCK cells. Am. J. Physiol. Cell Physiol. **291**(4), C600–C606 (2006)
34. R.I. Macey, R.E. Farmer, Inhibition of water and solute permeability in human red cells. Biochim. Biophys. Acta **211**(1), 104–106 (1970)
35. C.L. Chou, M.A. Knepper, Inhibition of urea transport in inner medullary collecting duct by phloretin and urea analogues. Am. J. Phys. **257**(3 Pt 2), F359–F365 (1989)
36. C. Yao et al., Triazolothienopyrimidine inhibitors of urea transporter UT-B reduce urine concentration. J. Am. Soc. Nephrol. **23**(7), 1210–1220 (2012)
37. M.O. Anderson et al., Nanomolar potency and metabolically stable inhibitors of kidney urea transporter UT-B. J. Med. Chem. **55**(12), 5942–5950 (2012)
38. O. Cil, M. Ertunc, R. Onur, The diuretic effect of urea analog dimethylthiourea in female Wistar rats. Hum. Exp. Toxicol. **31**(10), 1050–1055 (2012)
39. O. Cil et al., Salt-sparing diuretic action of a water-soluble urea analog inhibitor of urea transporters UT-A and UT-B in rats. Kidney Int. **88**(2), 311–320 (2015)
40. F. Li et al., A novel small-molecule thienoquinolin urea transporter inhibitor acts as a potential diuretic. Kidney Int. **83**(6), 1076–1086 (2013)

41. H. Ren et al., Thienoquinolins exert diuresis by strongly inhibiting UT-A urea transporters. Am. J. Physiol. Renal Physiol. **307**(12), F1363–F1372 (2014)
42. Z.Y. Zhang et al., Pharmacokinetics, tissue distribution and excretion of a novel diuretic (PU-48) in rats. Pharmaceutics **10**(3) (2018)
43. C. Esteva-Font et al., Diuresis and reduced urinary osmolality in rats produced by small-molecule UT-A-selective urea transport inhibitors. FASEB J. **28**(9), 3878–3890 (2014)
44. C. Esteva-Font et al., Structure-activity analysis of thiourea analogs as inhibitors of UT-A and UT-B urea transporters. Biochim. Biophys. Acta **1848**(5), 1075–1080 (2015)
45. S. Lee et al., Discovery, synthesis and structure-activity analysis of symmetrical 2,7-disubstituted fluorenones as urea transporter inhibitors. Medchemcomm **6**, 1278–1284 (2015)
46. J.H. Ran et al., Phenylphthalazines as small-molecule inhibitors of urea transporter UT-B and their binding model. Acta Pharmacol. Sin. **37**(7), 973–983 (2016)
47. S. Lee et al., Nanomolar-potency 1,2,4-triazoloquinoxaline inhibitors of the kidney urea transporter UT-A1. J. Med. Chem. **61**(7), 3209–3217 (2018)
48. Y. Zhao et al., Discovery and optimization of thienopyridine derivatives as novel urea transporter inhibitors. Eur. J. Med. Chem. **172**, 131–142 (2019)
49. M. Li et al., A thienopyridine, CB-20, exerts diuretic activity by inhibiting urea transporters. Acta Pharmacol. Sin. **41**(1), 65–72 (2020)
50. S. Wang et al., N-(4-acetamidophenyl)-5-acetylfuran-2-carboxamide as a novel orally available diuretic that targets urea transporters with improved PD and PK properties. Eur. J. Med. Chem. **226**, 113859 (2021)
51. Y. Xu et al., Preclinical pharmacokinetic studies of a novel diuretic inhibiting urea transporters. Molecules **27**(8) (2022)
52. Y. Ying et al., Urea transporter inhibitor 25a reduces ascites in cirrhotic rats. Biomedicines **11**(2) (2023)
53. N. Li et al., Urea transporter UT-A1 as a novel drug target for hyponatremia. FASEB J. **38**(13), e23760 (2024)
54. S.W. Oh, S.Y. Han, Loop diuretics in clinical practice. Electrolyte Blood Press **13**(1), 17–21 (2015)
55. O.M. Jolobe, Diuretic-induced hyponatraemia in elderly hypertensive women. J. Hum. Hypertens. **17**(2), 151 (2003)
56. C. Campo et al., Hyperuricemia, low urine urate excretion and target organ damage in arterial hypertension. Blood Press. **12**(5–6), 277–283 (2003)

Chapter 9
Urea Transport Mediated by Membrane Proteins of Non-urea-Transporters

Minghui Wang, Weidong Wang, and Chunling Li

Abstract Urea is generated by the urea cycle enzymes, which are mainly in the liver but are also ubiquitously expressed at low levels in other tissues of mammals. Urea is then eliminated through fluids, especially urine. Urea also serves as a readily available nitrogen source for the growth of many organisms, including plants and bacteria. Urea transporters are recognized as the primary membrane proteins responsible for urea transport in organisms. However, an increasing body of studies has identified additional membrane proteins in animals, plants, and microbes that exhibit urea transport capabilities or potential. The contribution of these membrane proteins to the maintenance of physiological homeostasis and their interactions with urea transporters remains to be fully elucidated. In this chapter, transport, characteristics, regulation, as well as cellular localization of non-urea-transporter membrane proteins facilitating urea transport, are reviewed to highlight their roles in physiology and pathophysiology. Specifically, the mammalian aquaporins AQP3, AQP6, AQP7, AQP8, AQP9, AQP10, and a sodium-glucose transporter (SGLT1) in the kidney are permeable to urea. In plants, tonoplast intrinsic proteins (TIPs), a member of aquaporin family, and the DUR3 orthologue, potentially play roles in low- and high-affinity urea transport, respectively. Two urea transporters pH-independent (Yut) and pH-dependent transporters (ureI) in bacteria are known to play roles in disease conditions.

Keywords Aquaporin · Urea transporter · DUR3 · UreI

M. Wang · C. Li (✉)
Department of Physiology, Zhongshan School of Medicine, Sun Yat-sen University, Guangzhou, China
e-mail: lichl3@mail.sysu.edu.cn

W. Wang
Department of Pathophysiology, Zhongshan School of Medicine, Sun Yat-sen University, Guangzhou, China

Urea, the end product of protein metabolism, is synthesized in the liver from ammonia and excreted by the kidney, serving as a non-toxic carrier of waste nitrogen. Ammonia accumulation leads to mitochondrial permeability transition and ultimately cell death [1]. When healthy individuals consume 0.33 g of protein nitrogen per kilogram of body weight ($BW^{3/4}$) daily, they excrete urea nitrogen at a rate of 10 ~ 15 mg per hour per kilogram of $BW^{3/4}$ [2].

In addition to being removed as metabolic waste, passive transport of urea through urea transporters contributes significantly to the osmotic pressure gradient from the renal cortex to the medulla, in conjunction with NaCl [3–5]. The distribution of urea in renal medullary tissue can reach up to 600 mOsm/kg through countercurrent exchange mechanism [3–5]. In the inner medullary collecting ducts, urea transporters facilitate the swift equilibration of urea between the luminal space and the interstitium [6]. Regarding the accumulation of urea in the medullary interstitium, the concentration of urea is influenced by a recycling process. During this process, urea is initially freely filtered by the glomerulus, then reabsorbed in the proximal tubule, followed by secretion into the thin descending limb of the Loop of Henle, and finally reabsorbed in the inner medullary collecting duct [7, 8].This mechanism plays a crucial role in avoiding water loss driven by the elevated urea concentrations within the urine [9].

Urea transporters (UTs) are recognized as the primary membrane proteins responsible for urea transport in organisms. However, an increasing body of studies has identified additional membrane proteins in animals, plants, and microbes that exhibit urea transport capabilities or potential. The contribution of these membrane proteins to the maintenance of physiological homeostasis and their interactions with UTs remain to be fully elucidated.

This chapter aims to provide a comprehensive overview of urea-permeable membrane channels other than the UT family. The discussion will focus on the discovery, distribution, functional roles, and transport mechanisms of these transporters. The unique characteristics and contributions of these channels to urea transport across cellular membranes will also be reviewed.

Urea Transport Mediated by Aquaporins in Mammals

Water permeation across cellular membranes is undeniably the primary function of aquaporins (AQPs), but some of these proteins also play a role in facilitating the transport of other solutes and gases. Certain AQPs demonstrate significant versatility by enabling the movement of various small non-water molecules, such as glycerol, hydrogen peroxide (H_2O_2) [10], urea [11], nitric oxide (NO) [12], ammonia (NH_3) [13], nitrate (NO_3^-) [14], or carbon dioxide (CO_2) [13]. Notably, while in vitro studies and molecular dynamics simulations have confirmed AQP-mediated transport of urea, NH_3, NO_3^-, and NO, the physiological significance of this transport is still largely unknown. In contrast, the transport of other solutes by AQPs has been shown to contribute, at least in part, to metabolic and regulatory processes [15].

General Features of Aquaporins

The existence of water channel proteins was predicted in the 1950s, but their molecular identity remained unknown until Peter Agre and his colleagues discovered a water channel protein in 1988 [16–18]. They purified this protein from the red blood cell membrane [19], with a non-glycosylated component of 28 kDa and a glycosylated component of 35 ~ 60 kDa. This protein was initially called "CHIP28" (channel-like integral protein of 28 kDa), later renamed aquaporin-1 (AQP1) [20, 21]. AQPs are found in membranes requiring rapid or regulated water passage, essential for cell and membrane functions. They alleviate osmotic stress from ion movement in signal transduction, energy production, and other cell activities [21].

To date, 13 water channels, AQP0 through AQP12, have been identified, which distribute extensively in human tissues (Table 9.1), implicating important physiological significance in humans. Based on the primary sequences, AQPs are subdivided into three subfamilies: aquaporins; aquaglyceroporins; and superaquaporins (Table 9.1). The first subfamily are the aquaporins, the water selective or specific water channels, also named "orthodox" or "classical" aquaporins, including AQP0, AQP1, AQP2, AQP4, AQP5, AQP6, and AQP8. The second subfamily is represented by aquaglyceroporins, including AQP3, AQP7, AQP9, and AQP10 [22]. They are permeable to water (to varying degrees), but also to other small uncharged molecules (ammonia, urea, and in particular, glycerol) [22]. They also facilitate the diffusion of charged and non-charged molecules of the metalloids, arsenic and antimony, and play a crucial role in metalloid homeostasis [23]. The third subfamily included AQP11 and AQP12 and is called "superaquaporins" [24]. Their NPA boxes, however, are quite different from those of previous AQPs (less than 20% homology at the amino acid level) [25].

All members of the AQP family are small, very hydrophobic, intrinsic membrane proteins. The amino acid sequences of human AQPs are approximately 30 ~ 50% identical. AQP family proteins have six membrane spanning helices connected by five loops and have intracellular N- and C-termini (Fig. 9.1a) [26–29]. Loops B and E feature short helical subunits that penetrate the plasma membrane, and interact with each other at highly conserved Asn-Pro-Ala (NPA) repeats, which are the signature sequences for AQPs (Fig. 9.1a). The six transmembrane domains, and B and E loop helices, form a compact channel, with the interacting NPA repeats marking its narrowest point (Fig. 9.1a). The AQPs also share another highly conserved sequence, the aromatic/arginine (ar/R) region, which exits at the extracellular side of the channel and constitutes the selectivity filter of the protein (Fig. 9.1b) [30].

In addition to their well-established function in water transport, aquaporins exhibit a remarkable versatility by facilitating the translocation of small, predominantly uncharged molecules such as glycerol, urea, ammonia, and even certain gases like carbon dioxide.

Table 9.1 Mammalian aquaporins

Organ expression		Chromosome	locus	Exon numbers	Transport		
Aquaporin							
Eye		12q13		4	Water		AQP0
Brain, eye, kidney, heart, lung, gastrointestinal tract, salivary	gland, liver, ovary, testis, muscle, erythrocyte, spleen	7p14		4	Water		AQP1
Kidney, ear, ductus deferens		12q13		4	Water		AQP2
Brain, kidney, salivary gland, heart, gastrointestinal tract,	muscle	18q22		4	Water		AQP4
Salivary gland, lung, gastrointestinal tract, ovary, eye, kidney		12q13		4	Water		AQP5
Brain, kidney		12q13		4	Water, urea (±),	anion	AQP6
Testis, liver, pancreas, ovary, lung, kidney		16q12		6	Water, urea (±),	ammonia	AQP8
Aquaglyceroporins							
Kidney, heart, ovary, eye, salivary gland, gastrointestinal tract,	respiratory tract, brain, erythrocyte, fat	9p13		6	Water, urea,	glycerol, ammonia	AQP3
Testis, heart, kidney, ovary, fat		9p13		6	Water, urea,	glycerol, ammonia	AQP7
Liver, spleen, testis, ovary, leukocyte		15q22		6	Water, urea,	glycerol	AQP9
Gastrointestinal tract		1q21		6	Water, urea,	glycerol	AQP10
Superaquaporins							
Testis, heart, kidney, ovary, muscle, gastrointesti nal tract,	leukocytes, liver, brain	11q13		3	Water?		AQP11
Pancreas		2q37		3	Unknown		AQP12

Ishibashi et al. Euro biophysic J, 2012; Litman et al. Handb Exp Pharmacol. 2009

Fig. 9.1 (continued) that resembles an "hourglass." (Reproduced from Ref. [31] with permission). (**b**) A cartoon representation of the consensus monomer of AQP7. Residues of the ar/R selective filter and NPA motifs are shown as sticks with corresponding cryo-EM density maps in gray. Transmembrane domains are represented by 1–6 while the two half helices by HX1 and HX2, and loops by A-E. (Image source: Huang et al. [30]. Shared under the CC BY 4.0 License. http://creativecommons.org/licenses/by/4.0/. No modifications were made)

Fig. 9.1 Secondary structure and topology of an aquaporin molecule. (**a**) AQPs have six membrane-spanning regions, both intracellular amino and carboxy termini, and internal tandem repeats. The tandem repeat structure with two NPA sequences form tight turn structures that interact in the membrane to form the pathway for translocation of water across the plasma membrane. Of the five loops in AQP1, the B and E loops dip into the lipid bilayer, and form "hemichannels" that connect between the leaflets to form a single aqueous pathway within a symmetric structure

Permeation of Urea by AQP3 and the Physiological Significance

In an early investigation, *Xenopus laevis* oocytes expressing human AQP3 were used as a positive control for urea and glycerol uptake, and human AQP1 was used for a negative control. After 10 min of incubation with 1 mM [^{14}C] urea, about 70 pmol of urea per oocyte was found in the AQP3 group on average, almost seven fold higher than that in the AQP1 group [32]. Urea uptake in *Xenopus* oocytes expressing rat AQP3 increased two fold after 30 min of treatment with [^{14}C] urea [24], and the degree of swelling tripled [33]. These studies indicate a potential role of AQP3 in urea transport.

Subsequent research revealed divergent findings on the potential of AQP3 to function as a urea channel [34, 35]. Although structural predictions and experimental validations indicate that AQP3 can transport urea, some studies suggest that AQP3 exhibits low efficiency in transporting urea. The addition of urea (1 mM) to AQP3-expressing oocytes caused an intracellular urea concentration of ~75 μM after a 10 min incubation. The oocytes remained significantly far from equilibrium (~10% of the expected equilibrium value), indicating that urea transport through AQP3, although present, was markedly slow [32, 36]. The concentration of urea is also a potential influencing factor for AQP3-expressing oocyte swelling and solute equilibrium. In conditions with a low urea concentration (20 mM) [34, 35], urea transport by AQP3 can hardly be detected [36], while when urea was 165 mM [24, 33], AQP3 in *Xenopus* oocytes increased urea uptake two-fold after 30 minutes [24], or threefold in oocyte swelling assays [33].

AQP3 appears to play a role in urea transport in the skin. AQP3 contributes to the net uptake of urea by keratinocytes. Some research suggests that uptake of urea through UTs and AQP3 improves epidermal barrier function and plays an important role in keratinocyte differentiation, lipid synthesis, and maintenance of epidermal homeostasis (Fig. 9.2) [37–39].

Permeation of Urea by AQP7 and the Physiological Significance

AQP7 and AQP9 were reported to transport urea (Table 9.1). In pancreas, urea (or glycerol) can activate beta cells via rapid uptake across the beta-cell plasma membrane, probably via AQP7, resulting in cell swelling, volume-regulated anion channel activation, electrical activity, and insulin release [40].

In the kidney, it has been proposed that the urea that is reabsorbed from thick ascending limbs enters the neighboring proximal straight tubules [41]; thus, complete urea recycling occurs between the descending limbs and ascending limbs of the loop of Henle, with AQP7 acting as a component of the pathway for urea in proximal straight tubules [42]. However, plasma and urine urea levels in AQP7 knockout mice do not differ from those in wildtype mice [43, 44], and there was also no difference between AQP7 knockout and wildtype mice in the urea content
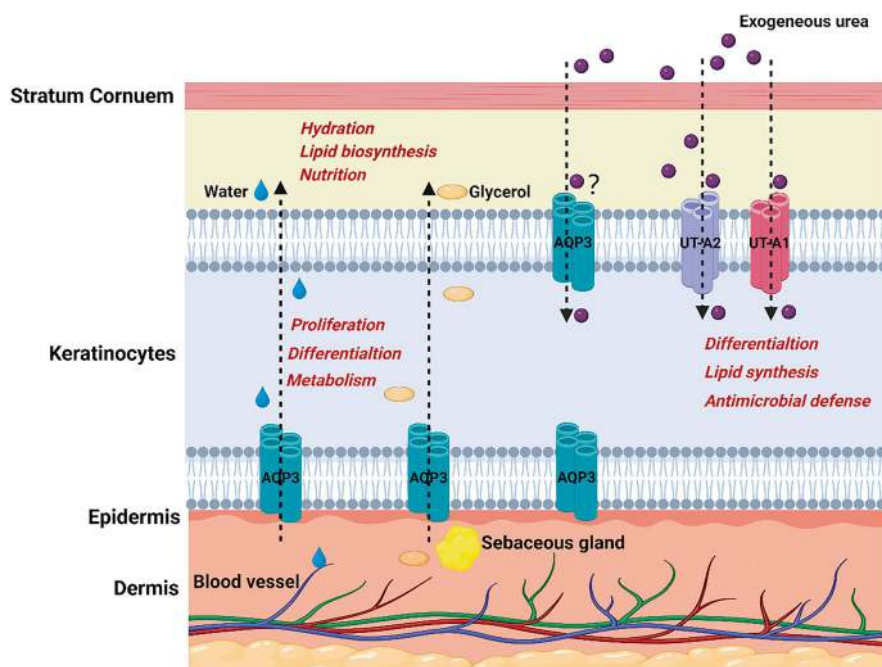
Fig. 9.2 Proposed mechanism of AQP3 function in epidermis. AQP3 facilitates water and glycerol transport from blood and sebaceous glands to keratinocytes. Steady-state glycerol content in epidermis and stratum corneum maintains skin hydration, lipid metabolism, and biosynthesis. AQP3-mediated transport of water and glycerol is also involved in proliferation and differentiation of keratinocytes. UT-A1, UT-A2, and AQP3 facilitate urea uptake in skin, which may induce keratinocyte differentiation and improve barrier and antimicrobial defense function of skin. Urea transporter (UT)

of the papilla. To detect small differences in urea levels, a low-protein diet, which limits the urea supply to the kidney, was provided. AQP7 knockout mice did not show impairment in urea accumulation in the papilla even with dehydration when compared with wildtype mice. They also did not show a urine concentrating defect with a low-protein diet and dehydration. Therefore, so far, there is no evidence that AQP7 plays a role in urea recycling in the kidney in vivo.

Permeation of Urea by AQP9 and the Physiological Significance

The erythrocyte expresses the urea transporter UT-B [45] and the urea-permeable AQP9 [46]. The ability to transport urea would mitigate osmotic shrinkage of erythrocytes while passing through the kidney, although AQP9 in erythrocytes may function more for the passage of glycerol.

AQP9 is a urea-permeable protein that is localized at the basolateral membrane of hepatocytes [47]. Ketogenic and high-protein diets, which are associated with increases in plasma β-hydroxybutyrate and urea levels, respectively, do not alter AQP9 levels in rat liver [48], indicating that urea transport is not the primary function of AQP9 in the liver. Consistently, AQP9 null mice do not show any difference in plasma or tissue urea levels [49]. A previous study on respective AQP9 knockout and UT-A1/3 knockout, as well as AQP9/UT-A1/3 double knockout mice, showed that an unidentified UT-A urea channel constitutes a primary but redundant urea facilitated transporter in murine hepatocytes, in addition to AQP9, for the export of urea to the blood [50]. This suggests that a primary function of AQP9 may be to make glycerol available for gluconeogenesis in hepatocytes, but not to contribute to the removal of urea from the liver.

The ability of AQP9 to transport urea in skin has been reported [51]. AQP9 transports water, glycerol, and urea, but also is permeable to a wide range of other solutes in oocytes [52].

Permeation of Urea by AQP10

AQP10 is only found in the small intestine. Initial studies in *Xenopus* oocytes determined that the shorter form of AQP10 has a low water permeability and no permeability to urea or glycerol [53], while the longer form transports water, urea, and glycerol [54]. The function and regulation of AQP10 in urea transport is less extensively studied.

Permeation of Urea by AQP8 and the Physiological Significance

AQP8's expression is markedly robust in the gastrointestinal organs, placenta, and heart, highlighting its physiological significance in these tissues [55, 56]. At the subcellular level, AQP8 is localized on the cell membrane and mitochondria [57]. It is still controversial regarding whether AQP8 functions as an urea channel. Early findings showed that AQP8 from mouse is the first aquaporin that is permeable to urea but not to glycerol [55]. In this work, mouse AQP8 holds a distinctive position among water channels due to its unique permeability characteristics and expression profile. Ten minutes uptake rate of urea in *Xenopus* oocytes expressing AQP8 reached around 25%, much higher than a negative control (AQP1) but less than a positive control (AQP3). This channel's selective permeability underscores its potential role in hepatocyte urea excretion. However, other investigations found that neither rat AQP8 nor human AQP8 could transport urea [58]. Researchers suggest that the species-specific differences in the permeability of AQP8 to urea may be attributed to variations in the amino acid residues at the ar/R filter (G207 in humans; A205 in mice) [36, 58].

Permeation of Urea by AQP6

Although AQP6 has been classified an orthodox aquaporin, an early study found out that AQP6 could be functionally characterized as an aquaglyceroporin [59]. AQP6 expressed in *Xenopus laevis* was permeable to neutral hydrophilic molecules such as glycerol and water [59].

Mercurials are known to inhibit the osmotic water permeability of most aquaporins, including AQP1, likely through binding to the residue Cys-189 of AQP1 [60] and occluding the pore [61–63]. Interestingly, AQP6 has a cysteine residue (Cys-190) [64] at the corresponding position to the Cys-189 in AQP1, and unlike other aquaporins, Hg^{2+} does not inhibit AQP6 but activates it instead [59, 65, 66]. A recent study using molecular dynamics (MD) simulations revealed that mercury ions activated AQP6 by binding to a pore-external cysteine residue, Cys-155 [67]. The pore opening of AQP6 was caused by mercury-induced conformational changes of residues His-181 and Arg-196 in the selectivity filter region in AQP6 [68].

Permeability to glycerol and urea is relevant to water transport by AQP6. Hg^{2+} opened a pathway in AQP6 to allow glycerol and urea to pass through. However, the activation effect of Hg^{2+}-induced uptake rate of glycerol and urea in native or AQP1-expressing oocytes was much lower than that of oocytes expressing AQP6 [59]. This study implied that water, glycerol and urea shared the same pathway in AQP6, since their reflection coefficients were far less than 1 [59]. This early study indicated a selectivity of AQP6 to urea, however, it needs to be independently replicated and the physiological significance of urea permeability of AQP6 remains to be determined.

Although there is no evidence showing that aquaporins play dominant roles in urea transport in normal conditions so far, it is still unknown whether aquaporins coordinate with UTs in transporting urea in pathophysiological conditions.

The Structural Basis for Urea Selectivity by AQPs

Using real-time molecular dynamic simulations of water movement through human AQP1, a two-stage filter model was proposed, in which the NPA motif forms a selectivity-determining region, and the aromatic/arginine (ar/R) region functions as a proton filter [61]. The ar/R region in AQP is the selectivity filter for uncharged solutes. Small solutes are filtered through a hydrophobic effect. For larger solutes such as glycerol, steric restraints combined with the arrangement of hydrogen bond donors and acceptors determine channel selectivity. Conformational changes of AQP structure may permit other molecules to pass through the plasma membrane, such as urea, glycerol, H_2O_2, and CO_2.

Two structurally conserved features within the channel have been identified as critical filters that prevent the transport of solutes larger than water, as well as protons. The first feature, a central constriction, is defined by the presence of the Asn-Pro-Ala motif (NPA constriction). Molecular dynamics and quantum mechanical

simulations have extensively demonstrated that the free energy barrier at the NPA constriction plays a vital role in proton exclusion [69].

Another predominant part of the channel constriction, referred to as the aromatic/arginine (ar/R) selectivity filter, contains a conserved arginine residue (in the second helical loop directly after the NPA motif). This constriction, close to the extracellular entrance of the pore, is the narrowest region in the AQP1 pore. The ar/R constriction is characterized by a highly conserved triad of residues: phenylalanine, histidine, and arginine, which is a hallmark of orthodox aquaporins [61, 69]. The ar/R region in AQP is the selectivity filter for uncharged solutes. Small solutes are filtered through a hydrophobic effect [70].

In orthodox aquaporins, additional elements of the filter include a phenylalanine residue situated on the upper portion of the pore-facing side of the second α-helix and a histidine located in a comparable site within the fifth transmembrane helix. In contrast, for AQPs that allow glycerol and urea to pass, the histidine residue is substituted by a smaller amino acid residue, such as glycine (as seen in AQP3, AQP7, AQP10) or alanine (as in AQP9) [36].

The negatively charged residues of arginine repel positively charged ions, contributing to the channel's selectivity for specific substances. Beyond this electrostatic exclusion, pore selectivity appears to be primarily based on the size exclusion of permeating entities. The ar/R constriction in conventional AQPs has a diameter that matches the size of a water molecule [62]. However, in solute channels like aquaglyceroporins, this constriction is broader and exhibits reduced polarity [71, 72]. This difference arises from the substitution of histidine with glycine, which allows space for an aromatic side chain from an adjacent tyrosine or phenylalanine residue [72]. Targeted site-directed mutagenesis of the ar/R region in AQPs can be instrumental in elucidating the role of the ar/R constriction in determining solute selectivity within AQPs [73]. Researchers investigated the functional roles of three key residues—Phe-56, His-180, and Arg-195—within the ar/R constriction of rat AQP1. Through site-directed mutagenesis, His-180 was substituted with alanine (AQP1-H180A) and Arg-195 with valine (AQP1-R195V), either individually or in combination (AQP1-H180A/R195V). These mutations did not alter the channel's water permeability. Notably, the AQP1-H180A/R195V double mutant exhibited urea permeability. Simultaneous substitution of Phe-56 and His-180 with alanine (AQP1-F56A/H180A) increased the maximum diameter of the ar/R constriction approximately threefold, thereby permitting the passage of both glycerol and urea. Furthermore, all four AQP1 mutants tested facilitated ammonia permeation. Contrary to expectations, the removal of the positive charge at Arg-195 in the AQP1-R195V and AQP1-H180A/R195V mutants appeared to be proton permeable. Collectively, these findings underscore the critical role of the ar/R constriction as a selective barrier for solute permeability.

The SLC6A18 Transporter Is Probably a Sodium-Dependent Glycine/Urea Antiporter

SLC6A18 has been identified as an apical sodium-dependent transporter for glycine [74]. The latest research further suggests that this transporter functions as a sodium-dependent antiporter, facilitating the exchange of urea and glycine [75]. The study identifies the SLC6A18 transporter as a potential Na-dependent glycine/urea antiporter located in the proximal straight tubule (PST) of the kidney, which is believed to be responsible for the active secretion of urea into the nephron. The study suggests that the energy-dependent transport of urea by SLC6A18 is essential for maintaining the high urea concentration gradient necessary for efficient urine concentration in mammals [75].

The proposed model for the SLC6A18 transporter describes a mechanism by which this protein facilitates the exchange of urea and glycine in the PST cells of the kidney. Glycine is initially absorbed from the blood into PST cells via the peritubular membrane, likely through the glycine transporter SLC6A9, which is critical for maintaining intracellular glycine levels and the subsequent exchange process. As an exchange, urea is secreted into the tubular lumen while glycine is reabsorbed into the cells, which is mediated by SLC6A18. Once glycine exits into the luminal membrane, it is suggested that it is rapidly reabsorbed back into the cell, although the mechanism is still under investigation. The permanent recycling of glycine is crucial for sustaining the transporter's function, ensuring a continuous supply of glycine for exchange with urea. Although not fully understood, it is probable that urea enters the PST cells from the basolateral side, potentially driven by the concentration gradient created by its continuous efflux on the luminal side via SLC6A18. Interestingly, the SLC6A18 transporter is also expressed in the thin descending limb of long-looped nephrons, indicating that this protein might contribute to urea handling in other parts of the kidney. This energy-dependent urea secretion mechanism plays a role in concentrating urine in some species adapted to arid environments.

The identification of SLC6A18 as a glycine/urea antiporter offers a new understanding of kidney function, particularly in the context of protein metabolism and its effects on kidney health. It also provides insights into how dietary protein intake can influence kidney function through its effects on urea handling, highlighting the importance of considering urea transport mechanisms in managing kidney health.

SGLT1 and NaGLT1

In the inner medulla (IM), several structures—including descending thin limbs (DTLs) and ascending thin limbs (ATLs) of Henle's loop, collecting ducts, and the vasa recta—collectively establish the osmotic gradient, with NaCl and urea serving as key osmolytes. Despite the well-established role of urea accumulation in the IM in promoting water conservation, the precise mechanisms by which these

components interact to regulate urine concentration remain inadequately understood [76, 77]. Notably, urea permeability is exceptionally high in ATLs and lower in DTLs within the IM in rat kidneys [78]. However, no specific urea transporter has been identified in these tubular segments.

Interestingly, an early study by Leung et al. proposed that rabbit Na+-glucose cotransporter (rbSGLT1), the rat Na+-iodide cotransporter, human Na-Cl-GABA transporter 1, and pig low-affinity SGLT3 are permeable to urea [79]. In oocytes expressing rbSGLT1, urea transport increased four-fold in the absence of sugar. This uptake was Na+-independent and exhibited a linear relationship with both incubation time and increasing urea concentrations. Urea uptake was inhibited by the rbSGLT1-specific inhibitor phlorizin in the presence of NaCl, while phloretin inhibited uptake regardless of Na+ presence. Interestingly, urea uptake was unaffected by urea analogues, but sugar addition enhanced urea transport, proportional to the Na+-glucose-H_2O cotransport rate. These findings indicated that in the absence of substrates, rbSGLT1 functioned as a urea channel, and under substrate-transporting conditions, it acts as a urea cotransporter.

Nawata et al. discovered some alternative channels permeable to urea within the rat inner medulla, which may play a contributory role in facilitating the high urea permeability of thin limb segments [80]. Rats that underwent water restriction for 72 h displayed increased mRNA levels of SGLT1a (a variant of SGLT1) in ATLs and elevated Na+-glucose transporter 1 (NaGLT1) mRNA expression in both ATLs and DTLs. Heterologous expression of these transporters in *Xenopus* oocytes facilitated the [^{14}C] urea uptake ratio. In Na+-free ND96 medium, NaGLT1 and SGLT1a increased [^{14}C] urea uptake into oocytes by twofold compared to water-injected controls, with similar results observed in Na-containing conditions. Phloretin or phloridzin significantly inhibited this urea transport, reducing it to levels comparable to those in control oocytes. However, unlike rabbit SGLT1 [79], the urea permeability of SGLT1a and NaGLT1 were Na independent and could be impaired by phloretin and/or phloridzin.

The physiological relevance of these multifunctional transporters remains unclear; however, it is conceivable that they may function as urea channels in cellular contexts where UTs are absent.

Urea Transport in Plants

Nitrogen is an important nutrient for higher plants and urea is a major nitrogen fertilizer, and it is also a naturally occurring and readily available nitrogen source in soil. Urea is also a plant metabolite derived either from root uptake or from catabolism of arginine by arginase. Various molecular players responsible for plant urea metabolism have been investigated including active and passive urea transporters, the urease catalyzing the hydrolysis of urea, and urease accessory proteins. This section of the chapter focuses on the transporters involved in plant urea transport.

Passive Transport of Urea in Plants

Aquaporin in Plants

Passive urea transport in plants, depending on the urea concentration gradient, is mediated by some subfamilies of the aquaporins. AQPs are critical for plants to maintain water homeostasis when facing abiotic and biotic stresses, such as cold, drought, salinity, nutritional imbalances, heavy metal and pathogen infections [81, 82]. Hundreds of AQPs have been discovered in plants [82], which have shown a large diversity in isoform, subcellular location and substrate. In plants, AQPs are in the plasma membrane and tonoplast, and play important roles in facilitating the transmembrane transport of water and regulating osmotic potential and hydraulic conductivity [81, 82]. In addition to facilitating water transport, these AQPs also facilitate transporting other small neutral molecules, such as urea, NH_3, CO_2, lactic acid, H_2O_2, and other molecules with physiological significance [81, 83].

These AQPs are sub-divided into several sub-families in which plasma membrane intrinsic proteins (PIPs) and tonoplast intrinsic proteins (TIPs) are the most abundant AQPs in the plasma membrane and tonoplast [81, 83]. Several other AQPs include the Nodulin26 (Nod26)-like intrinsic proteins (NIPs) [84], small basic intrinsic proteins (SIPs) [85] and uncategorized X intrinsic proteins (XIPs) [86], which are located in the plasma membrane or organelle membrane, respectively. PIPs are the major water transport channel and SIPs have a moderate activity to transport water. TIPs facilitate the transport of water and other small solutes in multifaceted vacuoles [87]. NIPs and XIPs are also involved in the transport of water and many other solutes [87]. The hybrid intrinsic proteins (HIPs) and the glycerol facilitator (GlpF)-like intrinsic proteins (GIPs) are present exclusively in moss [88–90]. HIPs and GIPs are absent in higher plants and are supposed to be lost during evolution [87].

Aquaporins Mediating Urea Transport in Plants

Studies on AQPs as urea transporters in plants are very extensive and have been reviewed comprehensively [87, 91–95]. Urea is a small uncharged solute that easily passes through the vacuolar membrane and endo-membrane via TIPs. TIPs likely function as urea transporters more than as water channels. This indicates that TIPs may affect urea levels by altering their uptake and translocation into vacuoles. The first identified urea-transporting TIP in plants is from the tonoplast of tobacco cells, named Nicotiana tabacum NtTIPa. When expressed in *Xenopus laevis* oocytes, NtTIPa show a high permeable to small non-electrolytes like glycerol and urea, in addition to water [96]. The urea permeability of plasma membranes is generally lower than that of the tonoplast, which correlates with the high urea transport rates in some TIPs compared to PIPs [96]. Later studies showed a plasma membrane PIP, NtAQP1 from tobacco, could transport urea, as could At-NIP6.1 [93, 97, 98].

During urea transport, an increasing pore diameter of AQP and specific residues are required for urea conduction [93, 98, 99].

Comprehensive studies subsequently revealed the role of AQPs in transporting urea. NtAQP1 ZmPIP1-5b that was isolated from maize hybrid F2F7 also exhibited urea transport activity in the *Xenopus* oocytes system [100]. Almost all of the subgroups of Arabidopsis TIPs were reported to facilitate urea transport, including AtTIP1;1, AtTIP1;2, AtTIP1;3, AtTIP2;1, AtTIP4;1, and AtTIP5;1 [101–103], indicating the role of TIPs in equilibrating urea concentrations between different cellular compartments [93]. Several members of PIPs and TIPs were determined to facilitate urea transport with a linear concentration dependency [96, 102]. Therefore, PlPs in plants may contribute to urea import with increasing concentrations of external urea, serving as a low-affinity uptake urea transporter, while TIPs would allow plant cells to load urea into the vacuole for transient storage of this nitrogen source [104]. Moreover, AtTIP1;3 and AtTIP5;1 were suggested as the water and urea channels in mature pollen and responsible for nitrogen remobilization in Arabidopsis [103, 105]. The AtTIP4;1 overexpression in Arabidopsis was reported to increase the urea uptake rate without causing detectable defects to plant growth and development [106]. NIPs showed urea permeability too. ZmNIP2;1, ZmNIP2;4, AtNIP5;1, AtNIP6;1, and CsNIP2;1 showed urea transport ability when expressed in *Xenopus* oocytes or yeast [98, 107, 108] and CsNIP2;1 from Cucumis sativus is shown to facilitates urea uptake when expressed in Arabidopsis thaliana [108].

High Affinity Active Transport of Urea in Plants

No sequence homologies of mammal UT-type and UreI (an integral membrane protein in *H. pylori* that mediates urea transport, see below) are found in any plant genome. However, plants possess a high affinity secondary active urea transporter that is responsible for taking up environmental urea and internal urea transport in addition to passive transport of urea. DUR3 (degradation of urea), a plasma membrane-localized transporter, was first characterized as a high affinity urea/H+ symporter for urea uptake [109, 110], which belongs to the sodium-solute symporter family. It was found by a genome-wide in silico search in which the Arabidopsis thaliana gene At5g45380 encodes an integral membrane protein consisting of 694 deduced amino acids [110]. AtDUR3 showed 41% sequence identity to the putative yeast urea transporter gene ScDUR3 [110]. Subsequent functional studies through yeast phenotype complementation and oocyte overexpression and kinetic analysis confirmed that atDUR3 was a proton symport-based urea transporter with high-affinity [109, 110].

DUR3 are present throughout the green lineage from algae [111] to higher plants, mostly encoded by single copy genes [112], such as rice and maize [113, 114]. In some algae and fungi DUR3 shows a higher number genes, which may enable them utilize urea in a more sophisticated nitrogen environment [115, 116]. All DUR3 proteins from fungi and plants share a relatively high sequence homology (with

38 ~ 95% sequence identity), but are clearly separated from mammalian and bacterial solute symporter family members [104, 112, 116]. AtDUR3 is predicted to contain 14 transmembrane domains with the N- and C- termini protruding into the outer side of the membrane [82]. In Arabidopsis roots, atDUR3 can sustain up to 90% of urea influx in the high-affinity range against a urea concentration gradient, while aquaporins mediate urea influx in the low-affinity range by diffusion [109, 110].

DUR3 may be differentially regulated by various stresses. The expression of the AtDUR3 gene is high during nitrogen starvation and can be repressed after resupply of NH_4^+ or NO_3^-; also it can be dramatically induced after resupply of urea [109]. Interestingly, different DUR3 transcript abundances in tomato showed a difference in nitrogen use efficiency [117]. A recent study demonstrated that besides urea acquisition and N-remobilization, CaDUR3 in coffee plants is differently regulated by water deficit, heat stress, salinity or infection [118]. In Arabidopsis atDUR3 is also regulated by the life phase and nutrient conditions, which is of significance in crop productivity [92, 119]. The latest evidence indicates that DUR3 is involved in nitrogen redistribution from leaves to panicles of rice during heading, and contributes to rice yield under nitrogen-deficient and field conditions [114].

Urea Transport in Bacteria

Urea is used by bacteria and fungi as a nitrogen source. Urea is hydrolyzed by the cytoplasmic ureases, producing bicarbonate and ammonia. Many prokaryotes synthesize energy-dependent transport systems for urea uptake, although urea is small and uncharged and easily passes the bacterial membrane. When present in high concentrations, sufficient urea crosses the cytoplasmic membrane by passive diffusion, while under conditions of nitrogen starvation an energy-dependent urea uptake system is synthesized in microorganisms.

In early 80's, the glycerol facilitator, GlpF, was found to allow the entry of polyols (glycerol and erythritol), urea, glycine into the *E. coli* under osmotic stimulation [120]. After that, more specialized transporters have been characterized including those active, energy-dependent uptake systems in *Methylophilus methylotrophus* [121], cyanobacteria [122] and *Corynebacterium glutamicum* [123, 124] and those facilitating urea diffusion in *Helicobacter pylori* (*H. pylori*) [125, 126], *Bacillus cereus* [127] and *Yersinia pseudotuberculosis* [125].

The first type is an ATP-activated urea transporter [128], which is an ABC (ATP-binding cassette) transporter that couples urea uptake directly to ATP hydrolysis [121–124]. These ABC-transporters consist of a urea binding protein delivering urea to the transporter, which is tied to the cytoplasmic membrane/transporter or located in the periplasm of bacteria [129, 130]. The other component of ABC transporters are transmembrane domains embedding in lipid bilayers to form translocation channels and nucleotide-binding domains for ATP hydrolysis [130, 131].

The second class of urea transporter in bacteria includes pH-independent and pH-dependent transporters. In *Y. pseudotuberculosis* Yut is a pH-independent

protein that is homologous to mammalian urea transporter, with a sequence identity to human UT-B [132]. The *yut* gene locates near the urease locus and encodes a putative membrane protein with weak homology to single-component eukaryotic urea transporters. Yut greatly increases urea permeability in the cell when expressed in *Xenopus* oocytes, while inactivation of Yut in *Y. pseudotuberculosis* results in reduced resistance to acidity in vitro when urea is present in the medium. Yut and the *H. pylori* UreI urea channel were shown to be functionally interchangeable in vitro and are sufficient to allow urea uptake in both bacteria [125].

The prototype for a pH-dependent urea transporter is the integral membrane protein UreI, in the human gastric pathogen *H. pylori*. It has a channel-like structure, which closes and opens at neutral and acidic pH (acid-gated), respectively [126, 133]. When the channel opens at an acidic pH, it allows rapid urea entry to access cytoplasmic ureases. *H. pylori* is restricted to the gastric mucosa of humans, which indicates that this bacterium must survive in the extremely acidic environment. Urease can hydrolyze the urea generating ammonia, which buffers the cytoplasm or periplasm to allow acid resistance, facilitating colonization and survival of *H. pylori* in the stomach [134, 135].

UreI encodes an integral cytoplasmic membrane protein with six transmembrane segments forming a urea-specific pore, which allows urea to reach the cytoplasmically-located urease enzyme [126, 133, 136]. Deletion of *ureI* prevents cytoplasmic urease activity and expression of UreI in *Xenopus* oocytes, resulting in acid-stimulated urea uptake, with a pH profile similar to activation of cytoplasmic urease. UreI-mediated transport is urea specific, passive, nonsaturable, nonelectrogenic, and temperature independent. Therefore, UreI functions as a H^+-gated urea channel regulating cytoplasmic urease that is essential for gastric survival and colonization [126].

The structure of UreI, and the mechanism of its transport and gating, has been extensively investigated [126, 133, 137–141]. Unlike bovine UT-B, which forms a trimer whose interface is formed by equivalent protein helices with a center [132], UreI contains oligomers of six channel protomers, arranged in a hexamer, with a lipid core at the center [136, 138, 141]. Six-fold symmetry extends the resolution of the closed and open channel. Each channel is roughly composed of three sections: a periplasmic domain and vestibule formed by N and C termini, a periplasmic loop 1 (PL1) and PL2, and transmembrane helices on the periplasmic side of the urea filter (Fig. 9.3). The urea filter near the center of the membrane is composed of a ring of side chains from several hydrophobic residues, and a cytoplasmic domain and vestibule (transmembrane helices and loops on the cytoplasmic side of the filter) [130, 138]. The conformational transitions of UreI exist in closely balanced equilibrium to shift both the shape and length of the channel in favor of urea passage at low pH [138]. The urea gating or filtration mechanism is accomplished by His131 on PL2, which triggers the sequential and cooperative movements of PL1, PL2, and the C terminus in the periplasmic domain, together with displacement of the transmembrane helices accompanied by reorientation of side chains lining the channel interior [138].
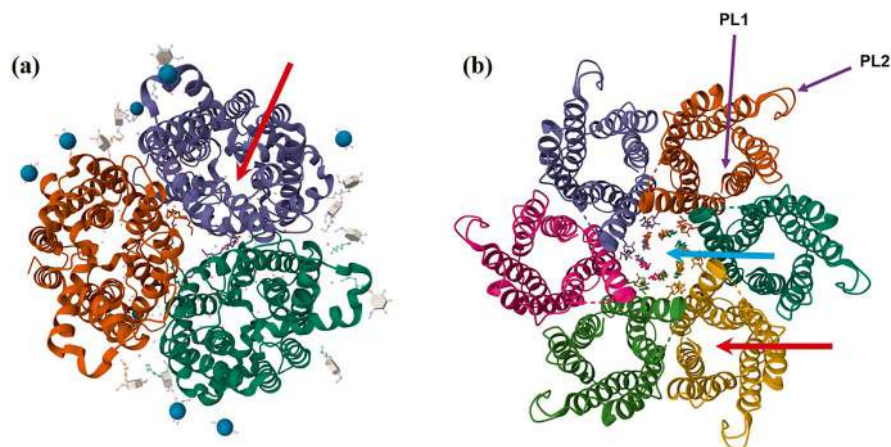
Fig. 9.3 Structure differences between mammalian UT and UreI in *H. pylori* [142]. (**a**) Ribbon diagram of trimer of bovine UT-B (PDB ID: 4EZC) obtained from RCSB PDB (https://doi.org/10.2210/pdb4ezc/pdb) [143] and the entrance to one of three urea channels (red arrow) [143]. (**b**) Ribbon diagram of hexamer of ureI (PDB ID: 6NSK) obtained from RCSB PDB (https://doi.org/10.2210/pdb6NSK/pdb), surrounding the lipids of the central bilayer (blue arrow) and the entrance to one of six urea channels (red arrow). Periplasmic loop 1 (PL1) and PL2 were indicated by purple arrow [138]

H. pylori infection is associated not only with peptic ulcer formation, but also with adenocarcinoma. UreI, as an essential virulence factor, potentially represents a new drug target that might be employed to help suppress or eradicate *H. pylori*. Indeed, aiming to target the *H. pylori* UreI channel and enable the delivery of antimicrobial compounds, urea-based nanosystems were developed [144, 145]. The strategies proved the efficacy of UreI channel-targeted drug delivery systems to improve antibiotic delivery inside *H. pylori*, although the effectiveness somehow is compromised due to the local environment of host gastric epithelium [146].

Structural Similarities and Differences of Urea Transporter Proteins in Mammals, Plants, and Microorganisms

Urea transporters in mammals, plants, and microorganisms share certain structural similarities, reflecting their roles in urea transport. UT, urea/amide   channel (UAC) and AQP channels exist as homologous multimers, where lipids are housed within the central cavity of the multimer, and urea is transported via the center of monomer [8, 22, 141]. The pores of these channels generally comprise three parts: the urea entrance, a selectivity filter formed by transmembrane α-helices, and the urea exit site. The amino acid residues that form the transport pore are highly conserved among subtypes within the same family. For example, the UT family displays the highly conserved LPXXTXPF motif [8], while HpUreI in *Helicobacter pylori*

conserves key residues in its third and fifth transmembrane helices [141], and the AQP family contains the NPA motif and the ar/R selectivity filter [147].

Although urea transporters across plants, bacteria, and mammals facilitate the movement of urea across biological membranes, their structural differences reflect adaptations to each organism's unique environment and physiological needs. DUR3 transporters typically have 14 or 15 transmembrane helices, with structural adaptations to facilitate active transport, moving urea against its concentration gradient with energy from proton co-transport [110, 113]. Bacterial UTs can have 6 or 7 transmembrane domains (Fig. 9.3b), depending on the species and the specific proteins [127, 138, 141]. Mammalian urea transporters are typically channel-like, with 10 transmembrane helices (Fig. 9.3a) [8, 143].

References

1. M.D. Norenberg, K.V. Rama Rao, A.R. Jayakumar, Ammonia neurotoxicity and the mitochondrial permeability transition. J. Bioenerg. Biomembr. **36**, 303–307 (2004). https://doi.org/10.1023/B:JOBB.0000041758.20071.19

2. D. Rudman et al., Maximal rates of excretion and synthesis of urea in normal and cirrhotic subjects. J. Clin. Invest. **52**, 2241–2249 (1973). https://doi.org/10.1172/JCI107410

3. J.M. Sands, Urea transporter inhibitors: En route to new diuretics. Chem. Biol. **20**, 1201–1202 (2013). https://doi.org/10.1016/j.chembiol.2013.10.003

4. M. Li, S. Zhang, B. Yang, Urea transporters identified as novel diuretic drug targets. Curr. Drug Targets **21**, 279–287 (2020). https://doi.org/10.2174/1389450120666191129101915

5. G. Stewart, The emerging physiological roles of the SLC14A family of urea transporters. Br. J. Pharmacol. **164**, 1780–1792 (2011). https://doi.org/10.1111/j.1476-5381.2011.01377.x

6. R.A. Fenton et al., Renal phenotype of UT-A urea transporter knockout mice. J. Am. Soc. Nephrol. **16**, 1583–1592 (2005). https://doi.org/10.1681/ASN.2005010031

7. S. Uchida et al., Impaired urea accumulation in the inner medulla of mice lacking the urea transporter UT-A2. Mol. Cell. Biol. **25**, 7357–7363 (2005). https://doi.org/10.1128/MCB.25.16.7357-7363.2005

8. C. Shayakul, B. Clemencon, M.A. Hediger, The urea transporter family (SLC14): Physiological, pathological and structural aspects. Mol. Asp. Med. **34**, 313–322 (2013). https://doi.org/10.1016/j.mam.2012.12.003

9. L. Bankir, B. Yang, New insights into urea and glucose handling by the kidney, and the urine concentrating mechanism. Kidney Int. **81**, 1179–1198 (2012). https://doi.org/10.1038/ki.2012.67

10. J.R. Thiagarajah, J. Chang, J.A. Goettel, A.S. Verkman, W.I. Lencer, Aquaporin-3 mediates hydrogen peroxide-dependent responses to environmental stress in colonic epithelia. Proc. Natl. Acad. Sci. USA **114**, 568–573 (2017). https://doi.org/10.1073/pnas.1612921114

11. C. Li, W. Wang, Urea transport mediated by aquaporin water channel proteins. Subcell. Biochem. **73**, 227–265 (2014). https://doi.org/10.1007/978-94-017-9343-8_14

12. Y. Wang, E. Tajkhorshid, Nitric oxide conduction by the brain aquaporin AQP4. Proteins **78**, 661–670 (2010). https://doi.org/10.1002/prot.22595

13. R.R. Geyer, R. Musa-Aziz, X. Qin, W.F. Boron, Relative CO(2)/NH(3) selectivities of mammalian aquaporins 0-9. Am. J. Physiol. Cell Physiol. **304**, C985–C994 (2013). https://doi.org/10.1152/ajpcell.00033.2013

14. M. Ikeda et al., Characterization of aquaporin-6 as a nitrate channel in mammalian cells. Requirement of pore-lining residue threonine 63. J. Biol. Chem. **277**, 39873–39879 (2002). https://doi.org/10.1074/jbc.M207008200

15. F.H. Login, L.N. Nejsum, Aquaporin water channels: Roles beyond renal water handling. Nat. Rev. Nephrol. **19**, 604–618 (2023). https://doi.org/10.1038/s41581-023-00734-9

16. G.M. Preston, P. Agre, Isolation of the cDNA for erythrocyte integral membrane protein of 28 kilodaltons: Member of an ancient channel family. Proc. Natl. Acad. Sci. USA **88**, 11110–11114 (1991). https://doi.org/10.1073/pnas.88.24.11110

17. G.M. Preston, T.P. Carroll, W.B. Guggino, P. Agre, Appearance of water channels in Xenopus oocytes expressing red cell CHIP28 protein. Science **256**, 385–387 (1992). https://doi.org/10.1126/science.256.5055.385

18. M.L. Zeidel, S.V. Ambudkar, B.L. Smith, P. Agre, Reconstitution of functional water channels in liposomes containing purified red cell CHIP28 protein. Biochemistry **31**, 7436–7440 (1992). https://doi.org/10.1021/bi00148a002

19. B.M. Denker, B.L. Smith, F.P. Kuhajda, P. Agre, Identification, purification, and partial characterization of a novel Mr 28,000 integral membrane protein from erythrocytes and renal tubules. J. Biol. Chem. **263**, 15634–15642 (1988)

20. C. Bondy, E. Chin, B.L. Smith, G.M. Preston, P. Agre, Developmental gene expression and tissue distribution of the CHIP28 water-channel protein. Proc. Natl. Acad. Sci. USA **90**, 4500–4504 (1993). https://doi.org/10.1073/pnas.90.10.4500

21. G. Benga, The first discovered water channel protein, later called aquaporin 1: Molecular characteristics, functions and medical implications. Mol. Asp. Med. **33**, 518–534 (2012). https://doi.org/10.1016/j.mam.2012.06.001

22. C. Pimpao, D. Wragg, I.V. da Silva, A. Casini, G. Soveral, Aquaglyceroporin modulators as emergent pharmacological molecules for human diseases. Front. Mol. Biosci. **9**, 845237 (2022). https://doi.org/10.3389/fmolb.2022.845237

23. G.P. Bienert, M.D. Schussler, T.P. Jahn, Metalloids: Essential, beneficial or toxic? Major intrinsic proteins sort it out. Trends Biochem. Sci. **33**, 20–26 (2008). https://doi.org/10.1016/j.tibs.2007.10.004

24. K. Ishibashi et al., Molecular cloning and expression of a member of the aquaporin family with permeability to glycerol and urea in addition to water expressed at the basolateral membrane of kidney collecting duct cells. Proc. Natl. Acad. Sci. USA **91**, 6269–6273 (1994). https://doi.org/10.1073/pnas.91.14.6269

25. K. Ishibashi, New members of mammalian aquaporins: AQP10-AQP12. Handb. Exp. Pharmacol. (190), 251–262 (2009). https://doi.org/10.1007/978-3-540-79885-9_13

26. P. Agre et al., Aquaporin water channels–From atomic structure to clinical medicine. J. Physiol. **542**, 3–16 (2002). https://doi.org/10.1113/jphysiol.2002.020818

27. J.S. Jung, G.M. Preston, B.L. Smith, W.B. Guggino, P. Agre, Molecular structure of the water channel through aquaporin CHIP. The hourglass model. J. Biol. Chem. **269**, 14648–14654 (1994)

28. S. Nielsen et al., Aquaporins in the kidney: From molecules to medicine. Physiol. Rev. **82**, 205–244 (2002). https://doi.org/10.1152/physrev.00024.2001

29. A.S. Verkman, A.K. Mitra, Structure and function of aquaporin water channels. Am. J. Physiol. Renal Physiol. **278**, F13–F28 (2000). https://doi.org/10.1152/ajprenal.2000.278.1.F13

30. P. Huang et al., Cryo-EM structure supports a role of AQP7 as a junction protein. Nat. Commun. **14**, 600 (2023). https://doi.org/10.1038/s41467-023-36272-y

31. M. Xiong, C. Li, W. Wang, B. Yang, Protein structure and modification of aquaporins. Adv. Exp. Med. Biol. **1398**, 15–38 (2023). https://doi.org/10.1007/978-981-19-7415-1_2

32. A. Herraiz, F. Chauvigne, J. Cerda, X. Belles, M.D. Piulachs, Identification and functional characterization of an ovarian aquaporin from the cockroach Blattella germanica L. (Dictyoptera, Blattellidae). J. Exp. Biol. **214**, 3630–3638 (2011). https://doi.org/10.1242/jeb.057406

33. M. Echevarria, E.E. Windhager, S.S. Tate, G. Frindt, Cloning and expression of AQP3, a water channel from the medullary collecting duct of rat kidney. Proc. Natl. Acad. Sci. USA **91**, 10997–11001 (1994). https://doi.org/10.1073/pnas.91.23.10997

34. A.K. Meinild, D.A. Klaerke, T. Zeuthen, Bidirectional water fluxes and specificity for small hydrophilic molecules in aquaporins 0-5. J. Biol. Chem. **273**, 32446–32451 (1998). https://doi.org/10.1074/jbc.273.49.32446

35. L.M. Holm et al., NH3 and NH4+ permeability in aquaporin-expressing Xenopus oocytes. Pflugers Arch. **450**, 415–428 (2005). https://doi.org/10.1007/s00424-005-1399-1

36. P. Kitchen et al., Beyond water homeostasis: Diverse functional roles of mammalian aquaporins. Biochim. Biophys. Acta **1850**, 2410–2421 (2015). https://doi.org/10.1016/j.bbagen.2015.08.023

37. W.B. Bollag, D. Xie, X. Zheng, X. Zhong, A potential role for the phospholipase D2-aquaporin-3 signaling module in early keratinocyte differentiation: Production of a phosphatidylglycerol signaling lipid. J. Invest. Dermatol. **127**, 2823–2831 (2007). https://doi.org/10.1038/sj.jid.5700921

38. M. Boury-Jamot et al., Expression and function of aquaporins in human skin: Is aquaporin-3 just a glycerol transporter? Biochim. Biophys. Acta **1758**, 1034–1042 (2006). https://doi.org/10.1016/j.bbamem.2006.06.013

39. K. Nakahigashi et al., Upregulation of aquaporin-3 is involved in keratinocyte proliferation and epidermal hyperplasia. J. Invest. Dermatol. **131**, 865–873 (2011). https://doi.org/10.1038/jid.2010.395

40. L. Best et al., Contrasting effects of glycerol and urea transport on rat pancreatic beta-cell function. Cell. Physiol. Biochem. **23**, 255–264 (2009). https://doi.org/10.1159/000218172

41. M.A. Knepper, F. Roch-Ramel, Pathways of urea transport in the mammalian kidney. Kidney Int. **31**, 629–633 (1987). https://doi.org/10.1038/ki.1987.44

42. K. Ishibashi, M. Imai, S. Sasaki, Cellular localization of aquaporin 7 in the rat kidney. Exp. Nephrol. **8**, 252–257 (2000). https://doi.org/10.1159/000020676

43. E. Sohara et al., Defective water and glycerol transport in the proximal tubules of AQP7 knockout mice. Am. J. Physiol. Renal Physiol. **289**, F1195–F1200 (2005). https://doi.org/10.1152/ajprenal.00133.2005

44. E. Sohara, T. Rai, S. Sasaki, S. Uchida, Physiological roles of AQP7 in the kidney: Lessons from AQP7 knockout mice. Biochim. Biophys. Acta **1758**, 1106–1110 (2006). https://doi.org/10.1016/j.bbamem.2006.04.002

45. S.M. Bagnasco, The erythrocyte urea transporter UT-B. J. Membr. Biol. **212**, 133–138 (2006). https://doi.org/10.1007/s00232-006-0872-x

46. Y. Liu et al., Aquaporin 9 is the major pathway for glycerol uptake by mouse erythrocytes, with implications for malarial virulence. Proc. Natl. Acad. Sci. USA **104**, 12560–12564 (2007). https://doi.org/10.1073/pnas.0705313104

47. M. Elkjaer et al., Immunolocalization of AQP9 in liver, epididymis, testis, spleen, and brain. Biochem. Biophys. Res. Commun. **276**, 1118–1128 (2000). https://doi.org/10.1006/bbrc.2000.3505

48. J.M. Carbrey et al., Aquaglyceroporin AQP9: Solute permeation and metabolic control of expression in liver. Proc. Natl. Acad. Sci. USA **100**, 2945–2950 (2003). https://doi.org/10.1073/pnas.0437994100

49. A.M. Rojek et al., Defective glycerol metabolism in aquaporin 9 (AQP9) knockout mice. Proc. Natl. Acad. Sci. USA **104**, 3609–3614 (2007). https://doi.org/10.1073/pnas.0610894104

50. S. Jelen et al., Aquaporin-9 and urea transporter-A gene deletions affect urea transmembrane passage in murine hepatocytes. Am. J. Physiol. Gastrointest. Liver Physiol. **303**, G1279–G1287 (2012). https://doi.org/10.1152/ajpgi.00153.2012

51. S. Grether-Beck et al., Urea uptake enhances barrier function and antimicrobial defense in humans by regulating epidermal gene expression. J. Invest. Dermatol. **132**, 1561–1572 (2012). https://doi.org/10.1038/jid.2012.42

52. H. Tsukaguchi et al., Molecular characterization of a broad selectivity neutral solute channel. J. Biol. Chem. **273**, 24737–24743 (1998). https://doi.org/10.1074/jbc.273.38.24737

53. S. Hatakeyama et al., Cloning of a new aquaporin (AQP10) abundantly expressed in duodenum and jejunum. Biochem. Biophys. Res. Commun. **287**, 814–819 (2001). https://doi.org/10.1006/bbrc.2001.5661

54. K. Ishibashi, T. Morinaga, M. Kuwahara, S. Sasaki, M. Imai, Cloning and identification of a new member of water channel (AQP10) as an aquaglyceroporin. Biochim. Biophys. Acta **1576**, 335–340 (2002). https://doi.org/10.1016/s0167-4781(02)00393-7

55. T. Ma, B. Yang, A.S. Verkman, Cloning of a novel water and urea-permeable aquaporin from mouse expressed strongly in colon, placenta, liver, and heart. Biochem. Biophys. Res. Commun. **240**, 324–328 (1997). https://doi.org/10.1006/bbrc.1997.7664

56. D. Gomes et al., Aquaporins are multifunctional water and solute transporters highly divergent in living organisms. Biochim. Biophys. Acta **1788**, 1213–1228 (2009). https://doi.org/10.1016/j.bbamem.2009.03.009

57. G. Calamita et al., The inner mitochondrial membrane has aquaporin-8 water channels and is highly permeable to water. J. Biol. Chem. **280**, 17149–17153 (2005). https://doi.org/10.1074/jbc.C400595200

58. K. Liu, H. Nagase, C.G. Huang, G. Calamita, P. Agre, Purification and functional characterization of aquaporin-8. Biol. Cell. **98**, 153–161 (2006). https://doi.org/10.1042/BC20050026

59. L.M. Holm, D.A. Klaerke, T. Zeuthen, Aquaporin 6 is permeable to glycerol and urea. Pflugers Arch. **448**, 181–186 (2004). https://doi.org/10.1007/s00424-004-1245-x

60. G.M. Preston, J.S. Jung, W.B. Guggino, P. Agre, The mercury-sensitive residue at cysteine 189 in the CHIP28 water channel. J. Biol. Chem. **268**, 17–20 (1993)

61. B.L. de Groot, H. Grubmuller, Water permeation across biological membranes: Mechanism and dynamics of aquaporin-1 and GlpF. Science **294**, 2353–2357 (2001). https://doi.org/10.1126/science.1066115

62. H. Sui, B.G. Han, J.K. Lee, P. Walian, B.K. Jap, Structural basis of water-specific transport through the AQP1 water channel. Nature **414**, 872–878 (2001). https://doi.org/10.1038/414872a

63. K. Murata et al., Structural determinants of water permeation through aquaporin-1. Nature **407**, 599–605 (2000). https://doi.org/10.1038/35036519

64. A. Hazama, D. Kozono, W.B. Guggino, P. Agre, M. Yasui, Ion permeation of AQP6 water channel protein. Single channel recordings after Hg2+ activation. J. Biol. Chem. **277**, 29224–29230 (2002). https://doi.org/10.1074/jbc.M204258200

65. M. Yasui et al., Rapid gating and anion permeability of an intracellular aquaporin. Nature **402**, 184–187 (1999). https://doi.org/10.1038/46045

66. H. Nagase et al., Molecular cloning and characterization of mouse aquaporin 6. Biochem. Biophys. Res. Commun. **352**, 12–16 (2007). https://doi.org/10.1016/j.bbrc.2006.10.110

67. S. Ma, H. Xie, K. Yu, J. Yang, Mechanism of unusual AQP6 activation by mercury binding to a pore-external residue C155. Biochem. Biophys. Res. Commun. **618**, 1–7 (2022). https://doi.org/10.1016/j.bbrc.2022.06.025

68. H. Xie et al., Molecular mechanisms of mercury-sensitive aquaporins. J. Am. Chem. Soc. **144**, 22229–22241 (2022). https://doi.org/10.1021/jacs.2c10240

69. B.L. de Groot, H. Grubmuller, The dynamics and energetics of water permeation and proton exclusion in aquaporins. Curr. Opin. Struct. Biol. **15**, 176–183 (2005). https://doi.org/10.1016/j.sbi.2005.02.003

70. J.S. Hub, H. Grubmuller, B.L. de Groot, Dynamics and energetics of permeation through aquaporins. What do we learn from molecular dynamics simulations? Handb. Exp. Pharmacol., 57–76 (2009). https://doi.org/10.1007/978-3-540-79885-9_3

71. E. Tajkhorshid et al., Control of the selectivity of the aquaporin water channel family by global orientational tuning. Science **296**, 525–530 (2002). https://doi.org/10.1126/science.1067778

72. D. Fu et al., Structure of a glycerol-conducting channel and the basis for its selectivity. Science **290**, 481–486 (2000). https://doi.org/10.1126/science.290.5491.481

73. E. Beitz, B. Wu, L.M. Holm, J.E. Schultz, T. Zeuthen, Point mutations in the aromatic/arginine region in aquaporin 1 allow passage of urea, glycerol, ammonia, and protons. Proc. Natl. Acad. Sci. USA **103**, 269–274 (2006). https://doi.org/10.1073/pnas.0507225103

74. D. Singer et al., Orphan transporter SLC6A18 is renal neutral amino acid transporter B0AT3. J. Biol. Chem. **284**, 19953–19960 (2009). https://doi.org/10.1074/jbc.M109.011171

75. L. Bankir, G. Crambert, R. Vargas-Poussou, The SLC6A18 transporter is most likely a na-dependent glycine/urea antiporter responsible for urea secretion in the proximal straight tubule: Influence of this urea secretion on glomerular filtration rate. Nephron **148**, 796–822 (2024). https://doi.org/10.1159/000539602

76. W.H. Dantzler, A.T. Layton, H.E. Layton, T.L. Pannabecker, Urine-concentrating mechanism in the inner medulla: Function of the thin limbs of the loops of Henle. Clin. J. Am. Soc. Nephrol. **9**, 1781–1789 (2014). https://doi.org/10.2215/CJN.08750812

77. J.M. Sands, H.E. Layton, Advances in understanding the urine-concentrating mechanism. Annu. Rev. Physiol. **76**, 387–409 (2014). https://doi.org/10.1146/annurev-physiol-021113-170350

78. C.M. Nawata, K.K. Evans, W.H. Dantzler, T.L. Pannabecker, Transepithelial water and urea permeabilities of isolated perfused Munich-Wistar rat inner medullary thin limbs of Henle's loop. Am. J. Physiol. Renal Physiol. **306**, F123–F129 (2014). https://doi.org/10.1152/ajprenal.00491.2013

79. D.W. Leung, D.D. Loo, B.A. Hirayama, T. Zeuthen, E.M. Wright, Urea transport by cotransporters. J. Physiol. **528**(Pt 2), 251–257 (2000). https://doi.org/10.1111/j.1469-7793.2000.00251.x

80. C.M. Nawata, W.H. Dantzler, T.L. Pannabecker, Alternative channels for urea in the inner medulla of the rat kidney. Am. J. Physiol. Renal Physiol. **309**, F916–F924 (2015). https://doi.org/10.1152/ajprenal.00392.2015

81. M. Wang et al., The interactions of aquaporins and mineral nutrients in higher plants. Int. J. Mol. Sci. **17** (2016). https://doi.org/10.3390/ijms17081229

82. A.K. Srivastava, S. Penna, D.V. Nguyen, L.S. Tran, Multifaceted roles of aquaporins as molecular conduits in plant responses to abiotic stresses. Crit. Rev. Biotechnol. **36**, 389–398 (2016). https://doi.org/10.3109/07388551.2014.973367

83. C. Maurel et al., Aquaporins in plants. Physiol. Rev. **95**, 1321–1358 (2015). https://doi.org/10.1152/physrev.00008.2015

84. I.S. Wallace, W.G. Choi, D.M. Roberts, The structure, function and regulation of the nodulin 26-like intrinsic protein family of plant aquaglyceroporins. Biochim. Biophys. Acta **1758**, 1165–1175 (2006). https://doi.org/10.1016/j.bbamem.2006.03.024

85. F. Ishikawa, S. Suga, T. Uemura, M.H. Sato, M. Maeshima, Novel type aquaporin SIPs are mainly localized to the ER membrane and show cell-specific expression in Arabidopsis thaliana. FEBS Lett. **579**, 5814–5820 (2005). https://doi.org/10.1016/j.febslet.2005.09.076

86. G.P. Bienert, M.D. Bienert, T.P. Jahn, M. Boutry, F. Chaumont, Solanaceae XIPs are plasma membrane aquaporins that facilitate the transport of many uncharged substrates. Plant J. **66**, 306–317 (2011). https://doi.org/10.1111/j.1365-313X.2011.04496.x

87. S. Sudhakaran et al., Significance of solute specificity, expression, and gating mechanism of tonoplast intrinsic protein during development and stress response in plants. Physiol. Plant. **172**, 258–274 (2021). https://doi.org/10.1111/ppl.13386

88. H.I. Anderberg, P. Kjellbom, U. Johanson, Annotation of Selaginella moellendorffii major intrinsic proteins and the evolution of the protein family in terrestrial plants. Front. Plant Sci. **3**, 33 (2012). https://doi.org/10.3389/fpls.2012.00033

89. S. Gustavsson, A.S. Lebrun, K. Norden, F. Chaumont, U. Johanson, A novel plant major intrinsic protein in Physcomitrella patens most similar to bacterial glycerol channels. Plant Physiol. **139**, 287–295 (2005). https://doi.org/10.1104/pp.105.063198

90. J.A. Danielson, U. Johanson, Unexpected complexity of the aquaporin gene family in the moss Physcomitrella patens. BMC Plant Biol. **8**, 45 (2008). https://doi.org/10.1186/1471-2229-8-45

91. L. Gao et al., Role of aquaporins in determining carbon and nitrogen status in higher plants. Int. J. Mol. Sci. **19** (2018). https://doi.org/10.3390/ijms19010035

92. M.P. Beier, S. Kojima, The function of high-affinity urea transporters in nitrogen-deficient conditions. Physiol. Plant. **171**, 802–808 (2021). https://doi.org/10.1111/ppl.13303

93. R. Kaldenhoff, M. Fischer, Functional aquaporin diversity in plants. Biochim. Biophys. Acta **1758**, 1134–1141 (2006). https://doi.org/10.1016/j.bbamem.2006.03.012

94. A.R. Fox, L.C. Maistriaux, F. Chaumont, Toward understanding of the high number of plant aquaporin isoforms and multiple regulation mechanisms. Plant Sci. **264**, 179–187 (2017). https://doi.org/10.1016/j.plantsci.2017.07.021

95. Q. Sun, X. Liu, Y. Kitagawa, G. Calamita, X. Ding, Plant aquaporins: Their roles beyond water transport. Crop J. **12**, 641–655 (2024)

96. P. Gerbeau, J. Guclu, P. Ripoche, C. Maurel, Aquaporin Nt-TIPa can account for the high permeability of tobacco cell vacuolar membrane to small neutral solutes. Plant J. **18**, 577–587 (1999). https://doi.org/10.1046/j.1365-313x.1999.00481.x

97. B. Otto, R. Kaldenhoff, Cell-specific expression of the mercury-insensitive plasma-membrane aquaporin NtAQP1 from Nicotiana tabacum. Planta **211**, 167–172 (2000). https://doi.org/10.1007/s004250000275

98. I.S. Wallace, D.M. Roberts, Distinct transport selectivity of two structural subclasses of the nodulin-like intrinsic protein family of plant aquaglyceroporin channels. Biochemistry **44**, 16826–16834 (2005). https://doi.org/10.1021/bi0511888

99. M. Dynowski, M. Mayer, O. Moran, U. Ludewig, Molecular determinants of ammonia and urea conductance in plant aquaporin homologs. FEBS Lett. **582**, 2458–2462 (2008). https://doi.org/10.1016/j.febslet.2008.06.012

100. M. Gaspar et al., Cloning and characterization of ZmPIP1-5b, an aquaporin transporting water and urea. Plant Sci. **165**, 21–31 (2003). https://doi.org/10.1016/S0168-9452(03)00117-1

101. F. Klebl, M. Wolf, N. Sauer, A defect in the yeast plasma membrane urea transporter Dur3p is complemented by CpNIP1, a Nod26-like protein from zucchini (Cucurbita pepo L.), and by Arabidopsis thaliana delta-TIP or gamma-TIP. FEBS Lett. **547**, 69–74 (2003). https://doi.org/10.1016/s0014-5793(03)00671-9

102. L.H. Liu, U. Ludewig, B. Gassert, W.B. Frommer, N. von Wiren, Urea transport by nitrogen-regulated tonoplast intrinsic proteins in Arabidopsis. Plant Physiol. **133**, 1220–1228 (2003). https://doi.org/10.1104/pp.103.027409

103. G. Soto, K. Alleva, M.A. Mazzella, G. Amodeo, J.P. Muschietti, AtTIP1;3 and AtTIP5;1, the only highly expressed Arabidopsis pollen-specific aquaporins, transport water and urea. FEBS Lett. **582**, 4077–4082 (2008). https://doi.org/10.1016/j.febslet.2008.11.002

104. S. Kojima, A. Bohner, N. von Wiren, Molecular mechanisms of urea transport in plants. J. Membr. Biol. **212**, 83–91 (2006). https://doi.org/10.1007/s00232-006-0868-6

105. G. Soto et al., TIP5;1 is an aquaporin specifically targeted to pollen mitochondria and is probably involved in nitrogen remobilization in Arabidopsis thaliana. Plant J. **64**, 1038–1047 (2010). https://doi.org/10.1111/j.1365-313X.2010.04395.x

106. S.H. Kim, K.I. Kim, H.W. Ju, H.J. Lee, S.W. Hong, Overexpression of gene encoding tonoplast intrinsic aquaporin promotes urea transport in Arabidopsis. J. Appl. Biol. Chem. **50**, 102–110 (2007)

107. R. Gu, X. Chen, Y. Zhou, L. Yuan, Isolation and characterization of three maize aquaporin genes, ZmNIP2;1, ZmNIP2;4 and ZmTIP4;4 involved in urea transport. BMB Rep. **45**, 96–101 (2012). https://doi.org/10.5483/BMBRep.2012.45.2.96

108. L. Zhang, J. Yan, O.K. Vatamaniuk, X. Du, CsNIP2;1 is a plasma membrane transporter from Cucumis sativus that facilitates urea uptake when expressed in Saccharomyces cerevisiae and Arabidopsis thaliana. Plant Cell Physiol. **57**, 616–629 (2016). https://doi.org/10.1093/pcp/pcw018

109. S. Kojima, A. Bohner, B. Gassert, L. Yuan, N. von Wiren, AtDUR3 represents the major transporter for high-affinity urea transport across the plasma membrane of nitrogen-deficient Arabidopsis roots. Plant J. **52**, 30–40 (2007). https://doi.org/10.1111/j.1365-313X.2007.03223.x

110. L.H. Liu, U. Ludewig, W.B. Frommer, N. von Wiren, AtDUR3 encodes a new type of high-affinity urea/H+ symporter in Arabidopsis. Plant Cell **15**, 790–800 (2003). https://doi.org/10.1105/tpc.007120

111. R. Terrado, A. Monier, R. Edgar, C. Lovejoy, Diversity of nitrogen assimilation pathways among microbial photosynthetic eukaryotes. J. Phycol. **51**, 490–506 (2015). https://doi.org/10.1111/jpy.12292

112. W.-H. Wang, B. Köhler, F.-Q. Cao, L.-H. Liu, Molecular and physiological aspects of urea transport in higher plants. Plant Sci. **175**, 467–477 (2008). https://doi.org/10.1016/j.plantsci.2008.05.018

113. G.W. Liu et al., Molecular identification and functional analysis of a maize (Zea mays) DUR3 homolog that transports urea with high affinity. Planta **241**, 861–874 (2015). https://doi.org/10.1007/s00425-014-2219-7

114. M.P. Beier et al., The urea transporter DUR3 contributes to rice production under nitrogen-deficient and field conditions. Physiol. Plant. **167**, 75–89 (2019). https://doi.org/10.1111/ppl.12872

115. M. Morel et al., Characterization and regulation of PiDur3, a permease involved in the acquisition of urea by the ectomycorrhizal fungus Paxillus involutus. Fungal Genet. Biol. **45**, 912–921 (2008). https://doi.org/10.1016/j.fgb.2008.01.002

116. M. Kakinuma, D.A. Coury, C. Nakamoto, K. Sakaguchi, H. Amano, Molecular analysis of physiological responses to changes in nitrogen in a marine macroalga, Porphyra yezoensis (Rhodophyta). Cell Biol. Toxicol. **24**, 629–639 (2008). https://doi.org/10.1007/s10565-007-9053-7

117. A. Lupini et al., Physiological and molecular responses in tomato under different forms of N nutrition. J. Plant Physiol. **216**, 17–25 (2017). https://doi.org/10.1016/j.jplph.2017.05.013

118. T.B. Dos Santos, V.Y. Baba, L.G.E. Vieira, L.F.P. Pereira, D.S. Domingues, The urea transporter DUR3 is differentially regulated by abiotic and biotic stresses in coffee plants. Physiol. Mol. Biol. Plants **27**, 203–212 (2021). https://doi.org/10.1007/s12298-021-00930-6

119. C. Muratore, L. Espen, B. Prinsi, Nitrogen uptake in plants: The plasma membrane root transport systems from a physiological and proteomic perspective. Plants (Basel) **10** (2021). https://doi.org/10.3390/plants10040681

120. K.B. Heller, E.C. Lin, T.H. Wilson, Substrate specificity and transport properties of the glycerol facilitator of Escherichia coli. J. Bacteriol. **144**, 274–278 (1980). https://doi.org/10.1128/jb.144.1.274-278.1980

121. J. Mills, N.R. Wyborn, J.A. Greenwood, S.G. Williams, C.W. Jones, Characterisation of a binding-protein-dependent, active transport system for short-chain amides and urea in the methylotrophic bacterium Methylophilus methylotrophus. Eur. J. Biochem. **251**, 45–53 (1998). https://doi.org/10.1046/j.1432-1327.1998.2510045.x

122. A. Valladares, M.L. Montesinos, A. Herrero, E. Flores, An ABC-type, high-affinity urea permease identified in cyanobacteria. Mol. Microbiol. **43**, 703–715 (2002). https://doi.org/10.1046/j.1365-2958.2002.02778.x

123. G. Beckers, A.K. Bendt, R. Kramer, A. Burkovski, Molecular identification of the urea uptake system and transcriptional analysis of urea transporter- and urease-encoding genes in Corynebacterium glutamicum. J. Bacteriol. **186**, 7645–7652 (2004). https://doi.org/10.1128/JB.186.22.7645-7652.2004

124. R.M. Siewe et al., Urea uptake and urease activity in Corynebacterium glutamicum. Arch. Microbiol. **169**, 411–416 (1998). https://doi.org/10.1007/s002030050591

125. F. Sebbane et al., The Yersinia pseudotuberculosis Yut protein, a new type of urea transporter homologous to eukaryotic channels and functionally interchangeable in vitro with the Helicobacter pylori UreI protein. Mol. Microbiol. **45**, 1165–1174 (2002). https://doi.org/10.1046/j.1365-2958.2002.03096.x

126. D.L. Weeks, S. Eskandari, D.R. Scott, G. Sachs, A H+-gated urea channel: The link between Helicobacter pylori urease and gastric colonization. Science **287**, 482–485 (2000). https://doi.org/10.1126/science.287.5452.482

127. G.H. Huysmans et al., A urea channel from Bacillus cereus reveals a novel hexameric structure. Biochem. J. **445**, 157–166 (2012). https://doi.org/10.1042/BJ20120169

128. T. Jahns, A. Zobel, D. Kleiner, H.J. Kaltwasser, Evidence for carrier-mediated, energy-dependent uptake of urea in some bacteria. Arch. Microbiol. **149**, 377–383 (1988)

129. T. van der Heide, B. Poolman, ABC transporters: One, two or four extracytoplasmic substrate-binding sites? EMBO Rep. **3**, 938–943 (2002). https://doi.org/10.1093/embo-reports/kvf201

130. S. Hailemariam, S. Zhao, Y. He, J. Wang, Urea transport and hydrolysis in the rumen: A review. Anim. Nutr. **7**, 989–996 (2021). https://doi.org/10.1016/j.aninu.2021.07.002

131. K.J. Tanaka, S. Song, K. Mason, H.W. Pinkett, Selective substrate uptake: The role of ATP-binding cassette (ABC) importers in pathogenesis. Biochim. Biophys. Acta Biomembr. **1860**, 868–877 (2018). https://doi.org/10.1016/j.bbamem.2017.08.011

132. E.J. Levin, M. Quick, M. Zhou, Crystal structure of a bacterial homologue of the kidney urea transporter. Nature **462**, 757–761 (2009). https://doi.org/10.1038/nature08558

133. D.L. Weeks, G. Sachs, Sites of pH regulation of the urea channel of Helicobacter pylori. Mol. Microbiol. **40**, 1249–1259 (2001). https://doi.org/10.1046/j.1365-2958.2001.02466.x

134. H.L. Mobley, L.T. Hu, P.A. Foxal, Helicobacter pylori urease: Properties and role in pathogenesis. Scand. J. Gastroenterol. Suppl. **187**, 39–46 (1991)

135. L.T. Hu, H.L. Mobley, Purification and N-terminal analysis of urease from Helicobacter pylori. Infect. Immun. **58**, 992–998 (1990). https://doi.org/10.1128/iai.58.4.992-998.1990

136. M. Rektorschek et al., Acid resistance of Helicobacter pylori depends on the UreI membrane protein and an inner membrane proton barrier. Mol. Microbiol. **36**, 141–152 (2000). https://doi.org/10.1046/j.1365-2958.2000.01835.x

137. R. McNulty, J.P. Ulmschneider, H. Luecke, M.B. Ulmschneider, Mechanisms of molecular transport through the urea channel of Helicobacter pylori. Nat. Commun. **4**, 2900 (2013). https://doi.org/10.1038/ncomms3900

138. Y. Cui et al., pH-dependent gating mechanism of the Helicobacter pylori urea channel revealed by cryo-EM. Sci. Adv. **5**, eaav8423 (2019). https://doi.org/10.1126/sciadv.aav8423

139. D.L. Weeks, G. Gushansky, D.R. Scott, G. Sachs, Mechanism of proton gating of a urea channel. J. Biol. Chem. **279**, 9944–9950 (2004). https://doi.org/10.1074/jbc.M312680200

140. S. Bury-Mone, S. Skouloubris, A. Labigne, H. De Reuse, The Helicobacter pylori UreI protein: Role in adaptation to acidity and identification of residues essential for its activity and for acid activation. Mol. Microbiol. **42**, 1021–1034 (2001). https://doi.org/10.1046/j.1365-2958.2001.02689.x

141. D. Strugatsky et al., Structure of the proton-gated urea channel from the gastric pathogen Helicobacter pylori. Nature **493**, 255–258 (2013). https://doi.org/10.1038/nature11684

142. H.M. Berman et al., The protein data bank. Nucleic Acids Res. **28**, 235–242 (2000). https://doi.org/10.1093/nar/28.1.235

143. E.J. Levin et al., Structure and permeation mechanism of a mammalian urea transporter. Proc. Natl. Acad. Sci. USA **109**, 11194–11199 (2012). https://doi.org/10.1073/pnas.1207362109

144. A. Qaiser et al., Design and synthesis of multifunctional polymeric micelles for targeted delivery in Helicobacter pylori infection. J. Mol. Liquids **363**, 119802 (2022)

145. Z.W. Jing et al., Design and evaluation of novel pH-sensitive ureido-conjugated chitosan/TPP nanoparticles targeted to Helicobacter pylori. Biomaterials **84**, 276–285 (2016). https://doi.org/10.1016/j.biomaterials.2016.01.045

146. R. Chitas, D.R. Fonseca, P. Parreira, M.C.L. Martins, Targeted nanotherapeutics for the treatment of Helicobacter pylori infection. J. Biomed. Sci. **31**, 78 (2024). https://doi.org/10.1186/s12929-024-01068-9

147. B. Ilan, E. Tajkhorshid, K. Schulten, G.A. Voth, The mechanism of proton exclusion in aquaporin channels. Proteins **55**, 223–228 (2004). https://doi.org/10.1002/prot.20038

Chapter 10
Energy-Dependent Urea Transports in Mammals and their Functional Consequences

Lise Bankir and Gilles Crambert

Abstract In lower organisms (bacteria, fungi, yeast), some species that express the enzyme urease take up urea from the surrounding medium as a source of nitrogen, by energy-dependent urea transporters. In contrast, in mammals, urea is an endproduct of nitrogen metabolism, and the energy-dependent urea transports are associated with either the need to excrete nitrogen efficiently, in the case of excess nitrogen intake, or the need to conserve nitrogen and re-use it, in the case of low nitrogen supply.

Three different energy-dependent urea transports have been characterized functionally in the mammalian kidney. One responsible for urea secretion in the straight segment of the proximal tubule (proximal straight tubule, PST), another for urea reabsorption in the upper third of the inner medullary collecting duct (IMCD), and one in the very late portion of the IMCD. But intriguingly, up to now, none of the membrane transporters responsible for these transports has been characterized molecularly.

This review describes these urea transports functionally and proposes a candidate transporter responsible for urea secretion in the PST. Based on the study of knockout mice, SLC6A18 has been characterized as a glycine transporter, but several previous observations suggest that it may also serve another function. SLC6A18 is very likely a urea/glycine, sodium-dependent antiport. These observations are described in detail.

Note. The "proximal tubule" of the mammalian nephron is subdivided into three subsegments S1, S2, and S3. The S1 and S2 segments correspond to the proximal convoluted tubule (PCT) and are located in the cortex. The S3 segment is often called the proximal straight tubule (PST) or "pars recta" and lies in the outer stripe of the outer medulla.

L. Bankir (✉) · G. Crambert
Laboratoire de Physiologie Rénale et Tubulopathies, Centre de Recherche des Cordeliers, INSERM UMRS 1138, Sorbonne Université, Université Paris Cité, Paris, France

CNRS EMR 8228, Métabolisme et Physiologie Rénale, Centre de Recherche des Cordeliers, Paris, France
e-mail: lise.bankir@inserm.fr; gilles.crambert@crc.jussieu.fr

Energy-dependent urea transport is suspected to also take place in two other organs that express facilitated urea transporters; in the testis, urea secretion could initiate a flux of fluid in seminiferous tubules to ensure sperm transport into the lumen; in the bladder, urea secretion could reclaim urea that is at permanent risk of dissipation, due to the large urea concentration difference between urine and blood and the high expression of the facilitated transporter UT-B on the basal membrane of the urothelium.

The energy-dependent secretion of urea in the PST has a number of consequences. (1) It allows a better efficiency of urea excretion and thus may prevent some toxicity of urea. (2) It provides a much better understanding of the urine concentrating mechanism. (3) It explains how urea may influence glomerular filtration rate, indirectly.

Keywords Nitrogen conservation · Urea · Kidney · Proximal straight tubule · Vasopressin · Glomerular filtration rate · Urine concentrating mechanism · Bladder · Testis

Abbreviations

AVR	Ascending vasa recta
CD	Collecting duct
CKD	Chronic kidney disease
DVR	Descending vasa recta
FEurea	Fractional excretion of urea
GFR	Glomerular filtration rate
IM	Inner medulla
IMCD	Inner medullary collecting duct
IS-OM	Inner stripe of the outer medulla
OS-OM	Outer stripe of the outer medulla
PCT	Proximal convoluted tubule
PST	Proximal straight tubule
TAL	Thick ascending limb
TDL	Thin descending limb
TGF	Tubulo-glomerular feedback
U/P urea	Ratio of urine-to-plasma urea concentrations
UT	Facilitated urea transporter

Introduction

Energy-dependent urea transport is observed in bacteria, fungi and yeast. Urea serves as a nitrogen source in species that express urease. A few urea transporters have been molecularly identified in these lower organisms (see review in [1]).

Energy-dependent urea transport has also been functionally well characterized in lower vertebrates. There, it is associated with nitrogen excretion and/or water conservation (urea secretion in the kidney of some frogs, and urea reabsorption in the ventral skin of some toads, respectively). The transporters responsible for these urea movements in lower vertebrates have not yet been characterized molecularly. See review in [1]. In this chapter, we will present several energy-dependent urea transports in mammals and explain what is their role in the overall nitrogen handling. We will also present a candidate transporter that is most likely responsible for an energy-dependent urea secretion in the mammalian kidney.

Mammals excrete most of their nitrogenous wastes in the form of urea and to a lesser extent ammonia. Their excretory needs for urea depend on the protein content of their diet and on their eating behaviour. Herbivores have a relatively low protein intake and thus need to conserve nitrogen rather than to excrete it. On the opposite, protein intake is quite high in carnivores. But because of their discontinuous large meals, they need to efficiently excrete large loads of urea, alternating with periods of fast during which they may need to conserve nitrogen. Omnivores, such as rodents, pigs and humans, who exhibit an intermediate situation with several meals per day, have a more regular need for nitrogen excretion.

The plasma urea level in mammals is kept at a relatively low level (3–10 mmol/L) so that, in carnivores and omnivores, urea is concentrated in the urine far above its concentration in plasma and body fluids in order to be excreted in a reasonable amount of water. However, there are marked species differences in the urine-to-plasma ratio of urea concentration, associated with different body size and other factors (Table 10.1). In some desert-adapted rodents, urine urea concentration can be 500-fold higher than that in plasma [2, 3]. Urea is very soluble in water and can thus be concentrated without risk of precipitation and kidney stones, contrary to uric acid. The excretion of urea in the feces is negligeable.

Most recent textbooks of renal physiology and nephrology do not include a specific chapter on urea excretion and its possible regulation, in spite of the fact that urea represents about 40% of all urinary solutes in humans (on a Western-type diet) and even more in laboratory rodents [4]. They ignore the fact that urea excretion is regulated, as will be explained below.

It is usually assumed that urea is freely filtered in the glomeruli and that a variable proportion is reabsorbed passively by diffusion along the nephron and collecting duct (CD), leaving a variable fraction of the filtered urea to be excreted. However, the magnitude of urea reabsorption along the nephron depends largely on the urine flow rate and thus, on the action of vasopressin. With slower flow and higher concentration of urinary solutes, more urea is reabsorbed in the CDs, partly because some urea is driven by simple diffusion along the whole CDs, due to a greater transepithelial concentration difference and a longer contact time, and partly because of the facilitated diffusion that occurs in the terminal IMCD where vasopressin-dependent facilitated urea transporters (UTs) are expressed. These vasopressin-dependent changes in urea excretion often obscure the results of some experimental studies if the level of vasopressin varies during the experiments.

Table 10.1 Water, urea and sodium handling in mice, rats, and humans

		Mouse	Rat	Human
Body weight (BW)	kg	0.03	0.3	70
Kidney weight	g/kg BW	13	6.6	4.3
Water and osmoles				
Urine osmolality	mosm/kg H_2O	2650	1500	650
Urine output	ml/d	2	12	1400
Osmolar excretion	mosm/d	5.3	18	900
U/P osmolality	—	8.8	5.0	2.2
Urea				
Daily urea excretion[a]	mmol/d	3.8	7.5	400
Daily urea excretion	mmol/d/kg BW	130	25	5.7
Plasma urea concentration	mmol/L	9	5	5
Urine urea concentration	mmol/L	1800	700	285
U/P urea	—	200	140	60
Sodium				
Daily Na excretion[a]	mmol/d	0.2	1.5	130
Daily Na excretion	mmol/d/kg BW	6.6	5.0	1.8
Plasma Na concentration	mmol/L	140	140	140
Urine Na concentration	mmol/L	60	125	95
U/P Na	—	0.45	0.90	0.68

[a]The daily excretions of urea and sodium depend on the protein and sodium content of the diet, respectively. The figures given here are rounded off and apply to healthy humans consuming a Western-type diet, and to normal rats and mice fed a usual rodent diet (values collected from several experimental studies and clinical investigations)

It has been understood since a long time that urea is accumulated in the inner medulla and that this accumulation allows urine to be concentrated by promoting water reabsorption. This high urea concentration in the inner medulla is depicted in Fig. 10.1. This accumulation is due to the influence of vasopressin which produces a "urea-selective" urine concentration. Urea plays an important role in urine concentration as a whole, improving the concentration of other solutes, but actually, most of the water economy resulting from the urine concentrating activity is devoted to the concentration of urea itself. Table 10.2 shows that the urine-to-plasma (U/P) ratio for urea is far higher than the U/P ratio for all osmoles as a whole, and the U/P ratio of sodium is actually lower than one.

It is well-known that vasopressin increases the permeability to water of the whole CD by inserting aquaporin 2 (AQP2) into the luminal membrane of principal cells along the CD. But less well-known is the fact that vasopressin also increases the permeability to urea of the deep inner medullary CD by activating the facilitated urea transporters UT-A1 and UT-A3. This allows urea, that has been concentrated upstream by water reabsorption, to diffuse out of the CD lumen into the inner medullary interstitium (Fig. 10.2a). Mice with knock-out of UT-A1/3 exhibit a marked urinary concentrating defect [5].
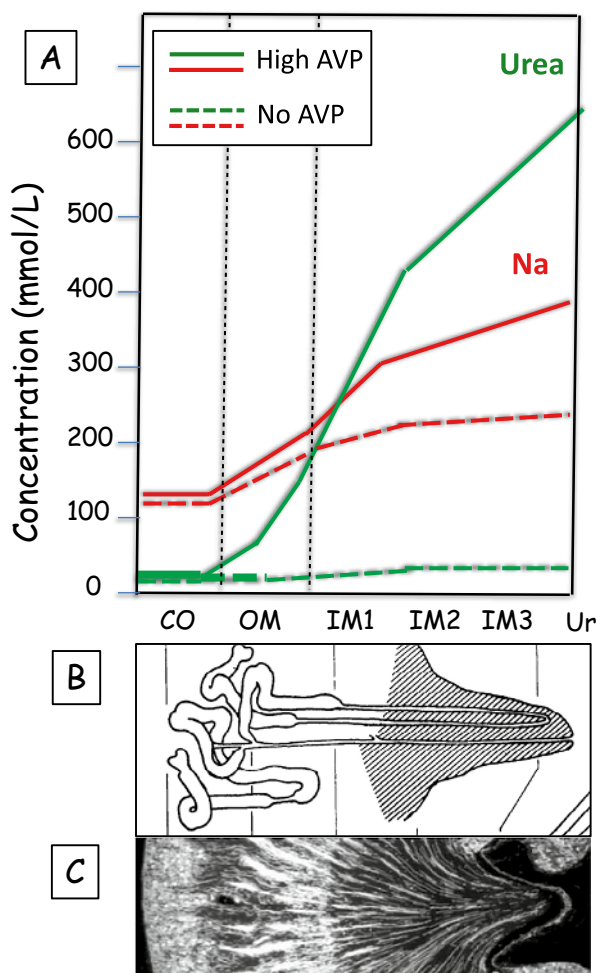
Fig. 10.1 (**a** and **b**) Concentrations of urea and sodium along the cortico-papillary axis in the rat kidney. Newly drawn from data published in Ref. [127]. CO, OM, IM1, IM2, IM3 and Ur = cortex, outer medulla, inner medulla at three different depths, and urine, respectively. From a low value in the cortex, urea concentration increases markedly in the medulla to reach a concentration at the tip of the papilla (IM3) about 100-fold higher than in the cortex. In contrast, sodium concentration increases in the outer medulla and only little in the inner medulla. In the absence of vasopressin (AVP), urea is not at all concentrated in the medulla, whereas sodium concentration is only modestly reduced. A nephron is drawn to show the different segments present in each kidney zone. (**c**) Picture of the central part of a kidney section showing the vascularization of the different kidney zones (white Microfil silicone rubber has been injected into the kidney via the renal artery). (Original picture by Lise Bankir)

Already reported several decades ago, but often forgotten now is the fact that this influence of vasopressin on urea reabsorption markedly reduces the efficiency of urea excretion. The fractional excretion of urea decreases markedly when urine is

Table 10.2 Fractional excretion of the main urinary solutes in rats with different urine concentrating activity

		Low CA	Normal CA	High CA	High/Low	ANOVA
Urine flow rate	ml/d	20.3 ± 1.5	11.1 ± 1.0	5.57 ± 0.18	0.27	$p < 0.001$
Urine osmolality	mOsmol/L	762 ± 44	1526 ± 139	3023 ± 87	3.97	$p < 0.001$
Inulin clearance	ml/min	1.06 ± 0.10	1.62 ± 0.16	1.93 ± 0.10	1.83	$p < 0.001$
Plasma urea	mM	4.3 ± 0.2	5.2 ± 0.5	7.8 ± 0.3	1,80	$p < 0.01$
FE urea	%	118 ± 18	67 ± 7	43 ± 1	0.37	$p < 0.001$
FE Na	%	1.2 ± 0.1	0.8 ± 0.1	0.7 ± 0.1	0.61	$p < 0.005$
FE K	%	10.1 ± 1.4	6.9 ± 0.6	6.8 ± 0.6	0.68	$p = 0.05$
FE creatinine	%	133 ± 12	107 ± 9	91 ± 6	0.69	$p < 0.05$

Rats in steady state. Data based on two 24-h urine collections in metabolic cages

CA urine concentrating activity. Fractional excretions (FE) calculated using inulin clearance as a marker of glomerular filtration rate. Data from Bouby et al (1996). Note that the FE of urea falls much more with increasing CA than that of sodium or potassium (much lower High/Low ratio for urea). This is explained by the greater reabsorption of urea that occurs in the collecting duct when urine flow rate declines, and to the dose-dependent influence of vasopressin on the terminal inner medullary collecting duct urea transporters

concentrated and urine flow rate relatively low, within the range of normal urine flows. This is well visible in the three examples shown in Fig. 10.2b. Thus, the contribution of urea to the urine concentrating mechanism has a negative counterpart by severely reducing the efficiency of its excretion. As explained elsewhere, a rise in glomerular filtration rate partially compensates this reduction [6].

The urine concentrating mechanism depends in part on several facilitated urea transporters, UT-A1/A3, UT-B and UT-A2 [7]. But importantly, the mammalian kidney also expresses energy-dependent urea transporters, as shown in Fig. 10.3. One is located in the pars recta of the proximal tubule (also known as proximal straight tubule (PST) or S3 segment) and is very likely SLC6A18 (see further). Two others have been functionally described, but have not yet been identified molecularly, "XXX" in the early part of the IMCD, responsible for urea reabsorption when protein intake is low, and "YYY" in the very terminal IMCD, that secretes urea. See further down for more details about these two urea transports.

The concept that urinary urea excretion results from filtration through the glomeruli followed by a variable amount of reabsorption along the tubules is much too simplistic. As already recognized more than 50 years ago [8, 9], in addition to this flow- and vasopressin-dependent reabsorption, urea excretion is regulated [8, 9]. Both energy-dependent urea reabsorption and energy-dependent urea secretion may occur through different transport processes, for the sake of either nitrogen salvaging or for more efficient urea excretion, respectively. A tendency for such a regulation is also apparent in humans, but to a much lesser extent [10]. As explained in more details below, experimental results suggest that the regulation associated with nitrogen conservation is a slow process (requiring weeks to occur) whereas the regulation associated with efficient urea excretion is rapid and probably under the control of peptidic hormones.
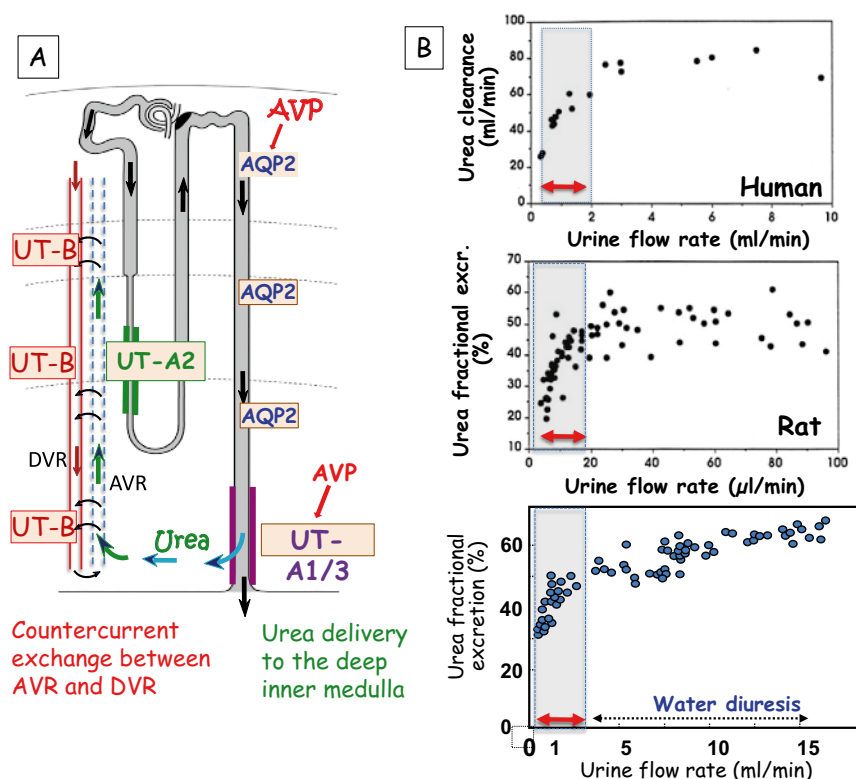
Fig. 10.2 Urea reabsorption in the collecting duct. Influence of urine flow rate on the fractional excretion of urea. A. Intrarenal urea recycling. UT-B, UT-A2, UT-A1/3 are facilitated urea transporters. Only UT-A1 and UT-A3 are activated by vasopressin (AVP). When AVP is present, part of the urea that flows in the terminal collecting duct diffuses into the medullary interstitium. Ascending vasa recta (AVR) take up this urea that is thus at risk of returning to the general circulation. But because they run in close contact with descending vasa recta, part of this urea undergoes counter-current exchange and can thus return to the inner medulla. This creates an "intrarenal urea recycling". (**b**) Relationship between urea clearance or fractional excretion and urine flow rate in three different studies. New figure drawn after data shown in [128] (top), [129] (middle) and [48] (bottom). With low flow rates observed in every day life (range shown by red double arrow), the efficiency of urea excretion declines sharply with declining urine flow rate (under the influence of vasopressin). These three examples show how urine concentration, associated with relatively low urine flow rates, dramatically decreases the efficiency of urea excretion. This marked decline in urea clearance or FEurea at low (but physiological) urine flow rates was shown in every text book 50 years ago (or more), but seems largely ignored in recent books

Experimental observations providing evidence for both acute and chronic regulation of urea excretion are shown in Figs. 10.4 and 10.5. Protein intake is known to increase the rate of glomerular filtration rate (GFR). As such, this can potentially increase urea excretion. But a regulation also occurs along the renal tubule. In the dog (a carnivore that has a greater load of urea to excrete), urea excretion rate is much greater after a protein meal than after an equivalent infusion of urea,

Fig. 10.3 Localization of urea transporters along the nephron and collecting duct. Energy-dependent transporters are shown in red. Others are facilitated urea transporters (see other chapters in this book). SLC6A18 is assumed to secrete urea in the pars recta. "XXX" is a transporter that allows reabsorption of urea in animals on a low protein diet. And "YYY" is a transporter that secretes urea in the very terminal inner medullary collecting duct. This secretion is very odd because, in the same structure, UT-A1 and UT-A3 allow urea reabsorption
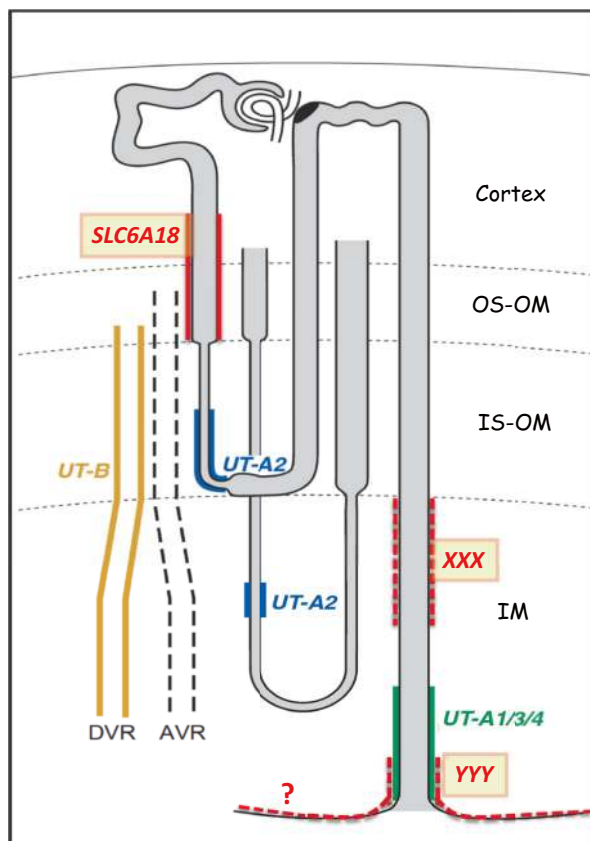

suggesting a specific regulation of this excretion (Fig. 10.4a) [11]. The regulation of urea excretion along the renal tubule is best evaluated by calculating FEurea, that is the fraction of the filtered urea that is excreted in the urine, often expressed as a percentage. FEurea is thus independent of the GFR. FEurea has been shown to increase after ingestion of a protein meal in both dogs and humans (Fig. 10.4b) [11, 12]. Glucagon, a hormone secreted in response to protein intake or to amino acid infusion also increases FEurea, as shown in two independent studies in rats (Fig. 10.4b) [13–15]. A long-term regulation of FEurea occurs in response to chronic changes in the protein content of the diet. A low protein diet for several weeks to humans or sheep results in much lower FEurea than on a normal protein diet [9], and these low values are reached whatever the level of urine concentrating activity (indicated by the urine-to-plasma concentration of inulin) (Fig. 10.5).
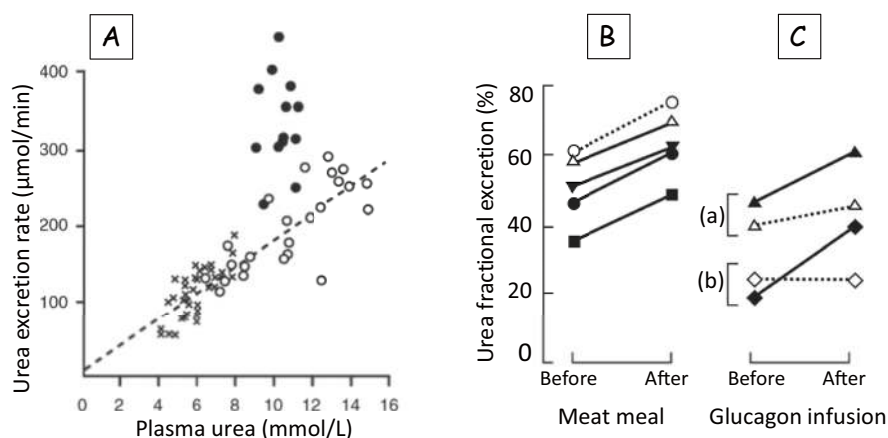
Fig. 10.4 Acute regulation of urea excretion. (**a**) Relationship between urea excretion rate and plasma urea concentration in one dog studied several times in three different conditions (8–10 experiments in each condition): control (crosses), after a meat meal (closed circles), and after an infusion of urea bringing the same amount of nitrogen as the meat meal (open circles). The influence of the protein meal clearly increased the urea excretion rate with little change in plasma urea concentration. In contrast, with an infusion of urea, urea excretion rate rose only in proportion to the rise in plasma urea concentration. Reproduced from Ref. [11]. (**b**) Influence of a protein meal on FEurea in dogs and humans. Black symbols show the results observed in three different dogs (mean of 8–10 experiments per dog). Adapted from Ref. [11]. White symbols (triangles and circles) show the mean results observed in 10 healthy humans studied in random order, either on a low (triangles) or a high (circles) hydration condition. Data for humans is adapted from data published in Ref. [12]. The meat meal increased FEurea by about 30% in both dogs and humans. (**c**) Influence of a glucagon infusion on FEurea in anesthetized rats during classical clearance experiments, in two independent studies (**a**) and (**b**). In each study, two different groups or rats received either an acute infusion of glucagon (solid line) or of vehicle (dotted line). Original data for (**a**) is from Ref. [15] and for (**b**) from Ref. [13]. In both studies, the infusion of glucagon increased FEurea by about 30% while the infusion of vehicle induced no change

Urea Reabsorption in the Kidney, as a Strategy for Nitrogen Conservation

Although mammals cannot breakdown urea because they do not express urease in any organ, some mammals can re-use urea nitrogen by virtue of two associated adaptations. One is the ability to reabsorb actively urea from the CD ("uphill" transport), thus reducing its urinary excretion. The other is hosting in their digestive tract bacteria that express urease and are thus able to hydrolyse urea, thus releasing carbon dioxide and ammonia. The former will pass into the blood and be excreted by the lungs, whereas the latter will have two possible fates (Fig. 10.6). Ruminants express the facilitated urea transporter UT-B in their rumen [16–19]. The bacteria will use urea nitrogen diffusing from blood into the rumen to build their own amino acids and proliferate [20]. The bacteria will subsequently be digested in the
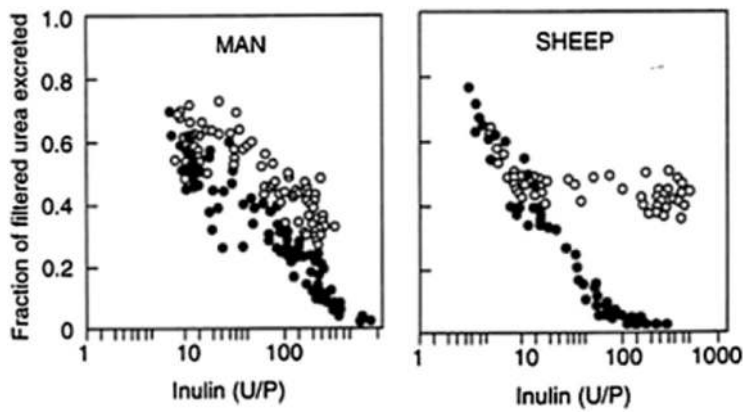
Fig. 10.5 Chronic regulation of urea excretion. Adapted from Ref. [130]. The two graphs show the fraction of filtered urea excreted in humans (MAN) and sheep in relation to the reabsorption of water measured as the inulin U/P ratio. A low protein diet (black symbols) significantly lowers FEurea relative to the filtration rate in both species but the effect is much more dramatic in the sheep than in man. The effect is graded according to urine flow and disappears at extreme water diuresis
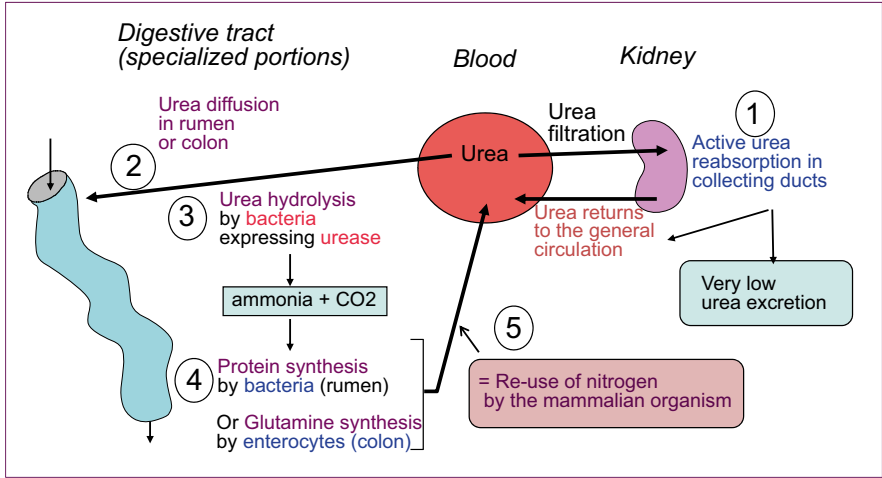
Fig. 10.6 Pathway for re-use of urea nitrogen in mammals (= nitrogen conservation). Filtered urea is reabsorbed in the early inner medullary collecting duct (as shown in low-protein fed rats) by an active transport, and is returned to the blood, thus reducing its renal excretion (1). Urea diffuses passively through facilitated UTs in the digestive tract (rumen in ruminants, or colon in other species) (2) where it is hydrolysed into ammonia and CO_2 by microorganisms expressing urease (3). Ammonia nitrogen can be re-used for protein synthesis (4), thus contributing to nitrogen conservation (5)

stomach, and their amino acids absorbed in the intestine, thus making nitrogen available again for the host. In other mammals, including humans, the bacteria able to hydrolyze urea are located in the colon which expresses UT-B [16, 21–27] or

UT-A [22, 23]. Ammonia resulting from urea breakdown will be used by the enterocytes of the host to make glutamine which can further be used for nitrogen metabolism (Fig. 10.6).

Because of the very low FEurea in sheep, Bodil Schmidt-Nielsen had assumed that an active urea reabsorption occured in their kidney [8, 9]. Sands and colleagues undertook several studies to characterize this urea reabsorption associated with low protein intake. They observed that an active urea reabsorption can be induced in rats by feeding them a low protein diet for several weeks. Using microperfusion of isolated segments of the inner medullary collecting duct (IMCD), they showed that this active absorption occurs in the early portion of the IMCD (closest to the outer medulla), increases with time up to a maximum after 3 weeks, depends on the presence of sodium in the lumen (but not in the bath), and can be inhibited by ouabain [28–32]. This suggests that a low protein diet induces the synthesis of a sodium-urea cotransporter and its insertion into the apical membrane of the early IMCD. Attempts to clone the transporter responsible for urea reabsorption in the rat kidney by either expression cloning or subtracting hybridization have not been successful [33–35].

In ruminants, the intensity of urea nitrogen recycling is regulated according to the protein content of the diet. With increasing level of protein intake, nitrogen recycling is reduced, along with reductions in urea reabsorption in the kidney, ruminal-wall urease activity and abundance of ruminal facilitated UT [17, 36].

Urea Secretion in the Kidney, Leading to Improved Nitrogen Excretion

It has been known for a long time that there is an addition of urea in the loop of Henle of superficial nephrons [37, 38]. This was assumed to result from facilitated diffusion of urea from ascending vasa recta into the thin limbs of Henle's loops which express the facilitated transporter UT-A2 in their lower half. This "recycling" of urea from blood to tubule was considered to play a significant role in the sequestration of urea in the inner medulla [4, 39]. This classical view, which prevailed for several decades, had to be revised when it was observed that mice with genetic deletion of UT-A2 do not show a urine concentrating defect [40, 41]. Thus, urea addition has to occur in some other site in the loop of Henle. *Note: the "loop of Henle" in micropuncture experiments includes all nephron segments comprised between the late proximal tubule and the early distal tubule accessible at the kidney surface: thus, it includes the pars recta of the proximal tubule, the thin descending limb and the medullary and cortical portions of the thick ascending limb, plus a very short piece of the early distal convoluted tubule.*

On the other hand, several authors had concluded from their observations that an active, energy-dependent urea transport probably occurs in the mammalian kidney [42–44]. About 50% of filtered urea is reabsorbed in the proximal convoluted tubule in the cortex at any level of urine concentration [37]. This reabsorbed urea is carried away by the intense cortical blood flow and cannot re-enter the nephron. However,

FEurea above 50% has been reported in a number of studies [45] (see Table 1 in [46]), suggesting that urea is added downstream of the late proximal convoluted tubule. Values above 100% have even occasionally been reported in rats, dogs, and humans (see review in [4]) and more recently in mice [4, 5]. Obviously, only a net tubular secretion of urea can account for these observations. This secretion most probably takes place in the pars recta of the proximal tubule [47–49]. Actually, a modest but significant urea secretion has been found in isolated cortical and medullary pars recta of the rabbit [42] (Fig. 10.7a). However, an active secretion is probably only modest in a herbivore such as the rabbit. A similar experiment, again in rabbit pars recta, did not reveal any urea secretion [50]. But the author used artificial solutions that contained no organic molecules. An important co-factor was missing in their experiment, as will be explained further below. Unfortunately, similar studies in pars recta of rats or mice are lacking. However, several authors reported
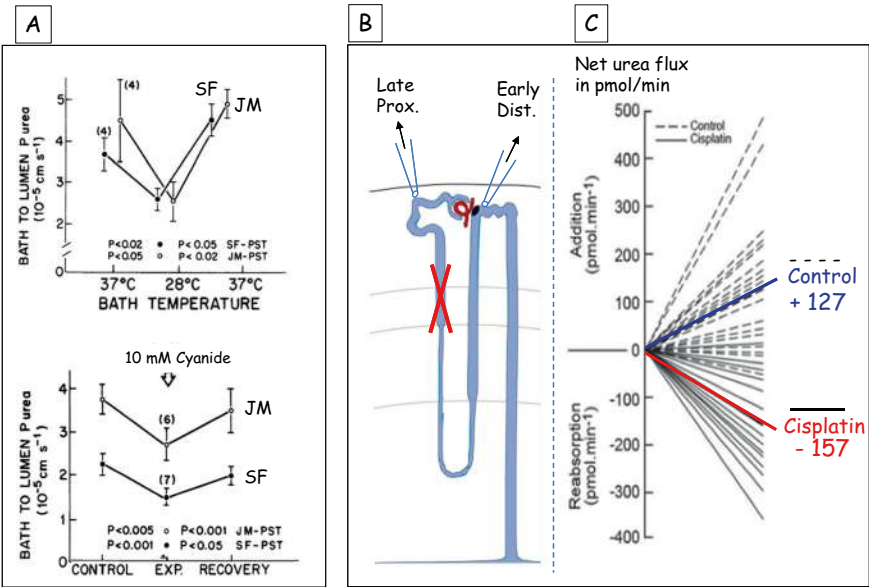
Fig. 10.7 Experimental results showing that urea is secreted in the pars recta. (**a**) Results obtained from microperfusion experiments of isolated rabbit PST and analysis of the collected perfusate. A positive bath-to-lumen flux of urea was observed in PST from superficial (SF) and juxtamedullary (JM) nephrons. This flux was largely and reversibly inhibited by a reduction in bath temperature or by addition of a metabolic inhibitor (cyanide), thus showing that this urea flux is energy-dependent. (**b**) Diagram of a nephron showing the two sites of fluid collection for analysis of tubular fluid, and the localization of the cisplatin influence on the pars recta (red cross). (**c**) Net urea mouvement between the late proximal and the early distal tubule in control rats and cisplatin treated rats. In control rats (dashed lines), a large amount of urea is added to the nephron lumen between these two sites. In contrast, when transport activity in the pars recta is impaired by cisplatin treatment, urea is largely reabsorbed. The magnitude of urea secretion in normal rats is thus equal to the difference between these opposite mouvements. Blue and red lines and numbers show the means of data in control and cisplatin-treated rats (in pmol/min), respectively. (Reproduced from Ref. [38]. No permission needed because this paper is in open access)

an accumulation of urea in rat cortical slices or in rat medullary rays that suggest active urea uptake by proximal tubule cells [51–55].

Additional evidence for active urea secretion into the pars recta comes from micropuncture studies in rats. Cisplatin is known to induce severe and selective damage in cells of the pars recta. The net addition of urea, observed between the late proximal and the early distal tubule in normal rats, was abolished and even reversed to a net reabsorption in rats treated for several days with cisplatin (Fig. 10.7b and c) [43]. This strongly suggests that the addition of urea into the loop of Henle, previously assumed to take place in the thin descending limb, is rather due to an active secretion into the pars recta.

In dogs (a carnivore which has greater loads of urea to excrete), urea excretion rate is much greater after a protein meal than after an equivalent infusion of urea, suggesting a specific regulation of this excretion [11]. FEurea rises markedly after a protein meal, an effect also reproduced by a glucagon infusion (Fig. 10.4) [13–15]. This suggests that glucagon, a hormone known to be secreted after a protein meal, may regulate the intensity of the active urea secretion [46].

Active urea secretion probably also occurs in the human kidney. This is suggested by the rare genetic anomaly resulting in "azotemia without renal failure" [47, 48, 56]. The affected subjects exhibit a selective three-to-four fold elevation in plasma urea concentration without any other sign of renal dysfunction. Their FEurea is extremely low (around only 10%). The relationship between FEurea and urine flow rate is shifted down to 30–50% lower values than in control subjects. This suggests that a large fraction of the excreted urea in normal subjects is due to a tubular process that is missing in these subjects. The defect is best explained by a mutation invalidating the function of a urea transporter contributing to secrete urea in the pars recta of the proximal tubule [46, 57].

Altogether, these observations strongly suggest that active urea secretion is part of the normal urea handling by the mammalian kidney. This secretion improves the efficiency of urea excretion, as is the case for other nitrogenous wastes (uric acid, ammonia). The pars recta of the proximal tubule is most likely the site of this urea secretion. It exhibits several anatomical features typical of a secretory segment and is known to secrete organic acids, uric acid, cyclic nucleotides and xenobiotics. It is surrounded mostly by ascending, venous vasa recta which provide this segment with its nutrient blood supply (capillaries issued from descending, arterial vasa recta are very scarce in the outer stripe of the outer medulla). We have recently proposed that the transporter likely responsible for this secretion is SLC6A18 [38]. However, this has not yet been proven experimentally. This will be explained in detail in the next section.

The secreted urea originates in unknown proportion from a mixture of urea present in medullary blood (urea never filtered, that remains in plasma after filtration in the juxtamedullary glomeruli), and from urea added to the inner medulla by the vasopressin-dependent action on the terminal CD and flowing up in ascending vasa recta blood. Red cells could also contribute significantly to supply urea during their relatively slow ascent in venous vasa recta because they express abundantly UT-B and may thus quickly equilibrate with surrounding plasma urea [58].

The amount of urea that could be added by secretion has been calculated [38] taking into account the percentage of plasma filtered into the juxtamedullary glomeruli from which DVRs originate, and the urea carried by erythrocytes. Calculations based on the experiments by Safirstein et al. [43] suggest that about 17 µmol/min urea are added by secretion into the loop of Henle in the rat. This figure is fully compatible with the amount of urea brought by DVRs into the outer medulla which amounts to 27.6 µmol/min. See detailed calculations in [38].

SLC6A18, the Transporter Likely Responsible for Urea Secretion in the Proximal Straight Tubule

The transporter that is most likely responsible for urea secretion in the PST is SLC6A18, a transporter that has been shown to transport glycine. A series of observations reported in the literature suggests that it could actually be a urea/glycine antiport [38]. This hypothesis of course requires confirmation by appropriate experiments in vitro, or by the study of knockout mice.

1. SLC6A18 is expressed only in the kidney, and there, only in the luminal membrane of cells of the S3 segment of the proximal tubule [59–61]. Figure 10.8 shows this localization in the S3 segment ("pars recta") of the proximal tubule.
2. Two independent studies investigated the consequences of SLC6A18 deletion in transgenic mice [62, 63]. Both reported a large rise in urinary glycine excretion and concluded that the function of SLC6A18 is to reabsorb filtered glycine that had not yet been reabsorbed upstream in previous subsegments of the proximal tubule. The transport of glycine by *SLC6A18* is sodium-dependent [63]. Humans with mutations of SLC6A18 also show an increase in urinary glycine excretion. But none of these studies measured plasma urea and urinary urea concentration.
3. In the study by Singer et al. [63] the amount of glycine excreted in the urine of knockout mice is huge (about 50 times that of wildtype mice) and the concentration of glycine in urine is 200 times higher than in plasma. How could so much glycine have escaped reabsorption upstream is difficult to understand. SLC6A19, another transporter of the same family, is expressed in the proximal tubule. It is a neutral amino acid transporter and reabsorbs amino acids in the S1 and S2 segments of the proximal tubule [64, 65]. Thus, only little glycine should remain in the lumen of the S3 segment.
4. Interestingly, in 1980, Barfuss et al. described that PST cells (but not cells of the proximal convoluted tubule) take up glycine from their basolateral membrane by an energy-dependent and sodium-dependent transport [66]. This may explain how so much glycine is excreted in the urine when the apical glycine transporter is deleted. But why would this nephron segment take up this amino acid from the blood?
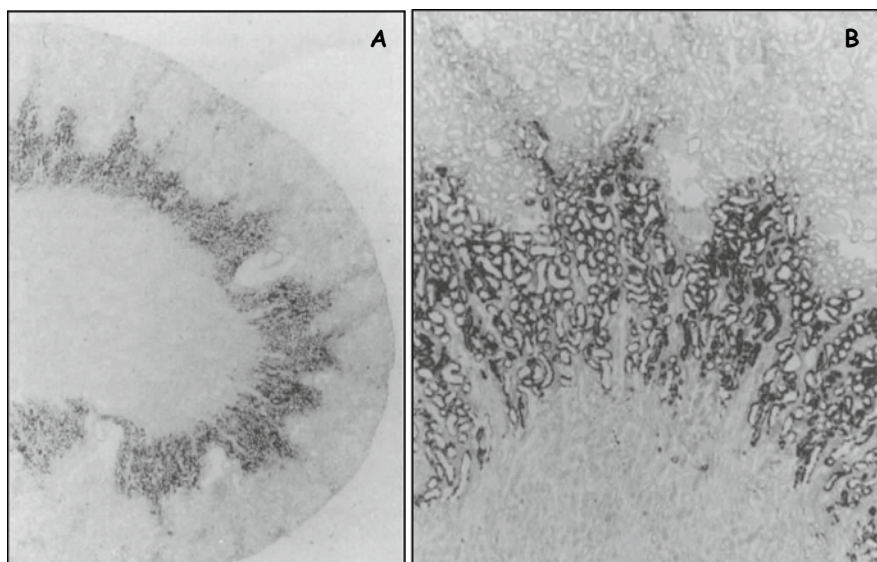
Fig. 10.8 In situ hibridization of SLC6A18 on a cryosection of an adult rat kidney. This picture reveals the localization of SLC6A18 mRNA. There is a strong and homogeneous labeling of the proximal tubules, exclusively in the deep part of the medullary rays in the cortex, and in the outer stripe of the outer medulla. This localization corresponds to the S2 and S3 segments of the proximal tubule (magnification in A × 14 and in B × 50). (Reproduced from Ref. [59]. No permission needed because this paper is in open access)

5. Glycine and urea are very close molecules. They have similar molecular mass (60 and 75 Da, respectively) with only one carbon atom. They are both neutral and show no chirality. This similarity led us to assume that both substances may be transported simultaneously and in opposite directions.

Altogether, these different observations led us to propose that SLC6A18 could be an antiport secreting urea against glycine, and that glycine could be recycled from the brush border back into the cells. Figure 10.9 shows how this counter-transport of urea against glycine operates, and how glycine recycling could work.

The failure of Knepper to find an active secretion of urea in the rabbit pars recta [50] (as Kawamura and Kokko had reported [42]) is most likely attributable to the fact that he used artificial solutions as bath and perfusate of the tubules, and thus no glycine was available in these fluids. Thus, an exchange of urea versus glycine could not take place.

AQP1 is abundantly expressed on both sides of all cells of the proximal tubule, including PST cells, and allows the abundant water reabsorption that takes place in this tubule. Intriguingly, the aquaglyceroporin AQP7 is expressed in the luminal membrane of PST cells, but not PCT cells, in addition to AQP1 [67, 68]. Why would an additional aquaporin be expressed there, and only in the luminal membrane? Probably not just to transport water. AQP7 can transport glycerol [67]. Glycine and
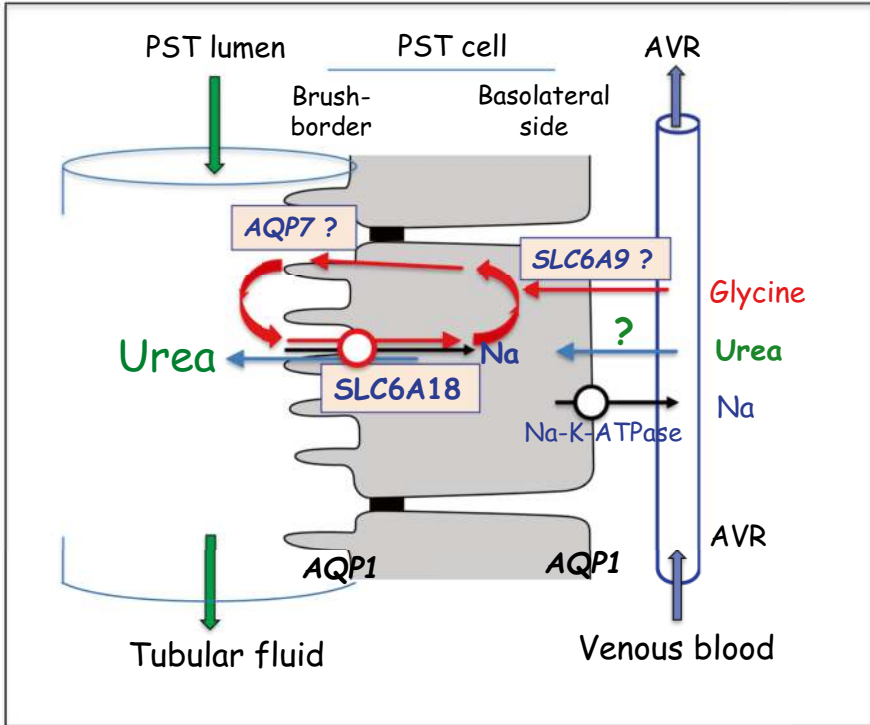
Fig. 10.9 Model of urea secretion in a PST cell, via the urea/glycine antiport. SLC6A18 is located in the luminal membrane (the brush border). Urea is secreted and glycine is reabsorbed along with sodium. The energy ensuring this counter-transport is provided by the sodium pumping at the basolateral Na-K-ATPase. Initially, the counter-transport of glycine and urea can be initiated by the uptake of some glycine from the basal side of the cell. An uptake of glycine could be provided by the glycine transporter SLC6A9 that is expressed in the pars recta. Glycine is not secreted into the lumen but is transciently stored in the brush border and is continuously recycled between the brush border and the cell body, while urea is secreted against one (or more) Na. Because AQP7 is expressed only in the PST, in addition to AQP1, it is possible to assume that it may play a special role there for recycling glycine, assuming that this aquaglyceroporin could indeed transport glycine. Blood flowing in the ascending vasa recta (AVR) supply urea and glycine to the pars recta cells. (Adapted with modifications from Ref. [38]. No permission needed because this paper is in open access)

glycerol show some similarities. It is attractive to assume that AQP7 could transport glycine and could contribute to glycine recycling in the brush border of PST cells. This is very speculative but could be easily evaluated by comparing in vitro the permeability of AQP7 to glycerol and to glycine in amphibian oocytes injected with AQP7 cRNA, as described previously [69, 70].

Which membrane transporters could allow glycine and urea to be taken up from the blood by PST cells? Another member of the SLC6 family, SLC6A9, is expressed in the same nephron segment as SLC6A18 and is described as a glycine transporter (https://esbl.nhlbi.nih.gov/Databases/SLC-kidney/). It could possibly allow glycine

uptake from the basolateral membrane of PST cells. This is of course just a hypothesis. Up to now, no known urea transporter could explain the uptake of urea in PST cells. But may-be there is no transporter involved. It is known that about 40–50% of filtered urea is reabsorbed in the proximal convoluted tubule (S1 segment) and no urea transporter has been characterized so far in this segment. If urea is secreted into the lumen of the PST, its intracellular concentration should be lower than that in peripheral blood and this should provide a driving force for blood urea to enter the cells.

Several observations across the animal kingdom suggest associations of SLC6A18 with ureotelism and/or with the need to conserve urea or to participate in urea excretion.

1. *SLC6A18* is among the genes that are lost in the transition of marine mammals to aquatic life [71]. Actually, these mammals do not need to concentrate urea in the urine because they can produce abundant urine volumes.
2. Most fish are ammoniotelic. But the fish Tilapia (living in an alkaline environment in the African lake Magadi) is ureotelic [72]. It expresses a facilitated urea transporter in its gills with high homology with urea transporters from mammals [73], and expresses SLC6A18 in its intestinal epithelium [74].
3. Elasmobranchs (rays and sharks) exhibit a very high urea concentration (>300 mM) in their internal milieu. They need to avoid the loss of urea through the gills, rectal gland and kidneys. Interestingly, *SLC6A18* sequence appears in the gene bank for several shark species (see details in [38]).
4. Most bony fish are ammoniotelic, but a few are ureotelic during their embryonic life. SLC6A18 has been identified in the zebrafish embryo [75].

Altogether, these observations bring an additional support for a role for SLC6A18 in urea handling.

Functional Consequences of Urea Secretion in the Proximal Straight Tubule

Benefits of Urea Secretion

The fact that urea is secreted into the nephron lumen in addition to the amount filtered improves markedly the efficacy of its excretion and limits the rise in plasma urea that takes place after each protein meal. Preventing or limiting the rise in the concentration of urea in plasma is important because urea can be toxic to some extent. It forms cyanate which induces carbamylation of proteins (similar to the glycation occurring with glucose in diabetic patients). The function of carbamylated proteins is reduced (decreased efficiency of immune cells, lower transport for oxygen by hemoglobin, etc....), and thus many regulations are impaired. In patients with CKD who exhibit increased plasma urea concentration, carbamylation of proteins becomes significant and its adverse effects have been well described [76–79].

The intensity of urea secretion is not easy to evaluate in vivo. A variable that can reflect this intensity is the urine-to-plasma ratio of urea concentrations. Urea secretion lowers plasma urea concentration and increases urine urea concentration. Thus, an increase in the U/P urea ratio means an increase in urea secretion (assuming no interference occurs, due to the influence of vasopressin which could stimulate urea reabsorption in the collecting duct).

Glucagon secretion is increased after a protein meal. Glucagon has been shown to have direct and indirect effects on the kidney [80]. Glucagon has been shown to increase markedly absolute and fractional excretion of urea in vivo [13, 15]. It is tempting to assume that glucagon could stimulate urea secretion in the pars recta by an indirect action mediated by liver-borne extracellular cAMP, as explained in detail elsewhere [6, 81]. This hypothesis requires confirmation by experiments in isolated perfused PST.

Influence of Urea Secretion on the Understanding of the Urine Concentrating Mechanism

It is important to understand the difference between counter-current exchange and counter-current multiplication. Both occur between structures that lie in parallel and with fluid flows running in opposite directions. Counter-current exchanges do not require energy and the transported solute(s) can only move "downhill". In contrast, counter-current multiplication requires energy to create an "uphill" concentration difference between the two structures.

The urine concentrating mechanism (UCM) that is presently described in all text books and chapters includes two main processes. (1) A counter-current multiplication of sodium concentration between the thick ascending limbs and the thin descending limbs in the inner stripe of the outer medulla providing the "single effect" that is multiplied within this kidney zone. (2) Passive movements of urea allowed by facilitated UTs and counter-current exchanges, explaining the accumulation of this solute in the inner medulla (see Figs. 10.1 and 10.2). The possible existence of an energy-dependent secretion of urea in the medulla is not mentioned except in rare reviews by Bankir et al. [1, 3, 4, 46]. Mathematical models simulating this "passive" concentrating mechanism fail to reach urine osmolarities observed in vivo [82–84]. Interestingly, a model including an active secretion of urea in the pars recta [85] revealed a "urea-selective" improvement in urine concentrating ability. The efficiency of urea excretion was improved without requiring a higher urine flow rate, and with only modest changes in the excretion of sodium and other solutes.

The renal handling of urea described in this review, including an energy-dependent urea secretion in the pars recta, creates a countercurrent multiplication of urea within the outer medulla, as described in Fig. 10.10. Urea concentration is "multiplied" because urea secreted into the pars recta in the OS-OM is transferred to AVR in the IS-OM, where is it carried up towards the OS-OM. It can then be
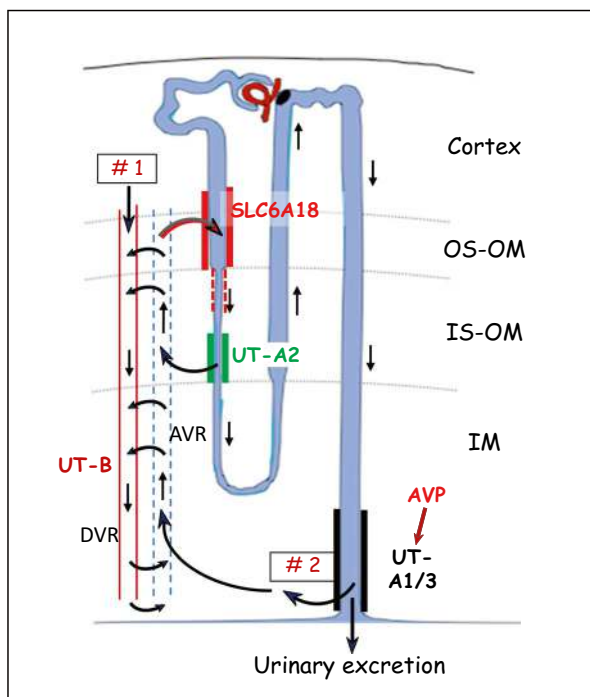
Fig. 10.10 Countercurrent multiplication of urea. Diagram of a nephron (combining a short-looped and a long-looped nephron) and a collecting duct, depicting urea handling in the kidney, and including urea secretion in the PST. The localization of the facilitated urea transporters UT-B, UT-A2 and AVP-stimulated UT-A1/3 is shown. DVR (red) and AVR (fenestrated) are descending (arterial) and ascending (venous) vasa recta, respectively. The four kidney zones of the kidney include the cortex, the outer and inner stripes of the outer medulla (OS-OM and IS-OM, respectively), and the inner medulla (IM). Thin straight arrows show the direction of tubular fluid flow. Thin curved arrows show countercurrent exchanges of urea between AVRs and DVRs. The thick red lines along the PST show the localization of SLC6A18 that allows the secretion of urea in exchange of glycine and one (or more) sodium. The urea available for secretion originates from two different sources. #1 shows urea entering the medullary circulation by DVRs issued from the efferent arteriole of juxtamedullary glomeruli, after about 25% of the plasma has been filtered. This never-filtered urea flows down in DVRs towards deeper regions of the medulla. #2 represents urea that was filtered, was carried in tubular fluid along the nephron, and reached the terminal IMCD where it diffused in the inner medullary interstitium through vasopressin-stimulated UT-A1/3. From the inner medullary interstitium, urea is taken up by AVRs and may be secreted into the PST in the OS-OM. That UT-A2 is expressed only in the deep part of the thin descending limbs of short loops has been well demonstrated by Nielsen et al. [131]. Urea from both sources (#1 and #2) can diffuse out of the thin limbs via UT-A2, ascend in AVRs and be secreted again in the PST. This amplifies urea concentration in the pars recta lumen and thus creates a countercurrent multiplication of urea. Moreover, it minimizes the return of urea into the venous circulation. (Reproduced with slight modifications from Ref. [38]. No permission needed because this paper is in open access)

secreted again, thus increasing its concentration in the pars recta lumen. Thus, in addition to the well understood counter-current multiplication for sodium that occurs between the thick ascending limb and the thin descending limbs, a counter-current multiplication for urea occurs between the pars recta and the ascending vasa recta. This energy-dependent urea transport accounts for the high urea concentration observed in the inner medulla (Fig. 10.1). This critical step of urea handling explains the large addition of urea well described in several species between the late proximal convoluted tubule and the early distal tubule accessible at the kidney surface by micropuncture (see Fig. 1 in [38]). It is dependent on the vasopressin-induced urea permeability of the terminal IMCD by UT-A1/3, as shown by results observed in UT-A1/3 knockout mice [5]. If urea does not diffuse from the lumen of the terminal IMCD into the inner medullary interstitium, the amount of urea susceptible to be secreted into the pars recta will be largely reduced. Two studies have shown that the knockout of UT-A2, expressed in the thin descending limbs does not result in a significant urine concentrating defect. This suggest that urea movements through this facilitated urea transporter play a role in the initiation and/or amplification of urea secretion, but not in steady state conditions. In some knockout mice models, the expected changes are best observed when the function of the proteins under study is evaluated during an acute stimulus (e.g. a sudden urea load [41, 86]).

Influence of Urea Secretion on GFR

The catabolism of dietary carbohydrates and lipids produces only CO_2 and H_2O (= metabolic water) which are easily excreted by the lungs and kidneys, respectively. In contrast, the catabolism of proteins produces a number of end-products that are excreted by the kidneys: urea, ammonia, uric acid, phosphates, sulfates, protons, etc. Moreover, because the concentrations of these solutes in plasma and extracellular fluids are relatively low (a few mmol/L or even μmol/L), their renal excretion imposes a need to concentrate them in the urine far above their concentration in the plasma for the sake of water economy (see Table 2 in [87]).

As recalled above, a single protein-rich meal or an amino acid infusion are known to induce a transient rise in glomerular filtration rate (GFR) (often referred to as "hyperfiltration") [12, 88–91]. And a sustained high protein intake (but not a high carbohydrate or lipid intake) induces a permanent increase in GFR [92, 93]. At least two hormones play a major role in this hyperfiltration, as described in details by Bankir et al. [6]. Protein-induced hyperfiltration does not occur in Brattleboro rats with hereditary central diabetes insipidus which cannot secrete vasopressin [94]. It also does not occur in pancreatectomized patients who can no longer secrete glucagon [95, 96].

This rise in GFR is likely due to a reduction in the tubulo-glomerular feedback operating at the juxtaglomerular apparatus, as shown in the elegant micropuncture study of Seney et al. in rats fed either a high or a low protein intake for 7–10 days [97]. In the fluid of the early distal tubule (the closest accessible site to the macula

densa), sodium and chloride concentrations were markedly lower in rats fed the high protein diet than in those fed the low protein diet. But interestingly, the osmolality of the tubular fluid was identical in the two conditions [97]. This means that another solute was present in the tubular fluid in much higher concentration on the high than on the low protein diet. This solute acts as an "osmotic buffer" limiting the risk of water leakage from the cortical thick ascending limb where the transepithelial difference in osmolarity becomes greater. This solute is obviously urea that is excreted in much larger amount on a high protein intake. Most likely, urea secretion is more intense on the high than on the low protein diet. Although not yet demonstrated experimentally, glucagon most likely stimulates urea secretion indirectly (as explained in [80, 98]. Vasopressin also favours urea secretion as explained above, by favouring urea delivery to the pars recta because of its action on urea transporters of the terminal IMCD that favour intrarenal urea recycling. The sequence of events by which glucagon and vasopressin each contribute to increase the GFR is schematized in Fig. 10.11.

As explained earlier in this chapter, the ratio of the concentration of urea in urine and plasma (urine-to-plasma concentration ratio = U/P urea) provides an index of the relative concentration of urea at the macula densa. In a number of studies in rats and humans, striking significant correlations have been observed between GFR (measured by inulin clearance) and the U/P urea ratio [6, 99, 100] (Fig. 10.12), or between the change in GFR (= hyperfiltration) and the change in this ratio in response to a glucagon infusion (see Fig. 4 in [15]). These correlations cannot establish a causality link. But the explanations given above strongly support such a causality.

Secondary Active Urea Transport in Other Organs

Table 10.3 summarize the different secondary active urea transports identified or suspected to occur in different tissues of mammals. Although well characterized functionally, the transporters responsible for two Na-dependent urea transports in the renal collecting duct have not been molecularly identified. Moreover, it seems highly likely that energy-dependent urea transport could take place in two other organs, the testis and bladder, as explained below.

Testis

In 1979, Turner et al. published a study suggesting the existence for an active transport of urea into the rat seminiferous tubules [101]. After an intravenous injection of radio-labeled [14C]urea, seminiferous tubules accumulated urea at a higher concentration than in the blood. This uphill movement of urea was inhibited by 2, 4-dinitrophenol and ouabain, thus providing evidence for active transport of urea
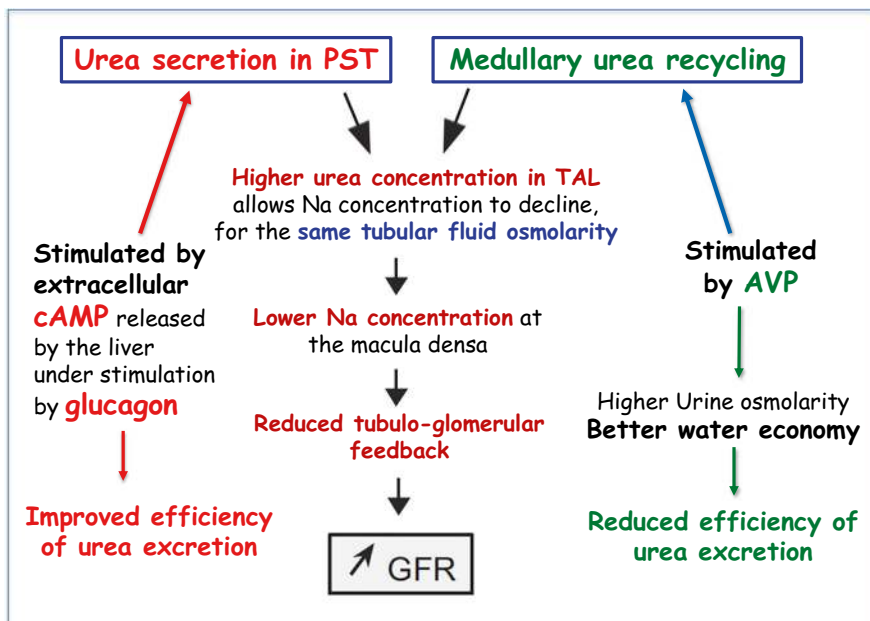
Fig. 10.11 Mecanism by which urea handling influences GFR. Both the secretion of urea in the PST and the medullary urea recycling induce a larger amount of urea to flow in the loop of Henle, and thus increase the concentration of urea in the thick ascending limb. This explains how urea, indirectly may influence the GFR. Vasopressin (AVP) stimulates urea recycling (well demonstrated). Glucagon probably stimulates urea secretion, indirectly (see text). (Reproduced with slight modifications from Ref. [38]. No permission needed because this paper is in open access)

into the rat seminiferous tubules. When facilitated urea transporters (UTs) were cloned 15 years later, two facilitated UTs were identified in the rat and mouse testis, UT-3 [102], and UT-A5 [103]. In the rat kidney, *UT-3 mRNA* is expressed in the inner stripe of the outer medulla, inner medulla, the papillary surface epithelium, and the transitional urinary epithelium of the urinary tract. In situ hybridization of testis revealed that UT-3 is located in Sertoli cells of seminiferous tubules. The signal was only detected in Sertoli cells associated with the early stages of spermatocyte development, suggesting that urea may play a role in spermatogenesis. *UT-A5 mRNA* is restricted to the peritubular myoid cells forming the outermost layer of the seminiferous tubules within the testes, and is not detected in kidney. *UT-A5 mRNA* level is coordinated with the stage of testes development and increases 15 days postpartum, commensurate with the start of seminiferous tubule fluid movement [103]. The functional significance of urea movements in the testis has not been evaluated in these studies.

In many epithelia where a secondary active transport is present, the energy-dependent transporter is expressed on one side of the epithelium and a facilitated traporter is expressed on the opposite side. For example, the sodium-coupled transporter SGLT2 is expressed on the apical membrane of the proximal convoluted
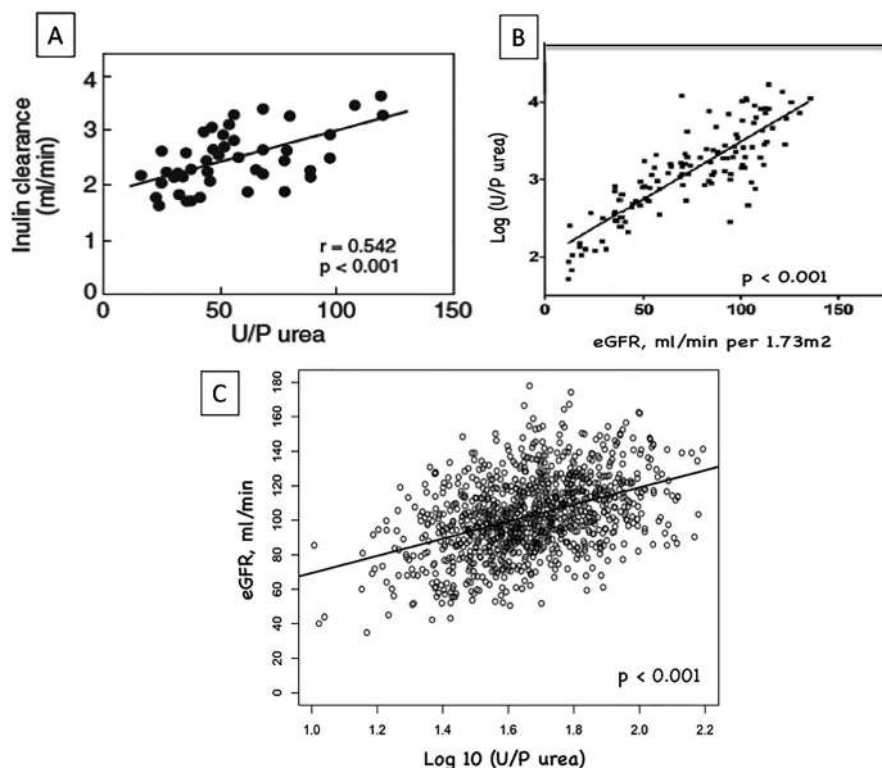
Fig. 10.12 Associations between the urine-to-plasma ratio of urea concentrations and GFR in rats (**a**) and humans (**b** and **c**). This U/P ratio is an accessible marker of the transepithelial concentration difference for urea (between tubular fluid and peritubular fluid) prevailing at the inaccessible macula densa. (**a**) Anesthetized normal rats (each point is the mean of 3 × 20 min clearance periods for one rat). (**b**) Patients with autosomal dominant polycystic kidney diease. (**a** and **b**) Reproduced from Ref. [6]. No permission needed because this paper is in open access. (**c**) Subjects from a population (SKIPOGH), reproduced from Ref. [100]. No permission needed because this paper is in open access)

tubule, and GLUT2 on the basolateral membrane [104]. Thus, the existence of facilitated UTs in the testis could be associated with an energy-dependent urea transporter. As mentioned above, the SLC6 family mostly encodes transporters for nitrogenous molecules. SLC6A18 most likely transports urea as a urea/glycine antiport, as explained above. Another member of this family, SLC6A16, is still an orphan transporter [105, 106]; no substrate has been characterized so far for this transporter. But genetic data bases indicate that its expression is extremely high in the testis (50 times higher than in other organs) (https://www.proteinatlas.org/ENSG00000063127-SLC6A16/tissue). This extremely high expression in the testis suggests that it probably plays an important role in this organ. Could SLC6A16 be involved in an uphill urea transport?

Table 10.3 Secondary active urea transports in mammals

Organ	Tissue	Direction of transport	Functional significance/ functional demonstration	Transporter
Kidney	PST	Secretion	Adding more urea in the nephron lumen for more efficient urinay excretion (compensating at least partially the abundant reabsorption via UT-A1/3)	SLC6A18 (very likely)
Kidney	Upper IMCD	Reabsorption	With low protein intake in the food (LP), limitation of urinary loss of urea. Reabsorbing filtered urea for the sake of nitrogen salvage. Probably constitutive in herbivores. Inducible in rats after 3 weeks on LP diet.	Transporter not known. Na-dependent. Inhibited if NaK-ATPase is inhibited by ouabain or by removing bath K, or perfusate Na, suggesting secondary active transport. Not inhibited by phloretin nor stimulated by vasopressin
Kidney	Terminal IMCD	Secretion	Suggestion: early expression of a transporter extending further down in the pelvic epithelium, ureters and bladder, to prevent dissipation of the high urea concentration in urine	Transporter not known. Secondary active Na-dependent urea transport, inhibited by phloretin, stimulated by AVP
Bladder	Urothelium	Secretion	Preventing diffusion of highly concentrated urea back into the blood when urine (with high urea concentration) stays for hours in the bladder lumen.	Not known (possibly the same as that in terminal IMCD?)
Testis	Seminiferous tubules	Secretion	Providing a driving force for fluid entry into the lumen of the tubules, in order to create a flow of fluid for driving the sperm cells in a flow of fluid along the tubules	SLC6A16 (suspected)

Abbreviations. *PST* proximal straight tubule. *IMCD* collecting duct running in the inner medulla

Actually, an issue that has been rarely addressed is how fluid enters in the seminiferous tubules to carry the sperm cells down along these long tubules. In the kidney of mammals (and of vertebrates in general), fluid enters the nephron lumen by filtration of plasma that occurs in the glomeruli. Further down, mostly in the S3 segment of the proximal tubule, certain solutes are secreted from peritubular blood to nephron lumen and this drives water along because the S3 epithelium is "leaky". A water flow is thus driven by the osmotic force generated by the solute transport.

Interestingly, in "aglomerular" fish (which nephrons do not possess a glomerulus), the transepithelial secretion of inorganic and organic solutes drives a secretory water flow in renal proximal tubules. Thus, the primitive urine provides exclusively from fluid and solutes secreted into the proximal tubule [107].

The abundant expression in the testis of facilitated urea transporters and of the Na-dependent transporter SLC6A16 suggests that a similar secretory process could take place in the testis to initiate a flux of fluid, driven by urea secretion, into seminiferous tubules. This totally novel hypothesis is supported by several observations. First, a few studies have shown that urea concentration in the lumen of seminiferous tubules is significantly higher than in the blood [108]. Second, Guo et al. [109] studied the role of the urea transporter UT-B in the testis and other organs by comparing urea handling in wildtype and UT-B knockout mice. Here, we will consider only the data reported for wildtype mice. In steady state conditions, the concentration of urea in testis was about 5.75 times higher than in serum, whereas it was only 1.1 times higher in the brain and 1.9 times higher in the liver (Fig. 10.13). The ratio of urea concentration in testis to blood was lower in very young mice than in older mice. In acute experiments, the uptake of urea by different organs was evaluated in mice in which renal blood flow was blocked (to prevent excretion of the radioactive marker). Five minutes after the administration of an intravenous bolus of [^{14}C]-labeled urea, the concentration of radioactive urea in testis was 3.6 times higher than in the blood (as calculated from Fig. 3 in [109]) (Fig. 10.13). Altogether, these data suggest that there is an uptake of blood urea by the testis. In vitro perfusion of seminiferous tubules [110] showed that addition of urea in the bath induced the appearance of urea in the lumen with a rate of influx reaching a steady state after about 20 min. The rate of urea influx was inhibited by about 50% by the inhibitor phloretin [110]. The authors did not determine if urea concentration in the lumen became significantly higher than in the bath, and did not evoke the possibility of an energy-dependent uptake or urea. But in view of the secretion described by Turner [101], of the studies showing that urea is more concentrated in the luminal fluid than in the blood, and in the observations described in Fig. 10.13, it seems possible that a secondary active urea transporter contributed to the urea influx reported by Fenton et al. [110].

Further experiments are needed (1) to study directly if seminiferous tubules take up urea from the blood and secrete it into the lumen, and (2) to study if SLC6A16 transports urea.

Bladder

The possibility that urea could undergo an active transport in the mammalian bladder is rarely addressed and generates little attention in the scientific community. This is however surprising in the light of the following observations.

Fig. 10.13 (**a**) The concentration of urea has been measured in blood serum, brain, liver and testis of normal mice. The concentration in the testis was much higher than in the brain and liver, and was about 5.75 times higher than in the serum. (**b**) Concentration of urea in serum and testis in mice at different ages (from 10 to 40 days). The concentration of urea was about five-fold higher than in serum in mice 15 weeks and older. Urea is concentrated in the rat testis. (Adapted from Ref. [109]. Permission requested by Dr Yang)
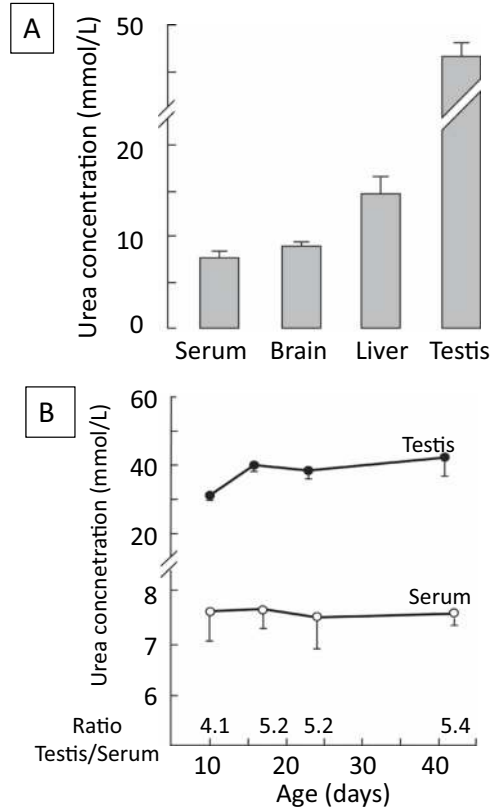
1. In most mammals, urea exhibits concentrations in the urine far higher than in the plasma. Typically, urea concentration in urine may be 20–100 times higher than in plasma for humans on a normal Western type diet. In laboratory rodents (rats and mice), the urine/plasma ratio of urea concentrations can reach 150–200 in normal conditions [86] and even more during dehydration or after administration of the vasopressin V2 receptor agonist dDAVP. And it can be as high as 500 in some rodent species adapted to arid life. It is difficult to understand how such huge transepithelial differences could be maintained inside the bladder for hours without an energy-dependent transport process.

2. The urothelium strongly expresses the facilitated urea transporter UT-B in its basolateral membrane [111]. Thus, the only barrier preventing equilibration of urea concentration between blood and bladder urine is the apical membrane. Even if the urothelium exhibits a unique anatomical structure and a low permeability to urea (as measured in vitro), it is difficult to imagine that it could prevent the diffusion of urea back into the blood when concentrated urine stays in the lumen for hours between micturitions. The permeability to urea of the rabbit bladder, studied in vitro, has been found to be low [112, 113]. But the rabbit shows a relatively low urinary urea concentration in the urine because of a low

urea excretion related to its vegetarian diet. Some urea (and water) may be reabsorbed along the urinary tract and bladder in dogs and rats [114] and this reabsorption is influenced by hydration and dietary protein intake [115, 116].

3. An intriguing observation has been made in the deepest subsegment of the IMCD in rats: urea was shown to be secreted by a Na-dependent transport system [117]. Net urea secretion was significantly inhibited by phloretin (SGLT inhibitor, added to the perfusate) and ouabain (Na,K-ATPase inhibitor, added to the bath). It was also inhibited by cooling the tubule to 23 °C. Net urea secretion was significantly stimulated by vasopressin (added to the bath). The functional meaning of such urea secretion in this site is very surprising because the facilitated urea transporters UT-A1 and UT-A3 allow an abundant and very fast diffusion of urea from IMCD lumen to the inner medullary interstitium [7]. Thus, it is difficult to understand what could be the functional meaning of a (small) urea secretion in opposite direction at this site. Actually, it is possible to interpret this secretion in a different way. The very late IMCD is in continuity with the urothelium lining the pelvis and the ureters. This urea secretion in the very late IMCD thus could be an early manifestation of the secretion that probably takes place in the perlvic space and along the ureter and bladder urothelium, in order to reclaim the urea susceptible to diffuse out of the urinary tract.

Thus, an energy-dependent urea secretion very likely takes place in the pelvic cavity of the kidney and along the urinary tract (ureters and bladder urothelium) as schematized in Fig. 10.14. This situation can be compared to that observed in the gills of elasmobranchs. They have a very high concentration of urea in the blood (about 300 mmol/L), to counteract the high osmolarity of the sea water. Thus, they are at continuous risk to loose urea through the gills which offer a very large area of exchange between the blood and see water. Fines et al. [118] showed, in Squalus acanthias, that there is an active sodium-coupled transport of urea from out of the gill's epithelium back into the blood, against the urea concentration gradient. This active urea transport, associated with special anatomical characteristics of the gill epithelium, contribute to urea retention by the gills. A similar situation occurs in the mammalian bladder, with a very special urothelium, and a strong transepithelial urea concentration difference. Studies intended to characterize this putative urea secretion in the mammalian bladder urothelium could be run using the experimental model of in situ isolated bladder designed by Spector et al. [115].

The knock out of UT-B in mice induces DNA damage and apoptosis in the bladder [119]. Actually, UT-B (SLC14A1) has been shown to be a biomarker and target in urothelial human cancer [120, 121]. It may be assumed that an imbalance between urea transport in both sides of urothelial cells (UT-B basolateral, and an apical transporter) may expose the cells to toxic concentrations of urea.
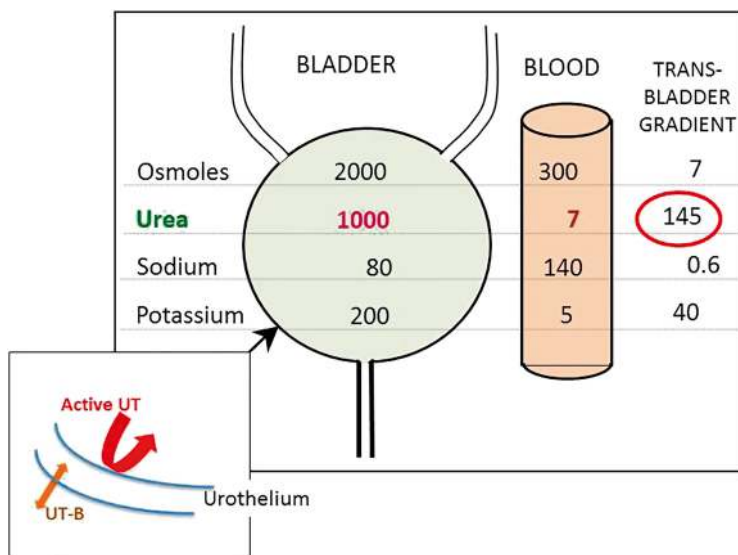
Fig. 10.14 Large urea concentration gradient between bladder and blood. Rounded values corresponding to the situation observed in normal rats. Urea is markedly more concentrated in the urine than in the blood, as shown by the large trans-bladder concentration gradient. Moreover, urine stays for long periods in the bladder lumen, and the facilitated urea transporter UT-B is expressed on the baso-lateral aspect of urothelial cells. Even with a very specialized urothelium structure, exhibiting a very low permeability to urea, we assume that the bladder could not maintain a high transurothelial gradient without an active urea transporter (red arrow) that continuously pumps back urea that is at risk of diffusing out of the bladder

Conclusion. Future Studies

This chapter is largely original because it presents several features of the renal handling of urea that are not frequently addressed. The attention has rarely been drawn on the existence of an energy-dependent urea secretion in the mammalian kidney. Evidence showing that urea is secreted has already been presented in several book chapters and reviews [1, 3, 4, 38, 46] but these papers have not been given much attention so far. Most renal physiologists were reluctant to accept the possibility of such a secretion in spite of the fact that it is difficult to understand how concentrating a large load of urea at a high level could not require some energy-dependent process. It is surprising that there has been so few experimental attempts to characterize a possible urea secretion. All the more so because all the mathematical models intended to simulate the urine concentrating mechanism failed to reach the urine osmolarity observed in vivo (as recalled above).

In classical acute clearance experiments in anesthetized rats, the rise in FEurea that could have revealed this secretion was probably compromised by the simultaneous action of vasopressin that markedly reduces urea fractional excretion (see Fig. 10.2b). Actually, it is known that anesthesia and surgery induce a rise in
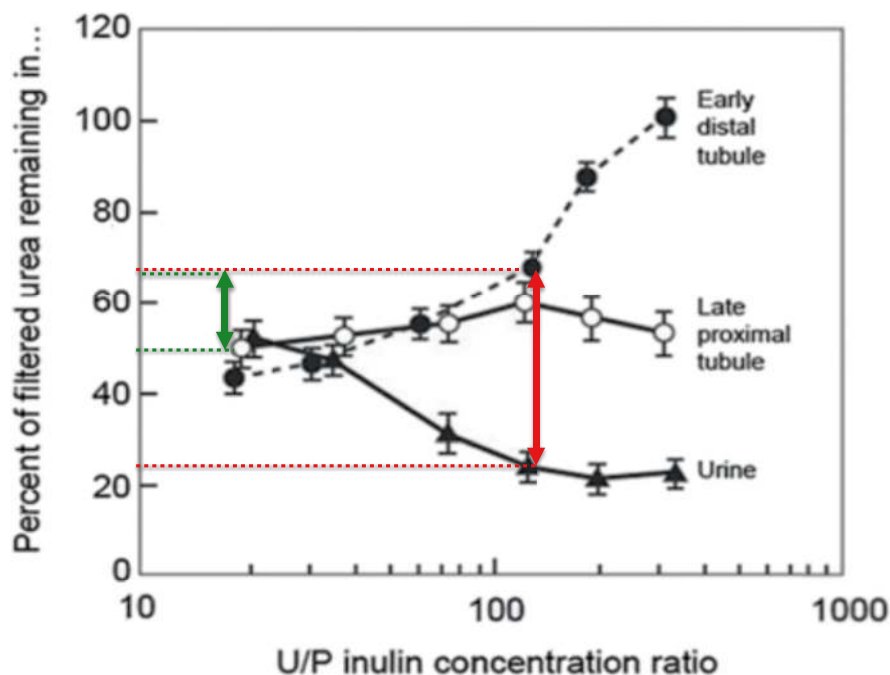
Fig. 10.15 Micropuncture studies reveal the amounts of urea secreted in the loop of Henle and reaborbed in the distal tubule and collecting duct. Modified from Ref. [1] in open access (based on micropuncture data by Ref. [37]). This figure depicts the fraction of filtered urea remaining in the late proximal tubule, the early distal tubule (close to the macula densa), and in the urine of normal rats, plotted against the urine-to-plasma ratio of inulin concentration (an index of water reabsorption and thus of tubular fluid or urine concentration). Note that the delivery of urea into the late proximal tubule is equal to about 50% of the filtered load over the whole range of urine concentration. The difference between the values in the late proximal tubule and the early distal tubule show how much urea is secreted. The difference between the values in the early distal tubule and the urine show how much urea is reabsorbed in the distal nephron and collecting duct. This reabsorption increases, and thus the fractional excretion of urea declines with increasing urine concentration (see also Fig. 10.2b, showing a similar decline in humans). For a U/P ratio of inulin concentrations of 120, FEurea is approximately 22%. Urea reabsorption between the early distal tubule and final urine (double red arrow) amounts to 38% of the filtered load (65–22%). Urea secretion between the end of the proximal tubule and the early distal tubule (double green arrow) amounts to 15% (65–50%). Thus, for this level of urine concentration, urea secretion compensates only part of the urea reabsorbed downstream

vasopressin secretion in experimental animals [122] as well as in humans [123, 124]. The amount of urea reabsorbed in the collecting duct under the influence of vasopressin has been largely underestimated. Figure 10.15 shows results of micropuncture studies [37]. For a urine/plasma ratio of Inulin concentrations of 120, as much of 40% of the filtered urea are reabsorbed between the early distal tubule and the final urine. Since the permeability of the distal tubule to urea is quite low, most of this urea is reabsorbed in the CD, and most of it in the IMCD through UT-A1/3

activated by vasopressin. *When FEurea is evaluated during chronic studies,* with urine collected in metabolic cages over 24 h without disturbance of the animals, the high fractional excretion of urea is clearly seen, as shown in Table 10.2. Fractional excretion of urea was above 50% in normal rats, and above 100% in rats with a low urine concentrating activity (induced by adding water to their food) [125].

Note FEurea does not need to exceed 100% to indicate the existence of significant urea secretion. About half of the filtered urea is reabsorbed in the proximal convoluted tubule, whatever the level of diuresis [37]. This urea has no chance to be reintroduced into the nephron because the very high blood flow in the cortex returns all reabsorbed solutes to the general circulation. Thus, even assuming there is no additional reabsorption of urea further down in the collecting duct, any figure of FEurea above 50% suggests that net tubular secretion occurs.

Another originality of this review is that it proposes a transporter responsible for this urea secretion, based only on the analysis of the literature. The experimental observations that support a urea/glycine counter-transport by SLC6A18 are very strong. But this will remain an attractive hypothesis until this transport will be proven experimentally. The best demonstration would be the study of transepithelial urea fluxes in isolated pars recta of rats or mice when glycine is available in the bath and lumen, as done in rabbit tubules by Kawamura [42]. Feeding the animals with a high protein diet for a few days before the experiments would probably increase the intensity of this transport. Studies in vitro in transfected cells will require the simultaneous transfection of SLC6A18 and collectrin (or ACE2), a chaperone that is required for the insertion of the transporter in the cell membrane [63, 126]. It should be easy to evaluate if AQP7 transports glycine in amphibian oocytes injected with AQP7 cRNA, as previously described [70].

If SLC6A18 is really responsible for urea secretion in the mammalian kidney, a clear phenotype should appear in mice with SLC6A18 knockout. The plasma concentration of urea should be significantly higher than in wildtype mice, and the fractional excretion significantly lower, a phenotype ressembling that of familial azotemia. Unfortunately, the investigators who studied such mice did not measure plasma urea.

Even if these validations are not yet available, it is important now to integrate in our concept of renal physiology that urea is secreted in the proximal tubule in significant amounts by an energy-dependent process. And that this secretion keeps the fractional excretion of urea within a reasonable range (30–50%) in spite of the marked reabsorption induced by vasopressin in the collecting duct. It will also be important to better characterize the role of urea secretion on the regulation of the glomerular filtration rate, and the possible stimulation of this secretion by liver-borne cAMP (under the influence of glucagon).

References

1. L. Bankir, Active urea transport in lower vertebrates and mammals. Subcell. Biochem. **73**, 193–226 (2014)
2. L. Bankir, C. de Rouffignac, Urinary concentrating ability: Insights from comparative anatomy. Am. J. Phys. **249**(6 Pt 2), R643–R666 (1985)
3. L. Bankir, M.M. Trinh-Trang-Tan, Urea and the kidney, in *The Kidney*, ed. by B.M. Brenner, 6th edn., (W B Saunders Company, Philadelphia, 2000), pp. 637–679
4. B. Yang, L. Bankir, Urea and urine concentrating ability: New insights from studies in mice. Am. J. Physiol. Renal Physiol. **288**(5), F881–F896 (2005)
5. R.A. Fenton, A. Flynn, A. Shodeinde, C.P. Smith, J. Schnermann, M.A. Knepper, Renal phenotype of UT-A urea transporter knockout mice. J. Am. Soc. Nephrol. **16**(6), 1583–1592 (2005)
6. L. Bankir, R. Roussel, N. Bouby, Protein- and diabetes-induced glomerular hyperfiltration: Role of glucagon, vasopressin, and urea. Am. J. Physiol. Renal Physiol. **309**(1), F2–23 (2015)
7. C. Shayakul, B. Clémençon, M.A. Hediger, The urea transporter family (SLC14): Physiological, pathological and structural aspects. Mol. Asp. Med. **34**(2–3), 313–322 (2013)
8. B. Schmidt-Nielsen, H. Osaki, Renal response to changes in nitrogen metabolism in sheep. Am. J. Phys. **193**, 657–661 (1958)
9. B. Schmidt-Nielsen, H. Osaki, H.V. Murdaugh Jr., R. O'Dell, Renal regulation of urea excretion in sheep. Am. J. Phys. **194**(2), 221–228 (1958)
10. H.V. Murdaugh Jr., B. Schmidt-Nielsen, E.M. Doyle, R. O'Dell, Renal tubular regulation of urea excretion in man. J. Appl. Physiol. **13**(2), 263–268 (1958)
11. W.J. O'Connor, R.A. Summerill, The excretion of urea by dogs following a meat meal. J. Physiol. **256**, 93–102 (1976)
12. A. Hadj-Aissa, L. Bankir, M. Fraysse, D.G. Bichet, P. Laville, P. Zech, et al., Influence of the level of hydration on the renal response to a protein meal. Kidney Int. **42**(5), 1207–1216 (1992)
13. M.A. Knepper, C.V. Gunter, R.A. Danielson, Effects of glucagon on renal function in protein-deprived rats. Surg. Forum **27**, 29–31 (1976)
14. M. Ahloulay, N. Bouby, F. Machet, M. Kubrusly, C. Coutaud, L. Bankir, Effects of glucagon on glomerular filtration rate and urea and water excretion. Am. J. Phys. **263**(Renal Fluid Electrolyte Physiol. 32), F24–F36 (1992)
15. M. Ahloulay, M. Déchaux, K. Laborde, L. Bankir, Influence of glucagon on GFR and on urea and electrolyte excretion: Direct and indirect effects. Am. J. Physiol. **269**(Renal Fluid and Electrolyte Physiol. 38), 225–235 (1995)
16. G.S. Stewart, C. Graham, S. Cattell, T.P. Smith, N.L. Simmons, C.P. Smith, UT-B is expressed in bovine rumen: Potential role in ruminal urea transport. Am. J. Physiol. Regul. Integr. Comp. Physiol. **289**(2), R605–RR12 (2005)
17. N.L. Simmons, A.S. Chaudhry, C. Graham, E.S. Scriven, A. Thistlethwaite, C.P. Smith, et al., Dietary regulation of ruminal bovine UT-B urea transporter expression and localization. J. Anim. Sci. **87**(10), 3288–3299 (2009)
18. S. Hailemariam, S. Zhao, Y. He, J. Wang, Urea transport and hydrolysis in the rumen: A review. Anim. Nutr. **7**(4), 989–996 (2021)
19. C. Zhong, R. Long, G.S. Stewart, The role of rumen epithelial urea transport proteins in urea nitrogen salvage: A review. Anim. Nutr. **9**, 304–313 (2022)
20. D. Kiran, T. Mutsvangwa, Effects of partial ruminal defaunation on urea-nitrogen recycling, nitrogen metabolism, and microbial nitrogen supply in growing lambs fed low or high dietary crude protein concentrations. J. Anim. Sci. **88**(3), 1034–1047 (2010)
21. H. Inoue, S.D. Jackson, T. Vikulina, J.D. Klein, K. Tomita, S.M. Bagnasco, Identification and characterization of a Kidd antigen/UT-B urea transporter expressed in human colon. Am. J. Physiol. Cell Physiol. **287**(1), C30–C35 (2004)
22. C.P. Smith, E.A. Potter, R.A. Fenton, G.S. Stewart, Characterization of a human colonic cDNA encoding a structurally novel urea transporter, hUT-A6. Am. J. Physiol. Cell Physiol. **287**(4), C1087–C1093 (2004)

23. G.S. Stewart, R.A. Fenton, F. Thevenod, C.P. Smith, Urea movement across mouse colonic plasma membranes is mediated by UT-A urea transporters. Gastroenterology **126**(3), 765–773 (2004)

24. H. Inoue, S.D. Kozlowski, J.D. Klein, J.L. Bailey, J.M. Sands, S.M. Bagnasco, Regulated expression of renal and intestinal UT-B urea transporter in response to varying urea load. Am. J. Physiol. Renal Physiol. **289**(2), F451–F458 (2005)

25. N. Lucien, P. Bruneval, F. Lasbennes, M.F. Belair, C. Mandet, J. Cartron, et al., UT-B1 urea transporter is expressed along the urinary and gastrointestinal tracts of the mouse. Am. J. Physiol. Regul. Integr. Comp. Physiol. **288**(4), R1046–R1056 (2005)

26. D. Collins, D.C. Winter, A.M. Hogan, L. Schirmer, A.W. Baird, G.S. Stewart, Differential protein abundance and function of UT-B urea transporters in human colon. Am. J. Physiol. Gastrointest. Liver Physiol. **298**(3), G345–G351 (2010)

27. D. Collins, C. Walpole, E. Ryan, D. Winter, A. Baird, G. Stewart, UT-B1 mediates transepithelial urea flux in the rat gastrointestinal tract. J. Membr. Biol. **239**(3), 123–130 (2011)

28. T. Isozaki, J.W. Verlander, J.M. Sands, Low protein diet alters urea transport and cell structure in rat initial inner medullary collecting duct. J. Clin. Invest. **92**(5), 2448–2457 (1993)

29. T. Isozaki, A.G. Gillin, C.E. Swanson, J.M. Sands, Protein restriction sequentially induces new urea transport processes in rat initial IMCD. Am. J. Phys. **266**(5 Pt 2), F756–F761 (1994)

30. T. Isozaki, J.P. Lea, J.A. Tumlin, J.M. Sands, Sodium-dependent net urea transport in rat initial inner medullary collecting ducts. J. Clin. Invest. **94**(4), 1513–1517 (1994)

31. A. Kato, J.M. Sands, Active sodium-urea counter-transport is inducible in the basolateral membrane of rat renal initial inner medullary collecting ducts. J. Clin. Invest. **102**(5), 1008–1015 (1998)

32. A. Kato, J.M. Sands, Urea transport processes are induced in rat IMCD subsegments when urine concentrating ability is reduced. Am. J. Phys. **276**(1 Pt 2), F62–F71 (1999)

33. Z.M. Ashkar, S. Martial, T. Isozaki, S.R. Price, J.M. Sands, Urea transport in initial IMCD of rats fed a low-protein diet: Functional properties and mRNA abundance. Am. J. Phys. **268**(6 Pt 2), F1218–23 (1995)

34. J.M. Sands, S. Martial, T. Isozaki, Active urea transport in the rat inner medullary collecting duct: Functional characterization and initial expression cloning. Kidney Int. **49**(6), 1611–1614 (1996)

35. G. Chen, Y. Yang, O. Frohlich, J.D. Klein, J.M. Sands, Suppression subtractive hybridization analysis of low-protein diet- and vitamin D-induced gene expression from rat kidney inner medullary base. Physiol. Genomics **41**(3), 203–211 (2010)

36. J.C. Marini, J.D. Klein, J.M. Sands, M.E. Van Amburgh, Effect of nitrogen intake on nitrogen recycling and urea transporter abundance in lambs. J. Anim. Sci. **82**(4), 1157–1164 (2004)

37. T. Armsen, H.W. Reinhardt, Transtubular movement of urea at different degrees of water diuresis. Pflugers Arch. **326**(3), 270–280 (1971)

38. L. Bankir, G. Crambert, R. Vargas-Poussou, The SLC6A18 transporter is most likely a Na-dependent glycine/urea antiporter responsible for urea secretion in the proximal straight tubule: Influence of this urea secretion on glomerular filtration rate. Nephron, 1–27 (2024)

39. M.A. Knepper, F. Roch-Ramel, Pathways of urea transport in the mammalian kidney. Kidney Int. **31**(2), 629–633 (1987)

40. S. Uchida, E. Sohara, T. Rai, M. Ikawa, M. Okabe, S. Sasaki, Impaired urea accumulation in the inner medulla of mice lacking the urea transporter UT-A2. Mol. Cell. Biol. **25**(16), 7357–7363 (2005)

41. T. Lei, L. Zhou, A.T. Layton, H. Zhou, X. Zhao, L. Bankir, et al., Role of thin descending limb urea transport in renal urea handling and the urine concentrating mechanism. Am. J. Physiol. Renal Physiol. **301**(6), F1251–9 (2011)

42. S. Kawamura, J.P. Kokko, Urea secretion by the straight segment of the proximal tubule. J. Clin. Invest. **58**(3), 604–612 (1976)

43. R. Safirstein, P. Miller, S. Dikman, N. Lyman, C. Shapiro, Cisplatin nephrotoxicity in rats: Defect in papillary hypertonicity. Am. J. Phys. **241**(2), F175–85 (1981)

44. K.H.J. Beyer, R.T. Gelarden, Active transport of urea by mammalian kidney. Proc. Natl. Acad. Sci. **85**, 4030–4031 (1988)

45. J.R. Clapp, Urea reabsorption by the proximal tubule in the dog. Proc. Soc. Exp. Biol. (New-York) **120**, 521–523 (1965)

46. L. Bankir, B. Yang, New insights into urea and glucose handling by the kidney, and the urine concentrating mechanism. Kidney Int. **81**(12), 1179–1198 (2012)

47. C.H. Hsu, T.W. Kurtz, P.U. Massari, S.A. Ponze, B.S. Chang, Familial azotemia. Impaired urea excretion despite normal renal function. N. Engl. J. Med. **298**, 117–121 (1978)

48. T. Armsen, V. Glossmann, M. Weinzierl, H.H. Edel, Familial proximal tubular azotemia. Elevated urea plasma levels in normal kidney function. Dtsch. Med. Wochenschr. **111**(18), 702–706 (1986)

49. K.H. Beyer, R.T. Gelarden, E.S. Vesell, Inhibition of urea transport across renal tubules by parazinoylguanidine and analogs. Pharmacology **44**, 124–138 (1992)

50. M.A. Knepper, Urea transport in nephron segments from medullary rays of rabbits. Am. J. Phys. **244**(6), F622–F627 (1983)

51. R.M. O'Dell, B. Schmidt-Nielsen, Retention of urea by frog and mammalian kidney slices in vitro. J. Cell. Comp. Physiol. A **57**(3), 211–219 (1961)

52. F. Roch-Ramel, G. Peters, Intrarenal urea and electrolyte concentrations as influenced by water diuresis and by hydrochlorothiazide. Eur. J Pharmacol. **1**, 124–139 (1967)

53. F. Roch-Ramel, F. Chomety, G. Peters, Urea concentrations in tubular fluid and in renal tissue of nondiuretic rats. Am. J. Phys. **215**(2), 429–438 (1968)

54. F. Roch-Ramel, J. Diezi, F. Chomety, P. Michoud, G. Peters, Disposal of large urea overloads by the rat kidney: A micropuncture study. Am. J. Phys. **218**(6), 1524–1532 (1970)

55. J. Hellerá, M. Kleinová, K. Janácek, R. Rybová, High concentration of urea in renal cortex, in *Kidney Metabolism and Function*, ed. by R. Dzúrik, B. Lichardus, W. Guder, (Martinus Nijhoff Publishers, Boston, 1985), pp. 298–302

56. G. Conte, A. DalCanton, M. Terribile, B. Cianciaruso, G. DiMinno, M. Pannain, et al., Renal handling of urea in subjects with persistent azotemia and normal renal function. Kidney Int. **32**, 721–727 (1987)

57. R.M. Hays, Familial azotemia. N. Engl. J. Med. **298**, 160–161 (1978)

58. L. Liu, T. Lei, L. Bankir, D. Zhao, X. Gai, X. Zhao, et al., Erythrocyte permeability to urea and water: Comparative study in rodents, ruminants, carnivores, humans, and birds. J. Comp. Physiol. B, Biochem. Syst. Environ. Physiol. **181**(1), 65–72 (2011)

59. N. Obermüller, B. Kränzlin, R. Verma, N. Gretz, W. Kriz, R. Witzgall, Renal osmotic stress-induced cotransporter: Expression in the newborn, adult and post-ischemic rat kidney. Kidney Int. **52**(6), 1584–1592 (1997)

60. K.F. Hilgers, S.K. Nagaraj, E.A. Karginova, I.G. Kazakova, R.L. Chevalier, R.M. Carey, et al., Molecular cloning of KS, a novel rat gene expressed exclusively in the kidney. Kidney Int. **54**(5), 1444–1454 (1998)

61. E. Romeo, M.H. Dave, D. Bacic, Z. Ristic, S.M. Camargo, J. Loffing, et al., Luminal kidney and intestine SLC6 amino acid transporters of B0AT-cluster and their tissue distribution in Mus musculus. Am. J. Physiol. Renal Physiol. **290**(2), F376–F383 (2006)

62. H. Quan, K. Athirakul, W.C. Wetsel, G.E. Torres, R. Stevens, Y.T. Chen, et al., Hypertension and impaired glycine handling in mice lacking the orphan transporter XT2. Mol. Cell. Biol. **24**(10), 4166–4173 (2004)

63. D. Singer, S.M. Camargo, K. Huggel, E. Romeo, U. Danilczyk, K. Kuba, et al., Orphan transporter SLC6A18 is renal neutral amino acid transporter B0AT3. J. Biol. Chem. **284**(30), 19953–19960 (2009)

64. R. Kleta, E. Romeo, Z. Ristic, T. Ohura, C. Stuart, M. Arcos-Burgos, et al., Mutations in SLC6A19, encoding B0AT1, cause Hartnup disorder. Nat. Genet. **36**(9), 999–1002 (2004)

65. C. Böhmer, A. Bröer, M. Munzinger, S. Kowalczuk, J.E. Rasko, F. Lang, et al., Characterization of mouse amino acid transporter B0AT1 (slc6a19). Biochem. J. **389**(Pt 3), 745–751 (2005)

66. D.W. Barfuss, J.M. Mays, J.A. Schafer, Peritubular uptake and transepithelial transport of glycine in isolated proximal tubules. Am. J. Phys. **238**(4), F324–F333 (1980)

67. E. Sohara, T. Rai, J. Miyazaki, A.S. Verkman, S. Sasaki, S. Uchida, Defective water and glycerol transport in the proximal tubules of AQP7 knockout mice. Am. J. Physiol. Renal Physiol. **289**(6), F1195–F1200 (2005)

68. E. Sohara, T. Rai, S. Sasaki, S. Uchida, Physiological roles of AQP7 in the kidney: Lessons from AQP7 knockout mice. Biochim. Biophys. Acta **1758**(8), 1106–1110 (2006)

69. K. Ishibashi, M. Kuwahara, Y. Gu, Y. Kageyama, A. Tohsaka, F. Suzuki, et al., Cloning and functional expression of a new water channel abundantly expressed in the testis permeable to water, glycerol, and urea. J. Biol. Chem. **272**(33), 20782–20786 (1997)

70. F.J. Moss, P. Mahinthichaichan, D.T. Lodowski, T. Kowatz, E. Tajkhorshid, A. Engel, et al., Aquaporin-7: A dynamic aquaglyceroporin with greater water and glycerol permeability than its bacterial homolog GlpF. Front. Physiol. **11**, 728 (2020)

71. M. Huelsmann, N. Hecker, M.S. Springer, J. Gatesy, V. Sharma, M. Hiller, Genes lost during the transition from land to water in cetaceans highlight genomic changes associated with aquatic adaptations. Sci. Adv. **5**(9), eaaw6671 (2019)

72. D.J. Randall, C.M. Wood, S.F. Perry, H. Bergman, G.M. Maloiy, T.P. Mommsen, et al., Urea excretion as a strategy for survival in a fish living in a very alkaline environment. Nature **337**(6203), 165–166 (1989)

73. P.J. Walsh, M. Grosell, G.G. Goss, H.L. Bergman, A.N. Bergman, P. Wilson, et al., Physiological and molecular characterization of urea transport by the gills of the Lake Magadi tilapia (Alcolapia grahami). J. Exp. Biol. **204**(Pt 3), 509–520 (2001)

74. Z.G.A. Orozco, S. Soma, T. Kaneko, S. Watanabe, Spatial mRNA expression and response to fasting and refeeding of neutral amino acid transporters slc6a18 and slc6a19a in the intestinal epithelium of Mozambique tilapia. Front. Physiol. **9**, 212 (2018)

75. N. Berman, M. Lectura, J. Thurman, J. Reinecke, A.C. Raff, M.L. Melamed, et al., A zebrafish model for uremic toxicity: Role of the complement pathway. Blood Purif. **35**(4), 265–269 (2013)

76. A.H. Berg, C. Drechsler, J. Wenger, R. Buccafusca, T. Hod, S. Kalim, et al., Carbamylation of serum albumin as a risk factor for mortality in patients with kidney failure. Sci. Transl. Med. **5**(175), 175ra29 (2013)

77. C. Nicolas, S. Jaisson, L. Gorisse, F.J. Tessier, C. Niquet-Léridon, P. Jacolot, et al., Carbamylation is a competitor of glycation for protein modification in vivo. Diabetes Metab. **44**(2), 160–167 (2018)

78. S. Kalim, A.H. Berg, S.A. Karumanchi, R. Thadhani, A.S. Allegretti, S. Nigwekar, et al., Protein carbamylation and chronic kidney disease progression in the Chronic Renal Insufficiency Cohort Study. Nephrol. Dial. Transplant. **37**(1), 139–147 (2021)

79. S. Kalim, S. Zhao, M. Tang, E.P. Rhee, A.S. Allegretti, S. Nigwekar, et al., Protein carbamylation and the risk of ESKD in patients with CKD. J. Am. Soc. Nephrol. **34**(5), 876–885 (2023)

80. L. Bankir, N. Bouby, B. Blondeau, G. Crambert, Glucagon actions on the kidney revisited: Possible role in potassium homeostasis. Am. J. Physiol. Renal Physiol. **311**(2), F469–F486 (2016)

81. L. Bankir, N. Bouby, R.C. Speth, G. Velho, G. Crambert, Glucagon revisited: Coordinated actions on the liver and kidney. Diabetes Res. Clin. Pract. **146**, 119–129 (2018)

82. M.A. Knepper, C.L. Chou, H.E. Layton, How is urine concentrated by the renal inner medulla? Contrib. Nephrol. **102**, 144–160 (1993)

83. A.T. Layton, H.E. Layton, W.H. Dantzler, T.L. Pannabecker, The mammalian urine concentrating mechanism: Hypotheses and uncertainties. Physiology (Bethesda) **24**, 250–256 (2009)

84. A.T. Layton, Mathematical modeling of urea transport in the kidney. Subcell. Biochem. **73**, 31–43 (2014)

85. A.T. Layton, L. Bankir, Impacts of active urea secretion into pars recta on urine concentration and urea excretion rate. Physiol. Rep. **1**(3) (2013)

86. L. Bankir, K. Chen, B. Yang, Lack of UT-B in vasa recta and red blood cells prevents urea-induced improvement of urinary concentrating ability. Am. J. Physiol. Renal Physiol. **286**(1), F144–F151 (2004)

87. L. Bankir, N. Bouby, E. Ritz, Vasopressin: A novel target for the prevention and retardation of kidney disease? Nat. Rev. Nephrol. **9**(4), 223–239 (2013)

88. J.P. Bosch, S. Lew, S. Glabman, A. Lauer, Renal hemodynamic changes in humans. Response to protein loading in normal and diseased kidneys. Am. J. Med. **81**(5), 809–815 (1986)

89. M. Giordano, P. Castellino, E.L. McConnell, R.A. DeFronzo, Effect of amino acid infusion on renal hemodynamics in humans: A dose-response study. Am. J. Phys. **267**(5 Pt 2), F703–F708 (1994)

90. C.E. Mogensen, Glomerular hyperfiltration in human diabetes. Diabetes Care **17**(7), 770–775 (1994)

91. M. Cortinovis, N. Perico, P. Ruggenenti, A. Remuzzi, G. Remuzzi, Glomerular hyperfiltration. Nat. Rev. Nephrol. **18**(7), 435–451 (2022)

92. S.W. Lew, J.P. Bosch, Effect of diet on creatinine clearance and excretion in young and elderly healthy subjects and in patients with renal disease. J. Am. Soc. Nephrol. **2**(4), 856–865 (1991)

93. A.N. Friedman, High-protein diets: Potential effects on the kidney in renal health and disease. Am. J. Kidney Dis. **44**(6), 950–962 (2004)

94. N. Bouby, M.M. Trinh-Trang-Tan, C. Coutaud, L. Bankir, Vasopressin is involved in renal effects of high-protein diet: Study in homozygous Brattleboro rats. Am. J. Phys. **260**(1 Pt 2), F96–100 (1991)

95. N.G. DeSanto, S. Coppola, P. Anastasio, G. Coscarella, G. Capasso, P. Castellino, et al., Pancreatectomy abolishes the renal hemodynamic response to a meat meal in man. Nephron **55**(1), 85–86 (1990)

96. G. Friedlander, F. Blanchet-Benque, A. Nitenberg, C. Laborie, R. Assan, C. Amiel, Glucagon secretion is essential for aminoacid-induced hyperfiltration in man. Nephrol. Dial. Transplant. **5**(2), 110–117 (1990)

97. F.D. Seney, A.E.G. Persson, F.S. Wright, Modification of tubuloglomerular feedback signal by dietary protein. Am. J. Phys. **252**(Renal Fluid Electrolyte Physiol. 21), F83–90 (1987)

98. M. Ahloulay, M. Déchaux, C. Hassler, N. Bouby, L. Bankir, Cyclic AMP is a hepatorenal link influencing natriuresis and contributing to glucagon-induced hyperfiltration in rats. J. Clin. Invest. **98**(10), 2251–2258 (1996)

99. D. Zittema, E. van den Berg, E. Meijer, W.E. Boertien, A.C. Muller Kobold, C.F. Franssen, et al., Kidney function and plasma copeptin levels in healthy kidney donors and autosomal dominant polycystic kidney disease patients. Clin. J. Am. Soc. Nephrol. **9**(9), 1553–1562 (2014)

100. D. Petrovic, L. Bankir, B. Ponte, M. Pruijm, T. Corre, J.P. Ghobril, et al., The urine-to-plasma urea concentration ratio is associated with eGFR and eGFR decline over time in a population cohort. Nephrol. Dial. Transplant. **39**(1), 122–132 (2023)

101. T.T. Turner, P.K. Hartmann, S.S. Howards, Urea in the seminiferous tubule: Evidence for active transport. Biol. Reprod. **20**(3), 511–515 (1979)

102. H. Tsukaguchi, C. Shayakul, U.V. Berger, T. Tokui, D. Brown, M.A. Hediger, Cloning and characterization of the urea transporter UT3: Localization in rat kidney and testis. J. Clin. Invest. **99**(7), 1506–1515 (1997)

103. R.A. Fenton, A. Howorth, G.J. Cooper, R. Meccariello, I.D. Morris, C.P. Smith, Molecular characterization of a novel UT-A urea transporter isoform (UT-A5) in testis. Am. J. Physiol. Cell Physiol. **279**(5), C1425–C1431 (2000)

104. C. Ghezzi, D.D.F. Loo, E.M. Wright, Physiology of renal glucose handling via SGLT1, SGLT2 and GLUT2. Diabetologia **61**(10), 2087–2097 (2018)

105. S. Bröer, The SLC6 orphans are forming a family of amino acid transporters. Neurochem. Int. **48**(6–7), 559–567 (2006)

106. S. Bröer, U. Gether, The solute carrier 6 family of transporters. Br. J. Pharmacol. **167**(2), 256–278 (2012)

107. K.W. Beyenbach, Kidneys sans glomeruli. Am. J. Physiol. Renal Physiol. **286**(5), F811–F827 (2004)

108. S.S. Howards, T.T. Turner, The blood-testis barrier: A morphologic or physiologic phenomenon? Trans. Am. Assoc. Genitourin. Surg. **70**, 74–75 (1978)

109. L. Guo, D. Zhao, Y. Song, Y. Meng, H. Zhao, X. Zhao, et al., Reduced urea flux across the blood-testis barrier and early maturation in the male reproductive system in UT-B-null mice. Am. J. Physiol. Cell Physiol. **293**(1), C305–C312 (2007)

110. R.A. Fenton, G.J. Cooper, I.D. Morris, C.P. Smith, Coordinated expression of UT-A and UT-B urea transporters in rat testis. Am. J. Physiol. Cell Physiol. **282**(6), C1492–C1501 (2002)

111. D.A. Spector, Q. Yang, J. Liu, J.B. Wade, Expression, localization, and regulation of urea transporter B in rat urothelia. Am. J. Physiol. Renal Physiol. **287**(1), F102–F108 (2004)

112. A. Chang, T.G. Hammond, T.T. Sun, M.L. Zeidel, Permeability properties of the mammalian bladder apical membrane. Am. J. Phys. **267**(5 Pt 1), C1483–C1492 (1994)

113. H.O. Negrete, J.P. Lavelle, J. Berg, S.A. Lewis, M.L. Zeidel, Permeability properties of the intact mammalian bladder epithelium. Am. J. Phys. **271**(4 Pt 2), F886–F894 (1996)

114. D.A. Spector, Q. Yang, J.B. Wade, High urea and creatinine concentrations and urea transporter B in mammalian urinary tract tissues. Am. J. Physiol. Renal Physiol. **292**(1), F467–F474 (2007)

115. D.A. Spector, J. Deng, K.J. Stewart, Hydration status affects urea transport across rat urothelia. Am. J. Physiol. Renal Physiol. **301**(6), F1208–F1217 (2011)

116. D.A. Spector, J. Deng, K.J. Stewart, Dietary protein affects urea transport across rat urothelia. Am. J. Physiol. Renal Physiol. **303**(7), F944–F953 (2012)

117. A. Kato, J.M. Sands, Evidence for sodium-dependent active urea secretion in the deepest subsegment of the rat inner medullary collecting duct. J. Clin. Invest. **101**(2), 423–428 (1998)

118. G.A. Fines, J.S. Ballantyne, P.A. Wright, Active urea transport and an unusual basolateral membrane composition in the gills of a marine elasmobranch. Am. J. Physiol. Regul. Integr. Comp. Physiol. **280**(1), R16–R24 (2001)

119. Z. Dong, J. Ran, H. Zhou, J. Chen, T. Lei, W. Wang, et al., Urea transporter UT-B deletion induces DNA damage and apoptosis in mouse bladder urothelium. PLoS One **8**(10), e76952 (2013)

120. R. Hou, X. Kong, B. Yang, Y. Xie, G. Chen, SLC14A1: A novel target for human urothelial cancer. Clin. Transl. Oncol. **19**(12), 1438–1446 (2017)

121. Z. Wan, Y. Wang, C. Li, D. Zheng, SLC14A1 is a new biomarker in renal cancer. Clin. Transl. Oncol. **25**(8), 2607–2623 (2023)

122. B. Corman, G. Geelen, Effects of blood sampling, anesthesia and surgery on plasma vasopressin concentration in rats. Experientia **48**(3), 268–270 (1992)

123. M. Haas, S.M. Glick, Radioimmunoassayable plasma vasopressin associated with surgery. Arch. Surg. **113**(5), 597–600 (1978)

124. A.C. Carvalho, A.T. Guillaumon, A. Cintra Ede, L.C. Figueiredo, M.M. Moreira, S. Araújo, Plasmatic vasopressin in patients undergoing conventional infra-renal abdominal aorta aneurysm repair. Rev. Bras. Cir. Cardiovasc. **26**(3), 404–412 (2011)

125. N. Bouby, M. Ahloulay, E. Nsegbe, M. Déchaux, F. Schmitt, L. Bankir, Vasopressin increases GFR in conscious rats through its antidiuretic action. J. Am. Soc. Nephrol. **7**, 842–851 (1996)

126. J.M. Vanslambrouck, A. Bröer, T. Thavyogarajah, J. Holst, C.G. Bailey, S. Bröer, et al., Renal imino acid and glycine transport system ontogeny and involvement in developmental iminoglycinuria. Biochem. J. **428**(3), 397–407 (2010)

127. K.H. Jarausch, K.J. Ullrich, Studies on the problem of urine concentration and dilution; distribution of electrolytes (sodium, potassium, calcium, magnesium, anorganic phosphate), urea amino acids and exogenous creatinine in the cortex and medulla of dog kidney in various diuretic conditions. Pflugers Arch. Gesamte Physiol. Menschen Tiere **262**(6), 537–550 (1956)

128. D.D. Van Slyke, The effect of urine volume on urea excretion. J. Clin. Invest. **26**(6), 1159–1167 (1947)

129. L. Bankir, M. Ahloulay, N. Bouby, F. Machet, M.M. Trinh-Trang-Tan, Direct and indirect effects of vasopressin on renal hemodynamics, in *Vasopressin*, ed. by P. Gross, (John Libbey Eurotext, 1993), pp. 393–406

130. B. Schmidt-Nielsen, Urea excretion in mammals. Physiol. Rev. **38**(2), 139–168 (1958)

131. S. Nielsen, J. Terris, C.P. Smith, M.A. Hediger, C.A. Ecelbarger, M.A. Knepper, Cellular and subcellular localization of the vasopressin- regulated urea transporter in rat kidney. Proc. Natl. Acad. Sci. USA **93**(11), 5495–5500 (1996)